UNIVERSITÁ DEGLI STUDI DI UDINE

Department of Medical and Biological Sciences

PhD Course in Clinical Sciences and Technologies

XXVI Cycle (2011-2013)

PhD Research Thesis

In Vitro Rejuvenation of Senescent Human Cardiac Stem Cells Enhances Their Therapeutic Efficacy in Repairing a Mouse Infarcted Heart

PhD student: Elisa Avolio

Supervisor: Prof. Carlo Alberto Beltrami

External supervisor: Prof. Paolo Madeddu

Tutor: Dr. Antonio Paolo Beltrami

Academic Year 2013 - 2014

UNIVERSITÁ DEGLI STUDI DI UDINE

Department of Medical and Biological Sciences

PhD Course in Clinical Sciences and Technologies

XXVI Cycle (2011-2013)

PhD Research Thesis

In Vitro Rejuvenation of Senescent Human Cardiac Stem Cells Enhances Their Therapeutic Efficacy in Repairing a Mouse Infarcted Heart

PhD student: Elisa Avolio

Supervisor: Prof. Carlo Alberto Beltrami

External supervisor: Prof. Paolo Madeddu

Tutor: Dr. Antonio Paolo Beltrami

Academic Year 2013 - 2014

ACKNOWLEDGMENTS

The work presented in this thesis represents a very important part of my PhD studies; I am really fond of this work and I strongly believe it can give important insights for the future applications of autologous stem cell therapy in the human heart.
During these 3 years, I always did my best in order to give my contribution to the realization of this study. But, since medical-science research is a team work, this study would have not been possible without the precious and essential contribution of several people.
I am very thankful to all of them, in particular to:

Dr. Antonio Paolo Beltrami and Dr. Daniela Cesselli, who designed the study and with whose invaluable help and under whose constant supervision the work was performed;

all the people from my lab in Udine: first of all Giuseppe and Angela, but also Emmanouil, Barbara, Ely, Marisa, Elisa, Anita and everyone else who contributed to this work making it possible;

Dr. Nicoletta Finato, for the help with the collection and analysis of the human hearts;

Dr. Carlo Vascotto and Arianna, for the help with molecular biology;

at the Bristol Heart Institute (BHI), University of Bristol, Dr. Rajesh Katare and Dr. Marco Meloni, for the execution of the *in vivo* experiments with mice; Dr. Hua Lin and Dr. Ben Littlejohns, for having supported me in the realization of the *in vitro* experiments with rat cardiomyocytes;

Prof. Carlo Alberto Beltrami, Prof. Paolo Madeddu (BHI) and Prof. Costanza Emanueli (BHI), for their expert guidance and for all the suggestions regarding the planning of the work;

Prof. Ugolino Livi and Dr. Giuseppe Aresu of the Cardiac Surgery of the University Hospital of Udine, who provided the human samples object of this study.

Last, I take advantage to thank all the people from my two labs, at both University of Udine and Bristol, who supported me and my work during my Ph.D. Even the smallest help and every little advice from each of you was precious for me; you all have contributed to my formation as a research scientist. Really hope to be a good one!!! :-)

Table of Contents

Abstract

Recently our group has demonstrated that human c-Kit$^+$ Cardiac Stem Cells isolated from explanted failing hearts (E-CSC) are characterized, *in vitro*, compared to those isolated from healthy donated hearts (D-CSC), by a senescent phenotype: a reduced telomere length and telomerase activity, the occurrence of telomere dysfunction foci and the accumulation of senescent markers, as $p16^{INK4A}$. The result is an impairment of CSC functional properties *in vitro*.

The aim of this study was to identify molecular mechanisms associated with CSC senescence and to pharmacologically modulate this latter, at the aim to rejuvenate senescent cells *in vitro*, before transplantation, and to improve the therapeutic potential of CSC *in vivo*.

With this work, we newly demonstrate that senescent E-CSC show an impaired regenerative ability when injected in the peri-infarct region of an infarcted mouse heart. 2 weeks post-Myocardial Infarction, E-CSC treated mice showed, with respect to the D-CSC ones, worst anatomical and functional parameters at echocardiographic analysis. Histologically, E-CSC treated animals displayed a larger scar size, a lower density of capillaries, small arterioles and cycling myocytes, an enrichment in senescent, apoptotic and LC3$^+$ myocytes and a reduced number of cardiac primitive/progenitor cells recruited in the site of injury. In addition, we demonstrated that the E-CSC secretome was strongly enriched in the pro-inflammatory IL-1β and unable to protect rat adult cardiomyocytes - exposed in vitro to SI/RO injury - from apoptosis and senescence, while the D-CSC's secretome did. The neutralization of IL-1β in cell supernatants restored E-CSC's secretome protective effect.

We then looked for possible mechanisms responsible for E-CSC dysfunction, focusing on molecular pathways associated with cell senescence and ageing.

We identified that E-CSC are characterized by an hyper-activation of the canonical NFκB pathway and of Caspase1, an increased activity of the TORC1 complex, an impairment of the authophagic flux and a reduction of AMPK, Akt and CREB activation, moreover leading to a decreased transcription of the cardio-protective microRNA-132.

On the basis of these findings, we screened drugs capable to interfere with the above described pathways; we identified that a 3-days treatment with a combination of Resveratrol (0,5μM) and Rapamycin (10nM) is able to reduce the fraction of E-CSC affected by cell senescence *in vitro* and to diminish the secretion of IL-1β, thus restoring the protective effects of CSC's secretome on cardiomyocytes exposed *in vitro* to SI/RO injury.

At the molecular level, all the alterations in E-CSC could be successfully reverted employing the cocktail of the two drugs: Rapamycin and Resveratrol-treated-E-CSC were characterized by a reduction in TORC1 activity and inflammasome activation, and an increase in AMPK, AKT, CREB, SIRT-1 and miR-132 levels, in addition to the restoration of the autophagic flux.

Last, we tested if the pre-conditioning of E-CSC with the combination of the two drugs, prior to the transplantation in the peri-infarct region in a mouse MI-model, is able to restore their reparative ability. The results were positive: mice treated with preconditioned E-CSC showed cardiac functional and dimensional parameters similar to those of D-CSC treated mice; histologically, hearts were characterized by an enhanced arteriolar density, a decreased cardiomyocyte senescence, apoptosis and autophagy and an increased recruitment of host CSCs, that resulted in the reduction of the infarct size.

In conclusion, we first demonstrate that senescent c-Kit$^+$ CSC resident in human failing hearts display an impaired *in vivo* reparative ability; importantly, the senescent phenotype is not irreversible, and senescent CSC can be rejuvenated *in vitro* with a short pharmacologic conditioning with a combination of Rapamycin and Resveratrol, finally boosting the *in vivo* cardiac regeneration.

These findings open new avenues to improve autologous CSC therapy in heart failure.

List of Abbreviations

CSCs	Cardiac Stem Cells
D-CSC	Cardiac Stem Cells isolated from Donor hearts
E-CSC	Cardiac Stem Cells isolated from Explanted, failing hearts
TR-E-CSC	E-CSC treated with Rapamycin and Resveratrol
Rapa+Resv	combination of Rapamycin + Resveratrol
AMI	acute myocardial infarction
HF	heart failure
SI/RO	Simulated Ischemia/ReOxygenation injury
DDR	DNA-Damage Response
CPDT	cell population doubling time
SASP	senescence associated secretory phenotype
VEGF	vascular endothelial factor
bFGF	basic fibroblast growth factor
HGF	hepatocyte growth factor
IL-1β	Interleukin-1β
TIF	telomere-dysfunction induced foci

Echocardiography (*in vivo* study)

LVAW	left ventricle anterior wall thickness
LVPW	left ventricle posterior wall thickness
LVESD	left ventricle end systolic diameter
LVEDD	left ventricle end diastolic diameter
LVESV	left ventricle end systolic volume
LVEDV	left ventricle end diastolic volume
LVSV	left ventricle stroke volume
LVEF	left ventricle ejection fraction
LVFS	left ventricle fractional shortening
CO	cardiac output
s	systole
d	diastole

I. Introduction

1- The Failing Heart

1.1 Heart Failure: definition

In the American Heart Association (AHA)/American College of Cardiology Foundation (ACCF) guidelines, Heart failure (HF) is defined as a complex clinical syndrome that can result from any structural or functional cardiac disorder that impairs the ability of the ventricle to fill or eject blood[1]. HF may be associated with a wide spectrum of left ventricular (LV) functional abnormalities, which may range from patients with normal LV size to those with severe dilatation and/or markedly reduced ejection fraction (EF). In most patients, abnormalities of systolic and diastolic dysfunction coexist[2]. The ACCF/AHA defines HF in two groups on the basis of the left ventricular ejection fraction[2]:

1. ***systolic HF****,* characterized by a *reduced ejection fraction* (EF≤40%), and
2. ***diastolic HF****,* when the *ejection fraction is preserved* (EF≥50%).

Randomized clinical trials in patients with HF have mainly enrolled patients with an EF ≤35% or ≤40% and it is only on these patients that efficacious cell therapies have been demonstrated to date. Patients with an EF in the range of 40% to 50% represent an intermediate group; their characteristics, treatment patterns and outcomes appear similar to those of patients with HF with preserved EF[2].

1.2 Classification

Both the AHA/ACCF and the New York Heart Association (NYHA) proposed a model in which HF is classified on the basis of functional parameters that emphasize its evolution, severity and progression. The ACCF/AHA stages of HF emphasize the progressive nature of this disease and can be used to describe individuals and populations, whereas the NYHA classes are merely symptomatic[2].

The ACCF/AHA stages of HF (table 1.1) recognize that both risk factors and abnormalities of cardiac structure are associated with HF. The stages are progressive and inviolate; once a patient moves to a higher stage, regression to an earlier stage of HF is not observed[2]. The NYHA functional classification (table 1.2) gauges the severity of symptoms in patients with structural

heart disease, primarily stages C and D; it represents an independent predictor of mortality. It is widely used in clinical practice and research and for determining the eligibility of patients for healthcare services[2]. In contrast with ACCF/AHA model, HYHA classes are reversible, and a patient with NYHA class IV symptoms might have improvements to class III with diuretic therapy alone[3].

ACCF/AHA Stages of HF	
Stage A	*At high risk for HF but without structural heart disease or symptoms of HF*
Stage B	*Structural heart disease but without signs or symptoms of HF*
Stage C	*Structural heart disease with prior or current symptoms of HF*
Stage D	*Refractory HF requiring specialized interventions*

Table 1.1 *ACCF/AHA classification of Heart Failure* [2; 3]

NYHA Functional Classification of HF	
Class I	*Patients with cardiac disease but without resulting limitation of physical activity. Ordinary physical activity does not cause undue fatigue, palpitations, dyspnea or anginal pain.*
Class II	*Patients with cardiac disease resulting in slight limitation of physical activity. They are comfortable at rest. Ordinary physical activity results in fatigue, palpitation, dyspnea or anginal pain.*
Class III	*Patients with cardiac disease resulting in marked limitation of physical activity. They are comfortable at rest. Less than ordinary physical activity causes fatigue, palpitation, dyspnea or anginal pain.*
Class IV	*Patients with cardiac disease resulting in inability to carry on any physical activity without discomfort. Symptoms of HF or the anginal syndrome may be present even at rest. If any physical activity is undertaken, discomfort is increased.*

Table 1.2 *NYHA classification of Heart Failure* [2; 4]

1.3 Epidemiology

HF is a burgeoning problem worldwide, with more than 23 million people affected. In the United States, prevalent cases of HF exceed 5,8 million and each year >550,000 new cases are diagnosed. The overall prevalence of HF in the adult population in developed countries ranges from 1% to 12% based on available data from the United States and Europe[5]. HF prevalence follows an exponential pattern, rising with age, and affects 6-10% of people over age 65. Although the relative incidence of HF is lower in women than in men, women constitute at

least one-half the cases of HF because of their longer life expectancy. In North-America and Europe, the lifetime risk of developing HF is approximately one in five for a 40-years-old. The overall prevalence of HF is thought to be increasing, in part because current therapies for cardiac disorders, such as myocardial infarction (MI), valvular heart disease and arrhythmias are allowing patients to survive longer[4].

1.4 Etiology

Any condition that leads to an alteration in LV structure or function can predispose a patient to developing HF. Among the risk factors for HF development, the most relevant are hypertension, diabetes mellitus, metabolic syndrome and atherosclerotic disease[2]. Although the etiology of HF in patients with a preserved EF differs from that of patients with reduced EF, there is considerable overlap between the etiologies of these two conditions[4]. A major cause of systolic HF is represented by coronary artery disease (CAD) with antecedent myocardial infarction. The prevalence of this form of HF is approximately 50%. Hypertension remains the most important cause of diastolic HF, with a prevalence of 60% to 89% from large controlled trials, epidemiological studies and HF registries, although other associated cardiovascular risk factors are represented by obesity, CAD, diabetes mellitus, atrial fibrillation and hyperlipidemia[2].
In 20-30% of the cases of HF with a reduced EF, the exact etiology is not known. These patients are referred to as having nonischemic, idiopathic cardiomyopathy if the cause is unknown. A large number of cases of cardiomyopathies are secondary to specific genetic defects, most notably those in the cytoskeleton (mutations of genes encoding for ß-myosin heavy chain, myosin-binding protein C, cardiac troponin T, desmin, and vinculin), in the nuclear membrane proteins (i.e. lamins) or ion channels[4].

1.5 Prognosis

Despite many recent advances in the evaluation and management of HF, the development of symptomatic HF still carries a poor prognosis, with 30-40% of patients die within 1 year of diagnosis[4] and 50% die within 5 years, mainly from worsening HF or as a sudden event (e.g. ventricular arrhythmia)[2]. Although it is difficult to predict prognosis in an individual, patients with symptoms at rest (NYHA class IV) have a 30-70% annual mortality rate, whereas patients with symptoms with moderate activity (NYHA class II) have an annual mortality rate of 5-10%. Thus, functional status is an important predictor of patient outcome[4].

1.6 Pathogenesis

HF may be viewed as a progressive disorder that is initiated after an index event either damages the heart muscle, with a resultant loss of functioning cardiac myocytes, or, alternatively, disrupts the ability of the myocardium to generate force, thereby preventing the heart from contracting normally. This index event may have an abrupt onset, as in the case of a myocardial infarction (MI); it may have a gradual or insidious onset, as in the case of hemodynamic pressure or volume overloading; or it may be hereditary, as in the case of many of the genetic cardiomyopathies. Regardless of the nature of the inciting event, the feature that is common to each of these index events is that they all in some manner produce a decline in the pumping capacity of the heart (fig. 1.1)[4; 6].

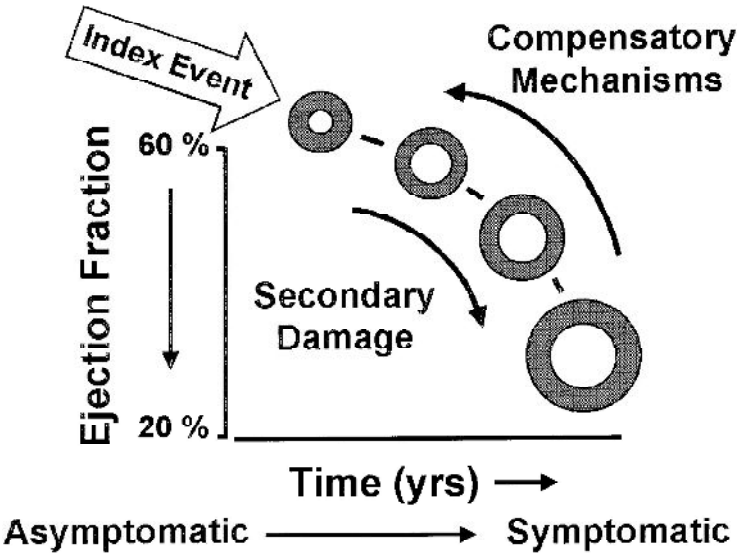

Figure 1.1 Pathogenesis of Heart Failure.
HF begins after an index event produces an initial decline in pumping capacity of the heart. A variety of compensatory mechanisms are activated. In the short term, cardiovascular function is restored to a homeostatic range. However, with time, the sustained activation of these systems can lead to secondary end-organ damage within the ventricle, with LV remodeling and cardiac decompensation. As a result, asymptomatic HF becomes symptomatic.
Taken from (Mann et al., 1999)

In most cases, patients remain asymptomatic or minimally symptomatic after the initial decline in pumping capacity of the heart or develop symptoms only after the dysfunction has been present for some time. One potential explanation is that a number of compensatory mechanisms become activated in the presence of cardiac injury and/or LV dysfunction allowing patients to sustain and modulate LV function for a period of months to years. These compensatory mechanisms include:

1. the activation of the renin-angiotensin-aldosterone (RAA) and adrenergic nervous systems, which are responsible for maintaining cardiac output through increased retention of salt and water, and
2. increased myocardial contractility.

3. In addition, there is the activation of a family of vasodilatory molecules (atrial and brain natriuretic peptides - ANP and BNP -, prostaglandins - PGE2 and PGI2 -, and nitric oxide - NO) that offset the excessive peripheral vascular vasoconstriction[4].

The transition to symptomatic HF is accompanied by increasing activation of neurohormonal, adrenergic and cytokine systems that lead to a series of maladaptive changes within the myocardium, collectively referred to as LV remodeling[4].

1.7 Basic mechanisms of left ventricular remodeling

LV remodeling develops in response to a series of complex events that occur at the cellular and molecular levels. It is defined as the process by which mechanical, neurohormonal and possibly genetic factors alter ventricular size, shape and function. Remodeling occurs in several clinical conditions, including myocardial infarction, cardiomyopathy, hypertension and valvular heart disease; its hallmarks include hypertrophy, loss of myocytes and increased interstitial fibrosis[3].

1.7.1 Myocardial infarction

Myocardial infarction (MI) is characterized by an acute loss of blood flow to a region of myocardium that results in myocyte necrosis, myofibroblast proliferation, cytokines release from injured myocytes and infiltration of circulating inflammatory cells. Much of this early inflammatory response results in reabsorption of necrotic tissue and the promotion of fibrotic scar formation prior to acute tissue remodeling[7]. In ischemic cardiomyopathy, changes in the ventricular architecture interest both the infarcted and noninfarcted tissue and remodeling is typically divided into acute and chronic stages ranging from hours to days and days to years[7]. The acute loss of myocardial cells results in abnormal loading conditions which induce dilatation and the change of the ventricular shape, rendering it more spherical, as well as causing hypertrophy (fig. 1.2)[3].

In its compensated stage, chamber dilation is produced by myocytes lengthening, whereas the ventricular number of cells is not altered. Importantly, myocyte diameter also increases, so that a modest absolute increase in wall thickness occurs and the ratio of wall thickness-to-chamber radius remains constant, keeping constant the cardiac wall stress, that follows Laplace law. In addition, the proportion between ventricular mass and chamber volume does not vary. When these relations are not preserved, decompensated concentric and eccentric hypertrophy develop, thus increasing cardiac wall stress[8]. Remodeling continues for months after the initial insult and the eventual change in the shape of the ventricle becomes detrimental to the overall function of the heart as a pump[3].

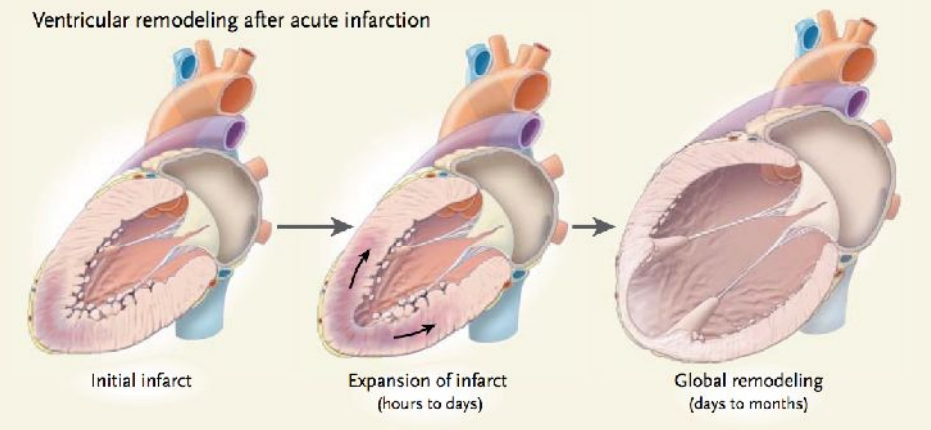

Figure 1.2 Ventricular remodeling after infarction. *Few hours-days after an acute myocardial infarction the area of myocardium affected by the infarction begins to expand and becomes thinner; within days to months, global remodeling can occur, resulting in overall ventricular dilatation, decreased systolic function and mitral valve dysfunction.*
Adapted from (Jessup et al., 2003)

1.8 Treatment

Once patients have developed structural heart disease, their therapy depends on their classification (fig. 1.3). For patients who have developed LV systolic dysfunction but remain asymptomatic (class NYHA I, ACCF/AHA stage A), the goal should be to slow disease progression by blocking neurohormonal system, reducing cardiac remodeling[3; 4]. For patients with heart failure and a low ejection fraction (Class NYHA II-IV, ACCF/AHA stage B-D) the primary goal is to alleviate symptoms, lessen disability, minimize risk factors and reduce the progression of disease, improving survival[3; 4]. These goals generally require a strategy that combines diuretics (to control salt and fluid retention) with neurohormonal interventions (to minimize cardiac remodeling)[4].

One third of patients with reduced EF and symptomatic HF (NYHA class III-IV) manifest abnormal inter- or intraventricular conduction with dyssynchronous ventricular contraction; the consequences of this latter include suboptimal ventricular filling, a reduction in LV contractility and prolonged duration of mitral regurgitation. *Biventricular pacing*, also termed *cardiac resynchronization therapy* (CRT), stimulates both ventricles nearly simultaneously, improving the coordination of ventricular contraction and reducing the severity of mitral regurgitation[4].

Implantation of *implantable cardiac defibrillators* (ICDs) in patients with mild to moderate HF (NYHA class II-III) and EF≤35% has been shown to reduce the incidence of sudden cardiac death in patients with ischemic or nonischemic cardiomyopathy. An ICD may also be combined with a biventricular pacemaker in patients with NYHA class III-IV HF[4].

Instead, for the management of patients with HF and preserved EF, there are no proven and/or approved pharmacologic or device therapies[4].

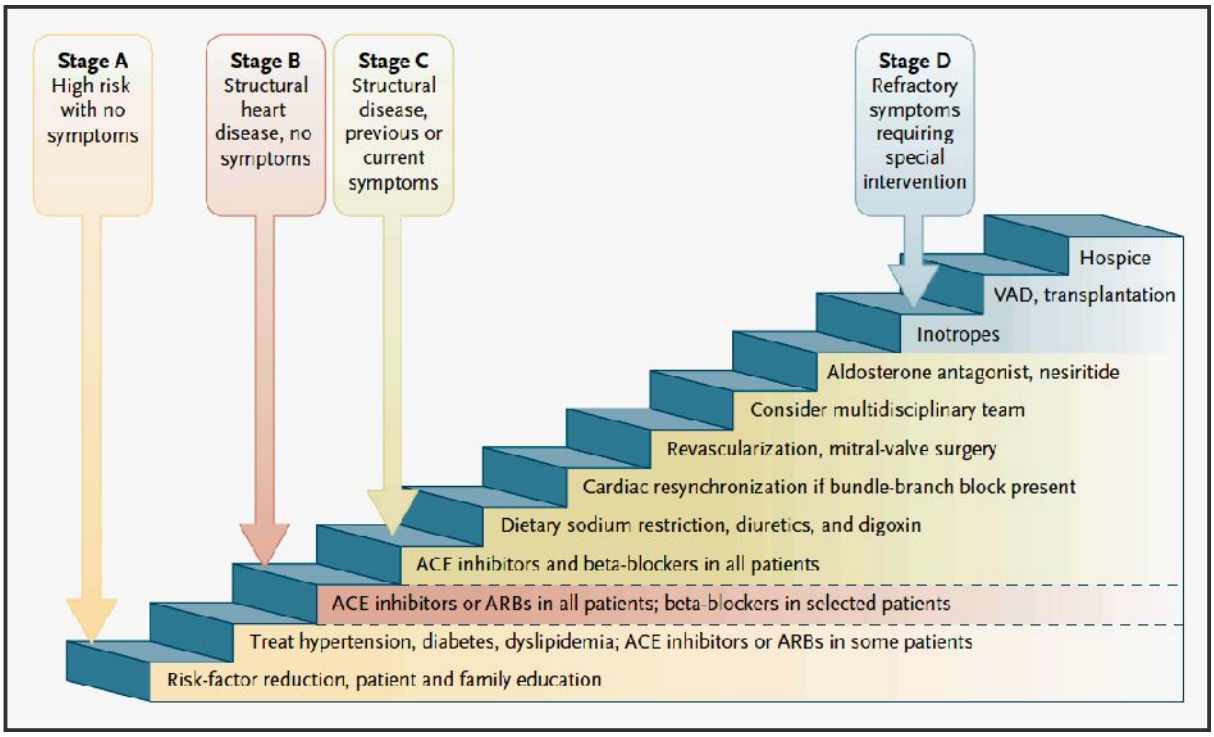

Figure 1.3 ***Stages of Heart Failure and treatment options for systolic Heart Failure***. *Taken from (Jessup et al, 2003)*

The final treatment for end-stage HF is represented by cardiac transplantation or prolonged assisted circulation. In the last years, a variety of extracorporeal pumps to provide circulatory support for variable periods of time have been developed. Although conceived of initially as alternatives to biologic replacement of the heart, left ventricular assisted devices (LVADs) were introduced as, and are still employed primarily as, temporary "bridges" to heart transplantation in patients who begin to fail medical therapy before a donor heart becomes available. However, improvements in this field have been so dramatic that now they can be regarded as destination therapy for a subset of patients that are not eligible for heart transplantation. Unfortunately, these long-term devices are not totally implantable yet and, because of this need for transcutaneous connections, all share a common problem with infectious complications. They also all share some tendency to thromboembolic complications as well as the expected possibility of mechanical device failure common to any machine. Last, a subset of patients with stage D or refractory end-stage HF who are younger and without significant comorbidities, can be considered as candidates for heart transplantation[4].

1.9 Looking at the future

Pharmacologic and interventional strategies have dramatically improved the outcomes of cardiac disease, but fail to adequately prevent disease progression. Current therapeutic options for end-stage HF patients are limited to cardiac transplantation (with the option of mechanical

cardiac assistance as a "bridge" to transplantation) or the option of permanent mechanical assistance of the circulation. Heart transplantation is limited by donor availability (increasing imbalance between supply and demand) and lifelong immunosuppression for transplant recipients; it suffers also of ethical problems concerning the transplantation of another person's organ[4; 9].

In the future, it is possible that genetic modulation of ventricular function or cell-based cardiac repair will be options for such patients. At the present, both approaches are considered to be experimental[4].

Current therapeutic approaches are palliative in the sense that they do not address the underlying problem of the loss of the cardiac tissue; the progression of the regenerative medicine is allowing the development of stem-cell based therapies that have the potential to transform the treatment of HF by achieving myocardial regeneration[10]. *Regenerative medicine* is defined as "the reconstruction of diseased or injured tissues by activation of endogenous cells or by cell transplantation"[11]. The role and contribution of stem cells in modern medicine is of paramount importance, both for their broad use in basic research and for the opportunities they give us to develop new therapeutic strategies in clinical practice. In addition, stem cells may be able to replace damaged tissues or even regenerate organs[12].

For the first time since cardiac transplantation, a therapy is being developed to eliminate the cause of HF, regenerate the lost tissue and not only to achieve damage control. Numerous preclinical and clinical studies have been performed that support the ability of various stem cell populations to improve cardiac function and reduce infarct size in both ischemic and nonischemic cardiomyopathy[10].

The discovery of myocardial regeneration and the applications of cell therapy for the regeneration of the damaged heart will be treated in *Chapter 3*.

2- Adult Stem Cells

2.1 What is a stem cell?

A stem cell is defined as a primitive, undifferentiated cell that can either extensively divide to reproduce itself (giving rise to identical daughter cells, by self-renewal, which maintain the quiescent pool population) or to give rise to more specialized cells (differentiated cells with more restricted properties) (fig. 2.1)[11; 13].

The major characteristics of stem cells are[12]:

- **self-renewal**, the ability to extensively proliferate,
- **clonality**, the ability to originate cells identical to themselves from a single cell,
- **potency**, the ability to differentiate into different cell types.

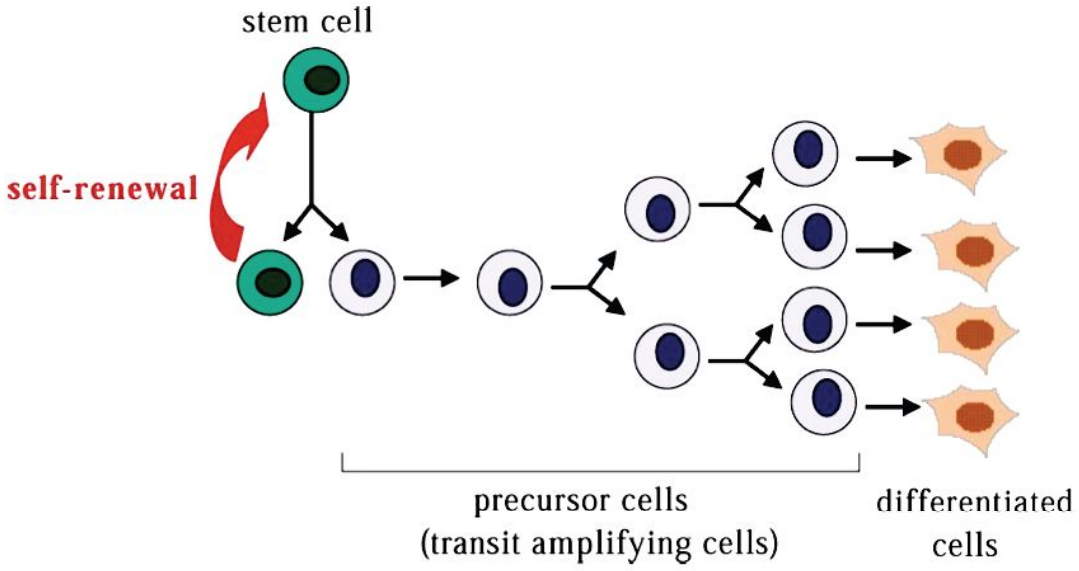

Figure 2.1 The possible choices for a daughter cell of a stem cell division. *It can either self-renew (that is, remain a stem cell) or commit to a pathway leading to differentiation. In many cases where it commits to differentiation, it first becomes a precursor cell, which proliferates before differentiating. Taken from (Raff, 2003)*

To define a cell as a stem cell, scientists have used four criteria[13]:

1. stem cells undergo multiple, sequential self-renewing cell divisions, a prerequisite to sustain the population;
2. single stem cell-derived daughter cells differentiate into more than one cell type (examples include hematopoietic stem cells, neural stem cells) although some adult stem cells may give rise to only a single mature cell type (corneal stem cell);

3. stem cells functionally repopulate the tissue of origin when transplanted in a damaged recipient;
4. stem cells contribute to differentiated progeny *in vivo* even in the absence of tissue damage.

Stem cells can be furthermore categorized according to their differentiation potential in[12]:

- **totipotent cells**, the most undifferentiated cells found in early development. They differentiate into both embryonic and extraembryonic tissues, thereby forming the embryo and the placenta; they are unable to be cultured *in vitro*;
- **pluripotent cells**, able to differentiate into cells that arise from the 3 germ layers - ectoderm, mesoderm and endoderm - from which all tissues and organs develop, including germ cells. They can not give origin to extraembryonic tissues. Pluripotent stem cells called embryonic stem cells (ESCs) were first derived from the inner cell mass of the blastocyst. In recent years, Takahashi and Yamanaka[14] generated pluripotent cells by reprogramming somatic cells: in 2007 the transduction of human fibroblasts with four genes encoding the transcription factors Oct3/4, Sox2, c-MYC and KLF4 gave origin to cells sharing similar characteristics with ESCs, called induced pluripotent stem cells (iPSCs);
- **multipotent cells**, found in most tissues and able to differentiate into several mature cell types, even originated from different germ layers. They do not generate germ cells;
- **oligopotent cells**, able to form 2 or more lineages within a specific tissue;
- **unipotent cells**, able to differentiate into only one specific cell type, forming a single lineage.

Last, stem cells can be divided in 2 categories based on their origin[11]:

- **embryonic stem cells**, pluripotent stem cell-lines derived from early embryos before formation of the tissue germ layers;
- **adult tissue stem cells**, derived from, or resident in, a fetal or adult tissue. These cells sustain turnover and repair throughout life in some tissues.

2.2 Tissue adult stem cells

Most, if not all, adult organs contain stem cells or, at least, can produce stem cells in culture; the ability of some tissues and organs in the adult to renew and repair following injury is critically dependent on these tissue-resident stem cells that generate tissue-specific, terminally differentiated cells[12]. The pathway to differentiation usually involves the daughter becoming a precursor cell, which proliferates before it differentiates[15]. The commitment, which is a program leading to differentiation, for a stem cell means the exit from self-renewal[11]. Because the proliferation amplifies the number of differentiated cells eventually produced, the precursors are often called transit amplifying cells (fig. 2.1). Specifically, these latter are called **progenitor**

cells when they express stemness markers and transcription factors that allow the cells to begin a differentiation program, while **precursor cells** if they already express proteins specific of the differentiated cell type they will generate. A progenitor cell possesses a greater developmental potential than a precursor cell[15].

It has been hypothesized that adult stem cells originate during ontogenesis (development of an organism) and remain in a quiescent state within adult tissues until local stimuli activate their proliferation, differentiation and migration[12].

The presumed ability of tissue-specific stem cells to acquire the fate of cell types different from the tissue of origin has been termed adult stem cell **plasticity**. This definition implies that a. different cell lineages are derived from a single initial cells, b. all differentiated cell types are functional *in vitro* and *in vivo*, and c. engraftment is robust and persistent in the presence and absence of tissue damage[13].

Different mechanisms have been proposed by Wagers and Weismann in 2004 to explain the plasticity of adult stem cells[16]:

1. **cell transdifferentiation**, the mechanism by which stem cells contribute to cell types of different lineages, following the activation of a dormant differentiation program to alter the lineage specificity of the cell;
2. **dedifferentiation** of a tissue specific cell to a more primitive, multipotent cell and subsequent **redifferentiation** along a new lineage pathway;
3. possibility that multiple distinct stem or progenitor cells contribute, consistent with their intrinsic lineage commitment and developmental potential, to each of the different lineages observed;
4. presence of single, rare pluripotent stem cells in the tissues;
5. **cell fusion**, between resident cells and guest cells, shown in neural cells.

It is now clear that stem cells are present in many adult tissues (including the bone marrow, heart, arteries, veins, gonads, skin and gut). The general consensus is that stem cells require a specialized microenvironment for their regulation: tissue-resident stem cells reside in **stem cell niches**, special microenvironments that control the self-renewal and differentiation of these cells[12; 17]. The niche microenvironment (fig. 2.2) consists of various signals from extracellular matrix and soluble mediators that mediate cell signaling and gene expression, regulating stem cell proliferation, migration, differentiation or apoptosis. The stem cell function is critically influenced by extrinsic signals from the microenvironment, therefore the niche plays a crucial role in stem cell homeostasis and tissue repair. The majority of tissue-resident stem cells are dormant but are activated by specific signals during injury and repair[12].

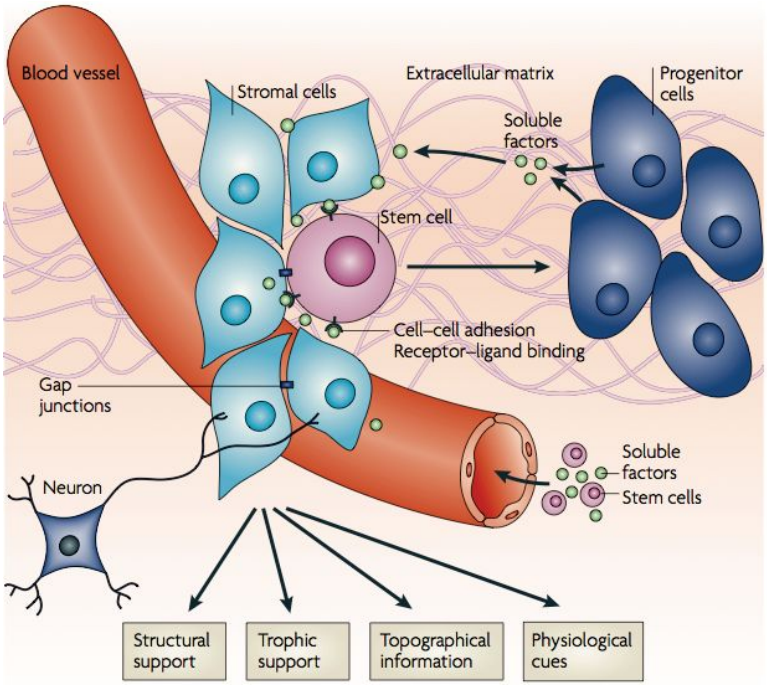

Figure 2.2 Schematic depict of the niche composition: *the stem cell itself, stromal cells, soluble factors, extracellular matrix, neural inputs, vascular network and cells adhesion components. It is important to note that, although many niche components are conserved, it is unlikely that every niche necessarily includes all of the components listed. Instead, niches are likely to incorporate a selection of these possible avenues for communication, specifically adapted to the particular functions of that niche, which might be to provide structural support, trophic support, topographical information and/or physiological cues.*
Taken from (Jones et. al, 2008)

The niche also controls the type of stem cell division[12]: **symmetrical cell division** results in identical daughter cells, which provides new cells to restitute damaged cells to following injury; it is important to underline that balance in stem cell homeostasis is required in order to avoid uncontrolled cell proliferation that causes hyperplasia or carcinogenesis, or a reduction in stem cells that would impair tissue repair. **Asymmetric division** occurs when a stem cell generates an identical daughter cell and a second differentiated daughter cell, allowing organ repair and regeneration while maintaining a population of stem cells.

Maintenance of a stem cell within the niche is influenced by[18]: a typical spatial localization, the anchorage of stem cells to supporting cells, the presence of a typical extracellular matrix and the integration of stimulatory as well as inhibitory signals.

Stem cells must retain their ability to self-renew in order to maintain tissue homeostasis, while they need to exit this self-renewal cycle and instead proliferate and differentiate when instructed by microenvironmental cues, including in response to tissue injury. This balance between self-renewal and proliferation and terminal differentiation is strictly regulated and its deregulation can have severe consequences, including cancer. Paradoxically, it has become evident in recent years that signaling pathways that induce stem cell proliferation may also be responsible for stem cell exhaustion and depletion. Indeed, when exposed to persistent proliferative signals, the stem cell compartment undergoes a transient amplification of the progenitor cell population, followed by a depletion of the tissue regenerative cells. Hence, it has been postulated that stem cells are endowed with a protective mechanism that results in

cell differentiation, death or senescence - the DDS response (fig. 2.3) - upon the aberrant stimulation of proliferative pathways, thereby preventing tumor progression[19].

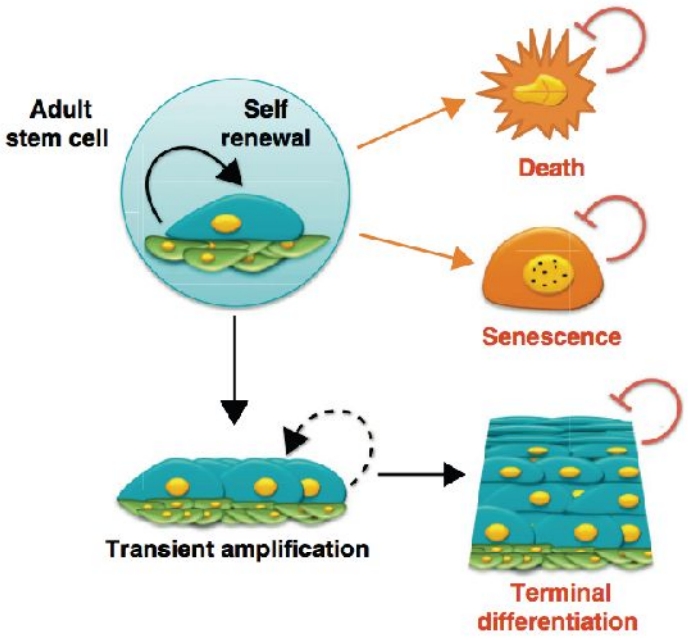

Figure 2.3 An exquisite balance between microenvironmental cues from the niche and cell autonomous signals is required to preserve the self-renewal and tissue regenerative capacity of stem cells. *Under physiological situations, stem cells undergo asymmetric cell division, thus self-renewing within their niche and generating daughter cells that proliferate rapidly, in a process known as transient amplification, followed by terminal differentiation. Environmental and intrinsic processes, including oncogenic stress, can cause stem cells to undergo cell death or senescence. The activation of cell differentiation, death or senescence programs results in the loss of proliferative potential of adult stem cells. The demise of stem cells may represent a natural protective barrier, preventing for example tumor formation. However, stem cell depletion may contribute to reduced tissue regenerative capacity and accelerated aging.*
Taken from (Iglesias-Bartolome et al., 2011)

However, stem cell depletion by the activation of the DDS response can contribute to reduced tissue regenerative capacity and accelerated aging. Hence, understanding the signaling circuitries (the most important of which are mTOR/Wnt, G-protein coupled receptors - GPCRs, Notch) regulating self-renewal capacity and DDS entry and escape within the stem/progenitor compartment might provide important insights into cancer initiation and a host of pathologies that involve the progressive loss of tissue-specific regenerating adult stem cells[19].

Among these signaling pathways is mTOR (mammalian Target of Rapamycin), which not only is important for its central role in cell growth and cancer progression, but an increase in its activity perturbs the ability of the whole organism to cope with stress, causing premature senescence and aging. Decreasing mTOR activity results in increased lifespan in multiple organisms, ranging from yeast, flies and worms, to mice[20]. The molecular mechanisms underlying this paradoxical contribution of mTOR to cancer growth while promoting stem cell senescence and reducing organismal life span are poorly understood. The hypothesis is that adult stem cells are prone to senescence in response to mTOR activation, thereby providing a mechanism protecting from malignant transformation of adult stem cells[19].

2.3 Stem cells and regenerative medicine

Regenerative medicine, built on emerging discoveries in stem cell biology, is defined as "the reconstruction of diseased or injured tissues by activation of endogenous cells or by cell transplantation"[11]. The role and contribution of stem cells in modern medicine is of paramount importance, both for their broad use in basic research and for the opportunities they give us to develop new therapeutic strategies in clinical practice. In addition, stem cells may be able to replace damaged tissues or even regenerate organs[12].

There are at least 3 essential requirements for practical use of stem cells in regenerative medicine: 1. the directed differentiation of stem cells to specific cell types (which is problematic to be reached in high percentages), 2. the achievement of high rates of cell survival after transplantation, and 3. the prevention of the occurrence of cancer or teratoma originated from implanted stem cells[21].

The scope of regenerative medicine was defined by Andre Terzic using the *"R^3" paradigm of therapeutic repair[22]: replacement, regeneration and rejuvenation,* integrated through the congruent "recycle", "restore" and "renew" processes. Replacement strategy refers to transplantation of a cell-based product that re-establishes homeostasis for the recipient through continuation of the tissue function from the donor; a significant limitation of this strategy remains the shortage of appropriate donors and the difficulty to match the immunological criteria for a safe and effective transplantation. Regenerative strategy refers to engraftment of progenitor cells that require *in vivo* growth and differentiation to establish recipient homeostasis through *de novo* function of the stem cell-based transplant. Last, rejuvenation strategy refers to self-renewal of tissues from endogenous, resident stem cells to maintain tissue homeostasis and promote tissue healing. This natural process of tissue recycling enables cells as they senesce to be replaced with younger cells that are inherently more resilient and equipped to provide adequate stress tolerance for tissue survival. Daughter cells can also be derived from reactivation of the cell cycle within mature cell types in response to (physio)-pathological stress. Rejuvenation ensures continuous production of renewable tissue required for long-term stress tolerance; however, most tissues are able to self-renew only partially. In the context of a massive acute injury, such as myocardial infarction, an inherent repair strategy results inadequate.

3- Dormant Stem Cells in the Adult Heart: Prospects for Self-Repair

3.1 The end of a dogma: the heart can self-renew

For centuries the heart has been considered as a static organ characterized by a large number of cardiomyocytes that are present at birth and live as long as the organism, without any form of cell turnover[23]. The paradigm that the heart is a post-mitotic organ incapable of regenerating parenchymal cells was established in the 1970s; this dogma has profoundly conditioned basic and clinical research in cardiology for the last 3 decades[24].

Two main clinical observations served as the basis for the old paradigm that the heart is a post-mitotic organ: 1. failure to observe mitotic figures in cardiac myocytes of tissue sections, and 2. rare observation of the occurrence of primary tumors arising from the myocardium in the adult mammalian heart[25]. Moreover, the formation of a fibrotic scar after an acute myocardial infarction and the lack of the complete regeneration (*restitutio ad integrum*) of the damaged tissue, strongly supported this thought. Since then, there has been a slow but steady reconsideration of this paradigm after a series of reports on the presence of cardiomyocyte renewal in the adult mammalian heart.

The main milestone in this paradigm shift was the demonstration of the intense myocyte proliferation that occurs, in human hearts, both acutely post-MI[26] and in cardiac hypertrophy secondary to aortic stenosis[27].

More recently, the quantification of the cardiomyocyte turnover making use of recent techniques as radiocarbon dating[28] or combining morphometric data with mathematical models[29], further enhanced the concept of cardiomyocytes turnover.

3.2 Cardiomyocytes and primitive cells renew the heart during life

Once accepted that cardiac myocytes could be generated postnatally, the next fundamental question that was addressed by the scientific community regarded the origin (still highly debated) of these renewing myocytes. Two alternative, but not mutually exclusive, possibilities were put forward: either a class of non terminally differentiated myocytes could persist in human hearts, or newly formed myocytes could arise from stem/progenitor cells[30].

In 2002, Quaini and colleagues[31] performed a study on the chimerism of transplanted hearts at the aim to verify if the origin of the proliferating cardiac myocytes was represented by non-terminally differentiated myocytes or primitive cells capable of migration, proliferation and

differentiation within the myocardium. In particular, female donor hearts implanted in male recipients showed a significant increase in cardiomyocyte and coronary vessel cells positive for the Y chromosome. This finding was the proof that male cells, coming from atria, colonized the heart and underwent a differentiation process in myocytes, endothelial and vascular smooth muscle cells. Moreover, primitive cells positive for the markers c-Kit, Sca1-like and MDR-1, of both donor and recipient origin, have been identified within the hearts. Identical cells have been identified also in control human hearts.

A completely analog study was carried out by Müller and Colleagues[32] during the same year. The study gave results similar to the previous cited: cardiomyocytes of male origin were identified in female hearts implanted in male recipients.

These early studies demonstrated that both poorly differentiated cells, expressing stem cell markers, and fully mature cells of recipient origin could be identified within transplanted hearts. This finding was regarded as the first indirect indication of the possible existence of cardiac resident stem cells[30]. Since c-Kit$^+$ cells, during the fetal life, colonize several organs expressing the Stem Cell Factor (SCF, the ligand of c-Kit receptor), it seems possible that also in the heart these primitive cells reside within the organ since the fetal life[33]. Moreover, the discovery of the rapid induction of SCF during a cardiac ischemia corroborates the hypothesis of the involvement of SCF in resident cardiac stem cells activation[33].

The unequivocal existence of the presence of cardiac stem cells in the mammalian heart is dated in 2003, when Beltrami and colleagues[34] discovered a population of c-Kit$^+$ Lin$^-$ cells endowed with the characteristics of cardiac stem cells (CSCs) in the rat heart. These cells were multipotent, clonogenic and self-renewing; both *in vivo* and *in vitro* they were able to originate cardiomyocytes, endothelial and vascular smooth muscle cells. When injected within an ischemic heart, CSCs were able to engraft, migrate and proliferate, giving origin to different cardiovascular cell types; the result was the formation of new blood vessels and myocytes that, contributing to the regeneration of part of the infarcted left ventricle, improved the cardiac function of the animals.

Two years later, the same group published a work that furthermore clarified how CSCs are organized and localized within the mammalian hearts[35]. The authors highlighted that cardiac niches contain both CSCs and lineage-committed cells, which are connected to supporting cells represented by myocytes and fibroblasts. Connexins and cadherins form gap and adherens junctions at the interface of CSCs-lineage-committed and supporting cells.

In 2007, always the group of Professor Anversa isolated, for the first time, CSCs from small biopsies of human myocardium[36], endowed with the same characteristics and potency of the rodent CSCs.

In the same year Hsieh et al.[37], to further address the question about the origin of the replicating myocytes, designed a genetic lineage tracing experiment that for the first time shed light on the cellular homeostasis that governs cardiomyocyte renewal. In a double transgenic MerCreMer/ZEG^{-} inducible cardiomyocyte reporter mouse, a tamoxifen-induced pulse caused an irreversible genetic switch - only in the cardiac myocytes - from β-galactosidase (β-gal) to the expression of GFP - green fluorescent protein (fig. 3.1). Hence, if during the chase any GFP^{-} stem or progenitor cells would form new myocytes, they would still express β-galactosidase. Two major findings emerged from this landmark report: 1. various models of myocardial injury (myocardial infarction model and chronic pressure overload) resulted in a significant increase in GFP-β-gal^{+} cardiac myocytes and a corresponding decrease in GFP$^{+}\beta$-gal^{-} cardiac myocytes, suggesting the formation of new cardiomyocytes from stem and progenitor cells, and 2. at the opposite, during normal aging of the rodent heart there was no decrease in GFP$^{+}\beta$-gal^{-} cardiac myocytes, suggesting an absence of stem cell-based physiologic cardiomyocyte renewal.

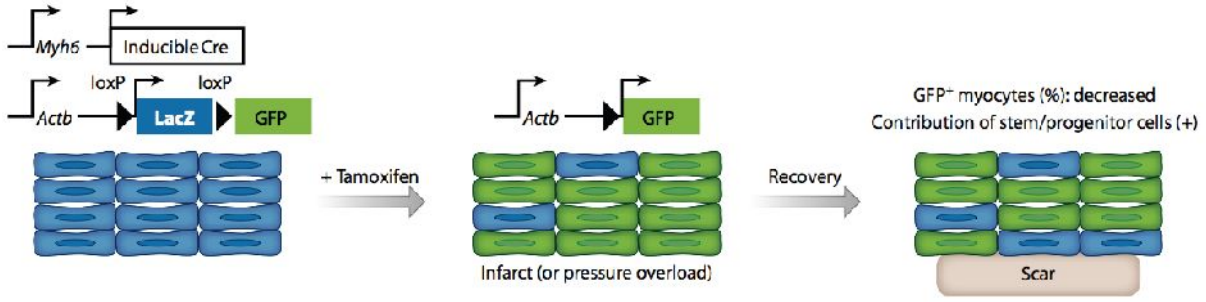

Figure 3.1 Origin of regenerating cardiomyocytes. *Fate-mapping experiments were performed in the adult mouse heart with an inducible GFP reporter (MerCreMer/ZEG^{-} mice). In pathological conditions (myocardial infarction and pressure overload) the formation of new cardiomyocytes from stem and progenitor cells (depicted in blue) is the prevalent process of regeneration. Reproduced from (Kikuchi et al., 2012)*

A very recent work[38] from the same Lee's group, that is in partial contradiction with the previously cited one[37], brought to light that, upon induction of MI, there is a high rate of cardiomyocyte turnover in the adult mammalian heart that originates from pre-existing GFP^{-} cardiac myocytes rather than non cardiomyocytes. The Authors calculated that, in young adult hearts, cardiac myocytes are replaced by proliferation of dedifferentiated pre-existing cardiac myocytes at an annual rate of 0.76%.

Always in the last year, a work from Marbàn's group[39] showed that new cardiac myocytes not only arise from pre-existing cardiac myocytes but also from stem/progenitor cells following MI. In line with previous reports, cardiomyocyte turnover predominantly occurs through proliferation of pre-existing cardiac myocytes at an annual rate of 1.3%-4% during normal aging.

Taken together, it seems that the mammalian heart appears to rely on two mechanisms for endogenous regeneration. The first source of stem/progenitor cells that upon differentiation and maturation reconstitute the lost cardiac myocytes as occurs in injury[31; 32; 34; 36; 37; 39] and second, the proliferation of dedifferentiated cardiac myocytes that can re-enter the cell cycle and can give rise to mononucleated, newly formed cardiac myocytes[38; 39]. To date, the debate on which one of the mechanisms is the prevalent in the adult hearts is still opened.

3.3 Resident Cardiac Stem Cells (CSCs) in the adult heart

Although primitive cells not residing in the heart, like bone marrow derived stem cells[40; 41; 42], can migrate to the heart, engraft and differentiate in cardiac cell types, contributing to the organ regeneration, stem cell scientists widely consider resident Cardiac Stem Cells the main cell type responsible for cardiac regeneration.

Piero Anversa and collaborators[24] defined Cardiac Stem Cells as undifferentiated, lineage-negative (LIN^-) cells - characterized by the absence of lineage-specific markers - that possess a high growth potential. At the single-cell level, CSCs are self-renewing, clonogenic and capable of differentiating in mature progenies *in vitro* and *in vivo* (fig. 3.2).

Phenotypically, CSCs share on their membranes, in different proportions, the stem cell-related antigens[24]:

- **c-Kit**: Stem Cell Factor receptor,
- **MDR1**: Multi-Drug Resistance 1 (receptor which belongs to the class of ABC transporters that mediate the Hoechst dye efflux from the cell),
- **Sca-1**: Stem cell antigen-1, in the murine heart; in the human heart an antigen similar to Sca-1, called *Sca-1-like,* has been more recently discovered, but it is still unknown.

In their undifferentiated state, CSCs express low levels of pluripotency markers such as OCT3/4, SOX2 and NANOG (fig. 3.3)[43].

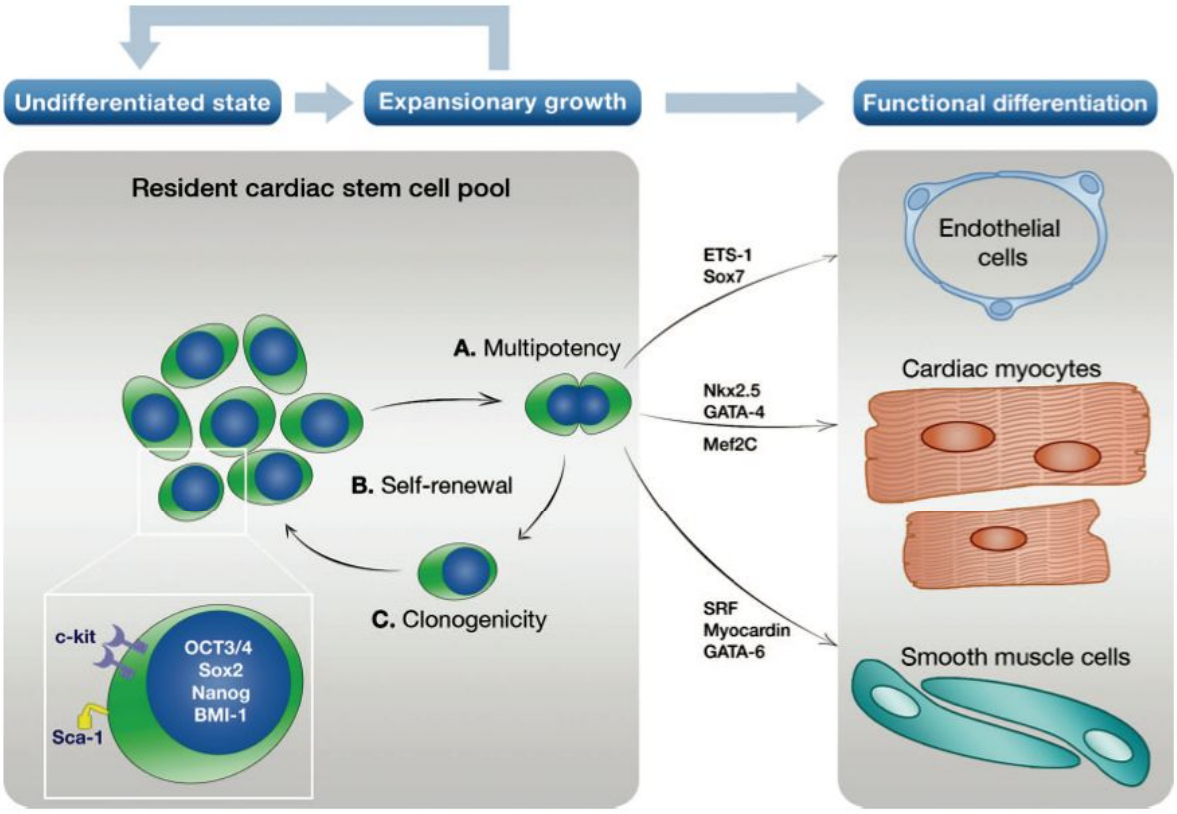

Figure 3.2 Cardiac stem/progenitor cell-based regeneration in the adult mammalian heart. *Cardiac stem/progenitor cells are multipotent (A), self-renewing (B), and clonogenic (C). In their undifferentiated state, CSCs express low levels of pluripotency markers such as OCT3/4, Sox2 and Nanog (see inset). The majority of CSCs also express key regulators such as BMI-1 that controls cell cycle inhibitors P19 and P21 to maintain and regulate their ability to proliferate. Once activated, CSCs can re-enter the cell cycle and subsequently can give rise to progeny that both maintain their own pool of undifferentiated stem cells and mature into three different lineages (endothelial cells, cardiac myocytes and vascular smooth muscle cells) under the influence of various lineage-specific transcription factors. Taken from (Koudstaal et al., 2013)*

The model by Anversa's group proposes a hierarchical classification of cardiac immature cells into 4 classes[24]:

1. ***cardiac stem cells****:* cell expressing stem cell antigens but lineage negative;
2. ***progenitors****:* cells expressing stem cell antigens and transcription factors of cardiac cells but that do not exhibit specific cytoplasmic proteins;
3. ***precursors****:* cells that possess stem cell antigens, transcription factors and membrane and cytoplasmic proteins typical of myocytes, smooth muscle cells (SMCs) and endothelial cells (ECs);
4. ***amplifying cells***: cells that proliferate before undergoing the complete mature differentiation in cardiomyocytes, SMCs and ECs.

These cell types can be viewed as subsequent steps in the progressive evolution from a more primitive (cardiac stem cell) to a more differentiated phenotype (amplifying cell). The first 3 cell types express c-Kit, MDR1, and Sca-1, whereas the last type no longer expresses these antigens. These cell categories can be identified in isolated cardiac cell preparations or in sections of atrial and ventricular myocardium[24].

Cardiac stem cells in the mammalian heart are organized in niches (fig. 3.3), protected areas exposed to low levels of hemodynamic stress, which are prevalently located in the atria and apex and consist of differentiated myocytes that surround clusters of CSCs and highly dividing amplifying cells. The interaction among CSCs, early committed cells and supporting cells - myocytes and fibroblasts - occurs via junctional proteins (cadherins and connexins)[33].

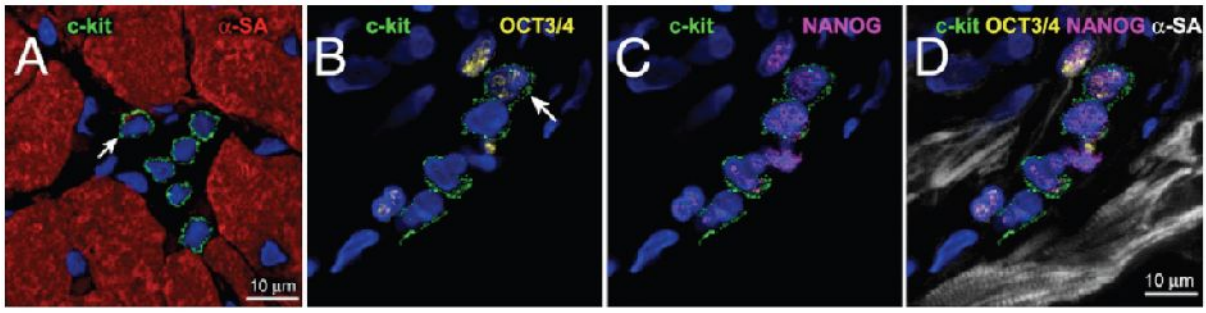

Figure 3.3 c-Kit⁺ stem cells niches in the normal human heart. ***A:*** *cluster of c-Kit⁺ cells (green). The cell indicated by arrow is a myocyte precursor, as we deduce by the expression of the contractile protein α-sarcomeric actin (α-SA, in red).* ***B–D:*** *c-Kit⁺ cells positive for OCT3/4 (yellow, indicated by arrow in B) and for NANOG (magenta). Myocytes are labeled by α-SA (white).*
Taken from (Cesselli et al., 2011)

The environment of the right atrial niches has the ability to maintain adult human CSCs in an undifferentiated state. Cell dynamics within the niches are tightly regulated; although new cardiomyocytes are continuously formed, the number of CSCs within the niches remains constant in the heart in a steady state. The myocardial niche maintains a significant level of developmental plasticity also in the diseased heart[44]. Niches in the senescent failing organ retain the ability to sense cell injury in the tissue of residence, and they respond to these needs by increasing the number of dividing CSCs[45]. Although prolonged pathological states alter the niche microenvironment and/or progenitor cells, CSCs can be longer collected from diseased myocardial samples[44].

Debates nowadays continue regarding the origin of CSCs: it is still unclear if these cells persist in the organ since birth[33] or if they colonize the heart only in a successive period[46].

Different classes of CSCs have been identified by various Authors on the basis of the different surface markers expression or cell localization (tab. 3.1); however, whether these cells represent different subsets of a common progenitor pool, or whether these populations partially overlap at certain cardiac developmental stages, remains unclear[47].

More recently Wu's group[48] performed an analysis of microarray based transcriptional profiling of 3 classes of rodent CSCs: c-Kit⁺, Sca-1⁺ and SP (*side-population*) cells, in the attempt to answer to the question if they are distinct categories of undifferentiated cells with diverse functional behavior, or whether they represent different phenotypic stages of the same cell

population. Comparison of the cells indicated that the c-Kit$^+$ population is most distinct and least correlated with Sca-1$^+$ and SP progenitors. While cardiac c-Kit$^+$ cells appear to be the most undifferentiated, the Sca-1$^+$ cells appear to be the most committed to differentiation, given their transcriptional similarity with cardiomyocytes. By comparison, cardiac SP appears to be intermediate between the cardiac c-Kit$^+$ and Sca-1$^+$ cells. Importantly, SP shares Sca-1 antigen, whereas neither of these two populations share the c-Kit surface marker, indicating a closer relationship between SP and Sca-1$^+$ cells. Hence, based on these study, the Authors believe that the cardiac c-Kit$^+$, Sca-1$^+$ and SP represent three distinct cell populations functioning at different levels of commitment to differentiation. However, in order to firmly establish whether the cell of origin for cardiac Sca-1$^+$ and SP is the c-Kit$^+$ cell, *in vivo* lineage tracing studies must be performed[48].

3.3.1 c-Kit$^+$ cardiac stem cells

The most extensively studied CSCs are based on the presence of the cell membrane c-Kit receptor. c-Kit, the receptor for stem cell factor (SCF), is expressed in a wide range of primitive cells, including hematopoietic stem cells, primordial germ cells, embryonic stem cells and melanoblasts. In the hematopoietic system, c-Kit is critical for proliferation, survival and differentiation. The activation of PI-3 (phosphoinositide-3) kinase, upon ligand binding of c-Kit, followed by recruitment of PKB (protein kinase B, also known as AKT) to the plasma membrane where PKB is activated, has been suggested to be an anti-apoptotic pathway and to be essential in regulating stem cell renewal[49].

c-Kit$^+$ CSCs, identified for the first time in 2003 from the Anversa's group in rodents, are characterized by the absence of lineage-specific markers (Lin$^-$) and possess the fundamental properties of stem cells: they are self-renewing, clonogenic and multipotent *in vitro* and *in vivo*; they give rise to cardiomyocytes, endothelial and smooth muscle cells; when injected into infarcted rat hearts, c-Kit$^+$ cells contributed to myocardial regeneration in the absence of cell fusion. In murine myocardium, c-Kit$^+$ Lin$^-$ cells have been identified at a frequency of about one cell per 10^4 myocytes[34].

In 2005, the *in vivo* potential of c-Kit$^+$ CSCs was further demonstrated by Dawn et al[50] showing that a few GFP$^+$ c-Kit$^+$ CSCs had formed GFP$^+$ cardiac myocytes in the infarcted myocardium in rats.

CSCs were subsequently identified also in human hearts. c-Kit$^+$ cells, isolated from small samples of myocardium, displayed the fundamental properties of stem cells *in vitro* (self-renewal, clonogenicity and multipotency) together with the ability to form arterioles, capillaries and cardiac myocytes when locally injected in the infarcted myocardium of immuno-compromised rodents; importantly, c-Kit$^+$ cells differentiated into functionally competent beating cardiomyocytes, without cell fusion[36].

In a very recently published work, Georgina Allison[51] and collaborators furthermore demonstrated the regenerative potential of c-Kit$^+$ CSCs. Employing experimental protocols of severe diffuse myocardial damage which, unlike an experimental infarct, spares the CSCs[52], in combination with several genetic murine models and cell transplantation approaches, the Authors demonstrated that c-Kit$^+$ CSCs are necessary and sufficient for myocyte regeneration, leading to complete cellular, anatomical, and functional myocardial recovery[51].

As regards the developmental origin of c-Kit$^+$ CSCs, it has been shown that among Nkx2.5$^+$ cells isolated from *in vitro* differentiated murine embryonic stem cells, c-Kit is the marker that allows isolating the most multipotent and clonogenic cells[53]. 28% of Nkx2.5$^+$ cells expressed c-Kit; these cells possessed the capacity for long-term *in vitro* expansion and differentiation into both cardiomyocytes and smooth muscle cells from a single cell. Moreover, c-Kit$^+$ Nkx2.5$^+$ cells from mouse embryos were capable of bipotential differentiation *in vivo*. Other experiments have demonstrated that c-Kit$^+$ cells colonize the heart during development, peak in the perinatal period and decline with age. Studies of developmental expression of c-Kit in myocardium of c-Kit-GFP transgenic mice, both in immunofluorescence microscopy and immunoblot analyses, showed that c-Kit$^+$ cells were highest 2 days and 1 week post-birth and then significantly decreased in 2- and 10-week-old hearts[46].

Table 3.1 Resident stem and progenitor cells in the mammalian heart

Cardiac Stem Cell class	stem cell molecular markers		species	source		stemness criteria	cardiac myocytes formation *in vitro*	cardiac myocytes formation *in vivo*	references *(make reference to Bibliography Table 3.1)*
	positive	negative		fetal/ neonatal	adult				
c-Kit	c-Kit, Sca-1, MDR-1, CD90	CD34, CD45	human, mouse, rat, dog, pig	yes	yes	multipotent, clonogenic, self-renewing	yes	yes	(Beltrami et al. 2003) (Dawn et al. 2005) (Bearzi et al. 2007) (Simpson et al. 2012) (Ellison et al. 2013)
Sca-1	Sca-1, c-Kit, CD105, CD31, CD90	CD14, CD34, CD45	mouse, human (Sca-1-like)	yes	yes	multipotent, clonogenic, self-renewing	yes	yes	(Oh et al. 2003) (Goumans et al. 2007) (Smits et al. 2009) (Wang et al. 2006)
Cardiospheres	c-Kit, Sca-1, Flk1, CD105, CD90, CD34, CD31	MDR-1, CD45, CD133	human, mouse, rat, pig	yes	yes	multipotent, clonogenic, self-renewing	yes	yes	(Johnston et al. 2009) (Smith et al. 2007) (Messina et al. 2004) (Makkar et al. 2012) (Chimenti et al. 2010)
Side Population (SP) cells	Abcg2, Sca-1, MDR-1, CD133	c-Kit, CD31, CD34, CD45	mouse, rat	yes	yes	multipotent, self-renewing, *not clonogenic*	yes	yes	(Martin et al. 2004) (Hierlihy et al. 2002) (Liang et al. 2011) (Oyama et al. 2007) (Mouquet et al. 2005)
Islet-1	Islet-1	Sca-1, c-Kit, CD31	human, mouse, rat	yes	No	multipotent, clonogenic, self-renewing	yes	yes	(Laugwitz et al. 2005) (Cai et al. 2003) (Moretti et al. 2006)
Flk1 (KDR or VEGFR2)	Flk1, islet-1, CD31, c-Kit	E-cadherin	human, mouse	yes	yes	multipotent, clonogenic, self-renewing	yes	yes	(Yamashita et al. 2005) (Kattman et al. 2006) (Bearzi et al. 2009) (Baba et al. 2007)
SSEA-1	SSEA-1, MHC	c-Kit, Sca-1	rat	yes	yes	multipotent	yes	yes	(Ott et al. 2007)
Epicardial cells	Wt1, Islet-1, Tbx18, c-Kit, CD34	CD45	mouse, human	yes	yes	multipotent	yes	predicted	(Martin-Puig et al. 2008) (Zhou et al. 2008) (Cai et al. 2008) (Limana et al. 2007)

3.4 Clinical trials employing Cardiac Stem Cells

Two novel strategies have been proposed for CSCs-based myocardial repair: 1. activation of endogenous CSCs by various means, like growth factors, non-cardiac stem cells or gene therapy; activated endogenous CSCs can proliferate and mature into newly formed cardiac myocytes; 2. delivery of autologous CSCs that have been isolated from small myocardial biopsies and scaled up outside the patient to sufficient numbers. In addition, exogenous CSCs are capable of activating the local endogenous CSCs compartment and are hypothesized to mature and differentiate into functional cardiac myocytes that are electromechanically coupled with the pre-existing cardiac myocytes[54].

An impressive array of preclinical studies performed in multiple species has demonstrated that injection of CSCs into animal models with ischemic cardiomyopathy slows the progression of LV remodeling and improves left ventricular (LV) function. The promising preclinical studies coupled with technologic advancements facilitating isolation and *ex vivo* amplification of autologous c-Kit$^+$ CSCs from heart biopsies of atrium or right ventricular septum set the stage for translational advancement of this field.

Bolli and colleagues built on the promising preclinical results and conducted a first-in-human clinical trial testing the therapeutic potential of cardiac c-Kit$^+$ CSCs. The SCIPIO (*Cardiac Stem cell Infusion in Patients with Ischemic Cardiomyopathy*) trial[55; 56] was the first randomized phase I study using c-Kit$^+$ Lin$^-$ autologous CSCs in patients with LV dysfunction (EF<40%). The CSCs were extracted from right atrial surgical appendage biopsies obtained during coronary artery bypass graft (CABG) surgery, and patients were treated with a single dose intracoronary injection of CSCs at approximately 4 months after surgery. At the 4-month time point, 20 patients who had received CSCs therapy demonstrated, when evaluated by a 3-dimensional echocardiography, an increase in LVEF from a baseline of 29.0±1.7% to 36.0±2.5% (P<0.001). Additionally, these patients also had an improvement in regional wall motion score in all segments assessed by echocardiography. This phase I trial established the safety profile of CSCs as no adverse effects were reported up to 2 years after therapy. Additionally, it demonstrated that interventions with autologous CSCs in patients with ischemic cardiomyopathy have a promising and beneficial impact that continued to increase until the 2-year follow-up time point.

The other important in-human clinical trial testing the therapeutic potential of CSCs is CADUCEUS[57] (*Cardiosphere-Derived Autologous Stem Cells to Reverse VentricUlar Dysfunction*), performed by Makkar and collaborators and employing cardiospheres.

As initially described by Messina et al.[58], under appropriate culture conditions, cells outgrow from pieces of myocardial tissue and, once expanded, form floating clusters of cells that can be expanded *in vitro* (cardiospheres). These floating spheres form in nonadhesive substrates.

Essentially, they are a conglomerate of both early-stage committed and primitive cells that in earlier descriptions contained a central core of c-Kit$^+$ stem cells (15%), layers of differentiating cells, and an outside cell layer of mesenchymal stromal cells. The presence of connexin-43 and gap junctions between undifferentiated and differentiated cells plays a crucial role in the proliferation of the undifferentiated lineage and also functions as an avenue for electrical coupling in cells committed to forming myocytes. These findings have led to the proposal that cardiospheres could potentially recapitulate cardiac niche biology in the *in vitro* environment.
CADUCEUS[57] is the first randomized prospective phase I trial that assessed the safety of intracoronary administration of autologous CDC (Cardiosphere-Derived Cells, cells derived from the disaggregation of cardiospheres and cultured in monolayer[59]) to 31 patients 1.5 to 3 months after an MI. The Authors demonstrated that the use of autologous CDC after MI was safe. There was no significant difference in end-diastolic volume and end-systolic volume seen in either the CDC or control groups. However, compared to the control group of patients, those treated with CDC showed increase in viable myocardium, regional contractility, and reductions in scar mass at the 6- and 12-month time point.

3.5 How do exogenous injected cells act in repairing the heart?

The clinical trials and the preclinical experiments using animal models outlined above were originally initiated with the aims of true cardiac regeneration. It was hypothesized that supplementation of the diseased heart with the correct type of cells would rectify the deficiency in numbers. However, several animal studies have shown that a significant muscle regeneration does not happen. Despite this, many studies have measured improvements in failing hearts. Even at the level of individual cardiomyocytes substantial functional changes can be demonstrated. The numerous clinical trials have suggested that a modest functional benefit might exist. However, for inherent limitations, clinical studies have not been able to follow the fate of the cells injected into human hearts. The demonstration that the functional characteristics of a diseased myocardium can be altered by cell therapy even in the absence of an obvious generation of new myocytes by donated cells (the studies mentioned so far suggest that at least some types of cell therapy are likely to improve cardiac function in chronic HF) has resulted in a search for alternative mechanisms of action. Although the mechanism(s) responsible for these beneficial effects is still unknown, different hypotheses have been proposed[10; 60] (fig. 3.4).

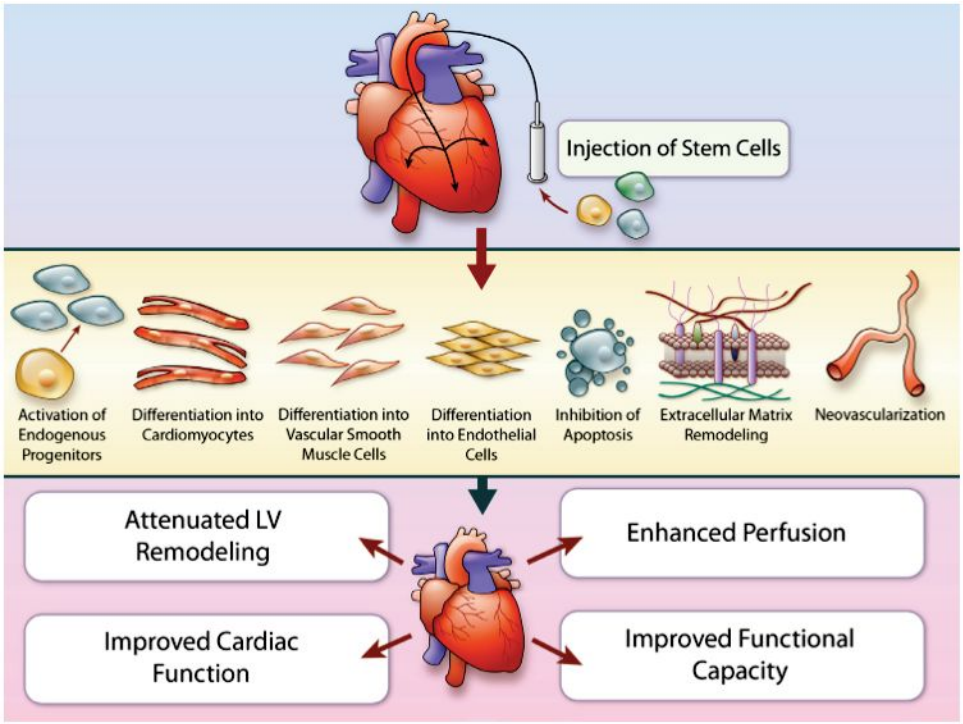

Figure 3.4 ***Potential mechanisms of action of stem cells.***
Implantation of stem cells in the injured heart initiates myocardial repair via several direct and indirect mechanisms: activation of endogenous precursors, differentiation into cardiac and vascular cells, promotion of neovascularization, favorable modulation of the extracellular matrix and inhibition of apoptosis. Together, these events reduce adverse cardiac remodeling and hypertrophy, increase perfusion and improve cardiac function, leading to improvement in clinical status. Taken from (Sanganalmath & Bolli 2013)

I. (Trans)differentiation of transplanted cells into cardiac cells

Although this may seem the most obvious explanation for the positive effects of stem cells, the evidence obtained so far does not support (trans)differentiation of transplanted cells as the only, or even the major, mechanism of action[10]. CSCs, when transplanted in injured hearts, give rise to vascular cells and to cells that express myocyte-specific proteins (although these cells are usually small and do not resemble adult myocytes). In some studies, particularly in models of acute MI, the magnitude of this regenerative process has been found to be substantial, but in a rat[61] and pig[62] model of chronic post-MI HF, differentiation of transplanted CSCs into myocytes or myocyte-like cells was quantitatively insufficient to account for the improvement in LV function. In the case of allogenic CDC transplantation in infarcted rat hearts[63], differentiation into cardiac cells has been reported to be either a minor mechanism of action or nonexistent[10].

II. Formation of new blood vessels from transplanted cells

Differentiation of transplanted cells into new blood vessels has been reported with various cells (mesenchymal stem cells, adipose-derived cells, $CD34^+$ cells and CSCs). This hypothesis relates to both acute myocardial infarction and chronic ischaemia and states that injected cells contribute towards the increased formation of collateral blood vessels[10; 60].

III. Cell fusion

In 2004, two works by Murry et al.[64] and Balsam et al.[65] proposed spontaneous cell fusion as an alternative mechanism by which transplanted bone marrow cells produce apparent regeneration of various adult tissues. Subsequent studies[66] from Anversa's group, however, concluded that c-Kit$^+$ bone marrow cells differentiated into myocytes and coronary vessels independent of cell fusion. The notion that cell fusion is an important mechanism underlying the positive effects of stem cells has lost support in recent years.

IV. Paracrine mechanisms

The inability to explain the salutary effects of transplanted stem cells on the basis of their differentiation has led to the paracrine hypothesis, widely defined by Gnecchi and collaborators[67]. For paracrine mechanism we intend the concept that transplanted cells induce myocardial repair by releasing signals (cytokines, chemokines, growth factors, possibly miRNA, exosomes or microparticles) within the surrounding tissue, which in turn promote a number of restorative processes including activation of endogenous CSCs, neovascularization, inhibition of apoptosis, inhibition of hypertrophy, and favorable alterations of the extracellular matrix (ECM). Collectively, these actions result in enhanced LV function, improved perfusion and myocardial repair[67].

- *Activation of endogenous CSCs*[10]: injected exogenous cells secrete growth factors (such as hepatocyte growth factor - HGF - and insulin growth factor-1 - IGF-1) that stimulate endogenous CSCs to migrate through the myocardial interstitium, proliferate and differentiate into myocytes and vascular structures.
- *Induction of neovascularization*[10]: many stem cells can induce neovascularization by secreting chemokines (stromal cell–derived factor-1 - SDF-1) and pro-angiogenic factors (vascular endothelial growth factor - VEGF -, basic fibroblast growth factor - bFGF -, hepatocyte growth factor - HGF -, insulin growth factor-1 - IGF-1 -, tissue growth factor β - TGFβ -, and angiopoietin-1). The resulting neovascularization may improve blood supply to the viable cells that remain in the infarcted region and thus improve cardiac function.
- *Inhibition of apoptosis*[10]: paracrine factors (such as IGF-1) released by stem cells after transplantation inhibit cardiomyocyte death by apoptosis.
- *Inhibition of hypertrophy*[10]: administration of stem cells in models of HF is associated with a reduction in the hypertrophic response of surviving myocytes.
- *Remodeling of the extracellular matrix (ECM)*. In body tissues, ECM formation and digestion and maintenance of optimal tissue structure are related to the fine balance between the activities of matrix metalloproteinases (MMPs) and tissue inhibitors of metalloproteinases (TIMPs). Pathological ventricular remodeling involves maladaptive changes in the ECM, which

leads to further myocardial deterioration. A net increase in ECM leads to interstitial fibrosis, and although this can be useful in limiting ventricular enlargement, it also decreases tissue compliance and adversely affects systolic and diastolic performance[60]. Stem cells can modulate various constituents of the ECM, thereby limiting infarct expansion, LV remodeling, and myocardial fibrosis. The importance of ECM alterations in CSCs-dependent repair is underscored by the findings of Rota et al.[68], who reported that CSCs increased MMP-2, MMP-9 and MMP-14 levels and decreased tissue inhibitors of MMP-4 levels in a rat model of post-MI HF.

4- Cellular Senescence

4.1 What is cellular senescence?

Cellular senescence is a specialized form of growth arrest, confined to mitotic cells, induced by various stressful stimuli and characterized by several, although not specific, markers[69].

Cellular senescence was formally described in 1965, when Hayflick showed that human fibroblasts had a limited ability to proliferate in culture despite the presence of ample space, nutrients and growth factors in the medium; non-dividing cells remained viable for many weeks but failed to grow[70]. This observation was interpreted in two different ways: 1. it could be a protective mechanism against cancer, a major life-threatening disease, or 2. it could represent the explanation for aging (loss of regenerative ability) of cells *in vivo*. In this latter case, cell senescence was considered deleterious because it contributes to decrements in tissue renewal and function[71].

Cell senescence may also be broadly viewed as a complex cell response to a variety of stressors, that includes, but is not limited to, growth arrest. Consistently, a response similar to cell senescence has been observed in terminally differentiated cells and has been named senescence after differentiation (**SAD**)[72].

4.1.1 What defines a senescent cell?

Senescent cells display several phenotypes which, all together, define the senescent state (fig. 4.1)[73].

Senescent cells arrest growth usually with a DNA content that is typical of G_1 phase, yet they remain metabolically active. Once arrested, they fail to initiate DNA replication despite adequate growth conditions. This replication failure is primarily caused by the expression of dominant cell-cycle inhibitors (see below). In contrast to quiescence, the senescence growth arrest is essentially permanent (in the absence of experimental manipulation) because senescent cells cannot be stimulated to proliferate by known physiological stimuli[71]. Senescent cells increase in size, sometimes enlarging more than two-fold relative to the size of non-senescent counterparts[70]; they usually express a senescence-associated β-galactosidase (**SA-β-gal**)[73].

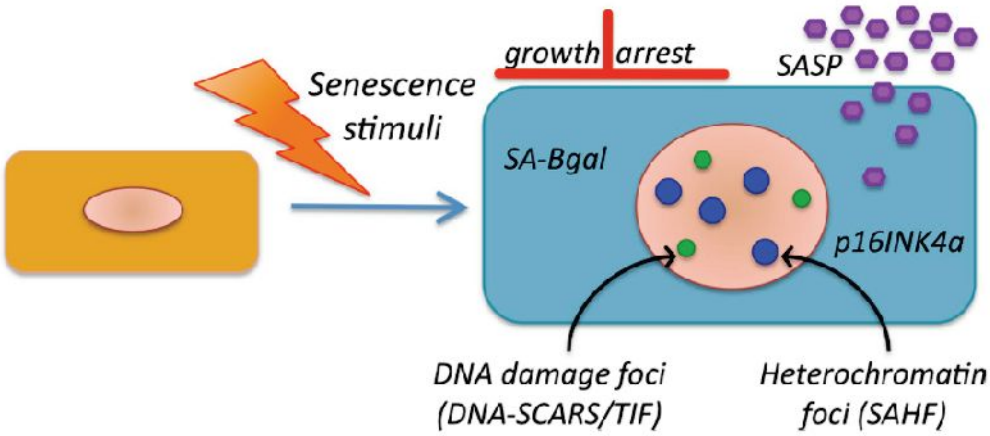

Figure 4.1 Characteristics of senescent cells. *Senescent cells differ from other non-dividing (quiescent, terminally differentiated) cells in several ways, although no single feature of the senescent phenotype is exclusively specific. Characteristics of senescent cells include an essentially irreversible growth arrest, expression of SA-βgal and p16^{INK4a}, robust secretion of numerous growth factors, cytokines, proteases and other proteins (SASP), and nuclear foci containing DDR proteins (DNA-SCARS/TIF) or heterochromatin (SAHF). Taken from (Rodier & Campisi 2011)*

Senescent cells are resistant to apoptosis. This latter is an extreme response to cellular stress and an important tumor-suppressive mechanism. But, whereas senescence prevents the growth of damaged or stressed cells, apoptosis quickly eliminates them. Many cell types acquire resistance to certain apoptotic signals when they become senescent. Resistance to apoptosis might partly explain why senescent cells are so stable in culture. This attribute might also explain why the number of senescent cells increases with age[71].

Although diverse stimuli can induce a senescence response, they appear to converge on either or both of two pathways that establish and maintain the senescence growth arrest. These pathways are governed by the gatekeeper tumor suppressor proteins p53 and pRB. Both these proteins are transcriptional regulators, and each lies at the heart of a pathway that includes a plethora of upstream regulators and downstream effectors[74].

Most of senescent cells express the cyclin-dependent kinase inhibitor (CDKI) **p16^{INK4a}**, a tumor suppressor which is not commonly expressed by quiescent or terminally differentiated cells. In some cells p16^{INK4a}, by activating the pRB tumor suppressor, causes the formation of senescence-associated heterochromatin foci (**SAHF**)[75], which silence critical pro-proliferative genes[76]. p16^{INK4a} is induced by culture stress and as a late response to telomeric or intra-chromosomal DNA damage. Moreover, p16^{INK4a} expression increases with age in mice and humans, and its activity has been functionally linked to the reduction in progenitor cell number that occurs in multiple tissues during aging[73]. Other CDKIs often expressed by senescent cells are p53 and p21[71].

Cells that senesce with persistent DNA damage response (**DDR**) signaling harbor persistent nuclear foci, termed DNA segments with chromatin alterations reinforcing senescence (**DNA-SCARS**). These foci contain activated DDR proteins, including phospho-ATM (ataxia

telangiectasia mutated protein), and are distinguishable from transient damage foci. DNA-SCARS include dysfunctional telomeres or telomere dysfunction-induced foci (**TIF**)[71]. Senescent cells with persistent DDR signaling secrete growth factors, proteases, cytokines and other factors that have potent autocrine and paracrine activities. This senescence-associated secretory phenotype (**SASP**) helps to explain some of the biological activities of senescent cells[77].

4.1.2 Mechanisms responsible for cell senescence

Several senescence-inducing stimuli have been identified. The limited growth of human cells in culture is due in part to telomere erosion, the gradual loss of DNA at the ends of the chromosomes (telomeres). Most cells do not express telomerase, the specialized enzyme that can restore telomeric DNA sequences *de novo*. DNA double strand breaks are especially potent senescence inducers. Eroded telomeres generate a persistent DNA damage response (DDR), which initiates and maintains the senescence growth arrest[78]. Many senescent cells harbor genomic damage at non-telomeric sites, which also generate the persistent DDR signaling needed for the senescence growth arrest[79].

Senescence can also occur, however, without detectable DDR signaling. Culture stress causes a senescence arrest without significant telomere erosion[80]. These stresses could include inappropriate substrata (e.g. tissue culture plastic), serum (most cells experience plasma, not serum, *in vivo*) and oxidative stress.

Intrinsic and extrinsic mechanisms have been identified as responsible for cell senescence; they have been reviewed in[81; 82] and summarized as follows.

Intrinsic inductors of cell senescence[81] act inside the cells and are represented by:

a. either the progressive telomere erosion that is associated with cell proliferation (**replicative senescence)** or
b. **telomere independent mechanisms**, which include a persistent DDR which keeps the cells alive but arrest their proliferation. These telomere-independent mechanisms include genomic and mitochondrial DNA damage, activated oncogenes, nucleolar dysfunction, RNA translation and turnover modifications, epigenetic changes, autophagy and alterations in miRNA expression.

Extrinsic inductors of cell senescence[81] are represented by extracellular signals that induce senescence in a paracrine fashion. Some examples are:

a. advanced glycation end products (AGEs),
b. angiotensin II,
c. senescence associated secretory phenotype (SASP - see below),
d. for stem cells, alterations in their niches, occurring with aging or pathology.

The figure 4.2 summarizes the possible origins of senescent cells.

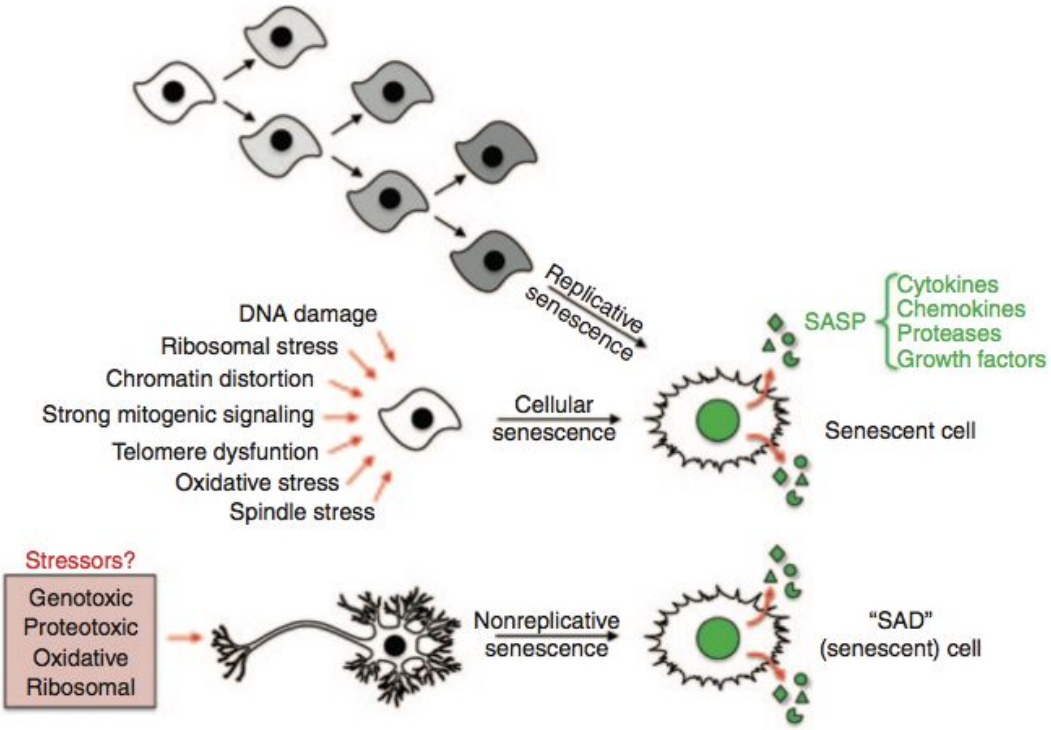

Figure 4.2 Different origins of senescent cells. *Cells that have reached their Hayflick limits have lost their ability to proliferate: this is termed replicative senescence. In cellular senescence, a variety of stimuli also cause an irreversible cell cycle arrest before cells lose their proliferative capacity. Emerging evidence suggests that there is a third possibility for the formation of senescent cells: terminally differentiated, nonproliferative cells acquire key features of senescent cells, including a SASP. These cells have been named SAD (senescence after differentiation) cells. SASP, senescence-associated secretory phenotype. Taken from (Naylor et al., 2013)*

4.1.3 How can senescent cells be recognized?

Several studies evidenced that cell senescence is a dynamic process, therefore cells progressively enter a deep senescence state, which is characterized by the loss of certain markers and acquisition of others[83]. It would be critically important to define the molecular and cellular markers of a deeply senescent cell versus an early senescent cell, since cell cycle reentry seems unlikely for cells that have entered deeper or late stages of senescence with respect to cells in an early senescent stage[83].

Despite several senescence-associated markers have been shown, no marker has been identified that exclusively identifies senescent cells and not all senescent cells express all possible senescence markers. Despite this awareness, several markers are currently used to identify senescent cells in culture and/or *in vivo*.

An obvious marker for senescent cells is the lack of DNA replication, which is typically detected by the incorporation of 5-bromodeoxyuridine (5-BrdU) or 3H-thymidine, or by immuno-staining for proteins such as PCNA (proliferating cell nuclear antigen) or Ki-67[71]. But these markers do not distinguish between senescent cells and quiescent or differentiated post-mitotic cells. Moreover, in the case of SAD, which characterizes post-mitotic cells, the lack of DNA replication does not represent a valid marker for cell senescence[72].

The first marker to be used for the more specific identification of senescent cells was SA-β-gal[84]. This marker is detectable by histochemical staining in most senescent cells. However, it is also induced by stresses such as prolonged confluence in culture.

In addition, p16 - an important regulator of senescence - is now used to identify senescent cells[85]. p16 is expressed by many, but not all, senescent cells. Recently, other three proteins were identified in oncogene-induced senescence: DEC1 (differentiated embryo-chondrocyte expressed-1), p15 (a CDKI) and DCR2 (decoy death receptor-2)[86]. Some senescent cells can also be identified by the cytological markers of SAHFs[76] and senescence-associated DNA-damage foci (SDFs)[87]. SAHFs are detected by the preferential binding of DNA dyes, such as 4,6-diamidino-2-phenylindole (DAPI), and the presence of certain heterochromatin-associated histone modifications, for example H3 Lys9 methylation, and proteins, for example heterochromatin protein-1 (HP1). SAHFs also contain E2F target genes, which SAHFs are thought to silence. SDFs contain proteins that are associated with DNA damage, for example the phosphorylated histone H2A variant at Serine 139 to generate γ-H2AX[88] and p53-binding protein-1 (53BP1). These foci result from dysfunctional telomeres and other sources of DNA damage. Last, senescent cells have been recognized by the combination of Ki67 negativity with high (n=5 per nucleus) γ-H2A.X foci density[89].

4.1.4 Senescent cells *in vivo* accumulate with age

In rodents, primates and humans, senescent cells are found in many renewing tissues. Notably, cells that express one or more senescence markers are relatively rare in young organisms, but their number increases with age. Estimates of senescent cells abundance in aged organisms vary widely depending on the study, species and tissue. Among the senescence markers that accumulate with age are SDFs that co-localize with telomeres, suggesting that, at least in some tissues, telomere dysfunction causes senescence *in vivo*[71].

Cells that express senescence markers are also found at sites of chronic age-related pathologies, such as atherosclerosis[90] or end-stage heart failure[43]. Thus, senescent cells are associated with aging and age-related diseases *in vivo*, as suggested by Hayflick's early experiments[91].

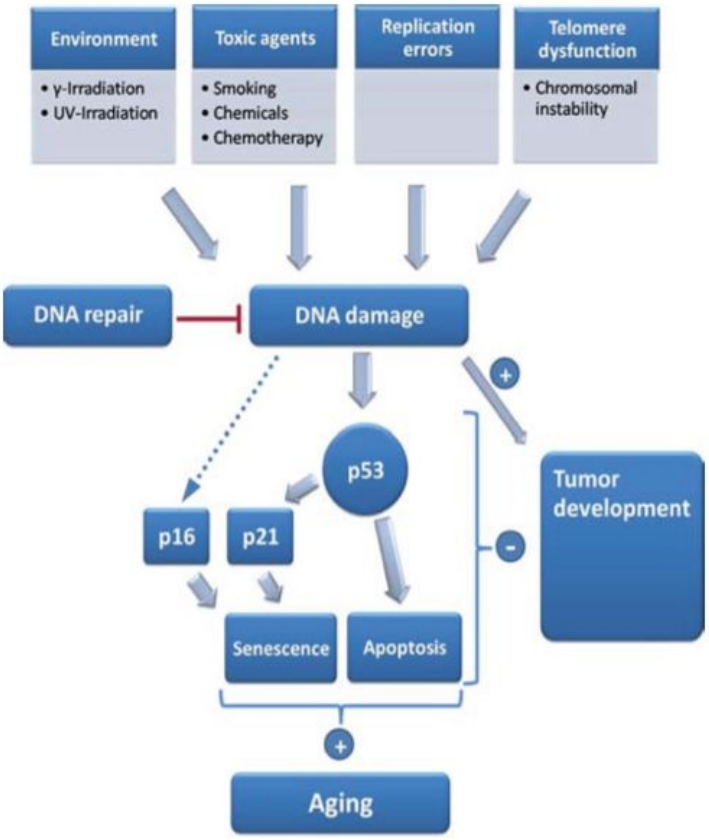

Figure 4.3 Mechanisms of aging. *Various factors contribute to accumulating DNA damage including environmental factors, toxic agents, replication errors, and telomere dysfunction. Accumulating DNA damage contributes to tumor development. To protect the organism, checkpoints are activated in response to DNA damage that inhibits tumor development by induction of apoptosis or senescence in cells with impaired genomic integrity. As a drawback, these mechanisms contribute to aging by impairing organ maintenance and regenerative capacities.*
Taken from (von Figura et al., 2009)

Recent findings suggest that senescent cells, at least those induced by acute p53 activation in murine tumor models, can be cleared by host mechanisms such as the immune system[92]. Nothing is known about how senescent cells are recognized by the immune system, whether additional mechanisms clear them *in vivo* or whether clearance mechanisms change with age or in age-related diseases[71].

p16 expression increases with age in the stem and progenitor cells of the mouse brain, bone marrow and pancreas, where it suppresses stem-cell proliferation and tissue regeneration[71]. Removal of p16-positive senescent cells can prevent or delay tissue dysfunction and extend healthspan[93]. The age-dependent rise in p16-positive stem and progenitor cells is consistent with the idea that stem-cell senescence might at least partly explain the age-related decline in brain and bone-marrow function and the development of type II diabetes. However, it is not known yet whether the p16-positive stem and progenitor cells are in fact senescent. So, it is possible that both the tumor-suppressive and pro-aging activities of p16 are partly due to growth suppression without senescence[71].

A second mechanism by which senescent cells might contribute to aging comes from their altered pattern of gene expression (SASP), explained below.

But how senescent cells might drive aging? Three possible explanations have been proposed:

a. cellular senescence can deplete tissues of stem or progenitor cells. This depletion will compromise tissue repair, regeneration, and normal turnover, leading to functional decrements[94];
b. the factors that senescent cells secrete affect vital processes (cell growth and migration, tissue architecture, blood vessel formation, and differentiation) and so are tightly regulated. The inappropriate presence of these factors can disrupt tissue structure and function[95];
c. the SASP includes several potent inflammatory cytokines[96]. Low-level, chronic inflammation is a hallmark of aging that initiates or promotes most, if not all, major age-related diseases. Chronic inflammation can destroy cells and tissues because some immune cells produce strong oxidants. Also, immune cells secrete factors that further alter and remodel the tissue environment, which can cause cell/tissue dysfunction and impair stem cell niches.

4.2 Senescent cells are active communicators: the SASP

Senescent cells with persistent DDR signaling do not display a passive behavior but they secrete growth factors, proteases, cytokines and other factors into their environment, affecting surrounding cells by activating various cell-surface receptors and corresponding signal transduction pathways that may lead to multiple pathologies, including cancer. This process is known as the senescence-associated secretory phenotype (SASP)[73; 97]. Senescent cells can induce a bystander effect, spreading senescence towards their neighbors *in vitro* and, possibly, *in vivo*[98]. SASP is responsible for some of the biological activities of senescent cells: it enforces cell cycle arrest, modifies the microenvironment and triggers immune surveillance of senescent cells[99]. SASP factors can be globally divided into the following major categories: soluble signaling factors (interleukins, chemokines, and growth factors), secreted proteases and secreted insoluble proteins/extracellular matrix (ECM) components[97].

The SASP is a plastic phenotype, that is proteins that are included in the SASP vary among cell types and, to some extent, with the stimulus that induced the senescence response[100].

The SASP functions in four areas[101]: a. an autocrine function that reinforces the development of senescence within the secreting cell; b. a pro-oncogenic effect on surrounding pre-malignant or transformed cells; c. an inflammatory effect driving infiltration of innate and adaptive immune system components; d. a paracrine function driving senescence development within normal cells surrounding the senescent secretory cell.

The SASP can have positive or negative effects depending on the context[102]. It can cause local and potentially systemic inflammation, disrupt tissue architecture, and stimulate growth of nearby malignant cells when the SASP is both pronounced or persistent, as in old age, massive obesity, or progerias[102]. Conversely, a localized, time-limited SASP may be important in resolving tissue damage, at least in younger individuals. Many factors that comprise the SASP

are important for tissue repair: growth factors and proteases that participate in wound healing, attractants for immune cells that kill pathogens, and proteins that mobilize stem or progenitor cells. Thus, the SASP may serve to communicate cellular damage/dysfunction to the surrounding tissue and stimulate repair, if needed[73]. Furthermore, SASP matrix metalloproteinases - MMPs - limit fibrosis following liver injury or during skin wound healing, which is beneficial. The SASP cytokines, IL-6 and IL-8, also reinforce the senescence growth arrest, at least in some senescent cells, which is beneficial in defense against cancer[102].

A very recent report by Gil and colleagues[77] reinforced the concept that the SASP can mediate paracrine transmission of cellular senescence. By co-culturing cells undergoing oncogene-induced senescence (OIS) with normal cells, the authors showed that the senescence phenotype could be transmitted to surrounding cells via the soluble SASP proteins.

By combining quantitative proteomics and screening with inhibitors, the authors identified key players mediating the paracrine transmission of senescence, including chemokines TGF-β, VEGF and CCL2 pathways. A search for upstream regulators of SASP pointed at IL-1 signaling and the inflammasome, molecules that operate cell autonomously to control SASP production and non-cell autonomously to spread the senescent phenotype via the SASP (fig.4.4).

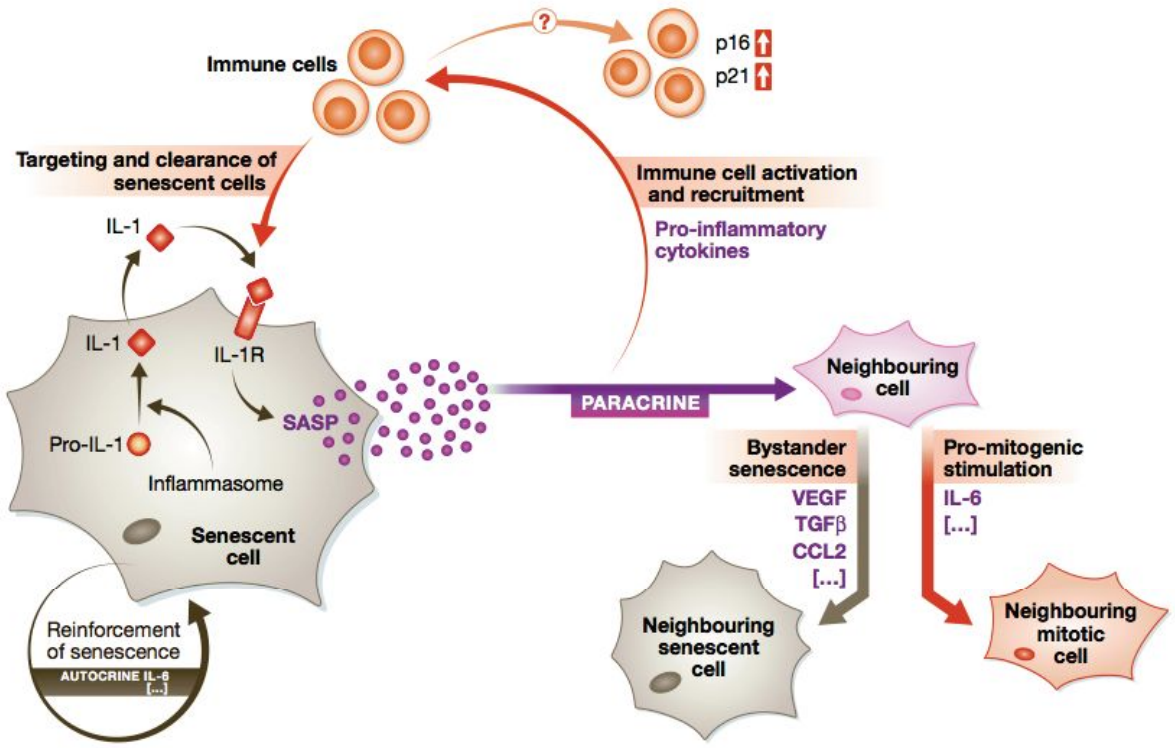

Figure 4.4 Autocrine and paracrine effects of cellular senescence. *Stress stimuli can trigger normal mitotic cells to go into senescence. This involves inflammasome-mediated activation of IL-1 signaling, which initiates the SASP response. The SASP reinforces the senescent phenotype via cytokines such as IL-6 in an autocrine manner. It also acts in a paracrine way to influence the cells in the surrounding environment. SASP components can trigger bystander senescence on neighboring cells and can also exert pro-mitogenic stimulation of neighboring cells via cytokines like IL-6, which appear to play dual roles depending on the context. Furthermore, the SASP can act on the immune system via pro-inflammatory cytokines, leading to immune cell recruitment and subsequent targeting and clearance of senescent cells. Alternatively, the SASP can trigger upregulation of p16 and p21 levels on neighboring immune cells. Taken from (Tasdemir et al., 2013)*

Transforming growth factor β (TGF-β) and IL-1 were identified as SASP factors able to trigger paracrine senescence[77]. Inhibition of each signaling pathway led to a partial bypass of paracrine senescence, consistent with a previous study reporting that TGF-β and IL-1 signaling cooperatively mediate paracrine senescence[103].

Acosta et al. studied the differences between autocrine and paracrine signaling networks. Whereas IL-1 signaling was involved in both autocrine and paracrine senescence, TGF-β contributed mainly to paracrine senescence[77]. **IL-1β** is active only in its mature form which requires the action of the **inflammasome**, a multi-molecular innate immune complex that forms in response to pathogen- or damage-associated signals, and consists of **caspase 1** (formerly known as IL-1 converting enzyme)[104]. Inflammasome-mediated activation of caspase 1 is critical in the subsequent processing and secretion of pro-inflammatory cytokines including IL-1β[104]. This latter is up-regulated during senescence[77; 103] and thus could be the major trigger of IL-1 signaling in paracrine senescence induced by the conditioned medium of OIS cells. Indeed, Acosta et al. found that the levels of inflammasome components, including caspase 1 activity, increased during OIS in culture and *in vivo*[77]. Further, caspase 1 inhibitors significantly reduced the cell cycle arrest in OIS cells and decreased the expression of many SASP components, including IL-1 α , IL-1β, IL-6 and IL-8[77]. Inflammasome may mediate a 'SASP cascade', with signaling effects that extend beyond acting solely on the initially stressed cells. Based on these findings, inflammasome seems to be at an interesting crossroad between inflammation and senescence[101].

The ability of senescent cells to propagate their phenotype is consistent with previous studies identifying IGFBP7 as a paracrine senescence regulator[105]. But the SASP may not always relay an arrest-inducing message onto the surrounding cells. Indeed, the SASP component IL-6 has been shown to elicit a pro-mitogenic response in a paracrine fashion[106]. Similarly, the SASP has been shown to be pro- and anti-tumorigenic depending on the micro-environment[107].

Among small non coding RNA (microRNA), the group of Judith Campisi showed that human senescent fibroblasts express, at high levels in culture, two microRNAs, mir-146a and mir-146b, in a SASP-dependent manner[108]. IL-1β induces the activation of NF-κB, which translocates inside the nucleus and begins the transcription of its targets, among them **micro-RNA-146**[109]. Cells undergoing senescence without induction of a robust SASP did not express mir-146a/b; these latter increase many days after IL-6 and IL-8 are maximally secreted and only in cells that secrete very high levels. IL-1 α neutralizing antibodies abolished both miR-146a/b expression and IL-6 secretion. These microRNAs modulate the inflammatory response and are expressed in response to rising inflammatory cytokines levels, as a negative feedback loop that limits excessive SASP activity[108]. In particular, when inflammatory cytokine secretion is high, elevated IL-1R signaling activates the downstream kinases IRAK1[108] and TRAF6[110], which ultimately

activate NF-κB. This transcription factor stimulates the expression of the SASP cytokines, IL-6 and IL-8, as well as miR-146a/b. By targeting IRAK1 and TRAF6 genes, miR-146a/b inhibit their expression, creating a negative feedback loop that restrains IL-1R signaling and limits senescence-associated cytokine production.
miR-146a/b are an example of another layer of complexity in the regulation of long-term senescence phenotypes.

4.3 Molecular pathways leading to cell senescence

Several intracellular molecular pathways have been associated to cell senescence; they are complex and interconnected. As follows, three main pathways are described.

4.3.1 AMPK/Akt/mTOR/autophagy pathway

Target of Rapamycin (TOR) is a serine/threonine kinase that belongs to the phosphoinositide 3-kinase (PI3K)-related protein kinases (PIKK) family, which comprises large proteins that enable organisms to cope with metabolic, environmental and genetic stresses[111]. TOR is implicated in disease states where growth is dysregulated and homeostasis is compromised, namely cancer, metabolic diseases and aging[111].
Mammalian TOR - **mTOR** - is the catalytic subunit of two distinct complexes called mTOR complex 1 (mTORC1) and mTORC2 (fig. 4.5). Unique accessory proteins distinguish these complexes: regulatory-associated protein of mTOR (RAPTOR) and Rapamycin-insensitive companion of mTOR (RICTOR) define mTORC1 and mTORC2, respectively. These companions function as scaffolds for assembling the complexes and for binding substrates and regulators. mTORC1 and mTORC2 share mammalian lethal with SEC13 protein 8 (mLST8) and the DEP domain-containing mTOR-interacting protein (DEPTOR), which function as positive and negative regulators, respectively[111]. In yeast and mammals, Rapamycin - a macrolide that is produced by a soil bacterium that is found on Easter Island - inhibits the ability of mTORC1, but not mTORC2, to phosphorylate its substrates. Rapamycin binds the small protein 12 kDa FK506-binding protein (FKBP12) and, in turn, Rapamycin–FKBP12 binds and inhibits RAPTOR-bound, but not RICTOR-bound, mTOR. Rapamycin might inhibit mTORC1 by dissociating RAPTOR from mTOR, thus preventing the access of mTOR to some substrates[111].
mTORC1 is a major regulator of ribosomal biogenesis and protein synthesis[112]. mTORC1 regulates these processes largely by the phosphorylation/inactivation of the repressors of mRNA translation 4E-binding proteins (4E-BPs) and by the phosphorylation/activation of ribosomal protein S6 kinase (S6K1)[113; 114] (fig. 4.5). When phosphorylated by mTORC1, 4E-BP1 dissociates from eukaryotic translation initiation factor 4E (eIF4E), allowing this latter to recruit the translation initiation factors. When phosphorylated by mTORC1, S6K1 promotes mRNA

translation by phosphorylating or binding multiple proteins[111; 115]. The phospho-rylation status of 4E-BP1 and S6K1 is commonly used to evaluate mTORC1 activity *in vivo*[113].
mTORC1 actively suppresses autophagy (see below) and, conversely, inhibition of mTORC1 (by small molecules or by amino acid withdrawal) strongly induces autophagy[111]. mTORC1 also controls the activity of several transcription factors that are implicated in lipid synthesis and mitochondrial metabolism[111].
mTORC2 is Rapamycin insensitive and activates Akt via phosphorylation at Ser473; it also activates serum- and glucocorticoid-regulated kinase (sGK) and protein kinase C (PKC), which all together regulate cell survival, cell cycle progression and anabolism[111]. Importantly, TORC1 antagonizes TORC2, inhibiting the PI3K-Akt pathway[115].

Upstream regulators of mTORC1 are nutrients, growth factors, energy and stress[111].
One key end point of growth factor signaling to mTORC1 is the small GTPase RHEB that, when loaded with GTP, stimulates the kinase activity of mTORC1 (fig. 4.5). Binding of insulin (or insulin-like growth factor - IGF) to its receptor activates the PI3K pathway, which leads to the phosphorylation and activation of Akt. In turn, Akt phosphorylates TSC2 (tuberous sclerosis protein 2), a large protein that, together with TSC1, forms the TSC1–TSC2 complex. This latter acts as a GTPase activating protein (GAP) for RHEB; because GDP-loaded RHEB is unable to activate mTORC1, TSC1-TSC2 effectively shuts off mTORC1 signaling. Akt-mediated TSC2 phosphorylation is likely to inhibit its GAP activity for RHEB, thus promoting mTORC1 activation[111; 115]. However, experimental evidences have been described which support also an activation of mTOR independently by Akt[116].
mTORC1 senses cellular energy. This is crucial, because mTORC1-driven growth processes consume a large fraction of cellular energy, and thus could be deleterious to starving cells.
Upon nutrient deprivation, cellular ATP levels quickly drop. The mTORC1 pathway indirectly senses low ATP by a mechanism that is centered on the AMP-activated protein kinase (AMPK). Both AMP and ATP are allosteric regulators of AMPK: when the AMP:ATP ratio increases, AMPK phosphorylates TSC2, possibly stimulating the GAP activity of TSC1-TSC2 towards RHEB to inhibit mTORC1 signaling (fig. 4.5). Moreover, AMPK phosphorylates RAPTOR, leading to the inhibition of mTORC1 through allosteric mechanisms[111].

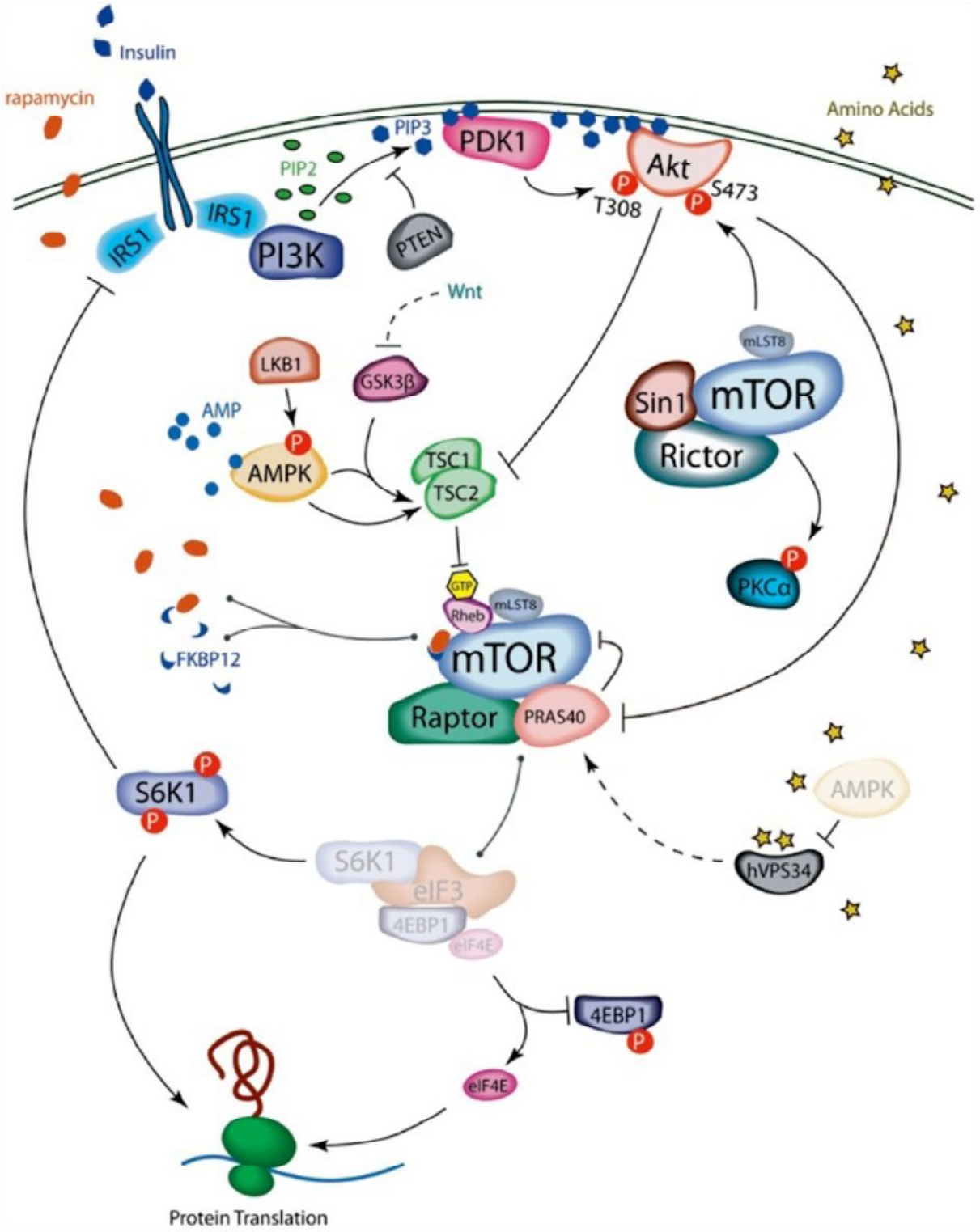

Figure 4.5 Scheme of AMPK-Akt-mTOR signaling pathway. *PI3K is activated by growth factors through direct interaction with receptors or through interaction with scaffolding adaptors, such as the IRS proteins. These interactions recruit PI3K to its substrate PtdIns(4,5)P2 (PIP2), allowing generation of the lipid second messenger PtdIns(3,4,5)P3 (PIP3). Akt and PDK1 are recruited to the plasma membrane through association with PtdIns(3,4,5)P3. This allows Akt to be activated through phosphorylation on Thr308 by PDK1 and Ser473 by mTORC2. Once active, Akt phosphorylates many downstream targets, including multiple sites on TSC2, which forms a functional complex with TSC1. Phosphorylation of TSC2 impairs the ability of the TSC1–TSC2 complex to act as a GAP towards the small GTPase Rheb, allowing Rheb–GTP to accumulate. Rheb–GTP potently activates mTORC1, which phosphorylates and inhibits 4E-BP1 and activates S6K1. A negative-feedback loop exists in which S6K1 directly phosphorylates IRS1 and block insulin or IGF-1 (insulin-like growth factor 1) signalling to PI3K. In addition, the TSC1–TSC2 complex appears to be involved in the phosphorylation of PKCα by mTORC2. The drug Rapamycin strongly and acutely inhibits mTORC1.*
Taken from (Vissing et al., 2013)

mTOR is a regulator of metabolism: when nutrients are available, mTOR is activated and drives anabolism as well as energy storage and consumption. Conversely, during fasting, mTOR must be suppressed to avoid the insurgence of conflicting metabolic signals. Finally, chronic overfeeding can lead to an excess of mTOR activation and metabolic derangements[111].

The TOR pathway is emerging as a key regulator of aging and inhibition of mTOR by Rapamycin or genetic deletion has been shown to expand life-span of invertebrates[117] and, even more strikingly, Rapamycin extends median and maximal life span of male and female mice[118].

mTOR plays a central role in cell senescence since its inactivation converts cellular senescence (a permanent exit from the cell cycle) into quiescence (a reversible cell cycle withdrawal)[119], as supported by the work of Korotchkina and colleagues, who demonstrated that p53-mediated senescence is irreversible in cells that maintain mTOR signaling; however, when mTOR signaling is inhibited, activation of p53 leads to quiescence[119]. In another study, inhibiting mTOR with Rapamycin increased the clonogenic capacity of primary human oral keratinocytes and their resident self-renewing cells by preventing stem cell senescence[120].

mTOR activation may instead determine stem cell exhaustion and aging.

Genetic studies have demonstrated that the deletion of one of several negative regulators of mTORC1, including PTEN and TSC1, leads haematopoietic stem cells (HSCs) to active cell cycling from quiescence, subsequent HSC exhaustion and defective long-term HSCs repopulating potential. These studies highlight the critical role of mTORC1-mediated cell growth signaling in the maintenance of HSC quiescence[121].

Aberrant growth signals or stress signals can accelerate stem cell senescence and tissue aging. Castilho and colleagues[122] showed that the persistent expression of Wnt proteins in mouse epidermis led to hyper-proliferation of epithelial stem cells, causing them to undergo senescence and exhausting the stem cell niche. Importantly, these actions seemed to occur through Wnt-mediated activation of the mTOR pathway: Rapamycin treatment prevented both the hyper-proliferation and premature senescence of epidermal stem cells that were exposed to excess Wnt.

In another study[123], the constitutive activation of mTORC1 through deletion of TSC1 led to increased expression of p16, p19 and p21 in mouse haematopoietic stem cells (HSCs), resulting in their depletion. An age-dependent increase in the activity of mTORC1 was detected and, moreover, prolonged Rapamycin treatment preserved the pool of HSCs to levels that were similar to those in young animals.

Furthermore, over-activation of the PI3K pathway by deletion of PTEN also led to the hyper-proliferation of HSCs followed by their depletion, probably through mTORC1. In fact, treatment

with Rapamycin restored the capacity of PTEN-null HSCs to reconstitute the blood lineage of irradiated mice[124].

The serine/threonine kinase **Akt**, also known as protein kinase B (PKB), is a downstream effector of PI3K (fig. 4.5). Akt is activated by extracellular signals that activate PI3K to generate phosphatidylinositol 3′ phosphate (PIP3). Akt activity is negatively regulated by phospholipid phosphatases (like PTEN) that dephosphorylate PIP3[113]. In mammals there are 3 Akt isoforms, differently expressed in various tissues.
The rate-limiting step in the activation of Akt is the binding of PIP3, which promotes Akt localization to the plasma membrane, where it is phosphorylated at two critical residues for its full activation: Thr-308 and Ser-473[113]. Following activation, Akt can phosphorylate an array of target proteins, most notably GSK3, FoxO1, FoxO3a, FoxO4 and TSC2[113].
Once Akt activates mTORC1, the latter elicits a negative feedback loop to inhibit Akt activity. This negative regulation of Akt activity by mTORC1 is attributed to the effect of S6K1 on IRS-1 downstream of IGF-1 and/or insulin receptors[125]. However, inhibition of Akt by mTORC1 has also been observed with other mechanisms. Regardless of the exact mechanisms by which mTORC1 inhibits Akt, this feedback inhibitory loop, taken together with the finding that mTORC2 is the activator of Akt, places Akt under positive and negative control mediated by mTOR. This also places mTORC2 upstream of Akt and mTORC1 both downstream and upstream of Akt, and, accordingly, mTORC1 activity should be dependent on mTORC2 activity. However, as recent findings suggest, the phosphorylation of Akt by mTORC2 is not required for Akt to phosphorylate TSC2 and to activate mTORC1, then mTORC1 is not dependent on mTORC2 activity[113].

Autophagy ("self-eating") is the controlled self-degradation pathway in eukaryotic cells that is essential for removing damaged organelles and macromolecules from the cytoplasm and recycling amino acids during periods of starvation. Autophagy is key in providing substrates for energy production during periods of low extracellular nutrients[126]. Autophagy is generally thought of as a survival mechanism, although its dysregulation has been linked to non-apoptotic cell death[127].
In macroautophagy, the major described type of autophagy, an isolation membrane (also termed phagophore) sequesters a small portion of the cytoplasm, including soluble materials and organelles, to form the autophagosome. This latter fuses with the lysosome to become an autolysosome and degrade the materials contained within it[128].
In response to food, the hormone insulin is produced, binds a receptor on the surface of cells and triggers a signaling cascade (fig. 4.6). An important part of this cascade is the enzyme class

I phosphatidylinositol-3-OH kinase (PI3K). This adds a phosphate group to a particular position on the lipid phosphatidylinositol, which is part of the cell membrane. Various proteins in turn bind the phosphorylated lipid and become activated, thus transmitting the external signal (in this case, insulin) into the cell. A central player in this pathway is mTOR, which suppresses autophagy[129]. This pathway provides a mechanism by which cells can block self-eating if the organism has just fed. On the flip side, the pathway also provides a means of inducing autophagy when the organism is starved: a lack of food (particularly of the sugar glucose) leads to a lack of insulin, leaving the pathway inactive and enabling the cell to tap into its storage reserves[129].

In mammalian cells, p70S6K, a downstream target of TORC1 involved in protein translation[111; 115], is activated at low-levels as a homeostatic mechanism even under nutrient-rich conditions and, moreover, subsequently to TORC1 is switched off, persists to be highly activated for a short period of time. This kinase exerts a negative feedback on signaling upstream of TOR, by inhibition of the activation of PI3K class 1 through an inhibitory phosphorylation of insulin receptor (InR) (fig. 4.6, purple lines), thus preventing cellular damages due to an excessive autophagy[130; 131; 132].

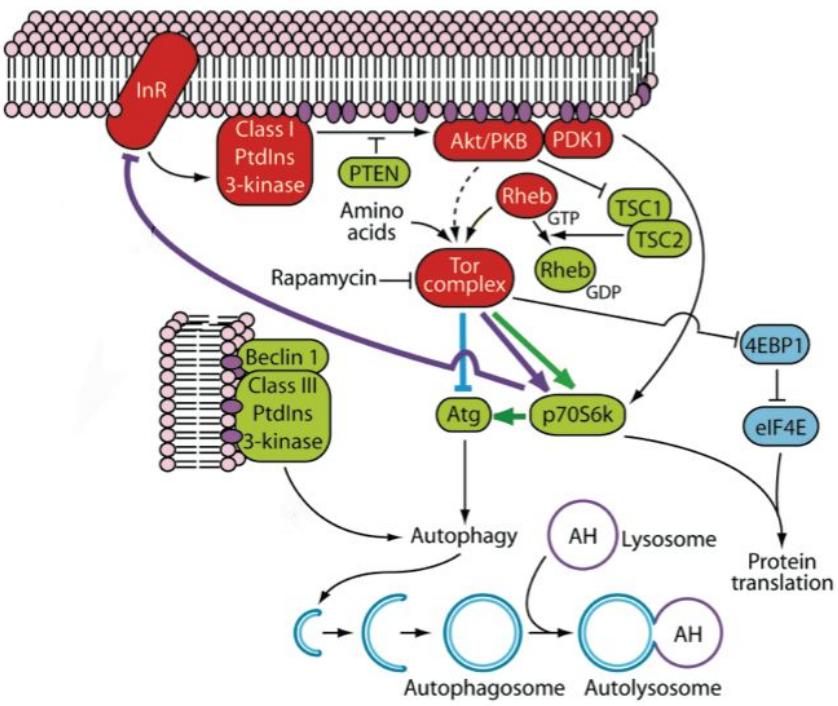

Figure 4.6 Different roles of p70S6K in the regulation of autophagy. *In the feedback model, low-level homeostatic activation of autophagy (**bold purple lines**) occurs even under nutrient-rich conditions through inhibition of the PI3K/Akt pathway. When nutrient levels drop, Tor inactivation allows autophagy to proceed at a higher level (**bold blue line**). During long-term starvation, the drop in p70S6k activity would remove the inhibition of PI3K and reactivate Tor to prevent excessive autophagy. Activation of p70S6k also stimulates autophagy directly (**bold green lines**), and independent of PI3K/Akt, although it was proposed that p70S6K may also act indirectly through effects on protein synthesis. In starvation conditions, the inhibition of Tor prevents further activation of p70S6K, which eventually limits autophagy and prevents excessive autophagy. InR, insulin receptor. Modified from (Klionsky et al., 2005)*

To be noted, in contrast with the previous data suggesting a negative role for p70S6K in stimulation of autophagy, a unique paper by Scott et al.[133] reported that, in the fat body of Drosophila melanogaster, p70S6K is instead a positive regulatory factor for autophagy (fig. 4.6,

green lines). Because p70S6K is needed for autophagy in Drosophila, the authors indicate that the inhibition of autophagy by TOR and the activation of p70S6K are effected through different branches of the TOR pathway. When TOR is switched on, p70S6K is activated and stimulates the autophagic process[130; 133]. But this mechanism seems to not be clear at all, since in Drosophila p70S6K activity would appear to be necessary but not sufficient to induce autophagy[133]. To date, this mechanism needs to be still examined in mammalian cells[130].

Multiple Atg proteins govern autophagosome formation. ATG, or autophagy-related genes, were first identified in yeast[134]. The core Atg proteins are highly conserved in other eukaryotes, including mammals, and they act in a similar hierarchical manner in yeast and mammals[128]. Atg3, Atg7, LC3-I and LC3-II (microtubule-associated protein light chain 3) are essential proteins for the autophagosomes formation in mammals[127]. In addition, Beclin 1 is a protein essential for the initiation of autophagocytosis, thus it has a critical role in cellular housekeeping and maintenance of homeostasis[135].

One of the best characterized substrates of selective autophagy is p62, which is also known as sequestosome 1/SQSTM1. p62 is an ubiquitously expressed cellular protein which directly interacts with LC3 on the isolation membrane; subsequently, p62 is incorporated into the autophagosome and then degraded[136]. Impairment of autophagy is accompanied by accumulation of p62. This leads to the formation of large aggregates, which include p62 and ubiquitin[137].

Evidence suggests that autophagic degradation declines with age, and it has been proposed that this leads to an accumulation of damage, such as protein aggregates and degenerate mitochondria, that contribute to age-related cellular dysfunction[126]. Activation of autophagy by inhibition of mTORC1 presumably maintains cellular function during aging by allowing enhanced degradation of aged cellular components. Evidence from studies in yeast and invertebrates supports the model that mTORC1-mediated induction of autophagy is required for lifespan extension from dietary restriction or from Rapamycin[138], although it remains to be determined whether induction of autophagy is sufficient to promote longevity in the absence of mTORC1 inhibition.

The role of autophagy in the occurrence of cell senescence is, however, still object of debate, corroborating the wide complexity of the autophagic process. In fact, this latter has been linked to both senescence and longevity with different mechanisms depending on the contest. Alongside the evidence that the autophagic degradation declines with age contributing to age-related cellular dysfunction[126], at the same time the opposite evidence that autophagy is activated in senescent cells is accumulating. Narita and coworkers[139] discovered spatial coupling of cells' catabolic and anabolic machinery: the TOR-autophagy spatial coupling compartment (TASCC), where (auto)lysosomes and mTOR accumulate during senescence

stimulating IL6 and IL8 secretion. TASCC contains mature autophagosomes, while early autophagosomes are mostly outside the TASCC. Thus, in senescent cells, autophagosomes form outside the TASCC at the cell periphery, out of reach of the inhibitory action of mTORC1, but they move inward as they mature. Autophagy is initiated at the cell periphery, spatially uncoupled from active mTOR in senescent cells. Coupling of mTOR and lysosomes occurs at the same location[139]. Importantly, the same author explained how autophagy can be a switch between apoptosis and senescence. In cultured HUVECs exposed to oxidative stress, autophagy is transiently activated following apoptosis, before cells become senescent[140]. Furthermore, the same Narita's group identified autophagy as a new effector mechanism of senescence[141]. Autophagy is activated during senescence and its activation is correlated with negative feedback in the PI3K-mTOR pathway. A subset of autophagy-related genes are up-regulated during senescence and induces autophagy and senescence. Autophagy, and its consequent protein turnover, mediates the acquisition of the senescence phenotype[141].

It has recently been reported that the decline of autophagy has a crucial role in the regulation of the aging process by increasing cellular senescence and inflammatory responses, since impaired autophagy can trigger inflammasome activation[135; 142].

Last, an impairment in autophagy has been described at the basis of pathogenesis of heart disease. Basal autophagy is critically required for protein quality control, removal of damaged organelles and recycling of intracellular elements to maintain cardiac homeostasis; excessive, or abrogated, autophagy is maladaptive[143; 144]. In support to this, mechanical unloading of the failing human heart decreases markers of autophagy, suggesting that autophagy may be an adaptive mechanism in the failing heart, and this phenomenon is attenuated by LVAD support[145]. But this phenomenon is not completely clear yet, thus it needs further clarifications.

AMP-activated kinase (**AMPK**) is a highly conserved sensor of increased levels of AMP and ADP originating from ATP depletion. Mammalian AMPK is a serine/threonine protein kinase which is composed of a catalytic α subunit and regulatory β and γ subunits. An elevated AMP/ADP concentration activates AMPK via allosteric regulation. Several upstream kinases can activate AMPK by phosphorylating the catalytic α subunit at Thr172. In turn, activated, phosphorylated AMPK can be inactivated by protein phosphatases (PP)[146].

AMPK has a central role since it coordinates a large signaling network of transcription factors and controls several cell processes like growth and autophagy, lipid and glucose metabolism, cell polarity[147].

Caloric restriction can stimulate AMPK activity whereas nutritional overload seems to impair AMPK activity and concurrently induce insulin resistance in many tissues thus promoting the

appearance of the components of the metabolic syndrome i.e. obesity, diabetes and cardiovascular diseases[146].

Recent studies demonstrated that the responsiveness of AMPK to different insults is clearly suppressed in aged tissues, reviewed in[147]. Characteristics which are affected by aging, i.e. oxidative stress[148] and endoplasmic stress[149] are augmented with aging, autophagic capacity is impaired[150] and a low-grade inflammation appears during aging[151]. In support to this, metabolic diseases are more common in old people.

AMPK controls autophagy inhibiting the activity of mTORC1 complex via two different mechanisms (fig. 4.5), either by directly phosphorylating the Raptor, a regulatory component of mTORC1, or by the phosphorylation of tuberous sclerosis protein 2 (TSC2), which subsequently suppresses the activity of mTOR[147]. AMPK can also directly stimulate autophagy through the phosphorylation of Ulk1[152], a protein involved in autophagosomes formation. Among its activities, AMPK controls also Sirt1, CREB and NFκB signaling.

4.3.2 Sirt1-CREB pathway

Yeast Sir2 and its orthologs **Sirtuins** are proteins possessing both NAD^+ dependent-protein deacetylase and ADP-ribosyltransferase activity. Mammalians possess at least 7 Sirtuins, termed Sirt1-7, that act as metabolic sensors linking environmental signals to metabolic homeostasis and stress response[82]. Sirtuins inhibit recombination of rDNA, relocalize to sites of DNA breaks and deacetylate histone proteins[153]. Sirt1 is the most studied mammalian Sirtuin; functionally, it controls gene expression, metabolism and aging, through a huge number of substrates which include p53, members of the FoxO family and NFκB[82]. Sirt1 is induced by caloric restrictions (CR) in rats, possibly as a consequence of the increased NAD/NADH ratio; moreover, in Sirt1 null mice, CR fails in extending lifespan[154].

Sirtuins are also involved in regulating cell fate decisions favoring stress resistance and inhibiting apoptosis; additionally, Sirt1 regulates cell death[155]. As regards cellular senescence, Sirt1 can antagonize OIS of mouse fibroblasts[156], while Sirt6 plays a prominent role in cellular senescence, regulating NFκB signaling[157]. The molecular mechanism through which Sirt1 could protect primitive cells have not been completely delineated yet[82]. However the most prominent ones are: positive regulation of telomeric length, the reduction of ROS production, the inhibition of p53 and the induction of autophagy[82].

As regards cell metabolism, a cycle linking Sirt1 and AMPK activation has been suggested, where both Sirt1 may activate AMPK and vice versa[158]. Last, Sirt1 is involved in autophagy by inhibiting mTOR through AMPK and by deacetylating several autophagy-relevant gene products (e.g. Atg5, Atg7 and Atg8/LC3)[159; 160].

Finally, Sirtuins have a positive impact on age-related pathologies. In this regard, Sirt1 can regulate endothelial Nitric Oxide Synthase (eNOS) activity[161]. Nitric oxide (NO) can regulate telomerase activity and is involved in endothelial function and inflammation[82].

cAMP-response element (CRE) binding protein (**CREB**) is a transcription factor that mediates the effects of fasting and feeding signals on the expression of metabolic programs in insulin-sensitive tissues[162]. It is also involved in age-related diseases[163].

CREB is a 46 kDa size protein residing in the nucleus that is capable of being activated by multiple pathways including cAMP/protein kinase A (PKA)-mediated signaling or the MAPK/ERK pathway. Upon activation, CREB is phosphorylated (pCREB) at its serine 133 residue, dimerizes with another pCREB, binds its cAMP response element (CRE) site on the DNA via a leucine zipper domain, and then recruits several co-activator proteins to assist with transcription (fig. 4.7). CREB transcriptome differs drastically depending on the tissue and cell type[163].

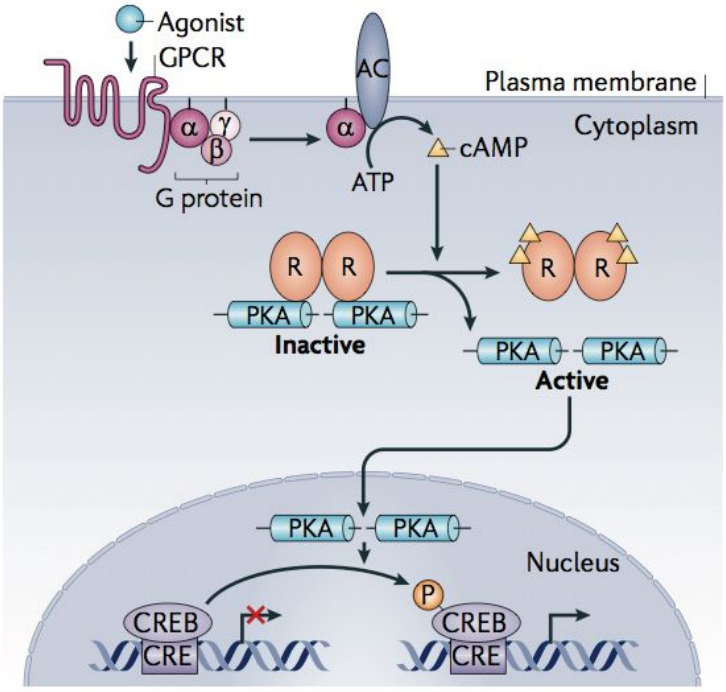

Figure 4.7 cAMP stimulates CREB phosphorylation.
The binding of ligand to G protein-coupled receptors (GPCRs) that are linked to the stimulatory G proteins, which are comprised of α-, β- and γ-subunits, leads to the activation of adenylyl cyclase (AC), which catalyses the synthesis of cyclic AMP. Increases in cellular cAMP stimulate protein kinase A (PKA) signalling. The liberated catalytic subunits enter the nucleus by passive diffusion and phosphorylate the cAMP-responsive element (CRE)-binding protein (CREB) at Ser133. Phosphorylated CREB promotes target gene expression at promoters containing CRE.
Taken from (Altarejos et al., 2011)

AMP-activated protein kinase (PKA) phosphorylates transcription factors of the CREB family[164]. cAMP levels in the cell depend strictly on adenylyl cyclase (AC) activity. cAMP levels tend to decrease with age, and several studies have demonstrated reductions in AC activity with age[163]. In addition CREB activity is critically reduced in the context of aging and of age-associated brain diseases[163; 165]. The abundance of CREB was markedly decreased in both whole cell and nuclear extracts of senescent fibroblasts; the marked decrement in expression of CREB with senescence suggests the possibility that the diminished expression of CREB may contribute to

altered CAMP-mediated regulation of gene expression with senescence[166]. CREB deficiency drastically reduces the expression of Sirt-1 and the induction of genes relevant to neuronal metabolism and survival in the cortex and hippocampus of dietary- restricted animals. Biochemical studies reveal a complex interplay between CREB and Sirt-1: CREB directly regulates the transcription of the sirtuin in neuronal cells by binding to Sirt-1 chromatin; Sirt-1, in turn, is recruited by CREB to DNA and promotes CREB-dependent gene expression[165].
Moreover, CREB is involved in Akt signaling pathway, since it has been demonstrated that Akt promotes cell survival at least in part by stimulating the expression of cellular genes via the CREB nuclear transduction pathway[167].
Last, CREB is involved in the regulation of several organism activities, ranging from metabolism - inducing Sirt1 expression in response to fasting[168] - to the circadian rhythm - regulating microRNA-132[169].

4.3.3 IKKβ-NFκB pathway

Nuclear factor (NF)κB (**NFκB**) signaling pathway is involved in the regulation of multiple cellular functions, as apoptosis, autophagy, cellular proliferation, differentiation, metabolism and adaptive and innate immunity responses[170].
The role of NFκB in senescence is controversial, as it is divisively associated with proliferation and tumor progression, and contrastingly with growth arrest and aging[171]. The NFκB family of transcription factors are ubiquitously expressed and regulate the response to cellular and environmental stress[172]. The IKK kinase complex includes IKKα, IKKβ and IKKγ (also called NEMO), upstream activators of NFκB signaling[170] (fig. 4.8).
In the canonical pathway, under resting conditions NFκB dimers are bound to inhibitory IκB proteins, which sequester NFκB complexes in the cytoplasm. Stimulus-induced degradation of IκB proteins is initiated through phosphorylation by the IκB kinase (IKK) complex, which consists of two catalytically active kinases, IKKα and IKKβ, and the regulatory subunit IKKγ (NEMO). Phosphorylated IκB proteins are targeted for ubiquitination and proteasomal degradation, releasing bound NFκB dimers to translocate to the nucleus where induce the expression of target genes[173]. The canonical pathway is activated by a wide array of receptors including those for inflammatory cytokines (IL-1β, TNFα), pathogen-associated molecules and antigen receptors and results in the activation of IKKβ[171].

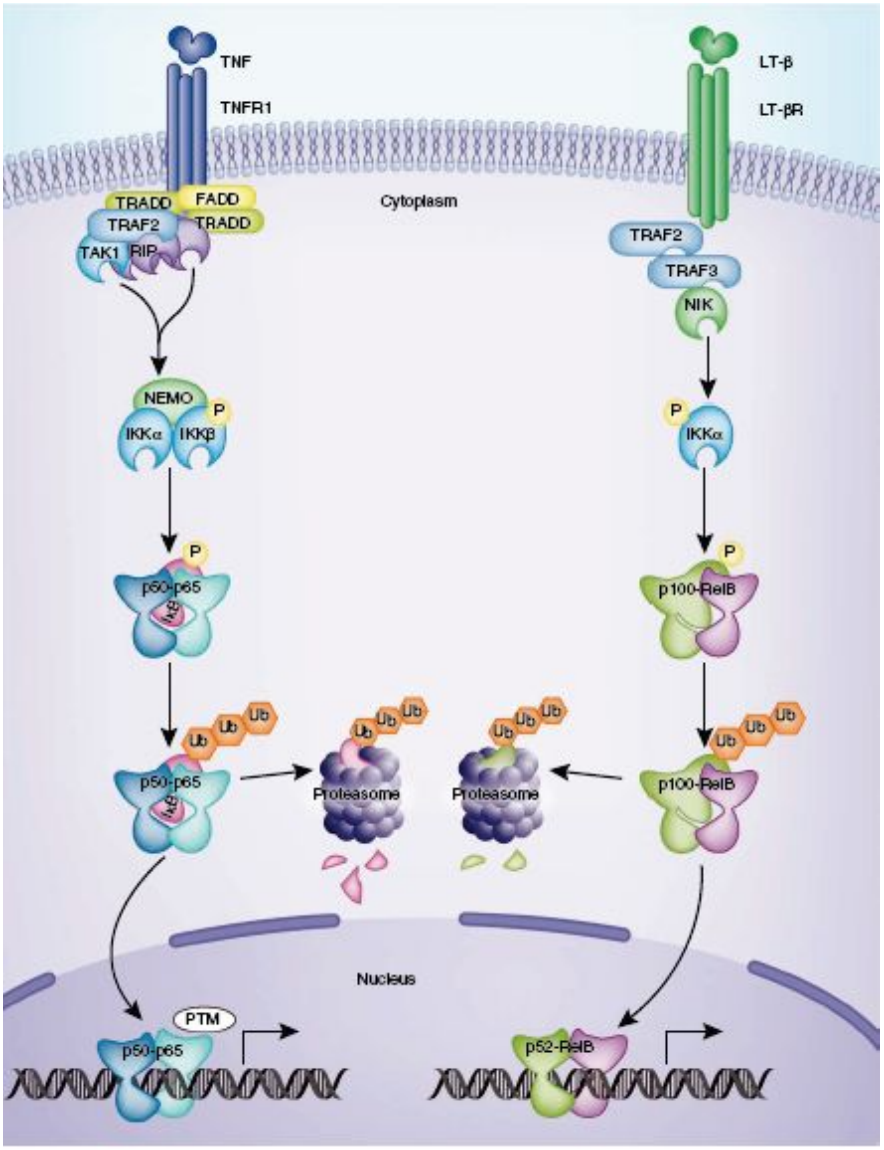

Figure 4.8 Canonical and non-canonical pathways of NF-κB activation. *Under resting conditions, NF-κB dimers (p50+p65) are bound to inhibitory IκB proteins, which sequester inactive NF-κB complexes in the cytoplasm. Stimulus-induced degradation of IκB proteins is initiated through phosphorylation by the IκB kinase (IKK) complex, which consists of two catalytically active kinases, IKKα and IKKβ, and the regulatory subunit IKKγ (NEMO). Phosphorylated IκB proteins are targeted for ubiquitination and proteasomal degradation, which thus releases the bound NF-κB dimers so they can translocate to the nucleus. NF-κB signaling is often divided into two types of pathways. The canonical pathway (left) is induced by most physiological NF-κB stimuli like TNFR1 signaling (represented here) or IL-1β signaling. The canonical pathway (right) is induced by certain TNF family cytokines, such as CD40L, BAFF and lymphotoxin-β (LT-β).*
Taken from (Oeckinghaus et al., 2011)

Chronic inflammation plays an important role in the aging process. Increased expression of inflammatory markers and an associated increase in NFκB DNA binding activity have been demonstrated in cells from older donors over cells from younger donors[174]. This may be partly due to the constitutive activation of NFκB as a result of accumulated oxidative stress during aging, which results in persistent inflammation[175]. NFκB has been shown to be strongly associated with progeria, a disease of premature aging. Aged tissues exhibit SA β-gal activity and enhanced $p16^{INK4A}$ expression, both of which are reduced upon NFκB inhibition. Moreover inhibition of NFκB in old tissue was shown to result in expression of genes characteristic of younger tissues[176].

Immunosenescence of adaptive immunity system enhances the activation of innate immunity responses which generates a proinflammatory phenotype, called inflammaging[177]. The major characteristics of inflammaging are the increased expression of genes associated with

inflammation in tissues[178] and augmented levels of cytokines, for example IL-6 and TNF-α, in serum[179]. These observations agree with earlier studies indicating that the NFκB system is activated with aging in many tissues[180]. Interestingly, inflammaging is also linked to a clear decline in autophagy[181] as well as apoptosis[182]. Moreover, it seems that the aging process *in vivo* also involves the appearance of senescent cells which are resistant to apoptotic cell death[183]. Campisi et al. showed that increased NFκB transcriptional activity due to p38MAPK activation was sufficient to induce the SASP of senescent fibroblasts[184,185].

NFκB system can also mediate the suppression of autophagy. Djavaheri-Mergny et al. observed that NFκB signaling inhibited the autophagy induced by TNF-α in different cell types[186]. They revealed that NFκB signaling activated mTOR kinase, which is the major inhibitor of autophagy. Moreover, suppression of NFκB signaling in this model stimulated the expression of Beclin 1 and subsequently triggered autophagy in TNF-α-treated cells. This response was mediated by ROS which can context-dependently promote autophagocytosis[186]. Upon TNF-α treatment, the activation of IKKα/β can repress TSC complex, a potent inhibitor of mTOR, and thus induce the activation of autophagy[187]. On the other hand, NFκB signaling, induced by TNF-α, can inhibit the expression of PTEN, a dual-specificity phosphatase that inhibits insulin/Akt pathway[188; 189]. The insulin/Akt pathway is a potent activator of mTOR and thus NFκB signaling can inhibit autophagy by stimulating this homeostatic pathway. Interestingly, signaling via insulin/IGF pathway can accelerate the aging process[190].

Inducible nitric oxide synthase (iNOS), induced by NFκB activation, stimulates the production of nitric oxide (NO) which has a crucial role as a messenger molecule. Recently, Sarkar et al. demonstrated that NO could inhibit autophagy by S-nitrosylating and thus inhibiting the activities of IKKβ and JNK1, potent inducers of autophagy[191].

IKKs were long thought to be highly specific for IκB proteins. However, evidence has accumulated indicating that IKKs target not only upstream mediators in NFκB cascades but also proteins unrelated to NFκB signaling[173]. Importantly, IKKβ is a potent activator of mTOR by phosphorylating and inhibiting TSC1. IKKβ-mediated phosphorylation of TSC1 is required for mTOR activation in response to pro-inflammatory cytokines such as TNF-α or IL-1β. Thus the signaling pathways activating IKKβ could trigger SASP via TASCC activation[187].

4.4 Cell senescence in the heart

Cardiac aging is manifested by maladaptation to stress, cardiac dysfunction and heart failure. Cardiac aging process involves cardiomyocytes and other cell types in the heart, such as interstitial fibroblasts and vascular cells. The morphological and functional changes of these cells with aging lead to cardiac hypertrophy, dilation and cardiac fibrosis due to chronic deposition and remodeling of extracellular matrix produced mainly by fibroblasts. Moreover, an

increased cardiac myocyte death due to necrosis and apoptosis with aging, and the accumulation of senescent cardiac stem cells, which are less proliferative, have a lower motility and release inflammatory cytokines - inducing paracrine senescence in the surrounding cardiomyocytes and vascular cells - also contributes to cardiac decompensation[192].

Imbalance between myocyte growth and death results in a premature increase in the number of senescent myocytes with depressed contractile performance. These structural and mechanical defects may lead ultimately to the onset of ventricular dysfunction and failure[193]. But also cardiac stem cells senesce. The forced entry of primitive cells into an irreversible quiescent state, coupled with an increased number of senescent myocytes, was identified in the human aged diseased heart by the expression of $p16^{INK4a}$ and very short telomeres. This led to a deficiency in cell regeneration with respect to cell death[45]. Similar findings were observed in Fischer rats[194]. Thus, activation of old CSCs, which undergo a limited number of doubling reaching cellular senescence and growth arrest, may be viewed as the process underlying cardiac aging[195].

Furthermore, experimental studies showed that, while acute ischemic heart disease is associated with the recruitment and activation of cardiac stem cells to injured areas, chronic cardiomyopathy is coupled with stem cell senescence and apoptosis[196].

4.4.1 Age and pathology affect human CSC function *in vitro*

Recently Cesselli and colleagues gave the direct demonstration that c-Kit-positive cardiac stem cells isolated from human explanted end-stage failing hearts (NYHA IV) express senescence markers ($p16^{INK4A}$, p21, phospho-p53) at high levels when cultured *in vitro* and show altered functional properties respect to CSCs isolated from healthy hearts donated for transplantation[43].

The authors demonstrated that CSCs isolated from donated and explanted hearts show a similar phenotype, that differs only for the expression of CD49a/α1 integrin, more represented in CSCs from explanted hearts[43]. Consistently, it was previously been reported that the α1 integrin isoform increases with cardiac aging and disease[197]. CSCs from explanted hearts show also lower cloning efficiency, migratory ability and maximum population doubling number than CSCs from donated hearts, while, at the opposite, they show a higher population doubling time. The differentiation ability is the same for both the cell populations[43].

Other important findings reported in this study[43] are that CSCs from explanted hearts are characterized by a reduced telomerase activity, a shorter telomere length and a stronger positivity to TIFs (recognized as the colocalization of 53 binding protein 1 (53bp1) or γH2AX with telomeric sequences) respect to CSCs from donated hearts (fig. 4.9)[43].

These results highlighted how prolonged pathology promotes dysfunctional telomeres and senescence of human CSCs, a phenomenon less apparent in adult donor hearts.

Moreover, the authors studied the correlation existing between age and pathology and the expression of senescence biomarkers in human CSCs. The multivariate analysis of the data showed that both age and pathology are independent predictors of telomerase activity, telomeric length, expression of TIFs, p16 and p21[43].

Last, authors analyzed the gene expression profile of both CSC populations, by microarray analysis. Among genes upregulated (at least 1.7 fold change) in CSCs from explanted hearts, are those encoding for pro-inflammatory cytokines (like IL-6). These cells present also an alteration in genes encoding for proteins involved in metabolic (lipids, carbo-hydrates, amino acids) pathways[43].

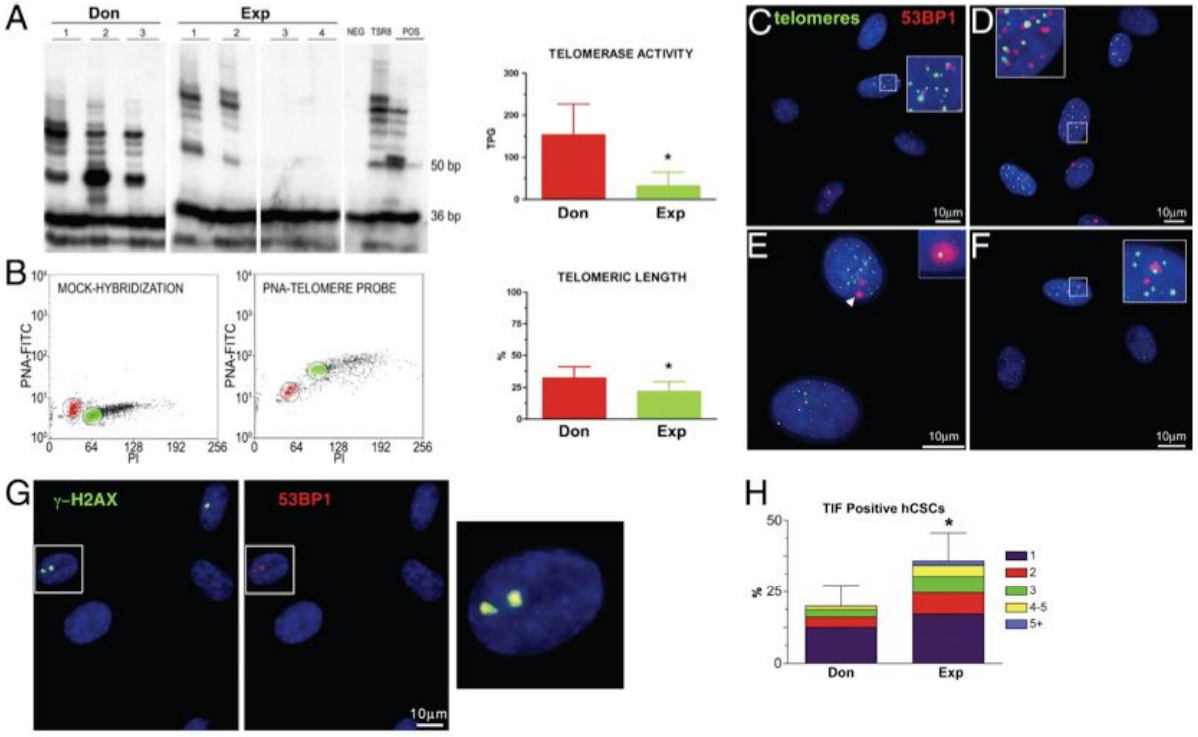

Figure 4.9 Telomere-telomerase axis in hCSCs from donor (Don) and explanted (Exp) hearts. ***A****: In CSC classes, products of telomerase activity display a 6-bp periodicity.* ***B****: Dot plots of CSCs hybridized without (mock-hybridization) and with the peptide nucleic acid (PNA) telomere probe. Gates were set around cells in the G0/G1 phase for both CSCs (red) and control cells, tetraploid 1301 cell line (green). PI, propidium iodide. Relative telomeric length was computed as the ratio of the telomere signal of CSCs and control cells.* ***C–F****: Four examples of telomere dysfunction-induced foci (TIFs) in which 53PB1 (red) colocalizes with telomere hybridization spots (green). Detail of interest is shown at higher magnification in the corresponding inset.* ***G****: γ-H2AX (green) and 53BP1 (red) colocalize at sites of DNA damage. The area included in the rectangles is shown at higher magnification on the right (yellow merged signals). In histograms, data are reported as means ± SD.* ***H****: fraction of CSCs with 1 to 5 TIFs.*
**P < 0.05 versus Don. Scale bars: 10 µm. Taken from (Cesselli et al., 2011)*

5- Can We Rejuvenate Senescent Stem Cells?

Age and pathological states can impair the *in vivo* regenerative properties of stem and progenitor cells, as demonstrated for endothelial progenitor cells (EPCs) and bone-marrow cells[198]. Young and functional stem cells should be selected at the aim to improve the quality of the cells used for stem cell therapy. At this purpose, two major strategies can be envisioned: a selection-based strategy and a drug/small molecule-based strategy[192]. Whereas the former is aimed at selecting the fraction of cells with the highest regenerative potential or devoid of senescent cells, the latter is meant to attenuate/revert the molecular pathways that characterize senescent cells[192].

The group of Professor Anversa has recently utilized antibodies that recognize insulin-like growth factor (IGF)-1 receptor (IGF1R) to select, within human CSCs, a subpopulation of younger cells (characterized by high telomerase activity and intact telomere length) which are endowed with a high ability to regenerate the murine infarcted myocardium. Therefore, $IGF1R^+$ human CSCs could represent a potent cell population for cardiac repair[199].

More recently, the Sussman's group rejuvenated senescent human CSCs, isolated from aged heart failure patients, by genetic modification using Pim-1 kinase. Pim-1 over-expressing CSCs showed an increases in proliferation, telomere length, survival, and a decrease in expression of senescence markers, factors that ameliorated CSCs regenerative properties[200].

A possible alternative to these approaches is to take advantage of the fact that senescent cells are functionally impaired and select for those cells whose stem cell properties are still preserved[192]. As described above, Cesselli and colleagues showed that single-cell-derived clones, obtained from hCSCs isolated from patients in end-stage heart failure, are less senescent than the overall population[43].

The problems of these described approaches are represented by the prolonged manipulation of cells, possible for research purposes but not permitted for the translation in clinical practice, and the large-scale expansion starting from a limited number of cells, which could finally undergo replicative senescence[192].

As an alternative, the drug-based strategy would improve the effects of stem cell therapy by addressing pharmacologically the molecular pathways that lead to cellular senescence[192]. Several molecular pathways have been associated either with the development of cell senescence or with organism longevity. Interestingly, the main molecular components linked to these two phenomena are common, and their manipulation may be explored both to ameliorate stem cell regenerative approaches and to prevent stem cell dysfunction and organ

pathology[192]. Figure 5.1 summarizes the primary pathways involved and the drugs that may target them.

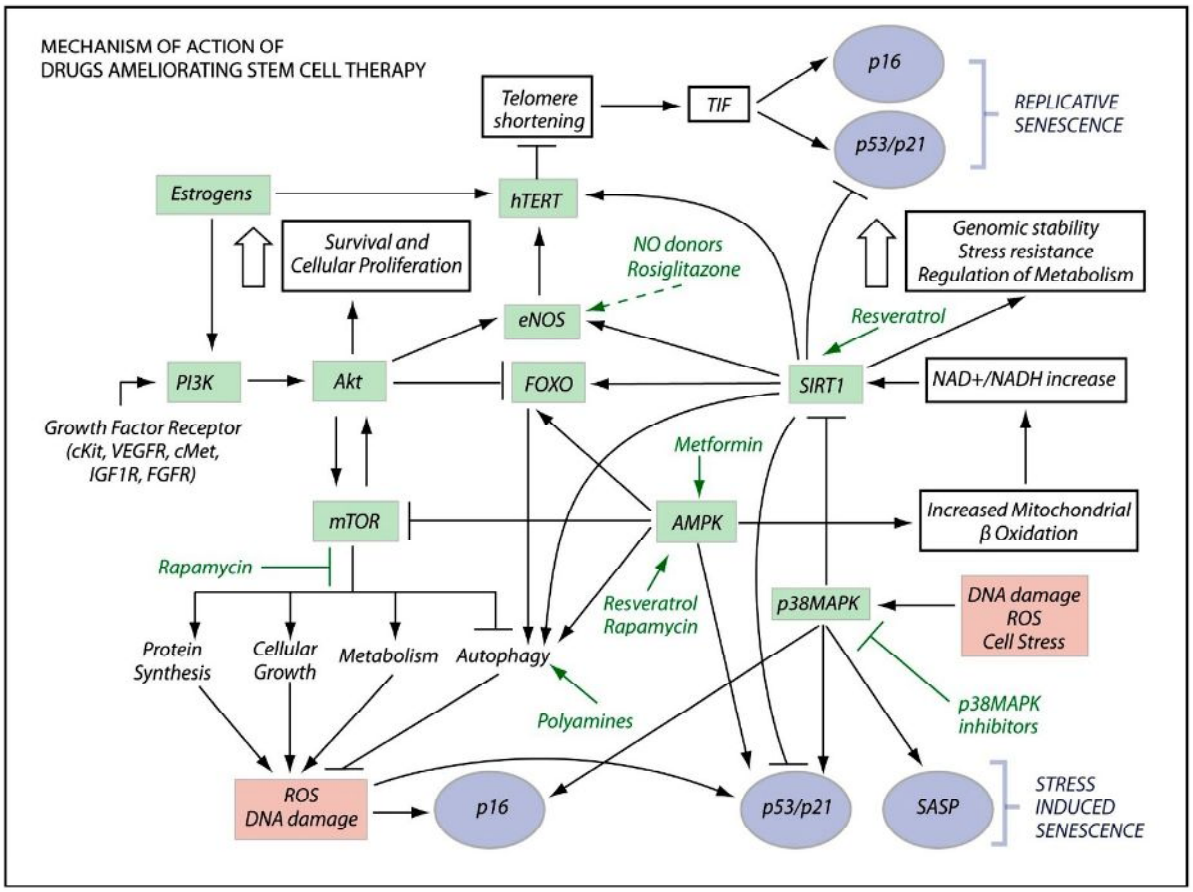

Figure 5.1 Mechanism of action of drugs ameliorating stem cell therapy. *The diagram summarizes the main molecular pathways leading to cellular senescence. Lines with sharp arrowheads indicate induction; lines ending with blunt arrowheads show inhibition. Drugs able to interfere with these pathways are shown in green. Taken from (Beltrami et al., 2012)*

5.1 Pharmacological approaches aimed at reverting cell senescence

The drug-based strategy has the aim to improve the effects of stem cell therapy by addressing pharmacologically the molecular pathways that lead to cellular senescence. Different drugs have been employed by researchers at this purpose: Rapamycin, Resveratrol, Metformin, Polyamines, p38MAPK inhibitors, Nitric Oxide donors[192]. As follows, some possible applications concerning the drugs object of this study are described.

5.1.1 Resveratrol

Resveratrol, a polyphenolic compound present in the skin of the red grape and thus in red wine, is emerging as a potent drug able to delay age-related deteriorations and to mediate cardioprotection, possibly by activating Sirt1. In fact, it possesses the ability to mimic the effects

of caloric restriction by activating Sirtuins and therefore acting modulating cell cycle, inhibiting apoptosis, increasing resistance to stress, and, finally, interfering with mTOR[201]. Resveratrol has shown beneficial effects against most degenerative and cardiovascular diseases: atherosclerosis, hypertension, ischemia-reperfusion, heart failure, diabetes, obesity and aging[201]. Importantly, in mice, pretreatment of either the infarcted heart or cardiac stem cells with Resveratrol prior to cell injection resulted in an improvement of the regenerative capacities of the injected cells, able to improve heart function[202].

Unlike Rapamycin, which antagonizes only one target, Resveratrol has multiple targets in the same nutrient-sensing network; in addition to Sirtuins, Resveratrol can also activate AMPK, antagonizing the mTOR pathway[203]. Furthermore, like the mTOR/S6K1 inhibitor Rapamycin, Resveratrol can inhibit S6K1 signaling; this resulted in decreased superoxide generation and enhanced NO levels in senescent endothelial cells in culture[204]. An enhanced S6K1 activity, an increased superoxide generation and decreased bioactive NO levels associated with eNOS uncoupling were also detected in aortas of old rats (aged 20–24 months) as compared to the young animals (1–3 months). Treatment of aortas of old rats with Resveratrol or Rapamycin inhibited S6K1 activity, oxidative stress, and improved endothelial NO production[204]. Thus, Resveratrol improves endothelial function in aging, at least in part, through inhibition of S6K1.

A recent study showed that the metabolic effects of Resveratrol can result from competitive inhibition of cAMP-degrading phosphodiesterases, leading to elevated cAMP levels. The consequence is an increase of NAD^+ and of the activity of Sirt1[205].

In another recent study, chronic treatment with 5 μM Resveratrol was able to reduce the senescence-associated secretory phenotype (SASP) in cultured human MRC5 fibroblasts, reducing both gene expression and release of pro-inflammatory cytokines. $p16^{INK4a}$ protein expression was not significantly modified, index that Resveratrol does not affect fibroblast replicative senescence, but improves tissue maintenance and repair during normal cellular aging[206].

Last, Resveratrol can trigger autophagy in cells from different organisms and ameliorate the fitness of human cells undergoing metabolic stress. These beneficial effects are lost when essential autophagy modulators are genetically or pharmacologically inactivated, indicating that autophagy is required for the cytoprotective and/or anti–aging effects of Resveratrol[207].

In a recent study published by the Beltrami's group[82], Resveratrol was able to attenuate human cardiac stem cells (CSCs) senescence *in vitro*. CSCs treated for 3 days with two different doses of the drug (0.5 and 1 μM), presented a larger fraction of Ki67-positive cells and an increased nuclear density. Importantly, the fraction of senescent cells resulted to be significantly reduced at both drug concentration used. In addition, Resveratrol was effective in reducing the fraction

of cells presenting DNA-damage foci, expressing p21 and dying by necrosis. These important results, essential to understand the aim of the study object of this thesis, are reported in (fig. 5.2).

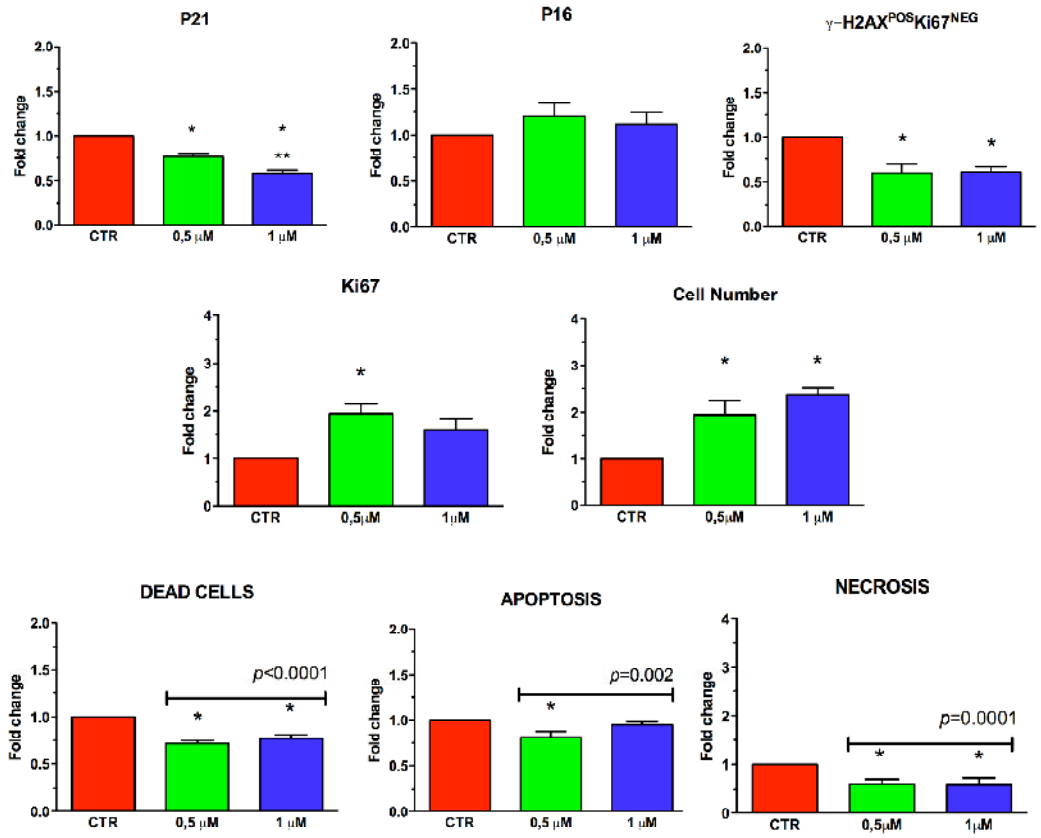

Figure 5.2 Effects of Resveratrol on human CSCs exposed for 3 days to 0μM, 0,5μM and 1μM of the drug. *Histograms represent the fold changes in the fraction of cells expressing senescence (p21, p16, γH2AX^{pos} Ki67^{neg}) and proliferation (Ki67) markers with respect to control (CTR), and the fold change in cell number and in the fraction of dead cells respect to CTR.*
** p<0.05 with respect to CTR; ** p<0.05 with respect to 0,5μM. Adapted from (Cesselli et al., 2012)*

5.1.2 Rapamycin

Because of the central role of mTOR in aging, Rapamycin has emerged as a very promising drug able to interfere with aging and, possibly, cell senescence[208]. Rapamycin is a macrolide produced by a soil bacterium that is found on Easter Island; it inhibits the ability of mTORC1 to phosphorylate its substrates. Rapamycin binds the small protein 12 kDa FK506-binding protein (FKBP12) and, in turn, Rapamycin-FKBP12 binds and inhibits RAPTOR-bound mTOR[111].
Rapamycin is already used in clinical practice for its immunosuppressant and anti-proliferative effects. Moreover, accumulated evidences display a possible role of Rapamycin in aging and cell senescence. In fact, Rapamycin can extend the maximum lifespan of mice, when given late in life, restore self-renewal of hematopoietic stem cells of aged mice, and prevent epidermal stem cell exhaustion induced by Wnt-1 in mouse skin[82].
In animal models, Rapamycin is able to prevent many age-related diseases such as cancer[209], obesity[132] and cardiovascular diseases[210].

Interestingly, many of the beneficial effects of Rapamycin have been shared with Resveratrol [211; 212], although the lifespan extending effect could be demonstrated with Rapamycin but not with Resveratrol in mice[118; 213]. Both Rapamycin and Resveratrol inhibit hyperactive mTORC1-S6K1 signaling, improve endothelial function in senescent cells and aging rat aortas[204], and also improve bone marrow-derived progenitor cell function and senescence[123]. All the results suggest that Rapamycin and Resveratrol may be used as anti-aging therapeutics in humans[214]. Rapamycin and analogs are indeed used in patients with organ transplantation and cancer and show clinical benefits[214].

In a recent study published by the Beltrami's group[82], Rapamycin was able to attenuate human cardiac stem cells (CSCs) senescence *in vitro*. CSCs treated for 3 days with two different doses of the drug (10nM and 100 nM), did not display changes in proliferation, as testified both by Ki67 expression and nuclear density. Rapamycin was instead effective in reducing the fraction of senescent cells acting primarily on the fraction of cells expressing p16 that, at a 10nM concentration, resulted to be halved. No changes in the fraction of cells with DNA-damage foci were observed. Interestingly, Rapamycin at both concentrations tested increased the fraction of cells undergoing cell death through apoptosis. These data, essential to understand the aim of the study object of this thesis, are reported in (fig. 5.3).

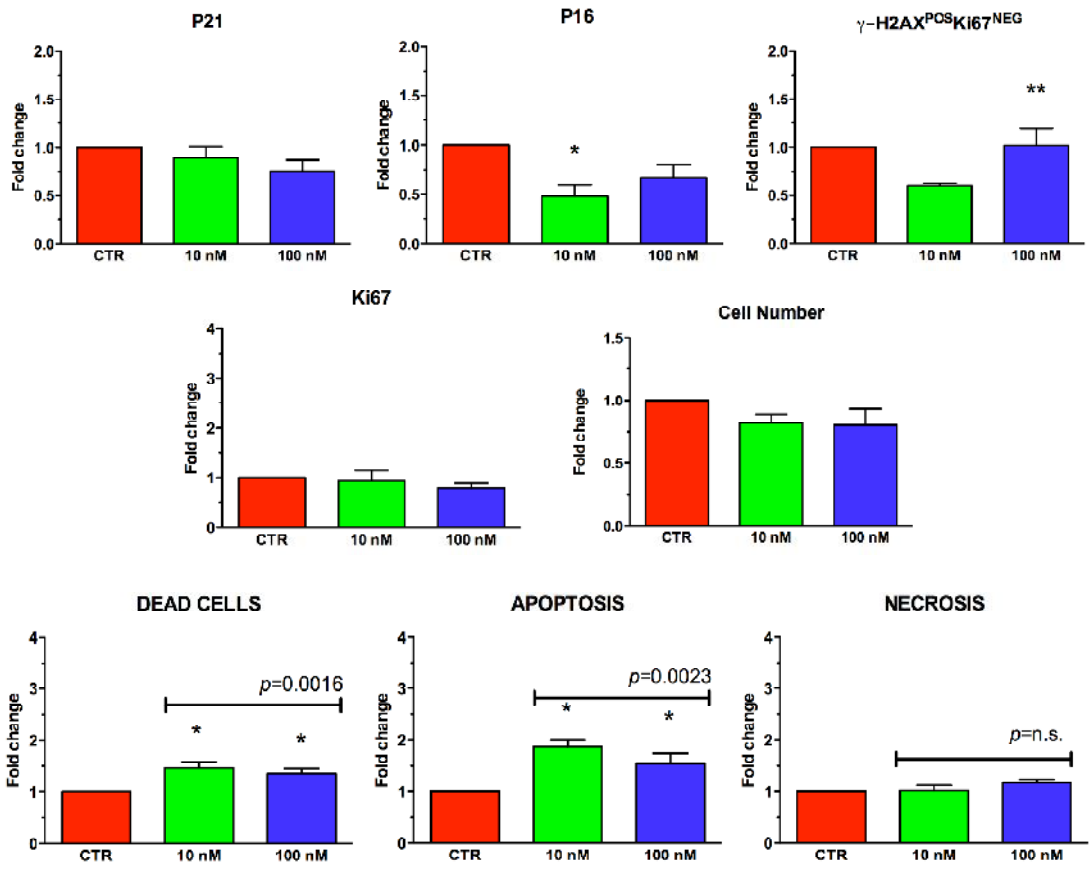

Figure 5.3 Effects of Rapamycin on human CSCs exposed for 3 days to 0nM, 10nM and 100 nM of the drug. *Histograms represent the fold changes in the fraction of cells expressing senescence (p21, p16, γH2AX^{pos} Ki67^{neg}) and proliferation (Ki67) markers with respect to control (CTR), and the fold change in cell number and in the fraction of dead cells respect to CTR.*
** p<0.05 with respect to CTR; ** p<0.05 with respect to 10nM. Adapted from (Cesselli et al., 2012)*

II. Rational and Aim

Heart failure (HF) is a complex clinical syndrome that can result from any structural or functional cardiac disorder that impairs the ability of the ventricle to fill or eject blood[5].

Mechanical, neurohormonal and possibly genetic factors alter ventricular size, shape and function, process named left ventricle remodeling[3]. Remodeling occurs in several clinical conditions, including myocardial infarction, cardiomyopathy, hypertension and valvular heart disease; its hallmarks include hypertrophy, loss of myocytes and increased interstitial fibrosis[3]. Remodeling continues for months after the initial insult and the eventual change in the shape of the ventricle becomes detrimental to the overall function of the heart as a pump[3]. HF overall prevalence is thought to be increasing, in part because current therapies for the cardiac disorders mentioned above are allowing patients to survive longer[4].

Although the current standard of care for HF improves outcomes, the syndrome continues to progress and there is a need for novel therapies that can prevent, further slow the progression, and/or reverse the structural and functional defects of the failing heart. Current therapeutic options for end-stage HF patients are limited to cardiac transplantation or the option of permanent mechanical assistance of the circulation. But heart transplantation is limited by donor availability and lifelong immunosuppression for transplant recipients[4; 9].

For these reasons, it is mandatory to investigate the mechanisms by which HF develops and to identify innovative therapies able to halt the progressive deterioration of cardiac function, also acting on the intrinsic repair mechanisms of the organ.

The discoveries of a cell turnover in the cardiac tissue[26] and of the presence of tissue-resident primitive cells, able to proliferate and differentiate in cardiac terminally differentiated cells[36], eventually improving the recovery of the organ, have opened new frontiers in the treatment of this pathology. The progression of regenerative medicine is allowing the development of stem-cell based therapies that have the potential to transform the treatment of HF by achieving myocardial regeneration[10].

Different groups have demonstrated the feasibility of isolating and expanding human CSCs from end-stage failing hearts[36; 44; 59; 215]; in addition, the recent early phase clinical trials SCIPIO[55] and CADUCEUS[57] employing autologous CSCs isolated from patients' hearts and expanded *in vitro* to obtain a sufficient number for transplantation, gave encouraging results. Despite this, accumulated evidences indicate that both aging and chronic age-related pathologies - such as

atherosclerosis[90] or end-stage heart failure[43; 199; 216] - are associated with human stem cell senescence and functional impairment.

Human CSCs obtained from failing hearts present reduced migration, proliferation and differentiation *in vitro*[43], features considered to be crucial for the regenerative potential of this autologous cell source. Moreover, these cells are characterized by a gene expression profile enriched in elements that are part of the SASP. Therefore, senescent human CSCs can contribute to create a microenvironment favoring, through a paracrine mechanism, senescence on neighbor cells, inflammation and extracellular matrix remodeling, thus creating a vicious circle hampering regenerative purposes[192]. The impact that cellular senescence exerts on CSCs biology *in vitro* has been demonstrated by different authors[43; 200]. Importantly, at present, the *in vivo* regenerative potential of CSCs obtained from normal hearts has not been directly compared with that of CSCs obtained from pathological hearts, currently employed in clinical trials.

In addition, in order to ameliorate autologous stem cell therapy, it would be mandatory any attempt aimed at improving the quality of the expanded cells, selecting the fraction of cells with the highest regenerative potential, excluding senescent cells[82]. The problems of this approach are represented by the prolonged manipulation of cells, not permitted for the translation in clinical practice, and the large-scale expansion starting from a limited number of cells, which could finally undergo replicative senescence[192]. As an alternative approach, rejuvenation of senescent human CSCs could improve the outcome of regenerative therapy. This latter purpose could be reached by a drug/small molecule-based strategy, meant to attenuate/revert the molecular pathways that characterize senescent cells[192]. Different anti-aging drugs have been employed by researchers with positive results on animal models of diseases[82,210,202]. Among them, there are Rapamycin and Resveratrol[192], already used in clinical practice.

For the reasons described above, with this study, the *in vivo* regenerative potential of senescent CSCs obtained from end-stage failure patients' hearts was first compared with that of CSCs obtained from normal hearts. After the demonstration, in an animal model of HF, that the first cell population's reparative ability was affected by senescence mechanisms, a drug-based strategy was adopted in the attempt to rejuvenate senescent CSCs, eventually ameliorating the cell therapy.

In details, the aims of this study were:

1. To compare the *in vivo* regenerative potential of human CSCs obtained from healthy hearts donated for transplantation (D-CSC) with that of human CSCs obtained from explanted end-stage failing hearts (E-CSC). For this purpose, a mouse model of acute myocardial infarction and heart failure was employed. D- and E-CSC lines were previously characterized *in vitro* to confirm the state of senescence and functional impairment of E-CSC, as already described[43].

2. To investigate for molecular pathways involved in aging mechanisms and that could be possibly altered in E-CSC. The pathways considered at this aim were:
   i. SASP-IKKβ-NFκB,
   ii.AMPK/Akt/mTOR/autophagy,
   iii.CREB/Sirt1.

3. To pharmacologically treat E-CSC, *in vitro*, with drugs capable to interfere with the above described senescence-associated molecular pathways, in the attempt to revert E-CSC senescence and restore cell functional properties. At this purpose, two drugs were employed: Rapamycin and Resveratrol[82].

4. Last, to verify if the *in-vitro* rejuvenation of E-CSC with Rapamycin and Resveratrol, prior to the injection in a mouse infarcted heart, was able to restore the *in vivo* regenerative potential of the cells, making it comparable to that of D-CSC.

III. Results

1- Cardiac Stem Cells from end-stage failing hearts show a senescent phenotype *in vitro*

For the present study, human Cardiac Stem Cells (CSCs) have been isolated from 20 hearts explanted from end-stage heart failure patients (E-CSC) and from 14 hearts donated for transplantation (D-CSC). Patients have been selected following the criteria illustrated in Table 1 (see par. 1 methods). Regarding the pathology, all patients enrolled in this study were affected by end-stage heart failure secondary to ischemic cardiomyopathy. Donors were younger than patients; patients were prevalently males. Clinical characteristics of patients and hearts are illustrated in Table 2 (see par. 1 methods).

1.1 Cell characterization

CSCs have been isolated using a protocol previously optimized by the prof. Beltrami's group[215], which requires an enzymatic digestion of the tissue followed by centrifugations and filtrations of the cell suspension to select cells lower than 40μm in diameter. Isolated cells have been cultured in a medium that allows the selection of undifferentiated mesenchymal stem cells for the first 2 passages, then cells were switched to an expansion medium (see methods); clusters of adherent spindle shaped cells were found 1-2 weeks after the isolation procedure. FACS analysis of CSC lines (**fig. 1.1**) revealed that a similar mesenchymal immunophenotype characterizes both D- and E-CSC, as shown by the expression of the cell surface markers CD13, CD44, CD73, CD105, CD49b and CD49d. Hematopoietic and endothelial markers are not expressed (data not shown). Both cell populations express at a high percentage (about 80%) the Stem Cell Factor receptor, c-Kit. D-CSC and E-CSC significantly differ only for the expression of CD49a, more expressed in E-CSC than in D-CSC.

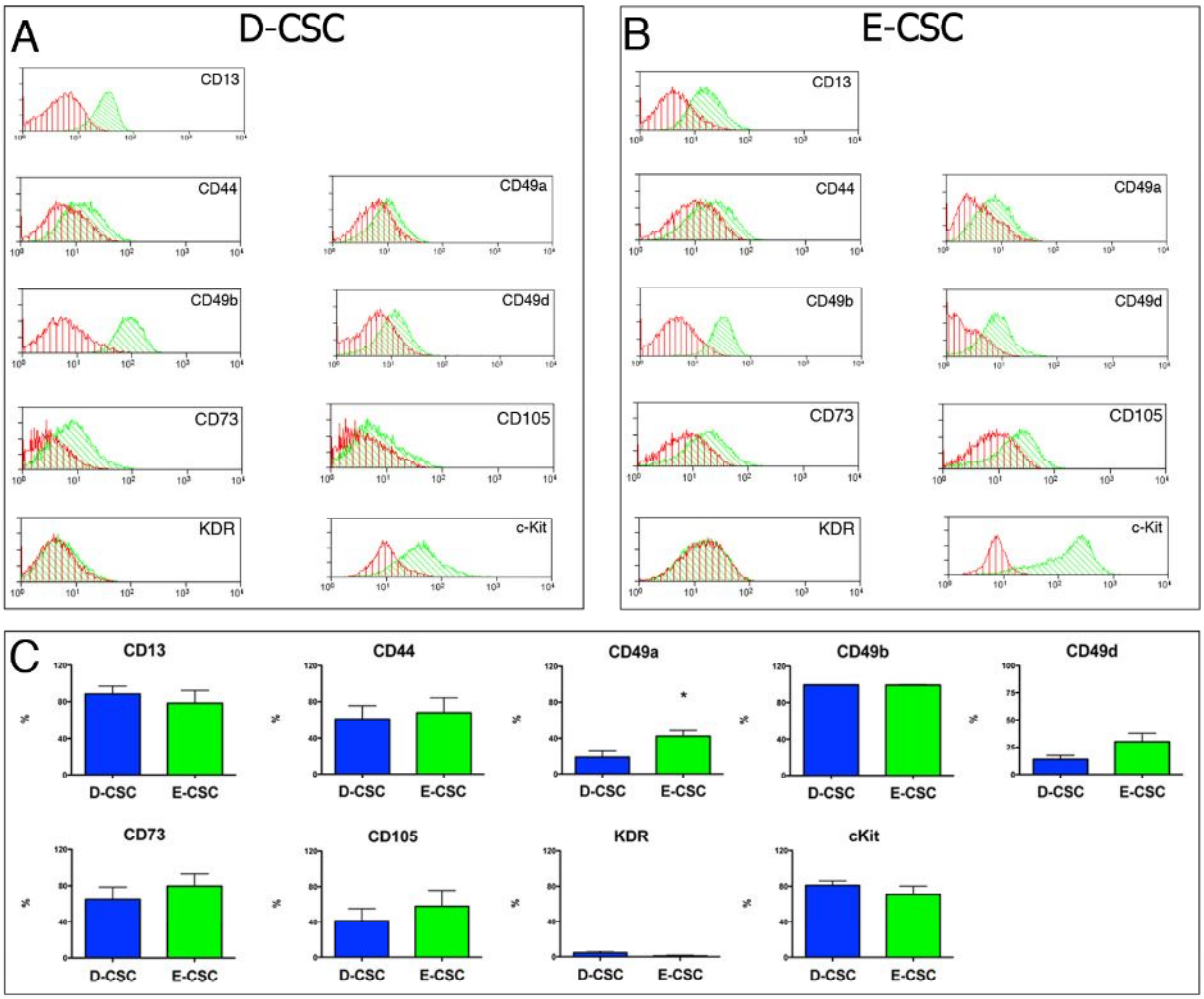

Figure 1.1 CSC immunophenotype. ***A*** *and* ***B****: Representative Flow-Cytometry histograms of D- and E-CSC. Red histogram represents the isotype control IgG staining profile, green histogram shows the specific antibody staining profile.* **C***: histograms summarize quantitative Flow-Cytometry data. Values are means±SEM. * p<0.05 vs D-CSC.*

Population doubling time is higher in E-CSC than D-CSC (**fig. 1.2**), which indicates that E-CSC are functionally impaired.

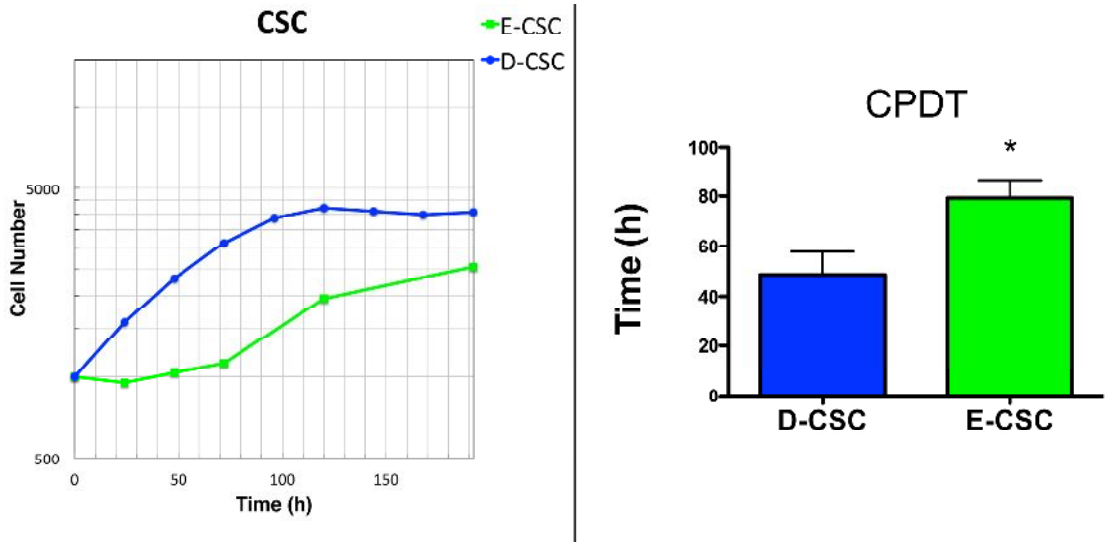

Figure 1.2 Growth curves and CPDT of CSC. *In the left panel, representative growth curves of D- and E-CSC. In the right panel, histograms summarizing cell population doubling time (CPDT) of D- and E-CSC. Values are means±SEM. * p<0.05 vs D-CSC.*

1.2 E-CSC express senescence markers at high levels *in vitro*

E-CSC and D-CSC at the 3rd passage in culture were compared, by immunofluorescence analysis, for the expression of senescence markers. E-CSC, with respect to D-CSC, are characterized by a higher percentage of cells expressing the senescence-associated marker p16; moreover, they present, at high levels, the phosphorylated histone H2A.X (at least n=5 foci of positivity per nucleus) in the absence of cell proliferation (Ki67 negativity). These results indicate that E-CSC are significantly enriched in senescent cells in comparison to D-CSC (**fig. 1.3A**). In addition, E-CSC are less proliferating and more apoptotic than D-CSC (**fig. 1.3B**).
Although both age and pathology may be responsible for E-CSC senescence, the pathological status was, in the present case study, the only independent predictor of the fraction of CSCs expressing either $p16^{INK4A}$ ($p<0.0001$) or γ-H2A.X ($p=0.004$).

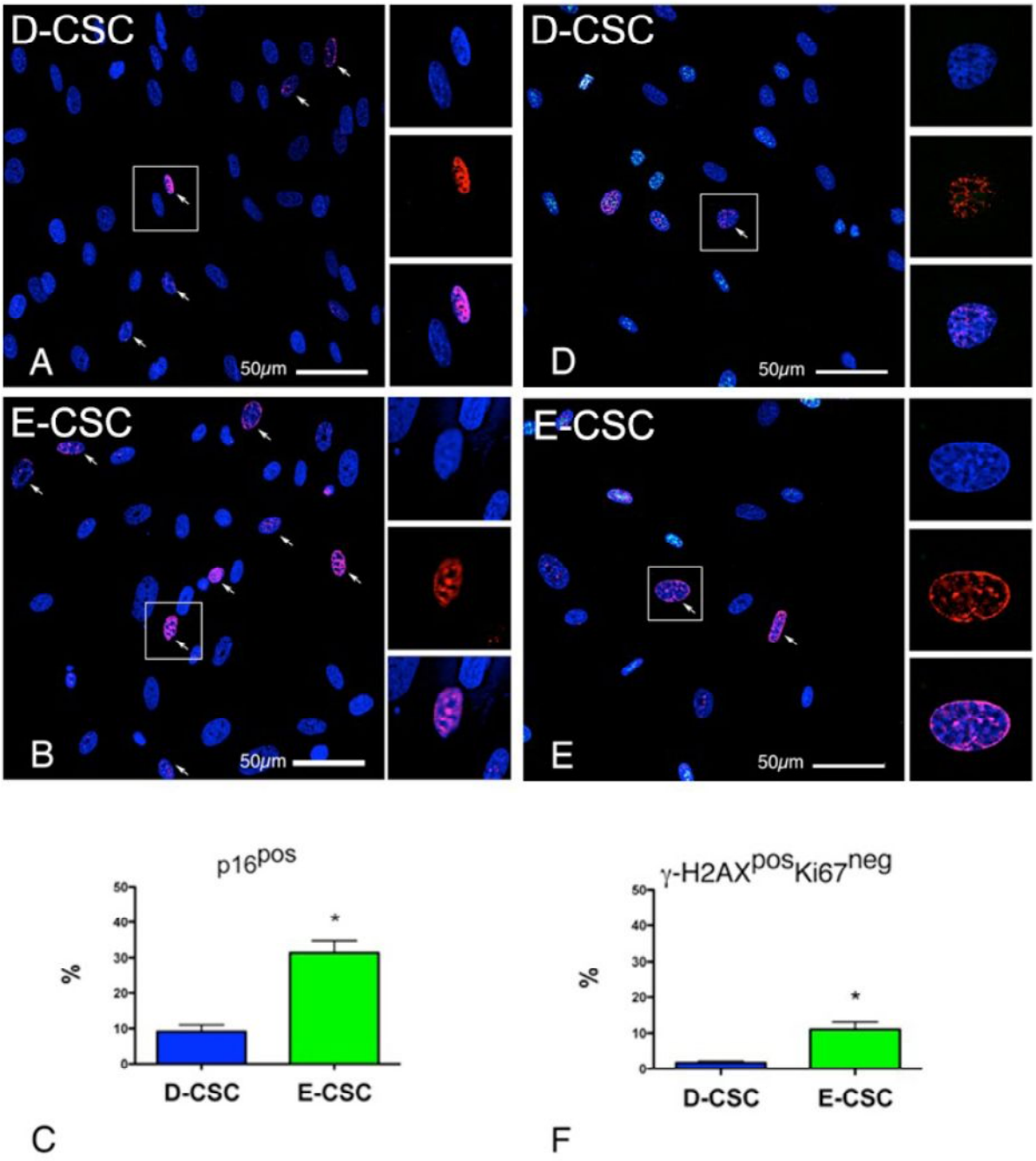

Figure 1.3A Expression of senescence markers in CSC. *Confocal images of D-CSC and E-CSC in culture (**A, B, D, E**). **A and B**: expression of $p16^{INK4A}$ in red fluorescence (arrows). **D and E**: expression of γH2AX histone variant in red fluorescence (arrows) in Ki67 (green fluorescence) negative cells, index of a persistent DNA-Damage Response (DDR). Nuclei are shown by the blue fluorescence of DAPI. **C and F**: histograms summarizing quantitative data of the above described immunostainings. Values are means±SEM. * p<0.05 vs D-CSC.*

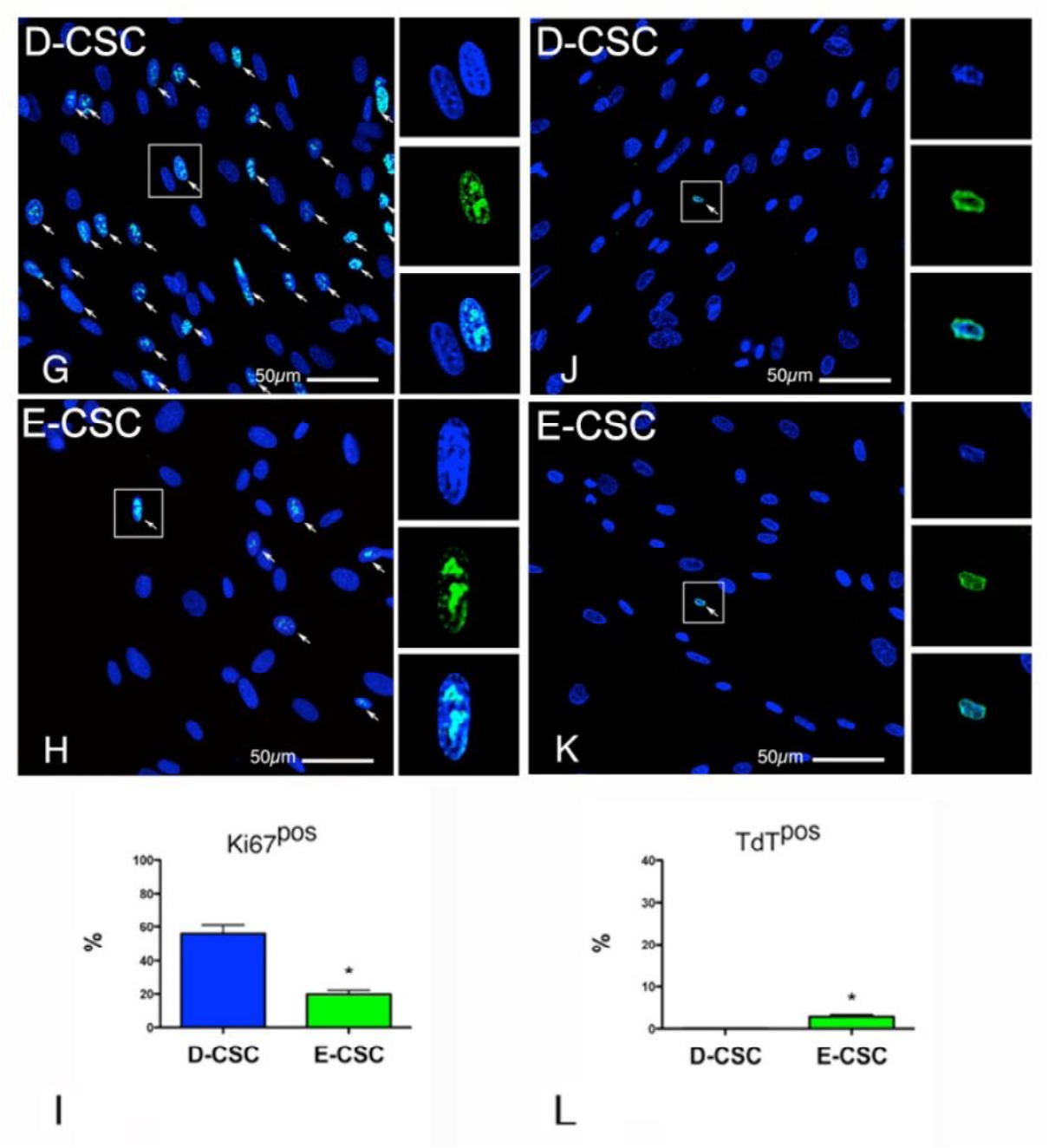

Figure 1.3B Expression of proliferation and apoptosis markers in CSC. *Confocal images of D-CSC and E-CSC in culture (**G, H, J, K**). **G and H**: expression of KI67 in green fluorescence (arrows) indicating cycling cells. **J and K**: TUNEL (TdT) positive cells (arrows) in green fluorescence, index of cell apoptosis. Nuclei are shown by the blue fluorescence of DAPI. **I and L**: histograms summarizing quantitative data of the above described immunostainings. Values are means±SEM. * p<0.05 vs D-CSC.*

1.3 E-CSC are characterized by an altered secretome (SASP)

Senescent cells release pro-inflammatory factors responsible for the paracrine transmission of cellular senescence and extracellular matrix remodeling. This phenomenon is named senescence-associated secretory phenotype (SASP)[73; 97].

The analysis of CSC secretome (**fig. 1.4**) showed that D- and E-CSC secrete similar levels of the pro-angiogenic and cardio-protective factors VEGF, bFGF and HGF; also the secretion of the pro-inflammatory and SASP-associated cytokines IL-6 and IL-8 is similar in both the cell populations. Instead, E-CSC supernatants are strongly enriched in the potent pro-inflammatory cytokine Interleukin-1β (IL-1β).

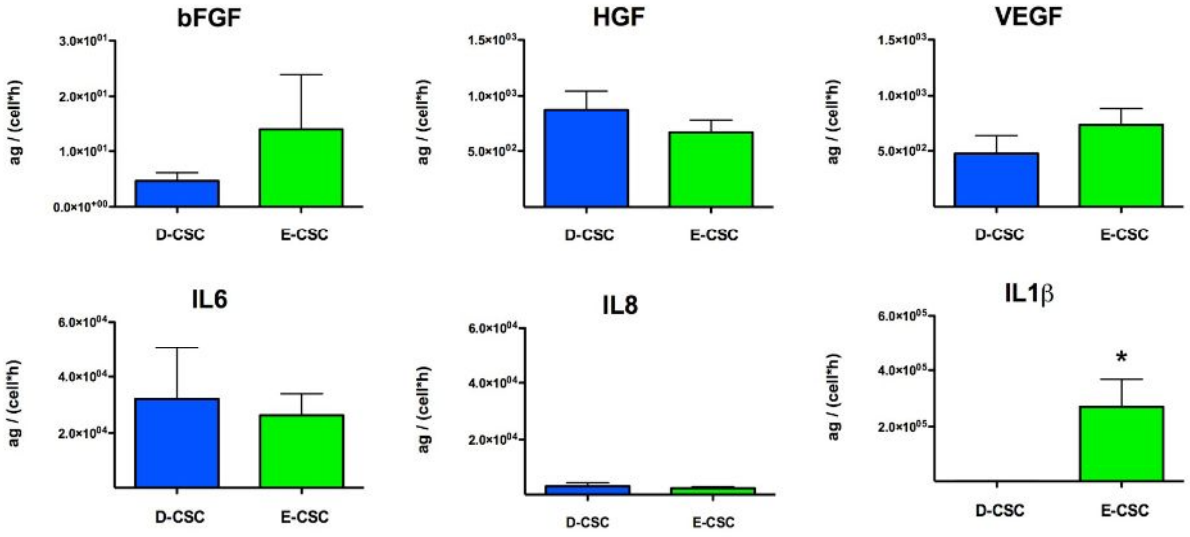

Figure 1.4 CSC secretome. *Histograms showing the quantity of pro-angiogenic (bFGF, HGF, VEGF) and senescence-associated (IL6, IL8, IL1β) cytokines released by D-CSC and E-CSC in the culture supernatant. The values have been normalized for the volume of the collected supernatant, the number of cells and the time of incubation. Values are means±SEM. * p<0.05 vs D-CSC.*

1.3.1 E-CSC secretome is not able to protect adult rat cardiomyocytes from a simulated ischemia-reperfusion injury *in vitro*

The biological effect of E-CSC secretome was evaluated on adult rat cardiomyocytes exposed *in vitro* to a simulated ischemia/reoxygenation injury (SI/RO), as previously described[217; 218].

Briefly, cardiomyocytes were incubated for 40 minutes with an "ischemia buffer" at pH=6.2 and under hypoxic conditions to simulate the *in-vivo* ischemia situation. After which cardiomyocytes were incubated for 17 hrs in normoxic conditions to simulate the phase of reperfusion that in animals follows the ischemic event; in fact, the border zone has a level of perfusion that is intermediate between the ischemic myocardium and the healthy one[219], and cardiomyocytes located in the myocardium bordering the ischemic area are reoxygenated as the result of the formation of new blood vessels (angiogenesis).

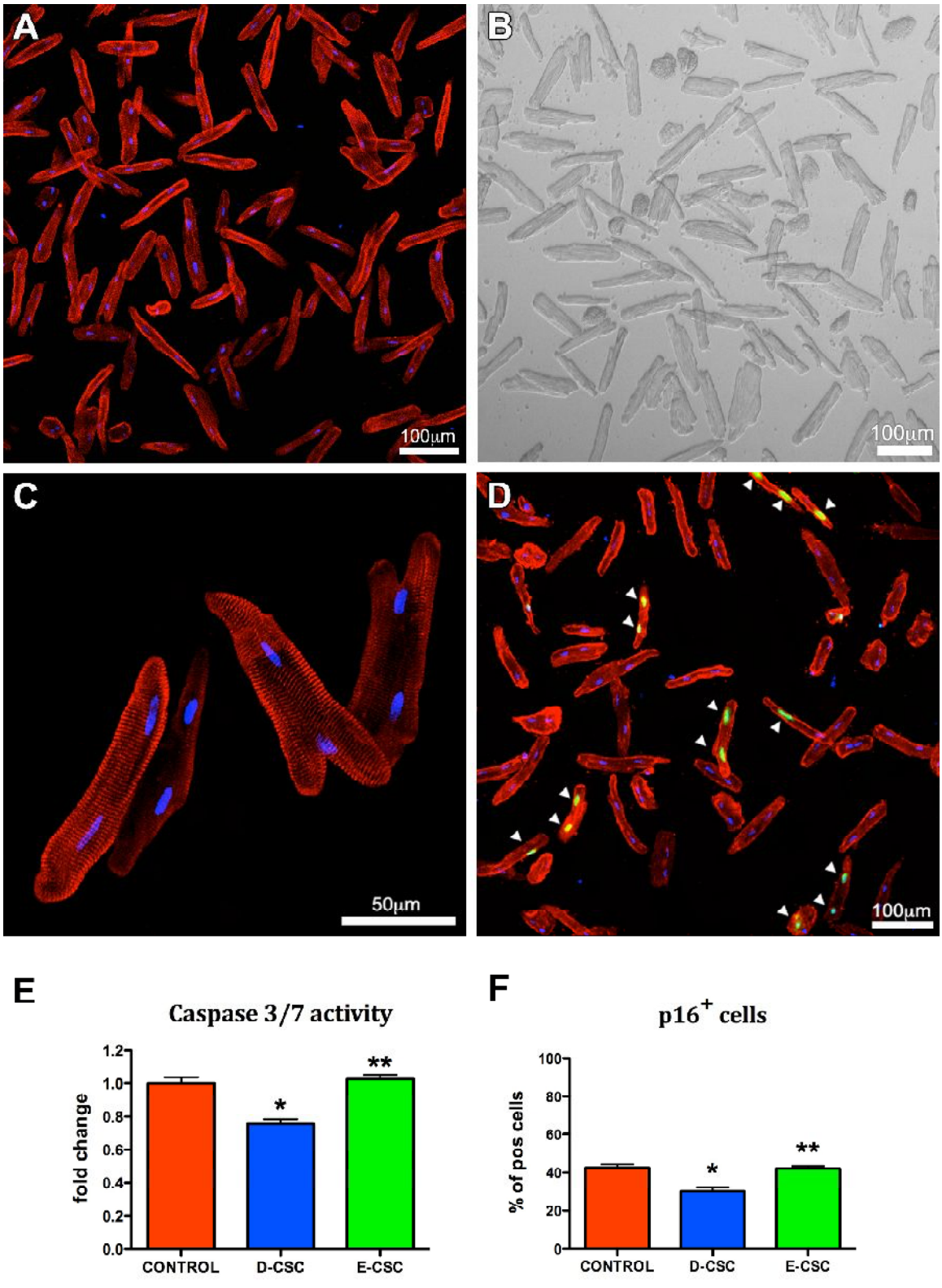

Figure 1.5 *In vitro* simulated ischemia-reperfusion experiment on isolated rat adult cardiomyocytes. *Confocal* ***(A, C, D)*** *and phase-contrast optical* ***(B)*** *images of cardiomyocytes in culture. Cells are shown at higher magnification in* ***(C)***. ***D****: senescent cardiomyocytes are recognized by the green fluorescence of p16 inside the nuclei (arrows). Cardiomyocytes cytoplasm is labelled by α-Sarcomeric Actinin depicted in red, while nuclei (DAPI) are shown in blue. Histograms summarize quantitative data of* ***(E)*** *apoptosis (measured as caspase 3/7 activity) and* ***(F)*** *senescence (measured as p16-positive cells) in cardiomyocytes after the simulated ischemia for 40min and 17h of re-oxygenation. Caspase activity was dosed by a luminescent assay. Values are means ±SEM. * p<0.05 vs Control; ** p<0.05 vs D-CSC.*

To evaluate the protective effect of D- and E-CSC secretome, the post-conditioning of cardiomyocytes was performed in D- or E-CSC conditioned medium. The results show that, while D-CSC's secretome is able to protect cardiomyocytes from apoptosis (evaluated as Caspase 3/7 activity) and senescence (evaluated as p16 expression), E-CSC's secretome does not (**fig. 1.5**).

Subsequently, to investigate the role played by the pro-inflammatory and pro-apoptotic IL-1β in the failure to protect cardiomyocytes, CSC conditioned media were supplemented with a blocking antibody for the cytokine prior to incubation on the cells. As shown in **fig. 1.6**, the neutralization of IL-1β in E-CSC supernatants restores the protective effect on cardiomyocytes, strongly reducing their apoptosis and senescence.
Importantly, the neutralization of IL-1β in D-CSC supernatants does not exert any effect, in support that the SASP characterizes only senescent E-CSC.

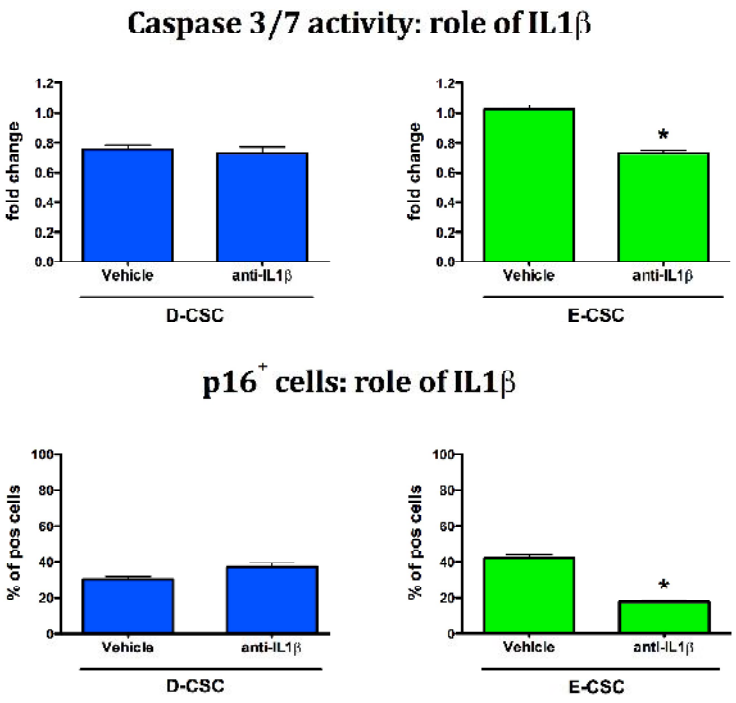

Figure 1.6 Effect of the pro-inflammatory cytokine IL1β, released by E-CSC in cell supernatant, on isolated rat adult cardiomyocytes. *Histograms summarize quantitative data of apoptosis (measured as caspase 3/7 activity, dosed by a luminescent assay, in the upper panel) and senescence (measured as p16-positive cells in immunofluorescence, in the bottom panel) in cardiomyocytes exposed to a simulated ischemia for 40min and re-oxygenated in CSC supernatant for 17h, with and without neutralization of* IL1β *in CSC supernatant using a neutralizing antibody. Values are means±SEM.*
** p<0.05 vs E-CSC Vehicle.*

1.3.2 E-CSC secretome is less efficient in stimulating angiogenesis in endothelial cells *in vitro*

Since angiogenesis is an important mechanism by which cells employed in cell therapy can contribute to the regeneration of the damaged heart, guarantying the perfusion of the new tissue, the capacity of D- and E-CSC's secretome to stimulate angiogenesis in endothelial cells (HUVECs) *in vitro* was investigated.

Both D- and E-CSC's secretomes are effective in stimulating the assembling of HUVECs in tubular networks when seeded on matrigel substrate, although E-CSC's secretome was less effective than D-CSC's one (**fig. 1.7**).

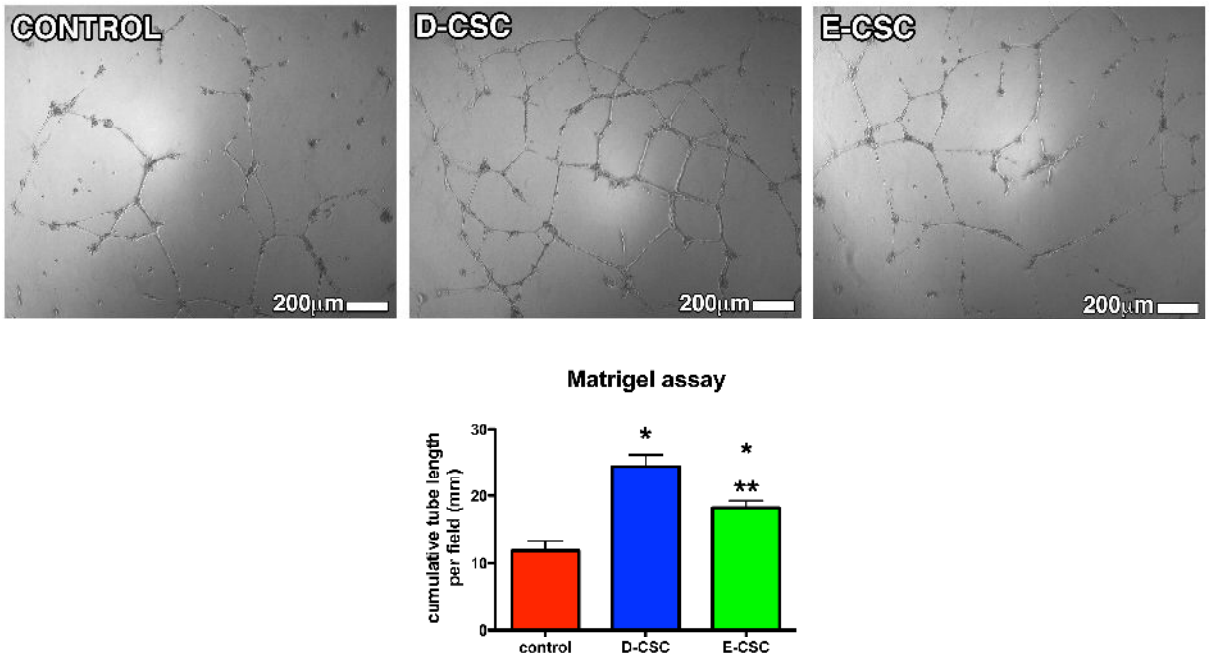

Figure 1.7 Effects of D- and E-CSC conditioned media on angiogenesis of endothelial cells *in vitro*. *Representative phase-contrast optical images of HUVECs forming tubular endothelial networks when cultured for 20 hours on matrigel substrate. Histograms summarize quantitative data of the length of tubes formed by HUVECs. Values are means±SEM.*
** p<0.05 vs Control; ** p<0.05 vs D-CSC.*

In conclusion, these data demonstrate that cultures of CSCs isolated from failing explanted hearts are significantly enriched in senescent cells, which are characterized by 1. a potent pro-inflammatory secretome and 2. a functional impairment.

2- Senescent Cardiac Stem Cells show a limited regenerative potential *in vivo*

Once demonstrated that E-CSC are senescent and functionally impaired *in vitro*, the impact that cellular senescence exerts on CSCs *in vivo* regenerative ability has been tested.
At this aim, a mouse model of acute myocardial infarction was selected as a model of heart failure, since animals develop an adverse cardiac remodeling after the permanent ligation of a coronary artery[220].
Myocardial infarction was induced in immunodeficient SCID/beige mice through the permanent ligation of the left anterior descending coronary artery, immediately after which D- or E-CSC or their vehicle were injected within the peri-infarct myocardium. After 14 days animals were sacrificed and hearts analyzed.

2.1 Hemodynamic and anatomic outcomes

As shown in **fig. 2.1**, cell therapy with both the cell types globally improved cardiac output respect to vehicle-treated mice. However, D-CSC were more effective than E-CSC in promoting the recovery of the organ regarding both 1. the dimensional parameters, including LVAW and LVESV, and 2. the functional parameters, including LVSV, LVEF, LVFS and dP/dT.

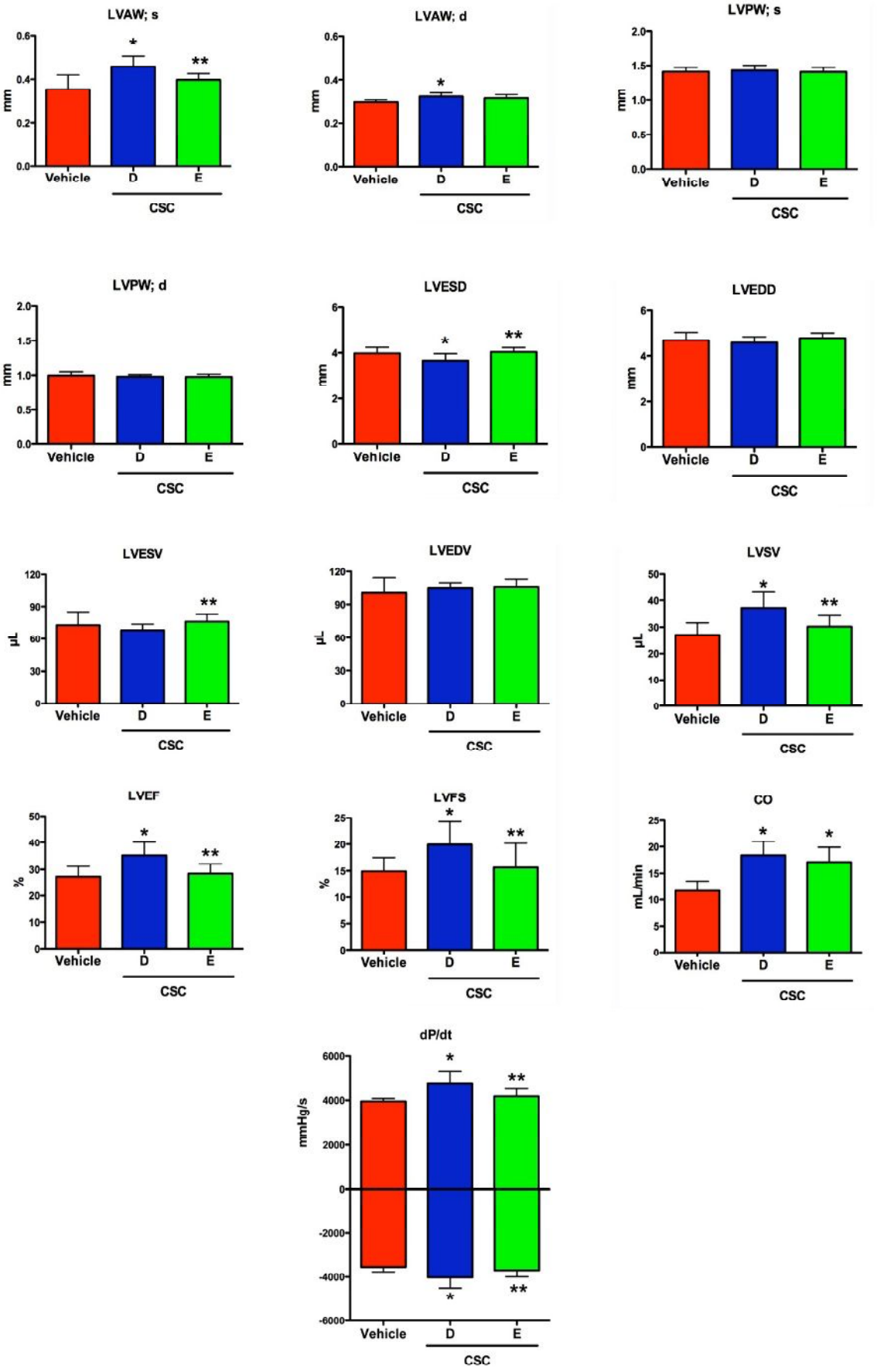

Figure 2.1 Anatomic and functional parameters *of infarcted mouse hearts injected either with Vehicle (n=17) or D-CSC (n=18) or E-CSC (n=17), 14 days post-MI. For abbreviations see the "List of abbreviations". Values are means±SEM.*
** p<0.05 vs Vehicle; ** p<0.05 vs D-CSC.*

2.2 E-CSC do not limit the scar size in infarcted ventricles

The loss of functional cells and the concomitant substitution of the vital tissue with fibrosis plays a key role in the establishment and progression of cardiac failure[221]. In order to study whether exogenous injected CSCs were able to limit this phenomenon, the size of the fibrotic scar was evaluated in the left ventricle.

As shown in **fig. 2.2**, only D-CSC were able to reduce the scar size compared to vehicle-treated mice.

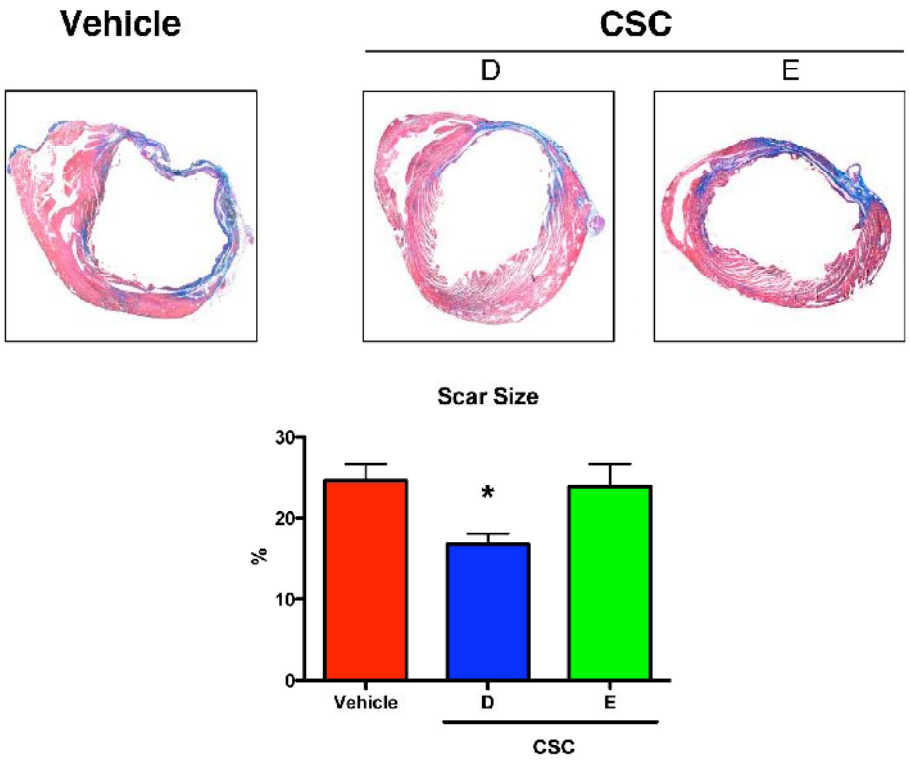

Figure 2.2 Scar size in the infarcted mouse hearts. *Histology images show Azan Mallory staining (in blue: collagen) of transverse sections of infarcted mouse hearts injected either with Vehicle (n=17) or D-CSC (n=18) or E-CSC (n=17), 14 days post-MI. Bar graphs show the fraction (%) of myocardium occupied by the scar. Values are means±SEM. * p<0.05 vs Vehicle.*

2.3 E-CSC do not stimulate angiogenesis in the infarcted heart

Many stem cells can induce neovascularization by secreting chemokines and pro-angiogenic factors (like VEGF, bFGF, HGF, IGF-1). The resulting neovascularization may improve blood supply to the viable cells that remain in the infarcted region and thus improve cardiac function. D-CSC but not E-CSC were able to stimulate the formation of capillaries and small arterioles in the infarcted ventricle, compared to vehicle-receiving mice (**fig. 2.3**). E-CSC showed a capacity to stimulate angiogenesis significantly reduced respect to that of D-CSC.

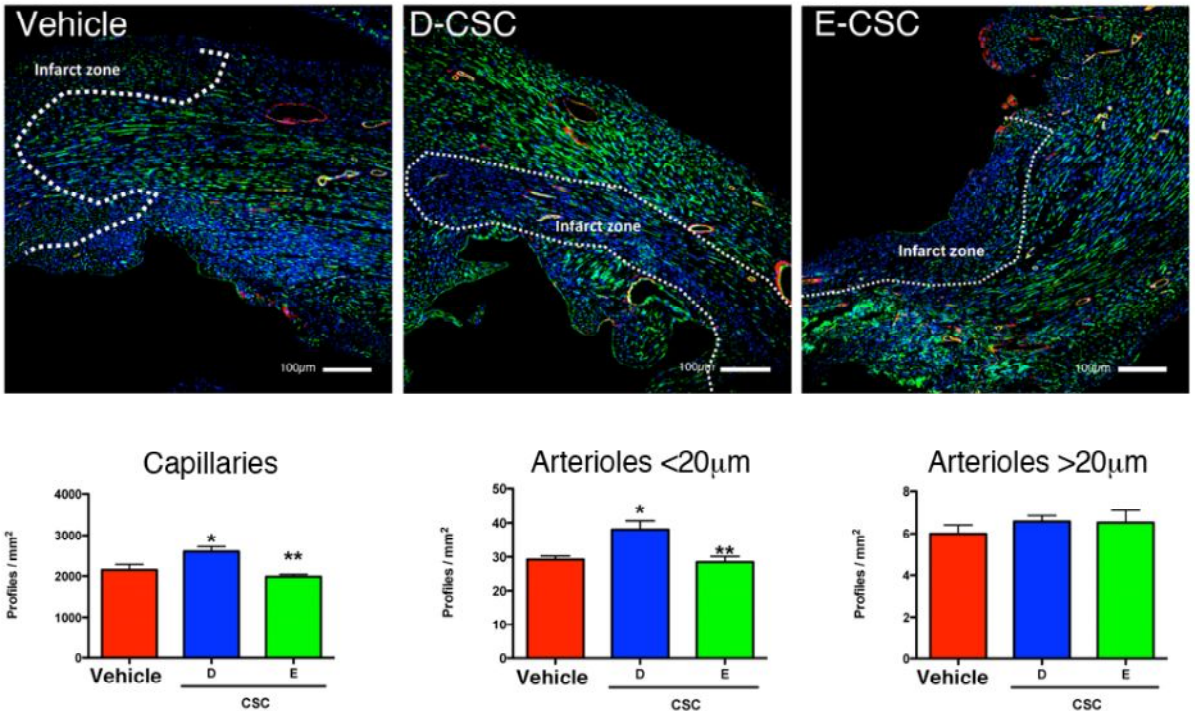

Figure 2.3 Angiogenesis in the infarcted mouse hearts. *Images show angiogenesis staining in transverse sections of infarcted mouse hearts injected either with Vehicle (n=17) or D-CSC (n=18) or E-CSC (n=17), 14 days post-MI. Capillaries are recognized by the green fluorescence of Isolectin B4, while arterioles are recognized by the red fluorescence of α-Smooth Muscle Actin. Nuclei are depicted in blue. Bar graphs show the density of capillaries, small (<20μm in diameter) and large (>20μm in diameter) arterioles in the peri-infarct zone. Values are means±SEM. * p<0.05 vs Vehicle; ** p<0.05 vs D-CSC.*

2.4 E-CSC are not able to protect ischemic cardiomyocytes *in vivo* and to recruit resident murine CSCs in the site of injury

Myocyte growth and death play an important role in myocardial repair. Myocyte proliferation is required to substitute cells lost during the injury, while apoptosis represents an important pathophysiologic mechanism causing progressive cardiomyocyte loss and left ventricular dilatation, even late after AMI. In addition, cardiomyocyte senescence should be avoided to preserve the regenerative capacity of the organ. Last, autophagy has been described to have a dual role: it can represent a process positive for the cells, helping their survival during starvation (as it happens during AMI) but it also plays a primary role in the transition towards the senescence state[141].

For all these reasons, the processes mentioned above have been analyzed in both the myocardial peri-infarct zone and the spared remote zone.

As shown in **fig. 2.4**, in the peri-infarct zone, only mice that received D-CSC were characterized by an increased number of proliferating myocytes and a reduced number of senescent and apoptotic myocytes respect to mice that did not receive any cell therapy.

Conversely, in peri-infarct myocardium, E-CSC increased cardiomyocyte senescence, apoptosis and the number of myocytes showing increasing levels of autophagic markers, compared to D-CSC treated animals. The increase in cardiomyocyte senescence was observed also in the remote myocardium.

The main goal of cell therapy in AMI is the replacement of lost tissue with viable, contracting myocardium with limited scarring and fibrotic tissue deposition. One important mechanism is the stimulation of endogenous primitive cells to produce new functional myocytes. Exogenous injected cells, of various sources and origins, used in cell therapy can activate endogenous progenitor cells, recruiting them in the site of injury and thus contributing to myocardial repair. For these reasons, the density of primitive cells in the infarcted ventricle was investigated. As shown in **fig. 2.5**, a significant increase in the density of cardiac primitive and progenitor cells was observed only in D-CSC injected animals.

Altogether, the data illustrated so far clearly demonstrate that E-CSC are not only functionally impaired *in vitro*, but they are also endowed with a blunted potential to regenerate a mouse infarcted heart, *in vivo*.

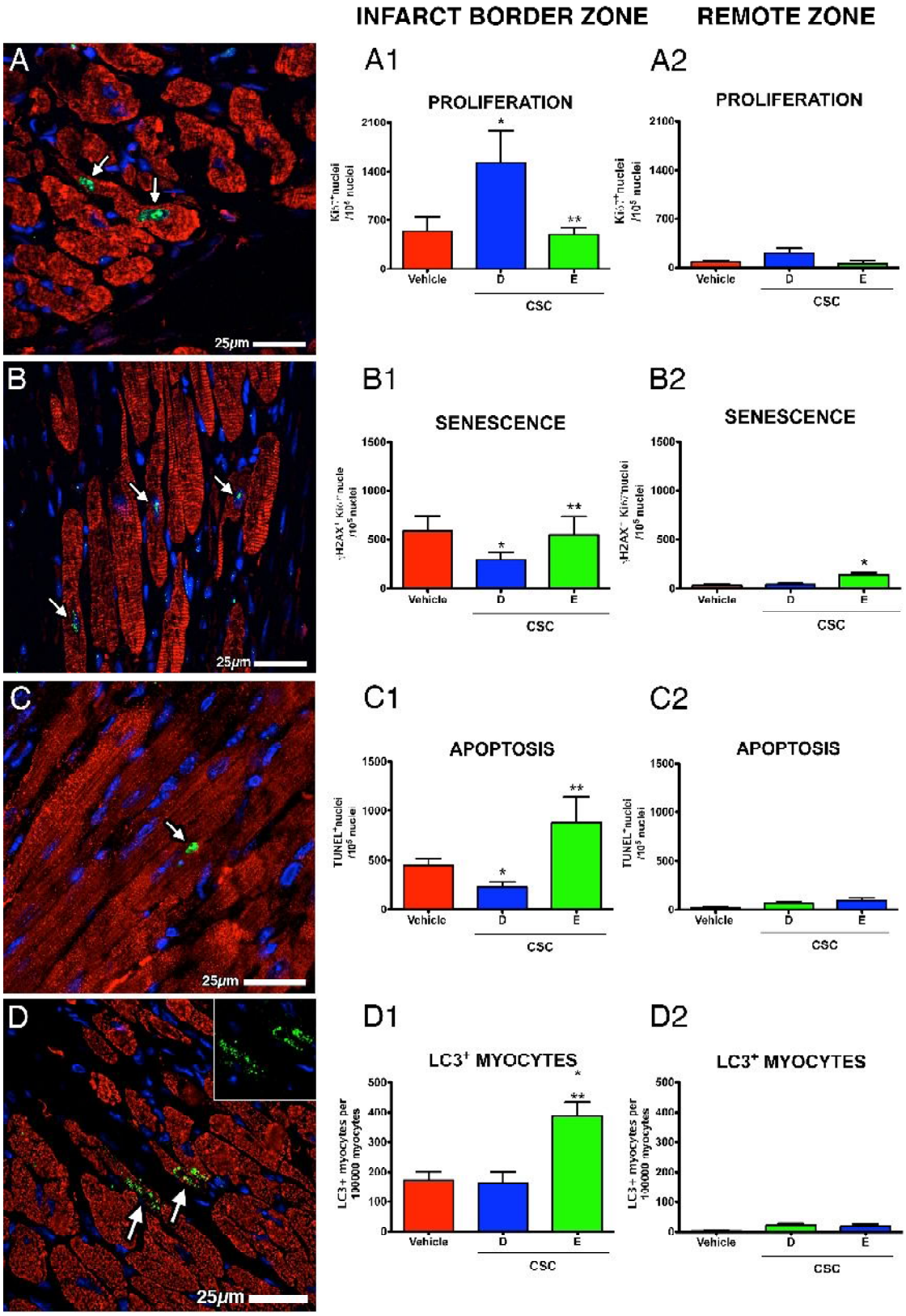

Figure 2.4 Cardiomyocytes in the infarcted mouse hearts. *Images show confocal staining of cardiomyocytes in transverse sections of infarcted mouse hearts injected either with Vehicle (n=17) or D-CSC (n=18) or E-CSC (n=17), 14 days post-MI.* ***A****: the green fluorescence of Ki67 indicates proliferating cardiomyocytes;* ***B****: the green fluorescence of γH2AX (in the absence of the proliferation marker Ki67) indicates senescent cardiomyocytes;* ***C****: the green fluorescence of TUNEL recognizes apoptotic cardiomyocytes;* ***D****: the green fluorescence of LC3 recognizes cardiomyocytes expressing autophagic markers.* ***(A-D)****: cardiomyocyte cytoplasm is labelled by the red fluorescence of α-Sarcomeric Actin. Nuclei are recognized by the blue fluorescence of DAPI. Histograms summarize quantitative data on cardiomyocytes proliferation* ***(A1, A2)****, senescence* ***(B1, B2)****, apoptosis* ***(C1, C2)*** *and autophagy* ***(D1, D2)*** *in the infarct border zone and remote zone. Values are means±SEM. * p<0.05 vs Vehicle; ** p<0.05 vs D-CSC.*

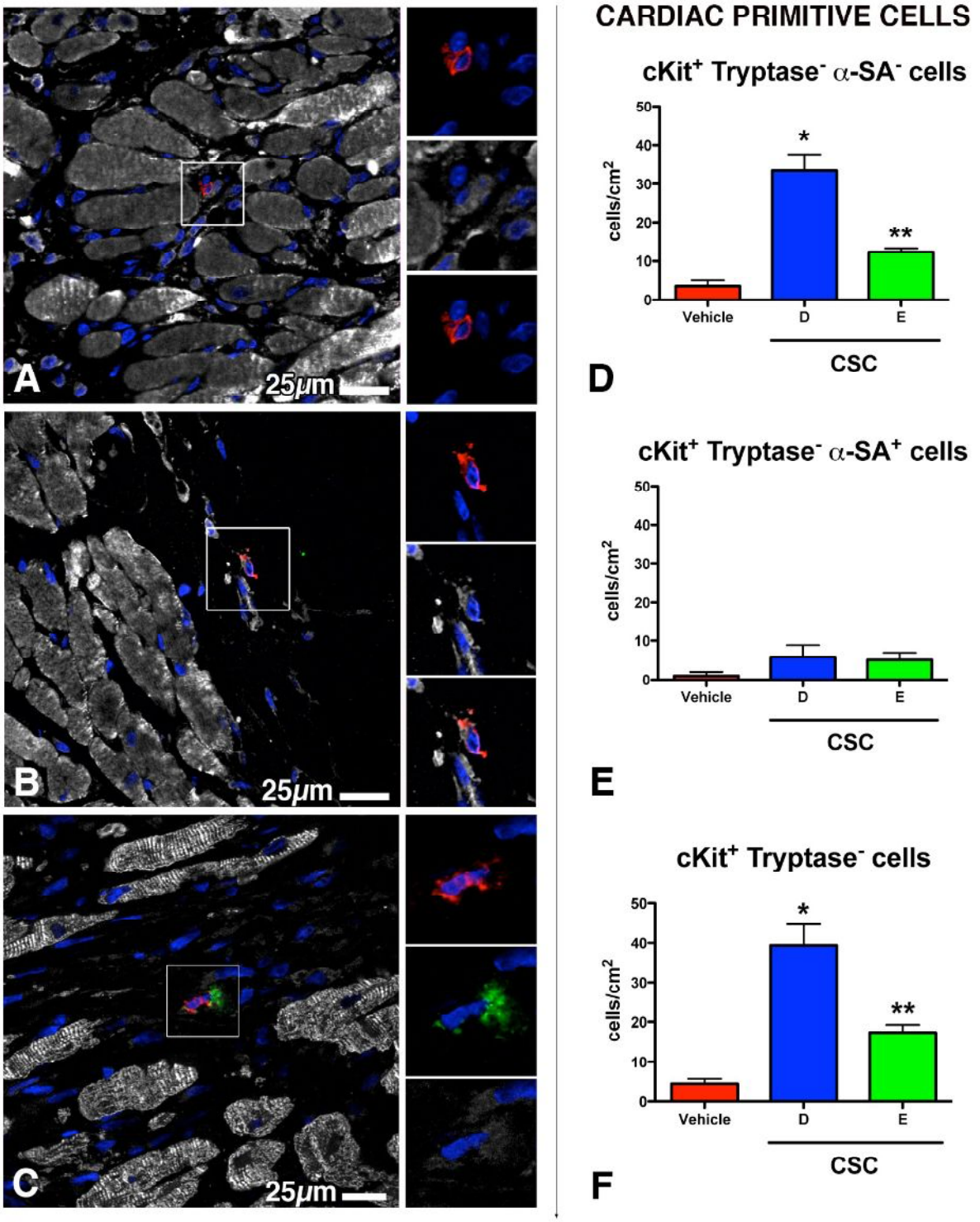

Figure 2.5 Primitive cardiac stem cells in the infarcted mouse hearts. *Confocal images of cardiac primitive cells in transverse sections of infarcted mouse hearts injected either with Vehicle (n=17) or D-CSC (n=18) or E-CSC (n=17), 14 days post-MI.* ***A****: cardiac stem/progenitor cell (c-Kit$^+$ aSA$^-$ Tryptase$^-$);* ***B****: cardiomyocyte precursor cell (c-Kit$^+$ aSA$^+$ Tryptase$^-$);* ***C****: mastocytes (c-Kit$^+$ Tryptase$^+$). c-Kit is depicted in red, Tryptase in green, α-Sarcomeric Actin in white and nuclei (DAPI) in blue. Histograms summarize quantitative data of the density of stem and progenitor cells* ***(D)****, cardiomyocyte precursors* ***(E)*** *and total cKit-positive cardiac primitive cells* ***(F)*** *in the infarct border zone of left ventricles. Values are means±SEM. * p<0.05 vs Vehicle; ** p<0.05 vs D-CSC.*

2.5 Human cells show a poor engraftment in the murine hearts

Last, in order to verify if human cells injected in mouse hearts directly contributed to the formation of new viable tissue, thus improving the cardiac function, the entity of CSC engraftment in mice hearts was evaluated. To this aim, sections of the left ventricle were stained with an antibody specific for human mitochondria.

As illustrated in **fig 2.6** (representative image) on the right, only single, very rare cells positive for the human marker could be detected in both D- and E-CSC treated mice.

This observation strongly suggests that transplanted human cells do not survive for long time in the animal tissues, and that 14 days after injection few human cells have been capable to survive, engraft and possibly differentiate in cardiac terminally differentiated cells. This observations corroborate the hypothesis of a paracrine mechanism of action of transplanted cells[67], supposed to be beneficial in the case of D-CSC, while limiting and destroying for the surrounding cells in the case of E-CSC, characterized by the SASP.

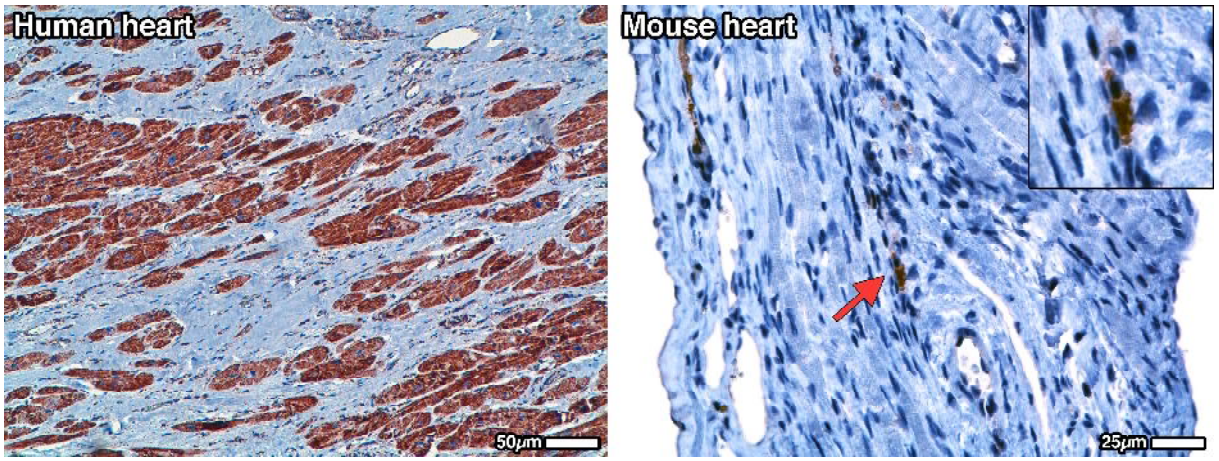

Figure 2.6 Human CSCs injected in the murine hearts show a poor engraftment 14 days after-MI and injection. ***On the left****, a representative image of a human infarcted heart tissue stained with an antibody anti-human mitochondria, as a positive control; the brown color of the viable cardiomyocytes is index of the presence of the antigen.* ***On the right****, an image of a murine infarcted left ventricle section stained with an antibody anti-human mitochondria. A human cell could be possibly observed. In general, no CSCs could be detected in rodents hearts 14 days post-MI, that means a poor engraftment of cells.*

3- Molecular pathways altered in senescent Cardiac Stem Cells

Once directly demonstrated that CSCs isolated from human failing hearts display a functional impairment both *in vitro* and, even more importantly, *in vivo*, failing to contribute to myocardial regeneration, the following step was the understanding of which, among the molecular pathways associated to cell senescence and aging, are altered in E-CSC and thus are possibly responsible for their behaviour.

3.1 IL-1β/NFκB signaling pathway

Moving from the assumptions that E-CSC are characterized by an altered secretome (SASP) and that, principally, release large amounts of the cytokine IL-1β in their culture supernatants, the pathway involving the activation of NFκB, activated by the binding of the cytokine to its receptor (IL-1R), was for first investigated. The activation of NFκB requires the degradation of the inhibitory IκB proteins, which sequester NF-κB complexes in the cytoplasm. Stimulus-induced degradation of IκB proteins is initiated through phosphorylation by the IκB kinase (IKK) complex, which consists of two catalytically active kinases, IKK α and IKKβ, and the regulatory subunit IKKγ (NEMO).

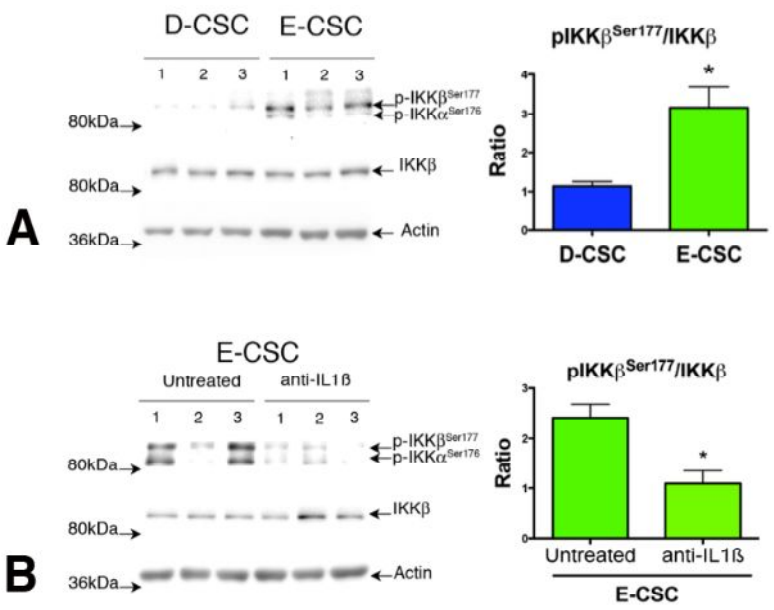

Figure 3.1 Molecular pathways associated with E-CSC dysfunction and senescence. *Representative Western Blot of cell extracts obtained from D-CSC and E-CSC samples **(A)** and E-CSC treated or not with an anti-IL-1β antibody **(B)**. Each lane was loaded with an independent sample (3 D-CSC and 3 E-CSC). Blotted proteins were incubated with antibodies directed against IKKβ and phospho-IKKβ^{Ser177}.*
Histograms show the results of the densitometric analyses as means±SEM.
** p<0.05 vs D-CSC or untreated E-CSC.*

The enhanced activation status of IKKβ in senescent E-CSC, compared to D-CSC, is confirmed by phosphorylation on Ser177 (**fig. 3.1A**). IKKβ phosphorylation is reduced when IL-1β in CSCs supernatants is neutralized using a blocking antibody (**fig. 3.1B**), in support that the cytokine is the responsible signal triggering the described pathway.

Activated NFκB translocates inside the nucleus and begin the transcription of its targets, among them the same IL-1β and the micro-RNA-146a; this latter is induced in senescent cells by the SASP[109] and acts as a negative feedback loop that limits excessive SASP activity, inhibiting the IL-1R[108].

Both the expression levels of IL-1β and micro-RNA-146a are higher in E-CSC than in D-CSC (**fig. 3.2A**).

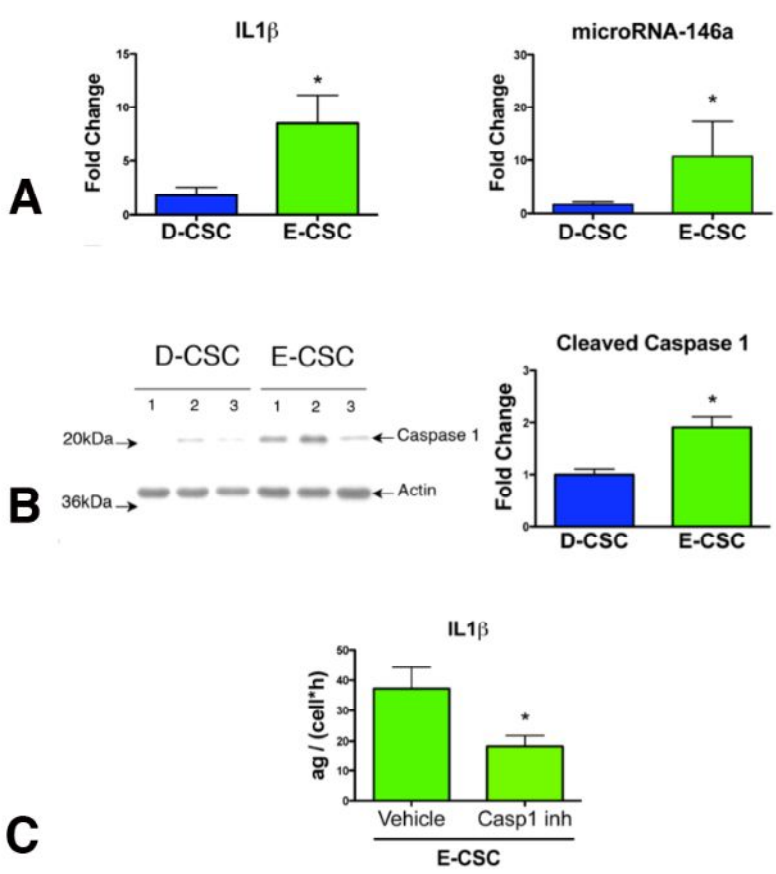

Figure 3.2 Molecular pathways associated with E-CSC dysfunction and senescence. ***(A)*** *Histograms show the expression levels of IL-1β and micro-RNA-146a in D- and E-CSC.*
(B)Representative Western Blot of cell extracts obtained from D-CSC and E-CSC samples. Each lane was loaded with an independent sample (3 D-CSC and 3 E-CSC). Blotted proteins were incubated with antibodies directed against Cleaved Caspase 1. Histograms show the results of the densitometric analyses. ***(C)*** *Histograms show the amount of IL-1β secreted by E-CSC either in the absence (Vehicle) or presence (Casp1 inh) of the caspase 1 inhibitor Z-YVAD-FMK.*
*(C)Data are presented as means±SEM. * p<0.05 vs D-CSC or E-CSC Vehicle.*

IL-1β is active only in its mature form which requires the action of the inflammasome, a multi-molecular innate immune complex that consists of caspase 1 (also known as IL-1 converting enzyme)[104]. Inflammasome-mediated activation of caspase 1 is critical in the processing and secretion of pro-inflammatory cytokines including IL-1β[104].

Consistently, the levels of activated cleaved Caspase 1 (the enzyme responsible for the processing of the precursor of IL-1β in its active form) are higher in E-CSC than D-CSC (**fig. 3.2B**). Moreover, the addition to E-CSC cultures of a Caspase1 inhibitor significantly reduces the amount of IL-1β released in cell supernatants (**fig. 3.2C**).

These data show that NFκB pathway is strongly activated in E-CSC, it is induced by the SASP and maintained by this latter with a positive feedback loop. The activation of IKKβ is of fundamental importance since IKKβ can crosstalk with another well known senescence associated molecular pathway: mTOR's one. In fact, IKKβ is a potent activator of mTOR by inhibiting TSC1[187].

3.2 AMPK/mTOR/Akt/Autophagy signaling pathway

AMPK/mTOR-associated signaling is the second molecular pathway that has been investigated.
The reasons behind the choice to study this pathway are different, among them: 1. E-CSC are characterized by an up-regulation of genes encoding for proteins involved in metabolic (lipids, carbohydrates, amino acids) pathways[43], and mTOR and AMPK are well known to be central energy sensors inside the cells[111]; 2. as told above, SASP is a potent activator of mTOR, which has an important role in controlling aging processes[187]; 3. mTOR controls autophagy, a process that drives cell senescence[141] and is associated with the SASP[139].

AMP-activated kinase (AMPK) is a highly conserved cell energy sensor; in particular, it senses increased levels of AMP[146]. This Ser/Thr kinase has a central role since it coordinates a large signaling network of transcription factors and controls several cell processes like growth and autophagy, lipid and glucose metabolism, cell polarity[147]. Among its activities, AMPK controls also NFκB signaling.
As indicated in **fig. 3.3A**, E-CSC show a significant reduction in activated phosphorylated AMPK levels respect to D-CSC.

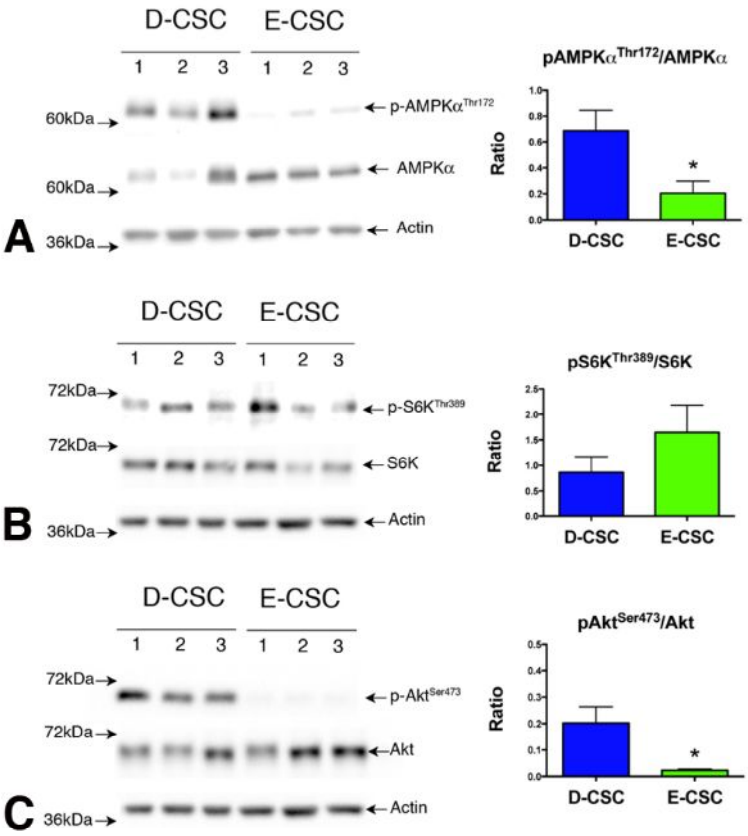

Figure 3.3 Molecular pathways associated with E-CSC dysfunction and senescence. *Representative Western Blot of cell extracts obtained from D-CSC and E-CSC samples. Each lane was loaded with an independent sample (3 D-CSC and 3 E-CSC). Blotted proteins were incubated with antibodies directed against AMPKα, phospho-AMPKα^{Thr172}, S6K, phospho-S6K^{Thr389}, Akt, phospho-Akt^{Ser473}. Histograms show the results of the densitometric analyses as means±SEM. * p<0.05 vs D-CSC.*

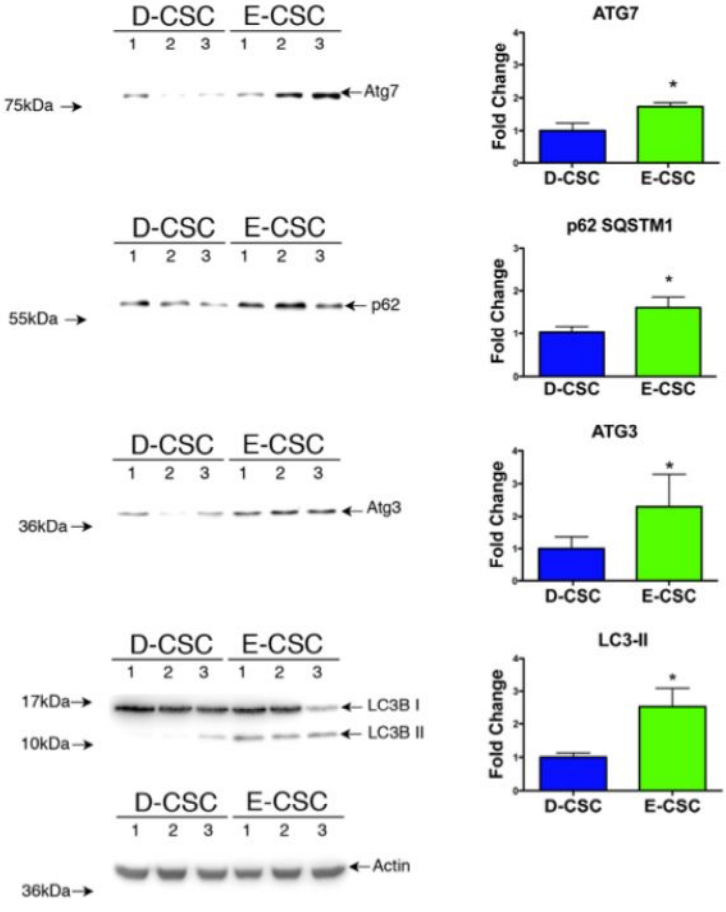

Figure 3.4 Molecular pathways associated with E-CSC dysfunction and senescence: autophagic markers. *Representative Western Blot of cell extracts obtained from D-CSC and E-CSC samples. Each lane was loaded with an independent sample (3 D-CSC and 3 E-CSC). Blotted proteins were incubated with antibodies directed against Atg7, p62/SQSTM1, Atg3, LC3-I and LC3-II. Histograms show the results of the densitometric analyses as means±SEM. * p<0.05 vs D-CSC.*

AMPK inhibits TORC1 by two different mechanisms, acting on both Raptor and TSC2[147].
While total levels of mTOR do not differ between D- and E-CSC, TORC1 hyper-activation in E-CSC is confirmed by three evidences: 1. the downstream TORC1 target S6K tends to be more activated in E-CSC than in D-CSC, as demonstrated by the phosphorylation on Thr389 (**fig. 3.3B**); 2. TORC1 negatively regulates Akt, and, in line, activation of this latter is reduced in E-CSC (**fig. 3.3C**); 3. autophagy, a process regulated by TORC1, is altered in E-CSC **(fig. 3.4)**, as shown by hyper-expression of autophagosomes related proteins (ATG3 and 7, LC3II) in E-CSC. In fact, although TORC1 directly suppresses autophagy, this latter is activated by p706SK[222], activated by TORC1. In addition, it is interesting to note that E-CSC present an arrest in the autophagic flux, as documented by the accumulation of p62/SQSTM1 protein, an ubiquitously expressed cellular protein which directly interacts with LC3 on the isolation membrane and that, after the formation of autophagosomes, is incorporated into these latter and degraded. Impairment of autophagy is accompanied by accumulation of p62[137].

3.3 CREB/Sirt1 signaling pathway

Last, since both AMPK and Akt[167] phosphorylate and activate CREB, a transcription factor that induces the expression of Sirtuins - proteins deacetylase that play a prominent role in cellular senescence and aging -, CREB signaling pathway was investigated in CSCs.
AMPK regulates the transcription of Sirt1, the most important mammalian Sirtuin[158]. Moreover, a marked decrement in the expression of CREB with senescence in cultured fibroblasts has been described[166].
In line with these considerations, levels of activated phospho-CREB are higher in D-CSC than in E-CSC (**fig. 3.5A**); however, the levels of Sirt1, a downstream target of CREB signaling, are similar between D- and E-CSC (**fig. 3.5C**).
CREB is involved in the regulation of the circadian rhythm - regulating its transcriptional target micro-RNA-132[169]. This latter, which represents a strong enhancer of myocardial healing[223], is significantly less expressed in E-CSC than in D-CSC (**fig. 3.5B**).
Finally, moving from the considerations that nitric oxide (NO) delays cell senescence[81] and may modulate CREB signaling[224], and moreover that Sirt1 can activate eNOS stimulating NO production, the concentration of nitrites in CSC supernatants and the levels of intracellular NO were measured. NO is a gaseous free radical with a short half-life *in vivo* of a few seconds or less (because it is lipid soluble, NO is not stored but is synthesized *de novo* and freely diffuses across lipid membranes). Therefore, the levels of the more stable NO metabolites, nitrite (NO_2^-) and nitrate (NO_3^-) are used in the indirect measurement of NO in biological fluids and as an indirect indicator of Nitric Oxide Synthase (NOS) activity.
As illustrated in **fig. 3.6**, neither NO nor nitrites levels differ between D- and E-CSC.

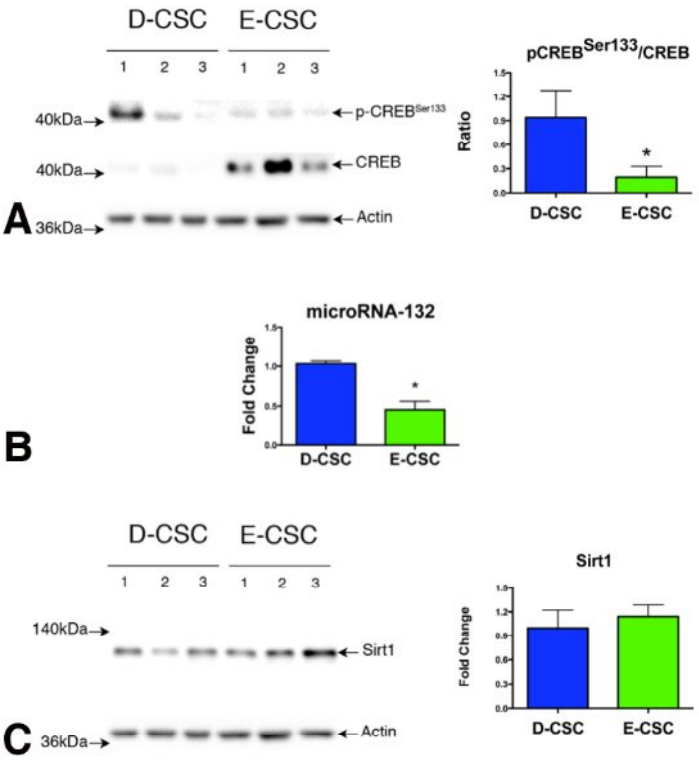

Figure 3.5 Molecular pathways associated with E-CSC dysfunction and senescence.
(A, C) *Representative Western Blot of cell extracts obtained from D-CSC and E-CSC samples. Each lane was loaded with an independent sample (3 D-CSC and 3 E-CSC). Blotted proteins were incubated with antibodies directed against CREB, phospho-CREB^{Ser133}, Sirt1. Histograms show the results of the densitometric analyses.*
(B) *Histograms show the expression levels of microRNA-132 in D- and E-CSC.*
Data are presented as means±SEM.
** p<0.05 vs D-CSC.*

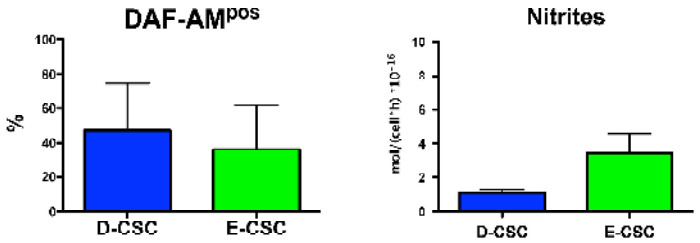

Figure 3.6 Detection of Nitric Oxide (NO) in CSCs. *Histograms summarize the quantitative analysis of the fraction of cells positive to intracellular NO (detected by flow-cytometry employing the fluorescent marker DAF-AM) and the amount of nitrites present in CSC culture supernatant. The values of nitrites have been normalized for the volume of the collected supernatant, the number of cells and the time of incubation. Values are means±SEM.*

Summarizing, overall these data indicate that senescent E-CSC are characterized by:

1. **an hyper-activation of IKKβ-NFκB signaling, triggered by IL-1β and the SASP, that through the further activation of Caspase 1 contributes to the creation of a self-maintaining loop;**
2. **an hyper-activation of TORC1, activated by IKKβ through an Akt-independent mechanism, and of its downstream target S6K (that tends to be more activated in E-CSC);**
3. **a reduced activation of Akt, AMPK and CREB;**
4. **an arrest of the autophagic flux, as demonstrated by an accumulation in p62.**

4- Rapamycin and Resveratrol rejuvenate senescent Cardiac Stem Cells *in vitro*

Once established that senescent E-CSC are functionally impaired, both *in vitro* and *in vivo*, and once identified three possible molecular pathways altered in these cells, the purpose was to interfere with these signaling pathways in the attempt to revert cell senescence, *in vitro*, ameliorating cell functional properties, *in vivo*.

Moving from the previous pilot study published by the Beltrami's group[82], the drugs selected at the aim to rejuvenate senescent E-CSC are Rapamycin and Resveratrol. The first is a TORC1 inhibitor[126] and it is also able to activate AMPK[225]; the second can activate AMPK[226] too, is able to reduce the SASP[206] and in addition it inhibits cAMP-degrading phosphodiesterases[205], leading to elevated cAMP levels required for CREB activation via PKA.

The previous pilot study[82], in which a dose-escalation screening of the drugs was performed, was fundamental to establish the optimal dosage of each drug which guarantees the best results - in term of reduction in CSC senescence - while causing the lowest cytotoxicity. Newly, with the present study, a combination of the drugs was tested on CSCs, at the aim to verify if a cocktail containing both the drugs was able to produce additive benefits on CSC biology, possibly contrasting the high cell death induced by Rapamycin with the high cell proliferation led by Resveratrol[82].

CSCs were treated for 3 days with a medium supplemented with Rapamycin (at a 10nm concentration), Resveratrol (0.5μM) or a combination of them, and analyzed for senescence markers, immunophenotype and functional properties.

In **fig. 4.1** representative images of the effects of the drugs on E-CSC at the end of the 3 days of treatment can be observed. It can be appreciated the pro-proliferative effect of Resveratrol respect to cells treated with vehicle, while Rapamycin promotes cell apoptosis[82]. In the combination of the drugs, Resveratrol is able to attenuate the cell death induced by Rapamycin.

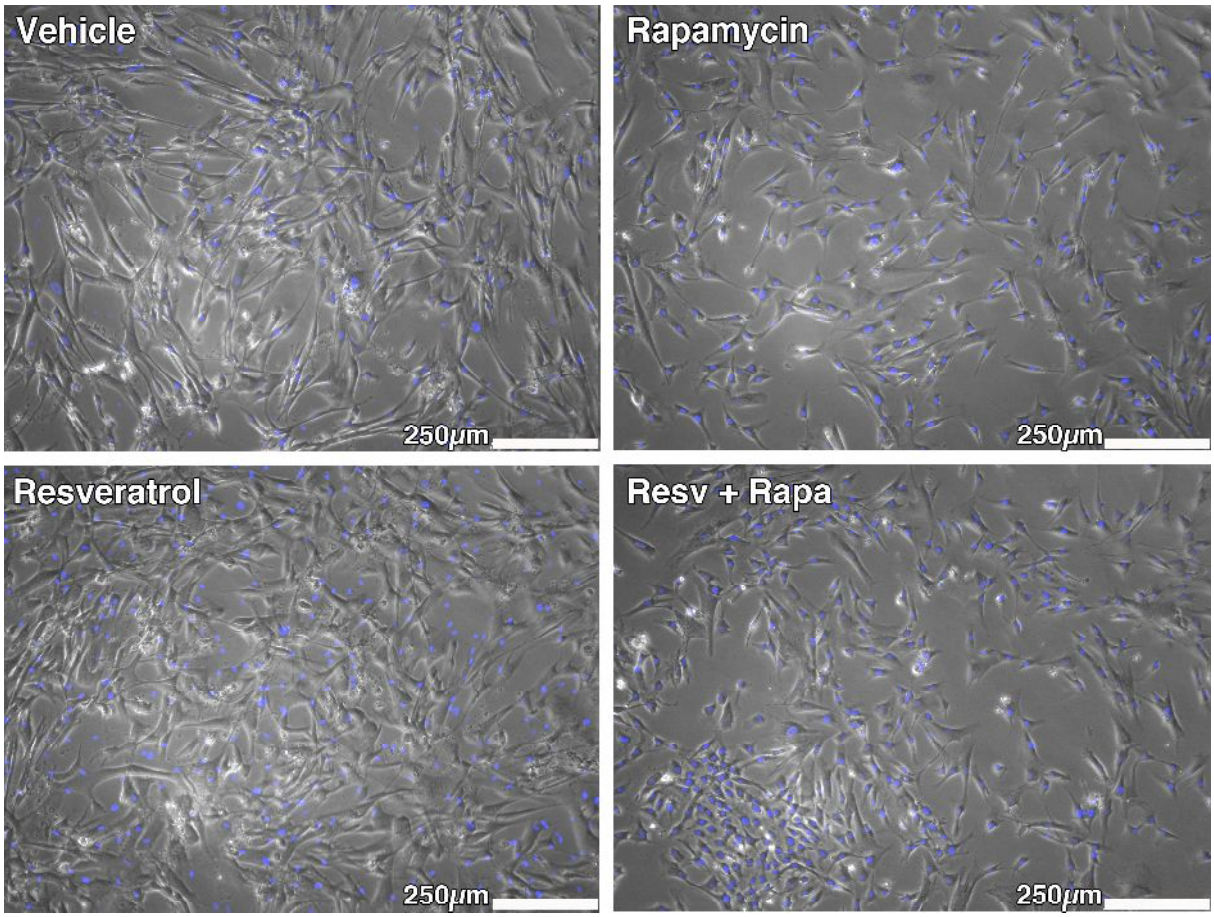

Figure 4.1 Phase contrast images of E-CSC after 72h of culture in a medium containing either Rapamycin or Resveratrol or a combination of the drugs or their Vehicle. *Nuclei are depicted in blue.*

4.1 Rapamycin and Resveratrol-treated CSCs: characterization

Both Rapamycin and Resveratrol singularly are effective in reducing E-CSC senescence (p16-pos cells), and the combined treatment does not add any additive effect; despite this, the combined treatment is fundamental in reducing the fraction of cells presenting DDR response, evaluated as γH2A.X positivity in the absence of cell proliferation (Ki67-negativity). Resveratrol but not Rapamycin reduces the fraction of apoptotic cells and, importantly, the first is able to attenuate the pro-apoptotic effect of Rapamycin when used in the combination of drugs. Last, the combination of Rapamycin and Resveratrol strongly stimulates E-CSC proliferation (**fig. 4.2**).

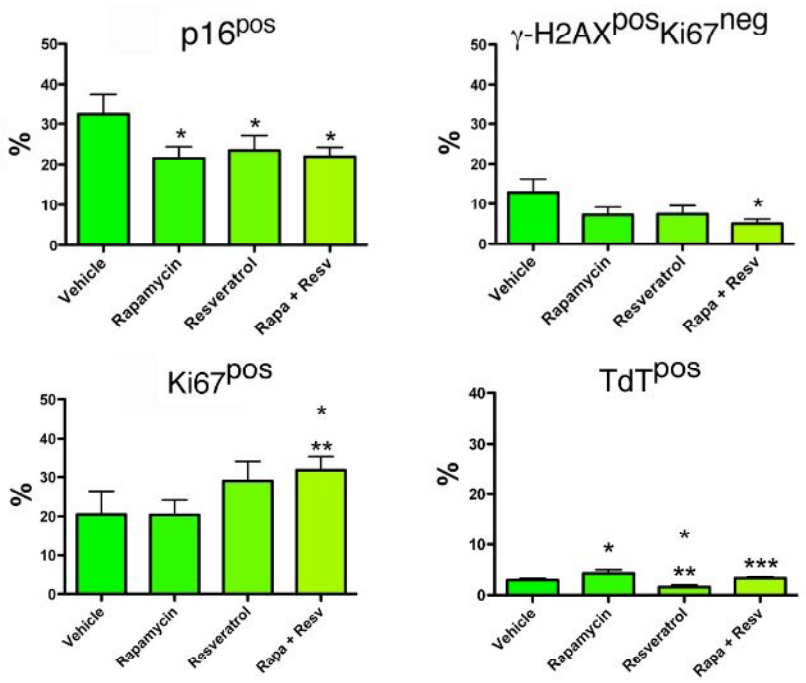

Figure 4.2 Effects of drugs treatment on E-CSC senescence, proliferation and apoptosis. *Histograms summarize the effects of Vehicle, Rapamycin, Resveratrol and Rapa+Resv (Rapamycin+Resveratrol) treatment on E-CSC senescence (represented by p16-positive cells and γ-H2AX-positive/Ki67-negative cells), proliferation (Ki67-positive cells) and apoptosis (TUNEL or TdT-positive cells).*
Values are means±SEM.
** p<0.05 vs Vehicle;*
*** p<0.05 vs Rapamycin;*
**** p<0.05 vs Resveratrol.*

Interestingly, the treatment of D-CSC with the drugs (**fig. 4.3**) does not exert any effect apart from stimulating cell proliferation when drugs are administered to the cells together.

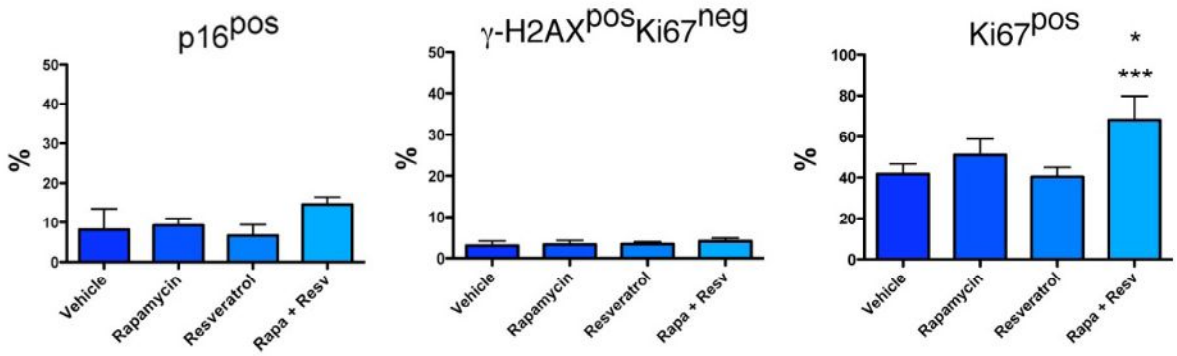

Figure 4.3 Effects of drugs treatment on D-CSC senescence and proliferation. *Histograms summarize the effects of Vehicle, Rapamycin, Resveratrol and Rapa+Resv (Rapamycin+Resveratrol) treatment on D-CSC senescence (represented by p16-positive cells and γ-H2AX-positive/Ki67-negative cells) and proliferation (Ki67-positive cells). Values are means±SEM.*
** p<0.05 vs Vehicle; *** p<0.05 vs Resveratrol.*

FACS analysis of drug treated D- and E-CSC showed that cell immunophenotype is not significantly modified by the drugs (**fig. 4.4**). The only exception regards the expression of the cardiac aging and disease associated CD49a marker[197] in E-CSC, which is positively attenuated by Rapamycin, in both the single treatment and in combination with Resveratrol.

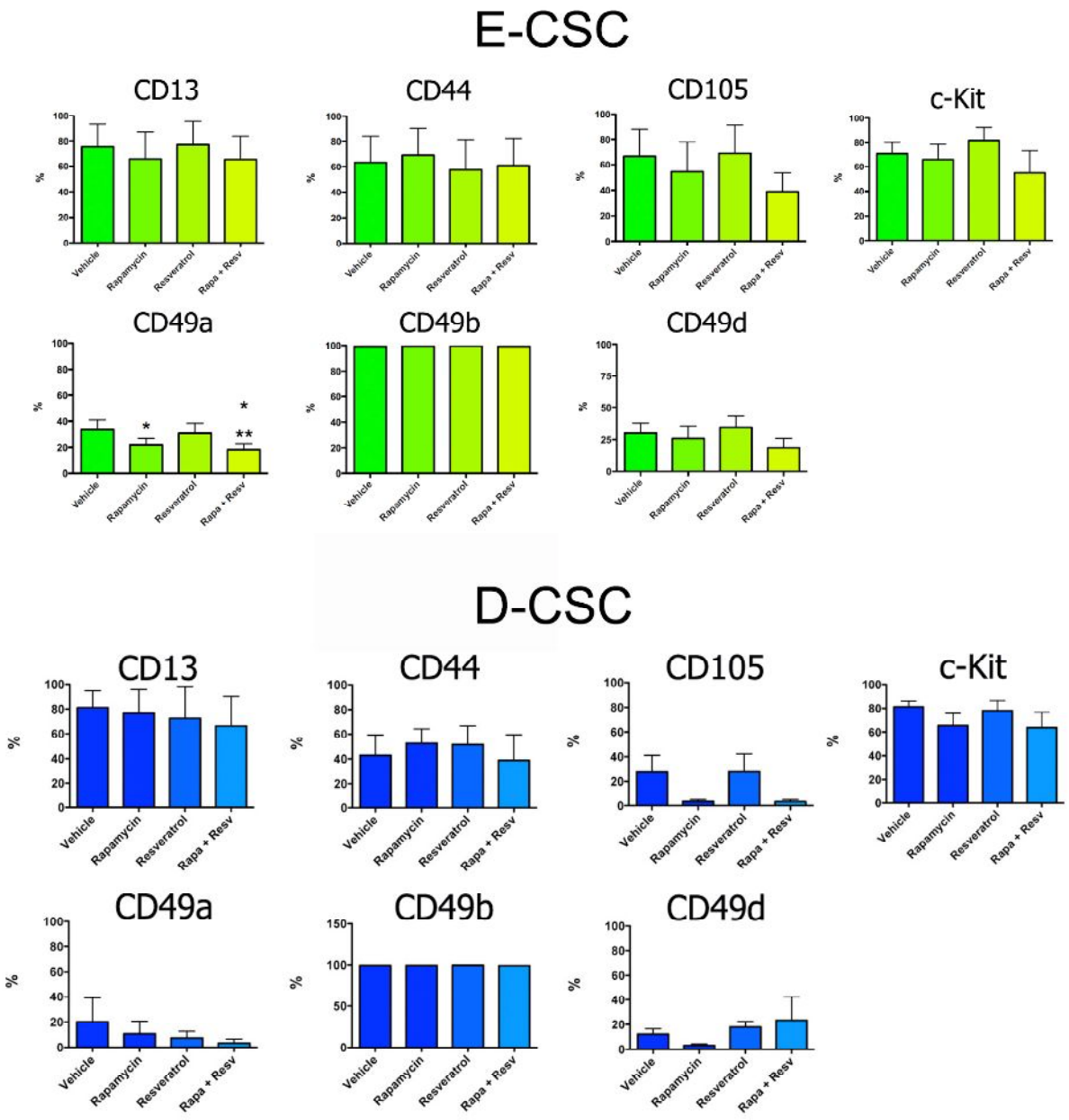

Figure 4.4 Effects of drugs treatment on D- and E-CSC immunophenotype. *Histograms summarize the effects of Vehicle, Rapamycin, Resveratrol and Rapa+Resv (Rapamycin+Resveratrol) treatment on CSC surface-antigen expression. Values are represented as means±SEM. * p<0.05 vs Vehicle; ** p<0.05 vs Rapamycin.*

Regarding the growth kinetic of CSCs, only Resveratrol is able to significantly reduce the cell population doubling time in E-CSC (**fig. 4.5**), improving cell functional properties. Conversely, drugs do not exert any effect on D-CSC CPDT.

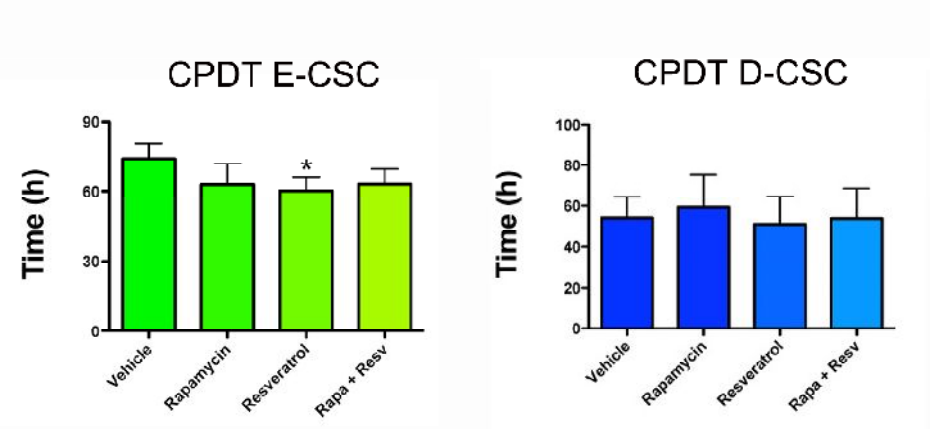

Figure 4.5 Effects of drugs treatment on D-CSC and E-CSC cell population doubling time (CPDT). *Histograms summarize the effects of Vehicle, Rapamycin, Resveratrol and Rapa+Resv (Rapamycin+Resveratrol) treatment on D-CSC and E-CSC CPDT. Values are represented as means±SEM. * p<0.05 vs Vehicle.*

Successively, the capacity of drugs to modify the migratory ability of E-CSC was tested.

A scratch assay was performed after that E-CSC were exposed for 3 days to the drugs. The mean scratch width did not differ significantly in the different culture conditions ($p>0.05$).

Fig. 4.6 shows that Resveratrol significantly increases cell motility compared to vehicle and Rapamycin treated cells. The cocktail of drugs only tends to increase cell migration speed, with Rapamycin reducing the improvement in migratory speed due to Resveratrol.

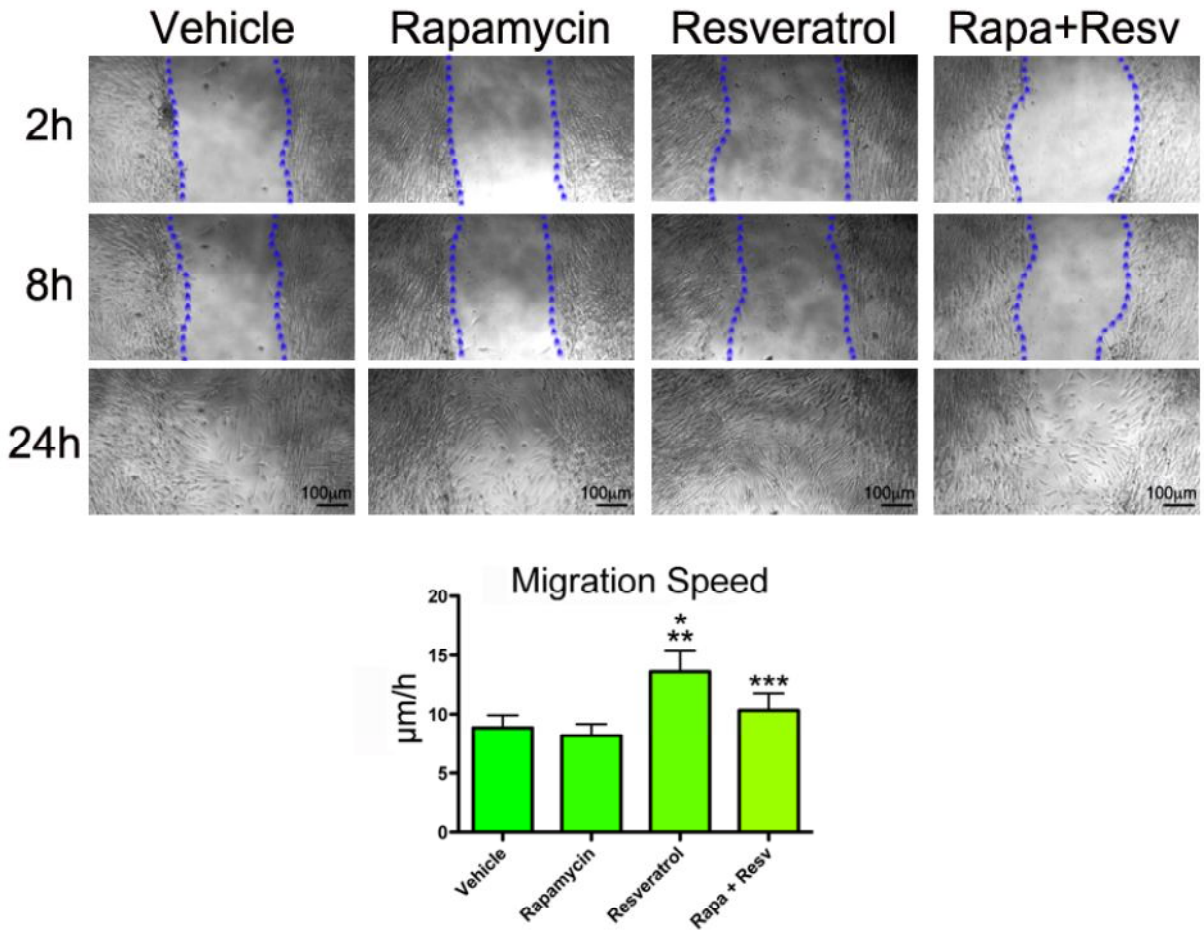

Figure 4.6 Scratch assay demonstrating the effects of drugs treatment on E-CSC motility. *Phase contrast images show the effects of Vehicle, Rapamycin, Resveratrol and Rapa+Resv (Rapamycin+Resveratrol) treatment on cell motility in a 24h-time period. After doing a scratch in the middle of the cells layer at high confluence, cells have been let to migrate for a time of 24h, until complete closure of the scratch. Images have been acquired, at a magnification of 50X, at time 0 and after 2, 8 and 24h. The blue hatches highlight the margins of the scratches. Migration speed has been calculated over the period of time between 2 and 8 hours. Histograms summarize E-CSC migration speed. Values are means±SEM.*
** p<0.05 vs Vehicle; ** p<0.05 vs Rapamycin; *** p<0.05 vs Resveratrol.*

4.2 The treatment with Rapamycin+Resveratrol improves E-CSC pro-inflammatory secretome

Preconditioning of E-CSC with Rapamycin and Resveratrol significantly modified cell's secretome. Importantly, the release of the pro-inflammatory cytokine IL-1β was remarkably reduced (**fig. 4.7**). This reduction is of fundamental importance, since the improved secretome of drugs-treated E-CSC is effective in protecting rat cardiomyocytes - exposed *in vitro* to a SI/RO injury - from apoptosis and senescence (**fig. 4.8**). No effect was observed with drug-treated D-CSC supernatants, supporting the statement that Rapamycin and Resveratrol exert their effect acting on specific molecular pathways, proper to senescent cells.

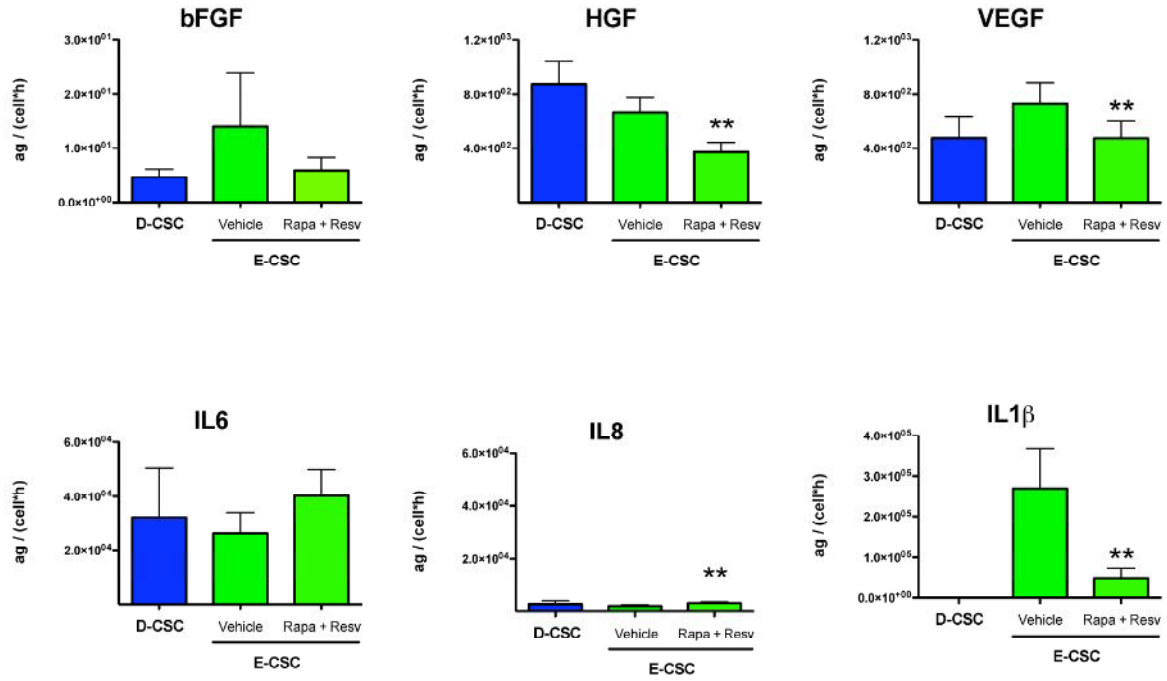

Figure 4.7 Effect of Rapamycin+Resveratrol treatment on E-CSC secretome. *Histograms showing the quantity of pro-angiogenic (bFGF, HGF, VEGF) and senescence-associated (IL6, IL8, IL1β) cytokines released by D-CSC, Vehicle-treated-E-CSC and Rapa+Resv-treated-E-CSC in the culture supernatant. The values have been normalized for the volume of the collected supernatant, the number of cells and the time of incubation. Values are represented as means±SEM. ** p<0.05 vs Vehicle-E-CSC.*

Figure 4.8 Effects of supernatants of E-CSC and D-CSC treated with Rapamycin+Resveratrol on isolated rat adult cardiomyocytes. *Histograms summarize quantitative data of apoptosis (measured as caspase 3/7 activity, dosed by a luminescent assay, in the upper panel) and senescence (measured as p16-positive cells in immunofluorescence, in the bottom panel) in cardiomyocytes exposed to a simulated ischemia for 40min and re-oxygenated for 17hrs in CSC supernatant preconditioned with Rapamycin +Resveratrol or their Vehicle. Values are means±SEM.*
** p<0.05 vs E-CSC Vehicle.*

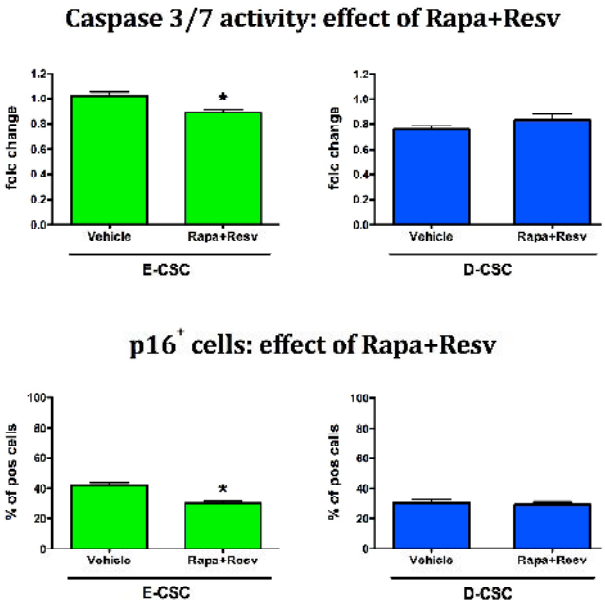

Last, supernatants of drugs-treated E-CSC are not able to stimulate the organization of endothelial cells (HUVECs) in tubular networks when seeded on matrigel substrate (**fig. 4.9**).

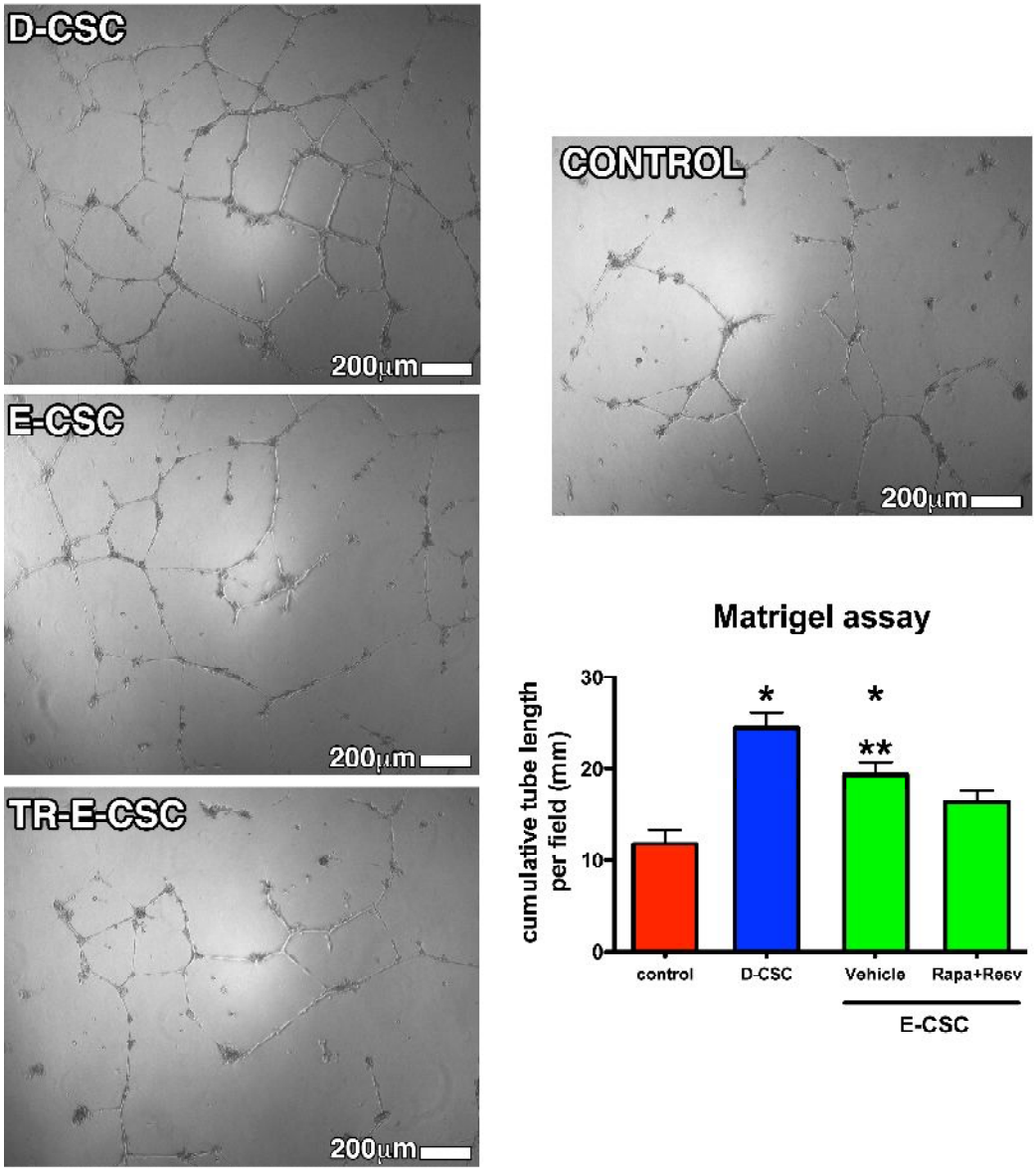

Figure 4.9 Effects of Rapa+Resv treated-E-CSC conditioned medium on angiogenesis of endothelial cells *in vitro*. *Representative phase-contrast optical images of HUVECs forming endothelial network when cultured for 20 hours on matrigel substrate. Histograms summarize quantitative data of the length of tubes formed by HUVECs. Values are means±SEM.*
** p<0.05 vs Control; ** p<0.05 vs D-CSC.*

All together, these data show that a 3 days pharmacological treatment of E-CSC with a cocktail of 10nM Rapamycin and 0.5μM Resveratrol reduces the fraction of senescent cells, improves cells functional properties *in vitro* and restores the ability of cell's secretome to protect rat cardiomyocytes from a SI/RO injury.

4.3 Molecular alterations in Rapamycin and Resveratrol-treated senescent CSCs

Last, the effects of the pharmacological treatment on E-CSC senescence-associated molecular pathways were investigated.

4.3.1 IL-1β/NFκB signaling pathway

Looking at the first signaling pathway altered in E-CSC, Rapamycin is able to reduce the activation of Caspase 1 in both the single and combined treatment (**fig. 4.10B**), important to counteract the activation of IL-1β, that eventually leads to the maintenance of the SASP.
Conversely, the levels of phospho-IKKβ are not modified by none of the drugs (**fig. 4.10A**). Similarly, the transcriptional levels of IL-1β and microRNA-146a are not modified (data not shown).

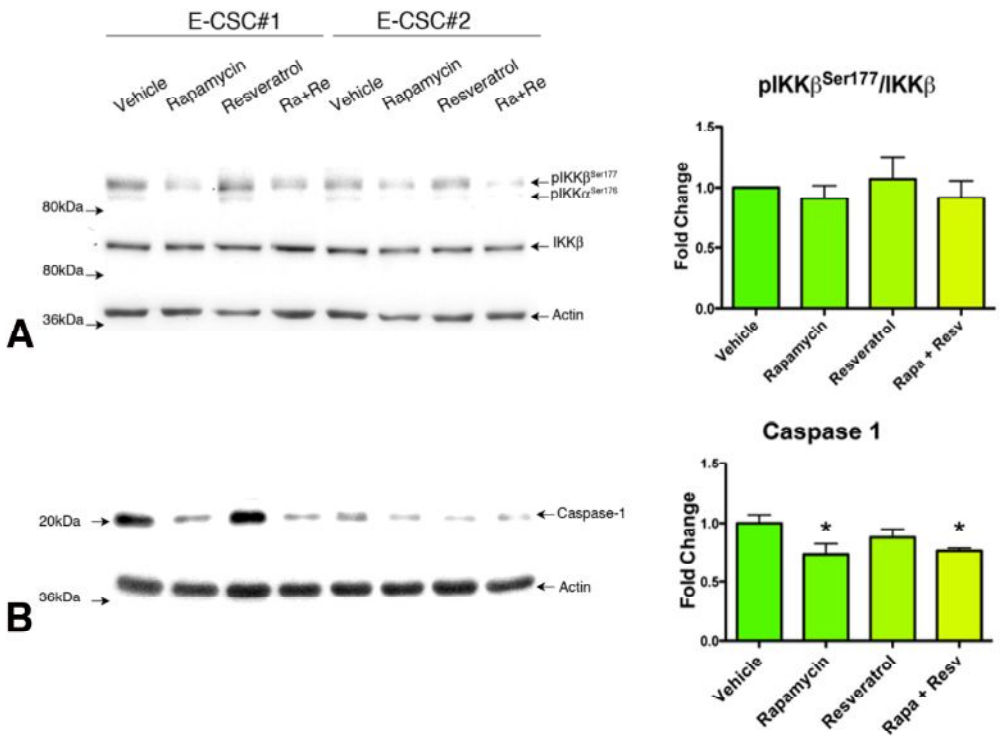

Figure 4.10 Effects of Rapamycin and Resveratrol treatment on E-CSC. *Western Blot analysis showing the effect of Vehicle, Rapamycin, Resveratrol and Rapamycin+Resveratrol treatment on* ***(A)*** *IKKβ, phospho-IKKβ^{Ser177} and* ***(B)*** *Caspase 1 levels. Blotted proteins were incubated with antibodies directed against IKKβ, phospho-IKKβ^{Ser177}, Caspase 1. Histograms show the results of the densitometric analyses as means±SEM. * p<0.05 vs Vehicle.*

4.3.2 AMPK/mTOR/Akt/Autophagy signaling pathway

Interestingly, the treatment of E-CSC with the combination of Rapamycin and Resveratrol is the only able to significantly increase the activation of AMPK (**fig. 4.11A**), that means that the drugs cooperatively work to activate AMPK.

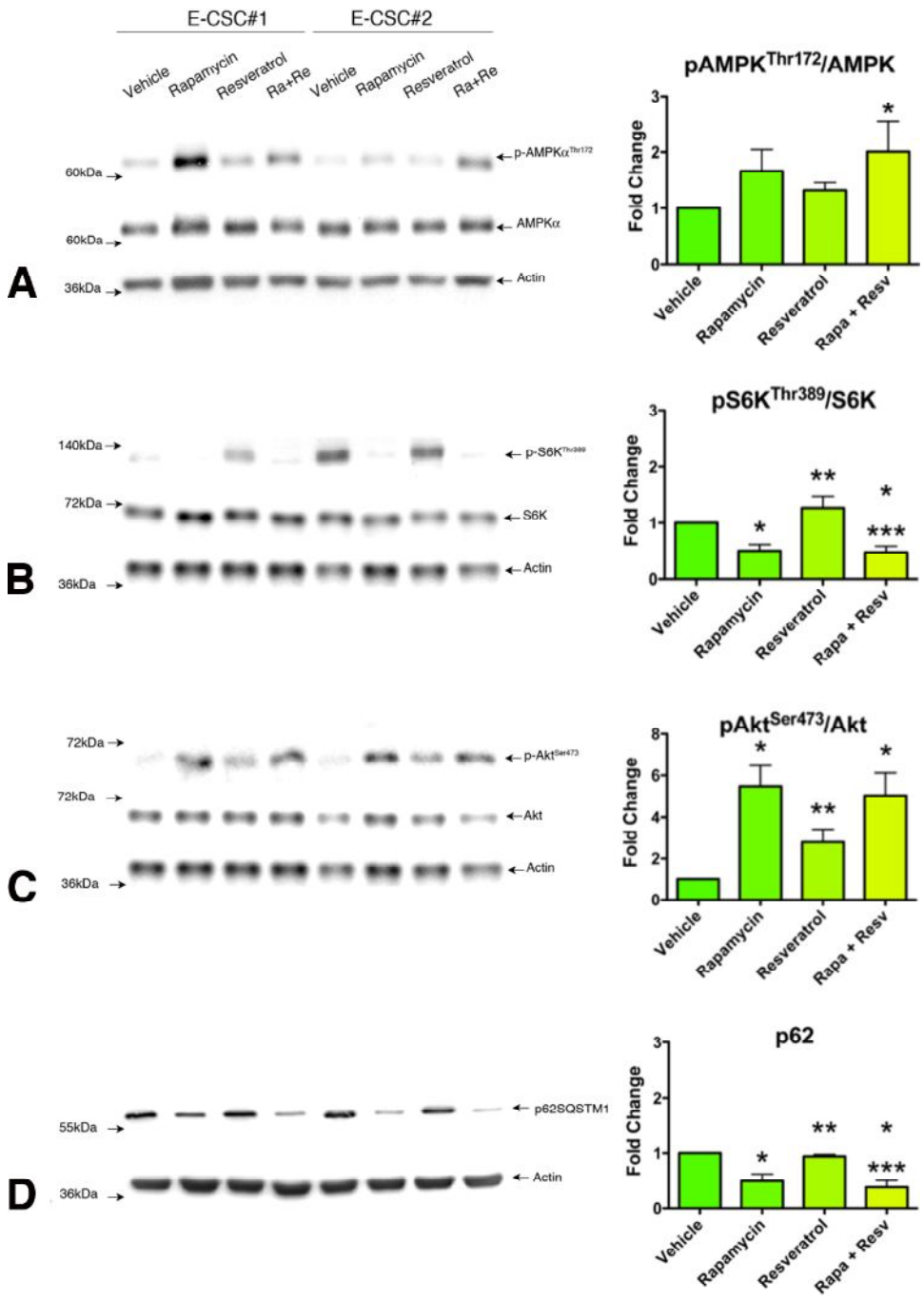

Figure 4.11 Effects of Rapamycin and Resveratrol treatment on E-CSC. *Western Blot analysis showing the effect of Vehicle, Rapamycin, Resveratrol and Rapamycin+Resveratrol treatment on* ***(A)*** *AMPKα, phospho-AMPKα^{Thr172},* ***(B)*** *S6K, phospho-S6K^{Thr389},* ***(C)*** *Akt, phospho-Akt^{Ser473},* ***(D)*** *p62/SQSTM1. Histograms show the results of the densitometric analyses as means±SEM.*
** p<0.05 vs Vehicle; ** p<0.05 vs Rapamycin; *** p<0.05 vs Resveratrol.*

Regarding mTOR pathway, the results show that Rapamycin is effective in reverting the molecular mechanisms altered in E-CSCs, while Resveratrol does not. In fact Rapamycin is able to reduce the activation of S6K (**fig. 4.11B**) and the levels of p62 (**fig. 4.11D**), suggesting that the arrest in the autophagic flux is reverted, moving towards normal levels. This can be observed although, as shown in **fig. 4.12**, autophagic markers are not modified by none of the drugs. In addition, Rapamycin is able to phosphorylate Akt, increasing its activation (**fig. 4.11C**). All these considerations support an inhibition of TORC1 activity. Moreover, TORC1 is the direct target of Rapamycin.

Conversely, Resveratrol does not seem to exert important effects on this pathway, failing to restore the molecular alterations proper to E-CSC; despite this, interestingly, Resveratrol does not limit the effects of Rapamycin when drugs are given to the cells together, thus the combined pharmacologic treatment is as effective as the single Rapamycin in rejuvenating senescent E-CSC.

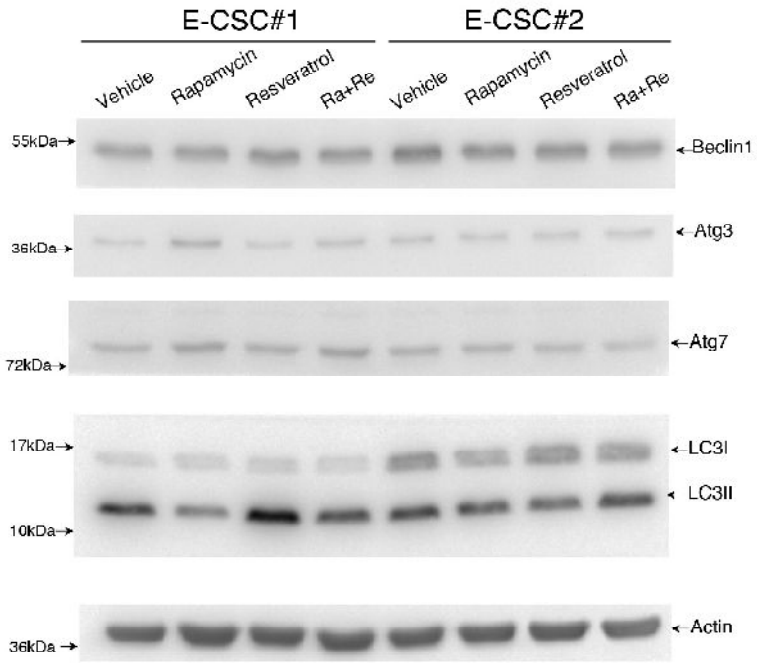

Figure 4.12 Effects of Rapamycin and Resveratrol treatment on E-CSC. *WesternBlot analysis showing the effect of Rapamycin +Resveratrol treatment on Beclin1, Atg3, Atg7, LC3I and LC3II levels.*

4.3.3 CREB/Sirt1 signaling pathway

Regarding the last molecular pathway analyzed, Resveratrol is able to increase Sirt1 levels, while Rapamycin does not (**fig. 4.13A**). Also the levels of the cardioprotective miR-132 are enhanced with Resveratrol treatment (**fig. 4.13C**). Unfortunately, in the combined treatment Rapamycin reduces the above cited properties of Resveratrol.

Instead, CREB's activation levels are not modified by none of the drugs (**fig. 4.13B**).

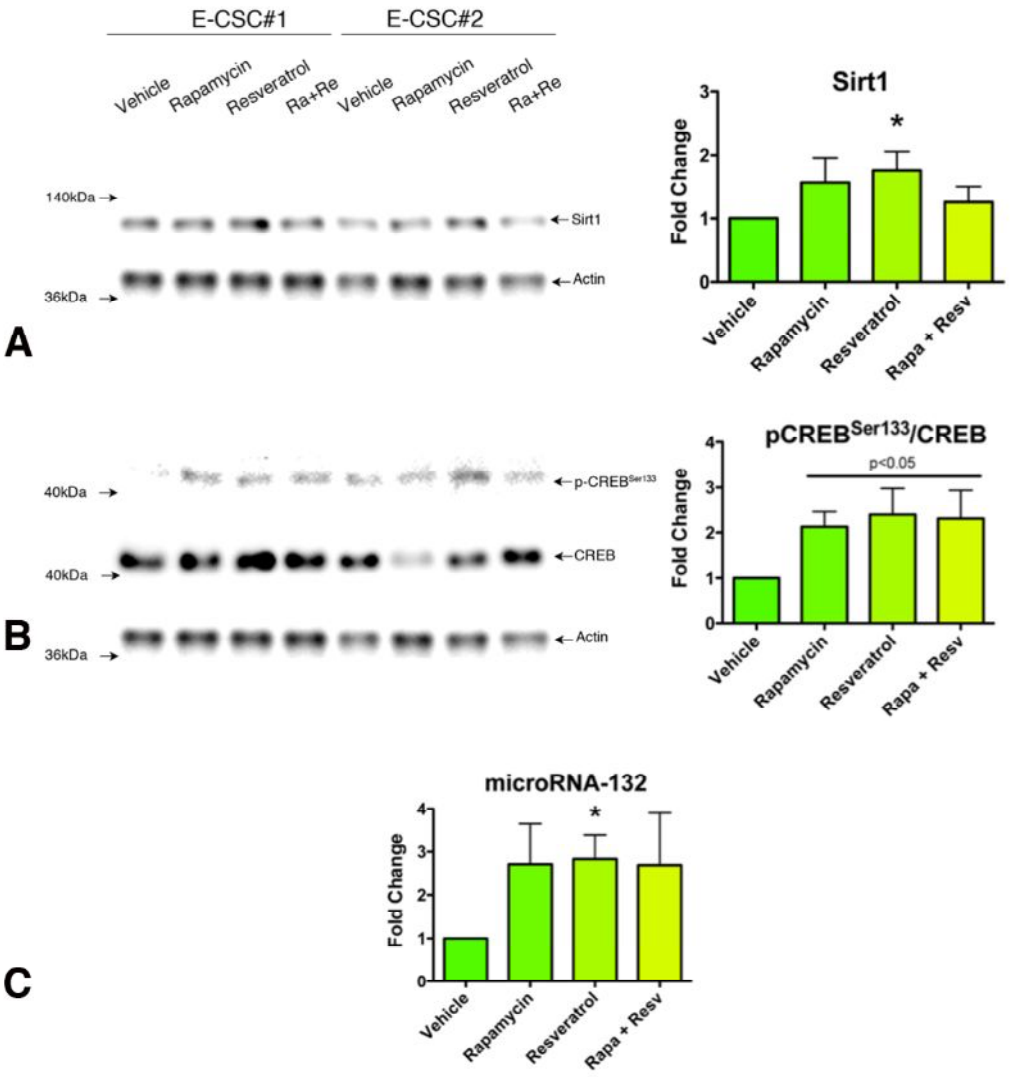

Figure 4.13 Effects of Rapamycin and Resveratrol treatment on E-CSC. ***(A-B)*** *Western Blot analysis showing the effect of Vehicle, Rapamycin, Resveratrol and Rapamycin+Resveratrol treatment on* ***(A)*** *Sirt-1 and* ***(B)*** *phospho-CREB^{Ser133}, CREB. Histograms show the results of the densitometric analyses as means±SEM. * p<0.05 vs Vehicle.* ***(C)*** *Histograms show the effect of drugs treatment on the relative expression of microRNA-132. Values are means±SEM. * p<0.05 vs Vehicle.*

Last, an increase in Sirt1 or CREB activation levels could suggest an activation of iNOS (inducible-Nitric Oxide Synthetase) with the subsequent production of nitric oxide, that exerts anti-senescence effects[81]. But none of the drugs modifies the levels of intracellular nitric oxide or of nitrites released in cell supernatants (**fig. 4.14**).

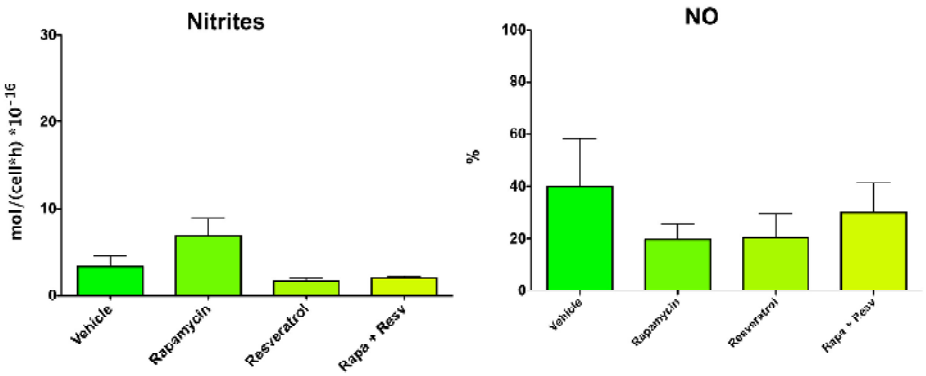

Figure 4.14 Detection of Nitric Oxide (NO) in E-CSC. *Histograms summarize the effects of Vehicle-, Rapamycin-, Resveratrol- or Rapamycin and Resveratrol-treatment (Rapa+Resv) on the fraction of E-CSC positive to the intracellular NO indicator DAF-AM and the concentration of nitrites present in the culture supernatants. The values of nitrites have been normalized for the volume of the collected supernatant, the number of cells and the time of incubation. Values are means±SEM.*

Summarizing, in Rapamycin and Resveratrol-treated-E-CSC:

1. **Rapamycin is able to reduce the activation of Caspase 1 by inflammasome, important to counteract the detrimental effects of the SASP and specifically of IL-1β through IKKβ and NFκB;**
2. **Rapamycin stimulates the activation of Akt, while both the drugs cooperatively work to activate AMPK;**
3. **Rapamycin inhibits TORC1 reducing the activation of S6K and the levels of autophagic markers; moreover, the levels of p62 are decreased, possibly reestablishing the autophagic flux to normal levels;**
4. **Resveratrol activates Sirt1 and induces the transcription of the cardio-protective miR-132.**

5- *in vitro* rejuvenation of senescent Cardiac Stem Cells restores their ability to repair a murine infarcted heart

5.1 Hemodynamic and anatomic outcomes

In order to ameliorate autologous stem cell therapy, it would be necessary any attempt aimed at improving the quality of the expanded cells, selecting the fraction of cells with the highest regenerative potential, excluding senescent cells[82]. As an alternative approach, rejuvenation of senescent human CSCs could improve the outcome of regenerative therapy. This latter purpose could be reached by a drug-based strategy, meant to attenuate/revert the molecular pathways that characterize senescent cells[192]. Rapamycin and Resveratrol represent 2 possible drugs to be used at this aim.

Resveratrol was able to improve E-CSC's functional properties *in vitro* (migration speed, proliferation, apoptosis, CPDT) more than Rapamycin, while at the molecular level Rapamycin was the most responsible for the reversion of senescence-associated signaling pathways; for these reasons, the combination of the drugs seems to be promising for the therapeutic rejuvenation of E-CSC at the aim of ameliorating autologous cell therapy.

After the demonstration that a pharmacologic treatment, for 3 days, with Rapamycin and Resveratrol is able to rejuvenate senescent E-CSC, the last phase of the study was the transplantation of drugs-treated E-CSC in the peri-infarct of infarcted mouse hearts, using the same model described above, to verify if the treatment was able to ameliorate the *in vivo* reparative ability of the cells. The effects of D-CSC, E-CSC and Rapamycin+Resveratrol-treated-E-CSC (TR-E-CSC) were compared.

Fig. 5.1 shows the anatomic and hemodynamic parameters of mice 14-days after which received vehicle or CSCs. Cell therapy with any of the three cell types improved cardiac output; however, D-CSC outperformed E-CSC with respect to both cardiac dimensional and functional parameters (see above). Importantly, animals implanted with preconditioned E-CSC (TR-E-CSC) showed an improvement in cardiac dimensional and functional parameters, matching the results obtained in animals implanted with D-CSC.

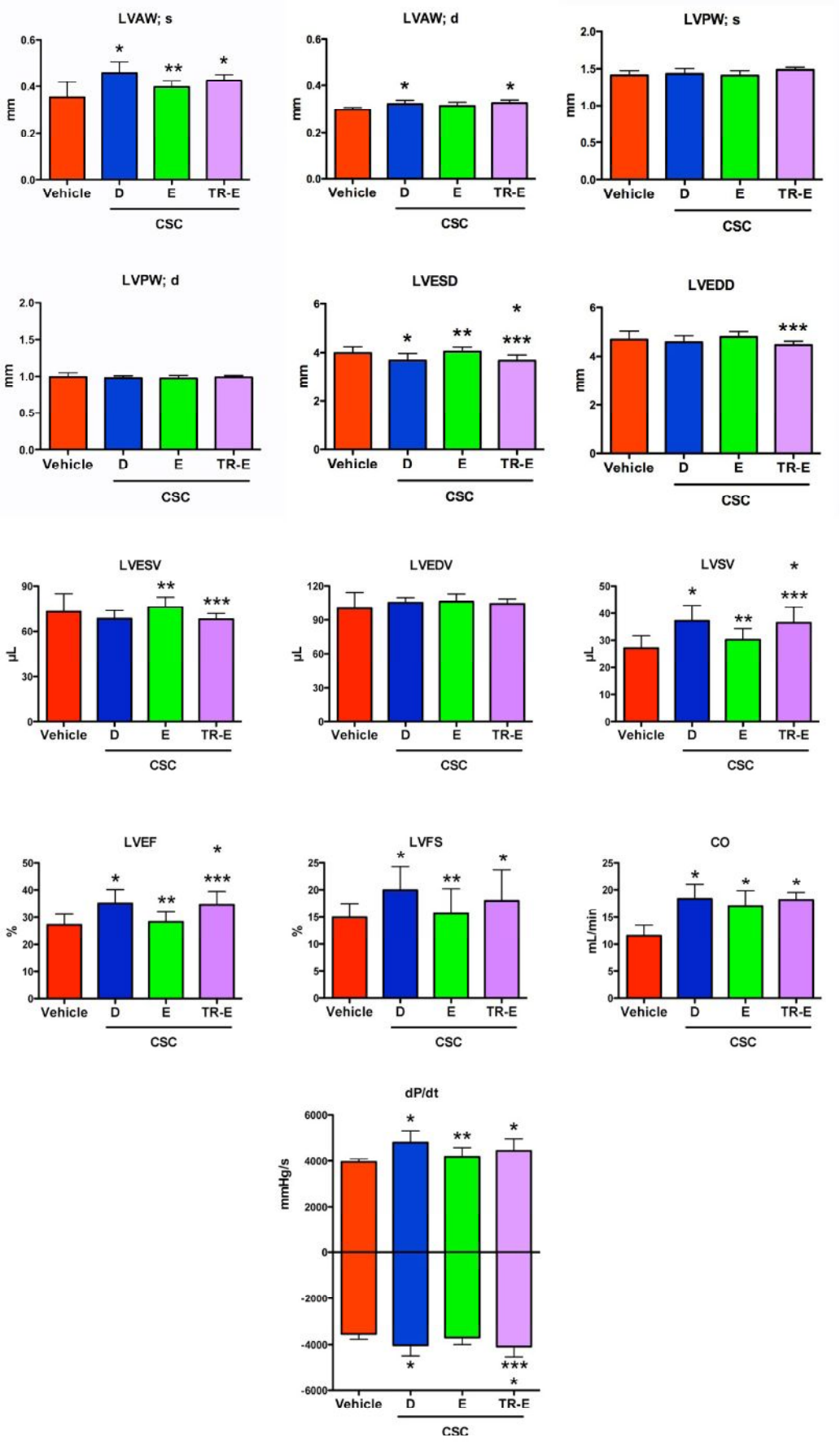

Figure 5.1 Anatomic and hemodynamic parameters of infarcted mouse hearts injected either with Vehicle (n=17) or D-CSC (n=18) or E-CSC (n=17) or Rapa+Resv-treated-E-CSC (TR-E-CSC) (n=18), 14 days post-MI. *For abbreviations see the List of abbreviations. Values are means±SEM. * p<0.05 vs Vehicle; ** p<0.05 vs D-CSC; *** p<0.05 vs E-CSC.*

5.2 Rejuvenated E-CSC reduce the scar size of infarcted hearts

TR-E-CSC were also able to reduce the scar size in left infarcted ventricles, as D-CSC did (**fig. 5.2**), improving the recovery of the animals.

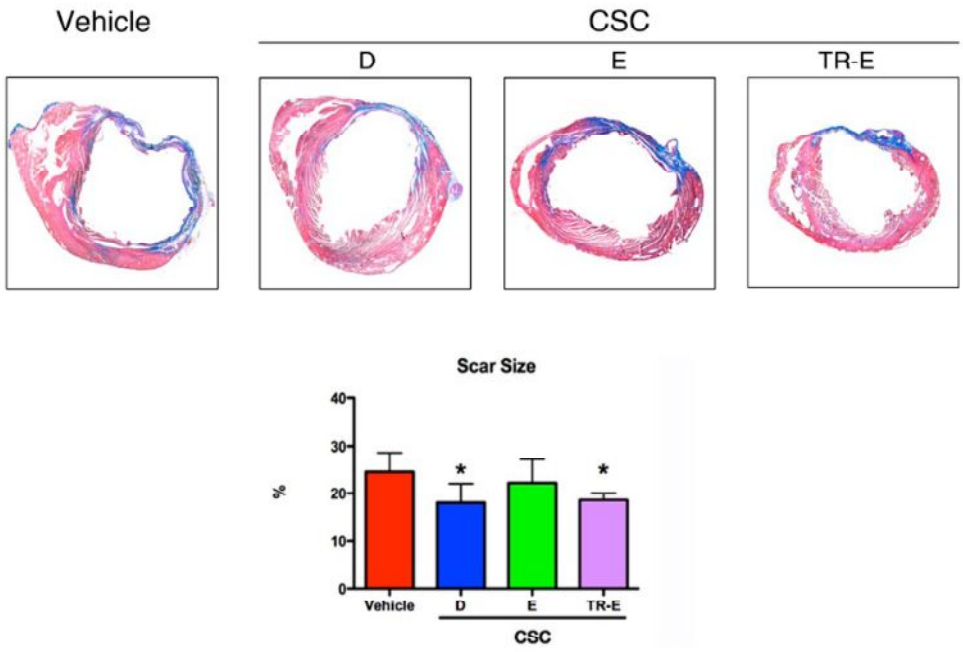

Figure 5.2 Pre-treatment of E-CSC with Rapamycin and Resveratrol improves scar size in the infarcted mouse hearts. *Histology images show Azan Mallory staining (in blue: collagen) of transverse sections of infarcted mouse hearts injected either with Vehicle (n=17) or D-CSC (n=18) or E-CSC (n=17) or Rapa+Resv-treated-E-CSC (TR-E-CSC) (n=18), 14 days post-MI. Bar graphs show the fraction (%) of myocardium occupied by the scar. Values are means±SEM. * p<0.05 vs Vehicle.*

5.3 Rejuvenated E-CSC improve arteriogenesis

While D-CSC incremented the density of both capillaries and small arterioles, TR-E-CSC enhanced only the density of large arterioles, indicating their main contribution to arteriogenesis (**fig. 5.3**).

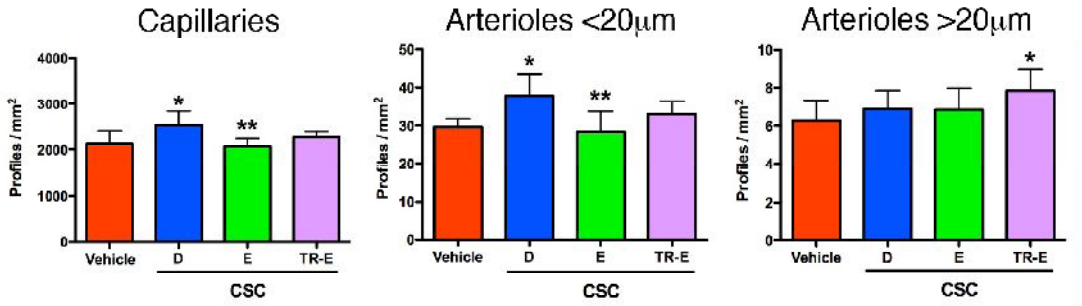

Figure 5.3 Effect of Rapamycin+Resveratrol treatment on angiogenesis in the infarcted mouse hearts. *Bar graphs show the density of capillaries, small (<20μm in diameter) and large (>20μm in diameter) arterioles in the peri-infarct zone of mouse hearts injected either with Vehicle (n=17) or D-CSC (n=18) or E-CSC (n=17) or Rapa+Resv-treated-E-CSC (TR-E-CSC) (n=18), 14 days post-MI. Values are expressed as means±SEM. * p<0.05 vs Vehicle; ** p<0.05 vs D-CSC.*

5.4 Rejuvenated E-CSC are able to protect cardiomyocytes in the mouse ischemic heart and to recruit resident murine CSCs in the site of injury

E-CSC pre-conditioned with Rapamycin and Resveratrol were able to significantly reduce the density of senescent and $LC3^+$ cardiomyocytes in the zone bordering the infarct, with respect to untreated E-CSC (**fig. 5.5**). Moreover, TR-E-CSC significantly reduced the apoptosis of cardiomyocytes, not only respect to E-CSC treated mice but also respect to vehicle-treated mice. Cardiomyocytes proliferation was instead increased in the border zone of TR-E-CSC injected mice respect to E-CSC's ones.

The effects of cell therapy in the myocardium distant from the infarct were less appreciable.

In addition to the positive effects on cardiomyocytes, a significant increase in the frequency of cardiac primitive/progenitor cells was observed in TR-E-CSC injected animals, respect to vehicle-treated ones (**fig. 5.4**), a process which is believed to be fundamental for the regeneration of the lost tissue[51].

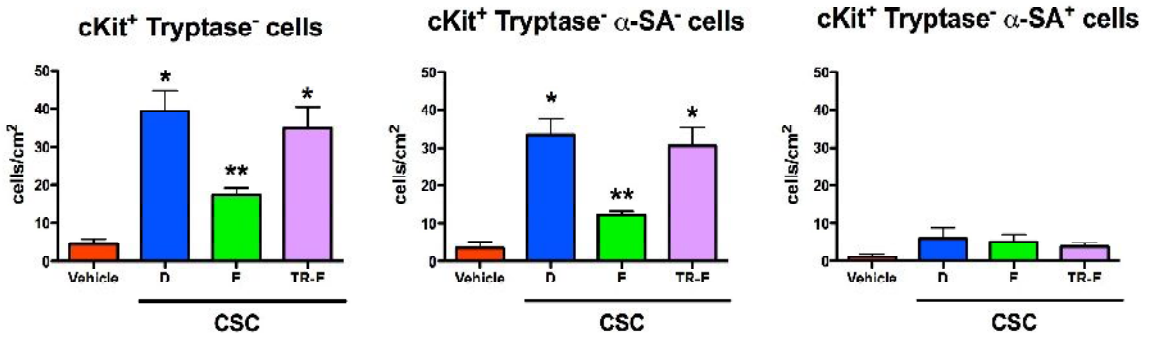

Figure 5.4 Pre-treatment of E-CSC with Rapamycin and Resveratrol restores their ability to recruit primitive cells in the mouse infarcted heart. *Histograms summarize quantitative data of the density of total cKit-positive cardiac primitive cells (c-Kit+ Tryptase-), stem and progenitor cells (c-Kit+ aSA- Tryptase-) and cardiomyocyte precursors (c-Kit+ aSA+ Tryptase-) in the infarct border zone of left ventricles of mice injected either with Vehicle (n=17) or D-CSC (n=18) or E-CSC (n=17) or Rapa+Resv-treated-E-CSC (TR-E-CSC) (n=18), 14 days post-MI. Values are means±SEM. * p<0.05 vs Vehicle; ** p<0.05 vs D-CSC.*

Altogether these data indicate that, although E-CSC show a blunted *in vivo* reparative ability, pharmacologic preconditioning with Rapamycin and Resveratrol restores the capacity of these cells to facilitate myocardial healing and to improve cardiac performance. Interestingly, this effect seems to be mediated mostly by potentiating their protective effect and by restoring their ability to recruit endogenous CSCs.

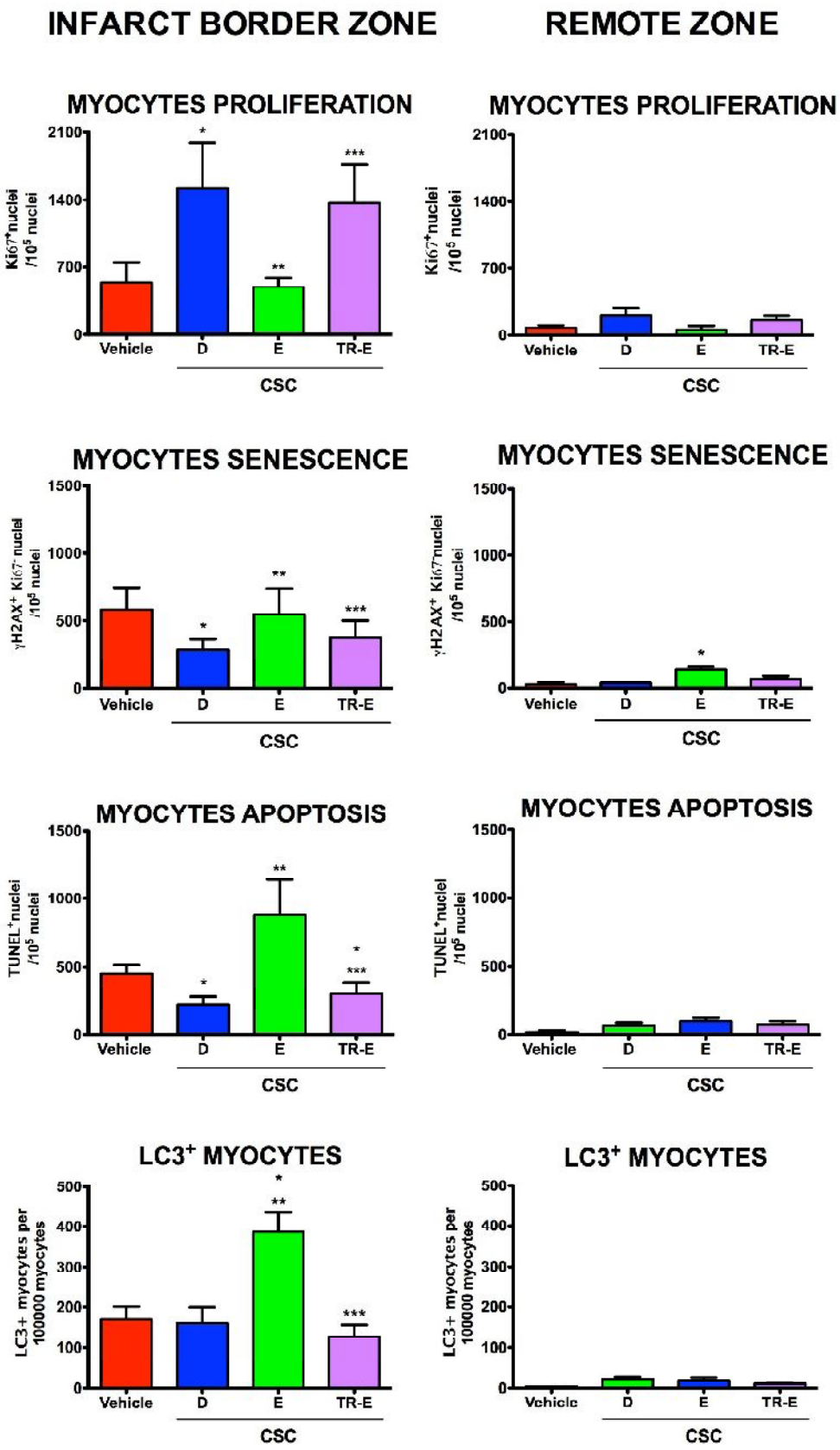

Figure 5.5 Pre-treatment of E-CSC with Rapamycin and Resveratrol let cells able to protect cardiomyocytes in the infarcted mouse hearts. *Histograms summarize quantitative data on cardiomyocytes proliferation, senescence, apoptosis and autophagy (meant as the presence of the autophagic marker LC3) in the cardiac infarct border zone and remote zone of mice injected either with Vehicle (n=17) or D-CSC (n=18) or E-CSC (n=17) or Rapa+Resv-treated-E-CSC (TR-E-CSC) (n=18), 14 days post-MI .*
*Values are means±SEM. * p<0.05 vs Vehicle; ** p<0.05 vs D-CSC; *** p<0.05 vs E-CSC.*

IV. Discussion

Heart failure (HF) is a complex clinical syndrome that can result from any structural or functional cardiac disorder that impairs the ability of the ventricle to fill or eject blood[5].

Mechanical, neurohormonal and possibly genetic factors alter ventricular size, shape and function, a process named left ventricle remodeling. This latter continues for months after the initial insult and the eventual change in the shape of the ventricle becomes detrimental to the overall function of the heart as a pump[3].

Although the current standard of care for HF improves outcomes, the syndrome continues to progress and there is a need for novel therapies that can prevent, further slow the progression, and/or reverse the structural and functional defects of the failing heart. Current therapeutic options for end-stage HF patients are limited to cardiac transplantation or the option of permanent mechanical assistance of the circulation. But heart transplantation is limited by donor availability and lifelong immunosuppression for transplant recipients[4; 9].

The discoveries of a cell turnover in the cardiac tissue[26] and of the presence of tissue-resident primitive cells, able to proliferate and differentiate in cardiac terminally differentiated cells[36], eventually improving the recovery of the organ, have opened new frontiers in the treatment of this pathology. The progression of regenerative medicine is allowing the development of stem-cell based therapies that have the potential to transform the treatment of HF by achieving myocardial regeneration[10].

Different groups have demonstrated the feasibility of isolating and expanding human CSCs from end-stage failing hearts[36; 44; 59; 215]; in addition, the recent early phase clinical trials SCIPIO[55] and CADUCEUS[57] employing autologous CSCs isolated from patients' hearts and expanded *in vitro* to obtain a sufficient number for transplantation, gave encouraging results, improving patients' cardiac function. Despite this, however, accumulated evidences indicate that both ageing and chronic age-related pathologies - such as atherosclerosis[90] or end-stage heart failure[43; 199; 216] - are associated with stem cell senescence and functional impairment, suggesting that these cells could not be optimal for employment in cell therapy and that this latter could be further improved to achieve better results.

In support of this hypothesis is the demonstration that human c-Kit$^+$ CSCs obtained from failing hearts are characterized by a shorter telomere length and a reduced telomerase activity; they also present reduced migration, proliferation and differentiation *in vitro*[43], features considered to be crucial for the regenerative potential of this autologous cell source. Moreover, these cells are characterized by a gene expression profile enriched in elements that are part of the SASP.

Therefore, senescent human CSCs can contribute to create a microenvironment favouring, through a paracrine mechanism, senescence on neighbour cells, inflammation and extracellular matrix remodeling, thus creating a vicious circle hampering regenerative purposes[192].
Although autologous c-Kit$^+$ CSCs have been used in the first in man clinical trial (SCIPIO[55]) for HF therapy, guided by Prof. Anversa and R. Bolli, with encouraging results, other groups gave the demonstration that cellular senescence affects CSCs functional properties *in vitro*[43; 200]. Thus, in order to ameliorate autologous stem cell therapy, it would be mandatory the improvement of the quality of the expanded cells, selecting the fraction of cells with the highest regenerative potential, excluding senescent cells[82]. This is possible using different strategies; for example, D'Amario and colleagues showed that IGF-1R$^+$ c-Kit$^+$ CSCs[199] are endowed with a superior *in vivo* regenerative ability.
At present, the *in vivo* regenerative potential, in a mouse model of AMI, of c-Kit$^+$ CSCs obtained from normal hearts has not yet been directly compared with that of CSCs obtained from pathological hearts. This was the **first aim** of this study.

In the first part of the work, CSCs isolated from end-stage HF patients' hearts (E-CSC) were compared to CSCs isolated from normal hearts donated for transplantation (D-CSC). D- and E-CSC share a similar mesenchymal immunophenotype, negative for endothelial and hematopoietic markers and enriched in the expression of c-Kit receptor (about 80% of cell positivity). Interestingly, the only marker that differed between CSC isolated from donors and patients hearts is CD49a, more expressed in E-CSC than in D-CSC. This marker has been associated to cardiac ageing and disease[197].
Cell characterization, *in vitro,* showed that E-CSC are functionally impaired, as supported by the following evidences:

1. E-CSC are enriched in senescent cells, as demonstrated by the presence of a high percentage of cells expressing p16^{INK4A} and presenting DDR-associated markers (presence of the phosphorylated histone variant γH2A.X in the absence of cell proliferation - meant as Ki67 negativity). Moreover, E-CSC are more apoptotic and less proliferating compared to D-CSC.
2. E-CSC are characterized by a lower growth kinetic respect to D-CSC.
3. E-CSC release an altered secretome, particularly enriched in the potent pro-inflammatory and senescence-associated cytokine IL-1β. Interestingly, as opposed to D-CSC, E-CSC's secretome was not able to protect rat adult cardiomyocytes exposed *in vitro* to a simulated ischemia - reoxygenation injury, favouring myocytes apoptosis and senescence. Since the role of IL-1β in triggering a. apoptosis (through activation of iNOS-Caspase 3/7)[227] and b. paracrine senescence (SASP mechanisms)[77] has been described in literature, a principal role played by this cytokine in the biological effect of E-CSC secretome on cardiomyocytes was

hypothesized. As hypothesized, the neutralization of IL-1β in E-CSC supernatants restored their protective ability on cardiomyocytes, reducing cell apoptosis and senescence to levels proper to D-CSC supernatants.

4. In addition, E-CSC showed a reduced ability, compared to D-CSC, to stimulate the formation of tubular networks in endothelial cells (HUVECs) cultured on matrigel substrate.

All these considerations confirmed that CSCs residing in human failing hearts are affected by senescence processes and are functionally impaired *in vitro*, as recently demonstrated[43].

Subsequently, to investigate if the functional impairment that characterizes E-CSC *in vitro* is reflected in a functional impairment *in vivo*, D- and E-CSC were transplanted in the peri-infarct myocardium of a murine infarcted heart. Vehicle was given to the animals as control. 14 days post-Myocardial Infarction (MI) and cell transplantation, animals which received E-CSC showed, with respect to the D-CSC ones, worst anatomical and functional parameters at echocardiographic analysis. In addition, the histological analysis of the left infarcted ventricles of E-CSC treated animals showed a larger scar size, a lower density of capillaries, small arterioles and cycling myocytes, an enrichment in senescent, apoptotic and $LC3^+$ myocytes and a reduced number of cardiac primitive/progenitor cells recruited in the site of injury.

These data corroborate the hypothesis of a functional impairment of senescent CSCs *in vivo* and for the first time a direct demonstration has been given.

Furthermore, the scarce presence of human cells, for both D- and E-CSC, in the mice hearts suggests that the biological effects of exogenous injected cells is due principally, if not exclusively, to their secretome, with paracrine mechanisms, as it has been widely described in literature[228]. If this assumption is true, the negative effects observed after E-CSC implantation can be explained by the cell's secretome rich of pro-senescent and pro-inflammatory cytokines, that contribute to create a microenvironment favoring the propagation of senescence on neighboring cells[101], thus hampering the regenerative process. This is in line with the increased frequency of senescent myocytes in the region distant from the myocardial infarction that has been observed in animals injected with E-CSC, with respect to both D-CSC and control.

Moving from these important results, the **second aim** of the work was trying to understand which molecular pathways, among the ones associated with cell senescence and ageing, were altered in E-CSC and thus could be possibly responsible for their negative behaviour.

3 are the molecular pathways analyzed:

1. SASP-IKKβ-NFκB,
2. AMPK/mTOR/Akt/autophagy,
3. CREB/Sirt1.

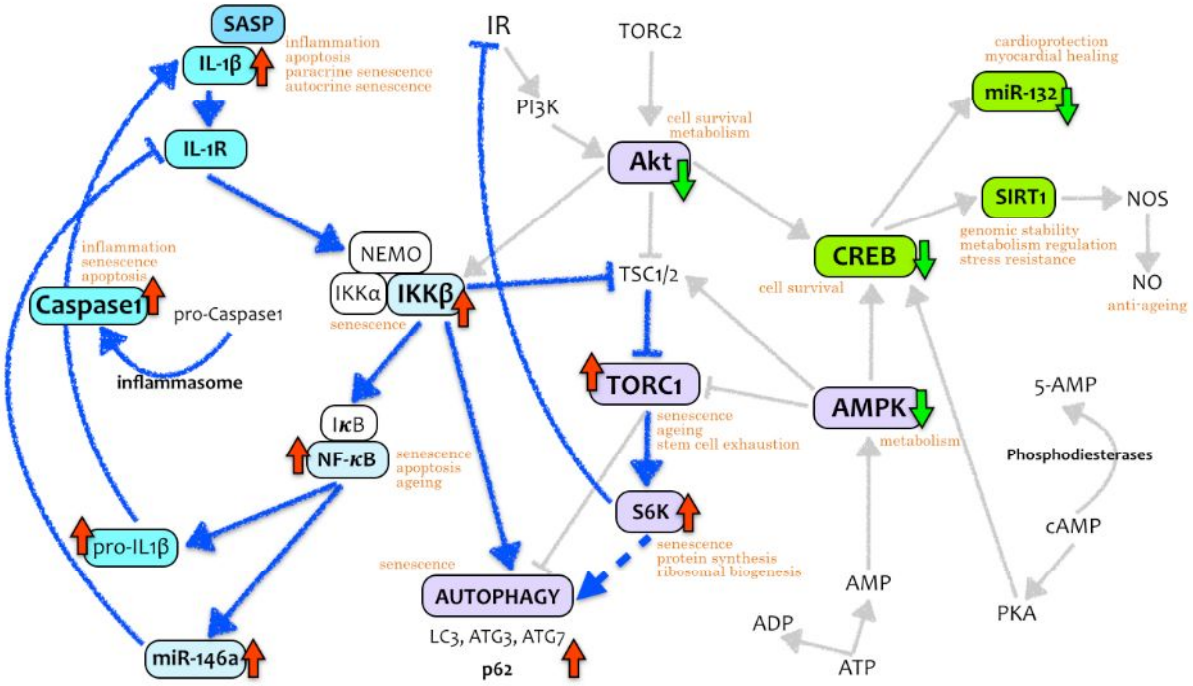

Figure 1. Cartoon illustrating the molecular pathways - associated with cellular senescence and ageing - altered (or hypothetically altered although not experimentally demonstrated) in E-CSC compared to D-CSC. *The bold blue arrows indicate the pathways predominant in E-CSC compared to D-CSC.* ***Red arrows*** *indicate an hyper-activation status in E-CSC with respect to D-CSC.* ***Green arrows*** *indicate a reduced activation in E-CSC with respect to D-CSC.*

The first pathway is activated by the SASP, that plays an important role in the autocrine maintenance and paracrine transmission of senescence[97], and IL-1β is a trigger signal. Since E-CSC secretome is strongly enriched in IL-1β, it was not surprising to find this pathway to be more activated in E-CSC compared to D-CSC. After the activation of IKKβ, this latter phosphorylates and activates NFκB, which translocates inside the nucleus and begins the transcription of its targets, among them the precursor of the same IL-1β (then processed and activated by the inflammasome and Caspase 1, thus establishing a positive feedback loop) and the micro-RNA-146a; this latter could act as a negative feedback loop on the IL-1R, limiting excessive SASP activity (figure 1).

The reasons behind the decision to study the second pathway are different, among them: a. E-CSC are characterized by an up-regulation of genes encoding for proteins involved in metabolic (lipids, carbohydrates, amino acids) pathways[43], and mTOR and AMPK are well known central energy sensors inside the cells[111]; b. mTOR has an important role in controlling ageing processes; c. SASP is a potent activator of mTOR[187]; d. mTOR controls autophagy, a process that drives cell senescence[141] and is associated with the SASP[139].

The results show that E-CSC, with respect to D-CSC, are characterized by a higher activity of TORC1/pS6K complex and an arrest in the autophagic flux, as stated by the accumulation of the p62 protein in E-CSC. Although the protein levels of total mTOR (comprehensive of mTOR

of both TORC1/2 complexes) do not differ between D- and E-CSC, the activation of TORC1 can be deduced by 3 evidences (figure 1): i. the downstream TORC1 target S6K tends to be more activated in E-CSC than in D-CSC; ii. TORC1 negatively regulates Akt (through the inhibition of Insulin Receptor by S6K, activated by TORC1) and, in line, activation of Akt is reduced in E-CSC; iii. autophagy, a process regulated by TORC1, is altered in E-CSC. In addition, E-CSC show a reduction in AMPK activation levels.

TORC1 can be activated by Akt, through an inhibiting phosphorylation of the TORC1 inhibitor TSC2[113] (figure 1); but since E-CSC present reduced levels in Akt activation, a possible explanation for TORC1 activation in E-CSC can be traced back to two mechanisms working synergistically and independently by Akt: 1) IKKβ, strongly activated by the binding of IL-1β to its receptor, inhibits TSC1[187], so activating TORC1; 2) the reduction in the AMPK activation levels and the subsequent lack of the inhibitory action on TORC1. This latter event has been described to occur both in ischemic and anthracyclin induced cardiomyopathies and possibly to govern the transition from cardiac injury to heart failure[229].

mTOR plays a central role in cell senescence since its inactivation converts cellular senescence (a permanent exit from the cell cycle) into quiescence (a reversible cell cycle withdrawal)[119], preventing stem cell senescence. mTOR activation may instead determine stem cell exhaustion[122] and aging[126]. Moreover, a subset of autophagy-related genes are up-regulated during senescence. Autophagy, and its consequent protein turnover, mediates the acquisition of the senescence phenotype[141]. Interestingly, an impairment in autophagy has been described at the basis of pathogenesis of heart disease. Basal autophagy is critically required for protein quality control, removal of damaged organelles and recycling of intracellular elements to maintain cardiac homeostasis; excessive, or abrogated, autophagy is maladaptive[143; 144].

Last, since both AMPK and Akt[167] phosphorylate and activate CREB, a transcription factor that induces the expression of Sirtuins - proteins deacetylase that play a prominent role in cellular senescence and aging - CREB signaling pathway was the third one investigated in CSCs. AMPK regulates the transcription of Sirt1, the most studied mammalian Sirtuin[158]. Moreover, a marked decrement in the expression of CREB with senescence in cultured fibroblasts has been described[166].

As shown in figure 1, the levels of activated phospho-CREB were lower in E-CSC than in D-CSC. CREB is involved in the regulation of the circadian rhythm - regulating its transcriptional target micro-RNA-132[169]. This latter, which represents a strong enhancer of myocardial healing[223], was significantly less expressed in E-CSC than in D-CSC. Differences in Sirt1 levels were not displayed.

Summarizing, senescent E-CSC are characterized by an increased activation of IKKβ-NFκB and TORC1 signaling, a reduced activation of Akt, AMPK and CREB, and an arrest of the autophagic flux (figure 1).

Since rejuvenation of senescent human CSCs could improve the outcome of regenerative therapy, the **third aim** of the work was to interfere with the above signaling pathways in the attempt to revert cell senescence, *in vitro*, possibly ameliorating cell functional properties, *in vivo*. It has been decided to use a drug-based strategy to attenuate or revert the molecular pathways that characterize senescent cells. Moving from the previous pilot study published by the Beltrami's group[82], the anti-aging drugs used at this aim are Rapamycin and Resveratrol. The first is a TORC1 inhibitor[126] and it is also able to activate AMPK[225]; the second could activate AMPK[226] too, reduce the SASP[206] and may inhibit the cAMP-degrading phosphodiesterases[205], leading to elevated cAMP levels required for CREB activation via PKA. A combination of the two drugs was newly tested on CSCs, to verify if a cocktail containing both the drugs was able to produce additive benefits on CSC biology with respect to the single drugs.
A 3-days treatment with a combination of Resveratrol (0,5μM) and Rapamycin (10nM) was able to reduce the fraction of E-CSC affected by cell senescence *in vitro;* importantly, in the combined therapy the pro-apoptotic effect of Rapamycin was counteracted by the anti-apoptotic action of Resveratrol. The cocktail of drugs also reduced of approximately 80% IL1ß secretion, thus restoring the ability of E-CSC's secretome to prevent cardiomyocyte death and senescence. The treatment of E-CSC with drugs globally improved functional properties of the cells *in vitro*.

At the molecular level, the improvements in E-CSC are associated with different mechanisms (figure 2). A reduction in TORC1 activity results principally from the dual action of AMPK, co-operatively activated by the drugs. A decrease in TORC1 activation results in a lower activation of S6K; moreover, the concomitant and beneficial restoration of the autophagic flux is suggested by a decrease in p62 accumulation.
A reduction in Caspase 1 activation, exerted by Rapamycin, positively results in the production of lower amounts of IL-1β and the reduction of its pro-inflammatory effects (linked to the SASP). Despite this, a reduction in IKKβ activation levels is not observed, probably due to the activation by Akt (activated by Rapamycin) that phosphorylates IKKβ keeping its activation levels almost unvaried.
Last, AMPK and Akt activate CREB, which in turn promotes the transcription of SIRT-1 (anti-ageing[230]) and miR-132 (promoter of myocardial healing[223]). Moreover, it has been described that Resveratrol can inhibit phosphodiesterases[205], increasing the levels of cAMP which activates PKA and finally CREB (figure 2).

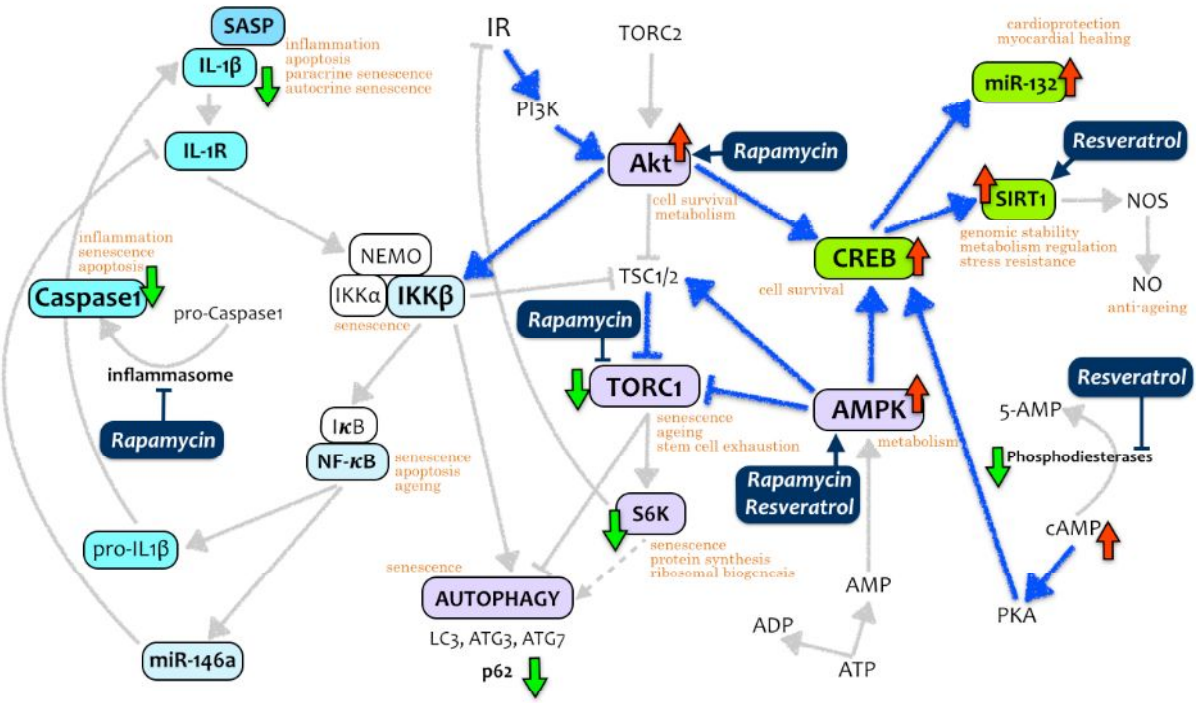

Figure 2. Model illustrating the effects of Rapamycin and Resveratrol treatment on the molecular pathways - associated with cell senescence and ageing - in Rapa+Resv-treated-E-CSC compared to untreated E-CSC. *The blue bold arrows indicate the pathways predominant in drugs-treated-E-CSC compared to E-CSC.* ***Red arrows*** *indicate an hyper-activation status in drugs-treated-E-CSC with respect to untreated E-CSC.* ***Green arrows*** *indicate a reduced activation in drugs-treated-E-CSC with respect to untreated E-CSC. The supposed targets of Rapamycin and Resveratrol are indicated in dark blue.*

In general, Rapamycin and Resveratrol result strongly effective in reverting the molecular alterations - linked to senescence and ageing - that characterize E-CSC compared to D-CSC, improving E-CSC functional properties *in vitro*.

More intriguingly, the pharmacologic treatment did not significantly modify D-CSC biology, corroborating the concept that drugs exert their effect on E-CSC, acting specifically on pathways associated to cell senescence and not altered in normal cells.

The **fourth aim** of the study was to verify if the pre-conditioning of E-CSC with the combination of the two drugs, prior to the injection in the peri-infarct region in a mouse MI-model, was able to restore their reparative potential.

This work gave the direct and first demonstration that the *ex vivo* pre-conditioning of E-CSC with a combination of Rapamycin and Resveratrol is able to restore the E-CSC *in vivo* reparative potential to levels observed with healthy D-CSC. This effects consisted of: an enhanced arteriolar density, a decreased cardiomyocyte senescence, apoptosis and autophagy and an increased recruitment of host CSCs, that resulted in the reduction of the infarct size and in the improvement of functional parameters. Angiogenesis is not increased by the pharmacologic preconditioning of E-CSC, and this could be explained by the reduction in the amount of pro-

angiogenic cytokines (VEGF, HGF, bFGF) secreted by the treated cells. The reduction in autophagy can be considered a positive result since this latter plays a central role in the establishment of senescence[140; 141] and in the onset of heart disease[143; 144]. The wide range of effects exerted by the *ex vivo* preconditioning suggests that rejuvenated E-CSC act through direct and indirect means probably via paracrine influence on various cellular components of the infarcted heart.

Conclusions

This study newly demonstrates that senescent CSCs obtained from end-stage failing hearts are characterized by an impaired reparative ability *in vivo*. The SASP characterizing senescent E-CSC plays a critical role in determining the blunted regenerative potential of senescent cells, also due to the propagation of senescence in the neighbor cells through paracrine mechanisms.
Importantly, this study demonstrates that the pathologic phenotype of E-CSC is not irreversible. In fact, the pharmacologic pre-conditioning was able to rejuvenate the patient-derived cells, boosting the *in vivo* cardiac regeneration.
To be emphasized, this aim was achieved without neither a prolonged manipulation of cells nor a genetic modification of CSCs, as the Sussman's group recently published[200], thus bypassing the risk of dangerous effects proper to gene therapy that makes use of virus-derived vectors. Another point in favour of this work is the preconditioning of CSCs *in vitro* with Rapamycin and Resveratrol prior to their injection in the animals, rather than the direct administration of the drugs to the animal, as already published in the past regarding Resveratrol in infarcted rats[231]. This is of fundamental importance since this approach avoids possible negative systemic effects.
These findings open new avenues for optimal regenerative treatments with autologous CSCs. The encouraging results obtained so far with clinical trials employing autologous CSCs in HF can be almost certainly improved by the rejuvenation of senescent cells prior to the re-implantation in the patient heart.
In conclusion, this work proposes a new possible protocol for autologous cardiac stem cells rejuvenation, with the future hope to boost the *in vivo* myocardial regeneration in the patient's heart.

V. Materials and Methods

1. ENROLLMENT OF PATIENTS AND ETHICS

In this study, patients suffering from end-stage heart failure (Stage D AHA classification), that underwent cardiac transplantation at the University Hospital of Udine, were enrolled. In order to be enrolled in the waiting list for organ transplantation, patients underwent an in-depth evaluation of their clinical status, which included: coronary angiography, cardiopulmonary exercise test, pulmonary function test, echocardiography, cardiac catheterization, assessment of pulmonary vascular resistance, electrocardiography and tests aimed at excluding the presence of malignancies and other vascular diseases. Furthermore, expert pathologists had access to the explanted organs, allowing the hearts to be evaluated macroscopically and histologically. For every patient enrolled in our case study, inspection of the coronary arteries confirmed the presence of stenosing atherosclerotic plaques shown by angiography, while histologic examination of the myocardium revealed the presence of segmental fibrosis and replacement fibrosis, defined as in (Beltrami et al, 1994)[221]. Clinical characteristics of patients and hearts are reported in **Table 1** and **2**.

The study, in accordance with the Declaration of Helsinki, was approved by the Ethics Committee of Udine (2 August 2011, reference number 47831) and written informed consent was obtained from each patient.

	No. of Patients	Age (yr.)	Sex (m/f)	Duration of Disease (mo)	Time from Heart Failure to Transplantation (mo)
Ischemic cardiomyopathy	20	60±7	19/1	119±94	42±44
Control	14	49±11	8/6	-	-

Table 1. Demographic, anatomic and functional characteristics of the subjects and hearts included in the study. *Data are presented as means±SD.*

	ISCHEMIC CARDIOMYOPATHY (N=20)	NORMAL VALUE*
LEFT VENTRICULAR DIAMETER (MM)		
SYSTOLIC	63.9±21.1	**20-35**
DIASTOLIC	78.2±30.6	**37-56**
RATIO OF WALL THICKNESS TO CHAMBER RADIUS	0.26±0.08	**0.32-0.39**
FRACTIONAL SHORTENING (%)	17.1±5.7	**34-44**
LEFT VENTRICULAR END-DIASTOLIC VOLUME (ML/M^2 OF BODY-SURFACE AREA)	122±36	**44-96**
EJECTION FRACTION (%)	24.7±9.4	**>50**
STROKE-VOLUME INDEX (ML/BEAT/M^2)	28±11	**20-41**
CARDIAC OUTPUT (ML/MIN)	4138±1367	**5000-7000**
CARDIAC INDEX (ML/MIN/M^2)	2220±775	**2600-4200**
MEAN PULMONARY-ARTERY EDGE PRESSURE (MMHG)	27±6	**1-10**
HEART WEIGHT (G)	521±120	**<350**

Table 2. Clinical characteristics of the patients whose hearts were studied. *Echocardiographic, hemodynamic and pathologic measurements. Data are presented as means±SD.*
** Normal value as in Olivetti G. et al., Apoptosis in the failing human heart. N Engl J Med. 1997 Apr 17;336(16):1131-41. Data are means±SD.*

2. *IN VITRO* EXPERIMENTS: CELLULAR BIOLOGY

2.1 Cardiac Stem Cells (CSCs) isolation and *in vitro* expansion

Human Cardiac Stem Cell lines (CSCs) employed in this study were isolated as in (Beltrami et al, 2007; Cesselli et al, 2013)[215; 232] from the following sources:

i. atrial specimens of explanted (E-) end-stage failing hearts (**E-CSC**, n=20) or

ii. discarded atrial specimens of hearts donated (D-) for transplantation (**D-CSC**, n=14).

Isolation was performed by washing atrial fragments (3-6g) in Basic Dissociation Buffer (BDB - see par.6) to eliminate blood from the tissue. Pericardial, adipose tissue and macroscopically apparent areas of fibrosis were then removed. The tissue underwent mechanic disaggregation with scalpels and scissors until fragments have a dimension not larger than 1 mm^3. The tissue was then washed with BDB and the cell solution was centrifuged 5 minutes at 500xg and supernatant discarded. The pellet was enzimatically dissociated by incubation in a 0.25% Collagenase type II solution (Worthington, Lakewood, NJ) in BDB in a volume at least two times the volume of the fragments. The enzyme/cell solution was incubated for 15-20 minutes at 37°C in a tube rotator. Usually fragments obtained from healthy donors were incubated for a

shorter period, while those collected from failing hearts required a longer incubation period (presence of fibrosis). Post-incubation Collagenase activity was stopped by the addition of blocking buffer (0.1% Bovine Serum Albumin in BDB, pH7.3 (Sigma-Aldrich, Dorest, UK)). The cell suspension was centrifuged at 100xg for 1 minute to pellet and discard the cardiac myocytes. The supernatant was centrifuged again at 500xg for 5 minutes. The resulting pellet was resuspended in 1 mL of BDB and filtered through a pre-wet 40μm filter (BD Falcon). The filtered suspension was centrifuged at 500xg for 5 minutes. The supernatant was discarded and cell pellet was resuspended in 1mL of medium (human MesenCult proliferation medium (STEMCELL Technologies, Manchester, UK)). Cells were cultured in the presence of 100 U Penicillin and 100 μg/L Streptomycin (Life Technologies, Paisley, UK). Cells were plated at a concentration of $1.5 \cdot 10^6$ in a 100-mm dish and maintained at 37°C, 5% CO_2. Colonies were usually observed 1 week after the isolation procedure.

2.1.1 Detachment and expansion of CSCs

To detach cells from substrate, the plate was washed twice with 5 mL of HBSS. 2 mL of TrypLE Express solution (Life Technologies, Paisley, UK) was added to the cells and incubated at 37°C, until the cells were observed to dissociate, after which 7 mL HBSS were added to the cells to inhibit enzymatic activity. Cell suspension was centrifuged at 500xg for 5 minutes and the supernatant was discarded. The cell pellet was resuspended in 1mL of culture medium. The cells were counted using a Burker Counting Chamber and plated at a density of 5000 cells/cm^2. After the second passage, the tissue culture plastic was coated with 10μg/mL human Fibronectin (Sigma-Aldrich, Dorest, UK) in HBSS and medium was switched to expansion medium (see par. 6). Medium is refreshed every 3-4 days.

2.2 Pharmacological treatment of CSCs with Rapamycin and Resveratrol

At passage 3, cells were treated with either **10 nM Rapamycin** (Sigma-Aldrich, Dorest, UK), **0.5 μM Resveratrol** (Sigma-Aldrich, Dorest, UK), or a combination of 10 nM Rapamycin and 0.5 μM Resveratrol diluted in the culture medium. The cells were incubated with the pharmacologic treatment for **72hrs**. The Rapamycin and Resveratrol were reconstituted as per manufacturer's instructions. For a control, cells were treated with the vehicle alone (DMSO and ethanol). After the incubation period, the cells were incubated for 48hrs in a drug-free expansion medium. These resulting cells were used for the *in vitro* (expression of senescence, proliferation and apoptosis markers; immunophenotype; migration ability; growth kinetics; collection of RNA and proteins; intracellular NO quantification; matrigel assay) and *in-vivo* (injection in the animals) experiments.

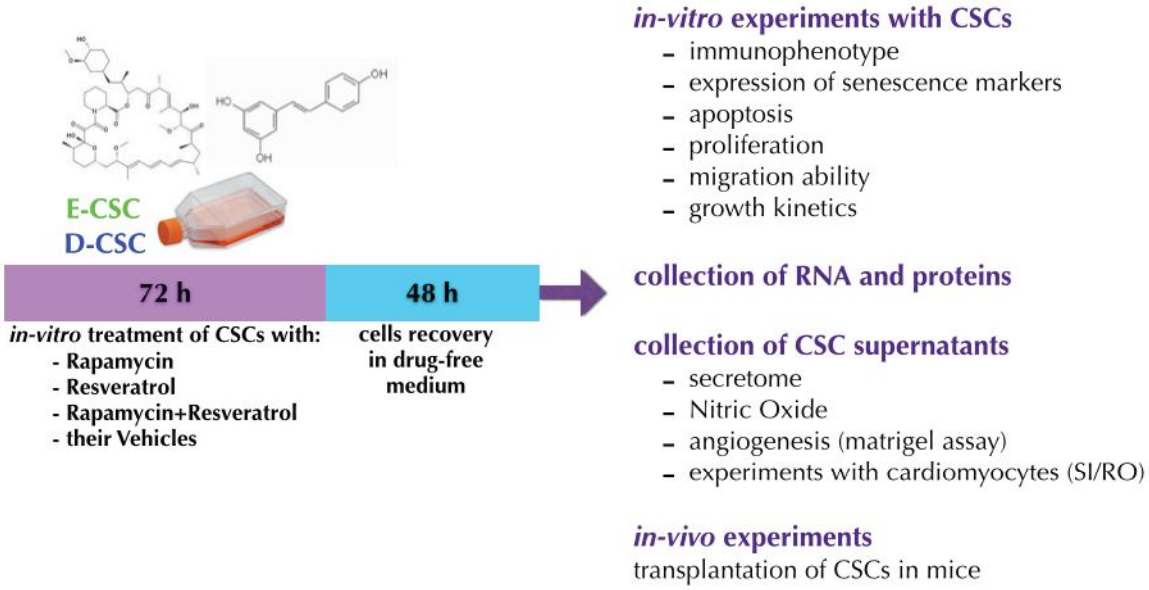

2.2.1 Collection of CSC supernatants for the analysis of the secretome

For the analysis of the secretome (for cytokine, nitrite production and endothelial networks formation assay) supernatants incubated for 48hrs with vehicle and drug-treated CSCs, were collected. The volume was measured and the supernatants were centrifuged at 4°C for 15 minutes at 1000xg to remove debris. Cells were detached and counted. Supernatants were stored at -80°C until use. To avoid repeated freezing-thawing cycles, the supernatants were thawed only once.

To study the protective role of the CSC-conditioned medium in SI/RO injury on isolated rat cardiomyocytes, CSCs after pharmacologic or vehicle treatment were cultured in drug-free cardiomyocyte culture medium for 48hrs in hypoxic conditions (1% O2, 5%CO2), to mimic the release of cytokines in the *in-vivo* ischemia situation. Supernatants were collected and incubated on rat cardiomyocytes.

2.3 Evaluation of Caspase-1 activity on IL1β secretion

E-CSC at the fourth passage in culture were incubated for 4 hours at 37°C, in serum free medium added with either 2nM Caspase-1/ICE Inhibitor, Z-YVAD-FMK (Biovision), or with vehicle. Cell culture supernatants obtained from vehicle- treated and inhibitor-treated E- CSC were collected, added with 0,5% w/v BSA (Sigma-Aldrich, Dorest, UK) and centrifuged at 10000xg, at +4°C. The supernatants of centrifuged samples were collected and, once volumes were measured, they were stored at -80°C until analysis. At the end of the incubation period, vehicle- treated and inhibitor-treated E-CSC were detached from culture plates and counted.

IL1β levels were measured employing the Bio-Plex Pro Human Cytokine 17-plex Assay (Bio-Rad) following manufacturer's instructions. Cytokine concentrations were normalized for the volume of collected supernatant, number of E-CSC and hours of incubation.

2.4 CSC growth kinetic (CPDT)

For the determination of the cell population doubling time (CPDT), CSCs were seeded at a density of $5 \cdot 10^3$ cells/cm^2. Cells were treated with drugs or vehicles for 3 days; at the end of the 48hrs of release period, cells were detached and seeded into 6well-plates at a density of $3 \cdot 10^3$ cells/cm^2 in expansion medium. At different time points (on day 1-2-3-5-8 of culture) cells were detached and counted using a Burker Counting Chamber. Population doubling time was calculated during the log-phase of growth.

2.5 Flow cytometry

To perform flow-cytometric analysis, CSCs were detached from the culture substrate (2.1.1). Detached cells were washed in HBSS, resuspended in 200 μL of calcium and magnesium-free HBSS and incubated with the appropriate antibodies (listed in **Table 3**) for 20 minutes at room temperature (RT), in the dark.

The c-Kit antigen required a different procedure as it was an unconjugated antibody. After the first incubation with the c-Kit antibody (30 minutes at 37°C), cells were washed with HBSS and incubated with a labelled secondary antibody for 20 minutes at 37°C. Isotype matched antibodies were employed as negative controls. After incubation, cells were washed, resuspended in 250μL of HBSS and analyzed.

Cell analysis was carried out with a FACSCanto analyzer (Becton Dickinson, Franklin Lakes, NJ, USA). Cells of interest were gated on the basis of their physical parameters (side scatter (SSC) and forward scatter (FSC)). Cell doublets were gated-out by plotting fluorescence area vs width. Mean fluorescence intensity was calculated by dividing the mean fluorescence of labeled cells by the mean fluorescence of the negative control.

Table 3. FACS antibodies				
Antigen	**Antibody**	**Company**	**Time, Temp**	**secondary antibody**
CD13	Alexa647-conjugated mouse monocl	eBioscience	20′ RT	-
CD44	FITC-conjugated mouse monocl	BD	20′ RT	-
CD49a	PE-conjugated mouse monocl	BD	20′ RT	-
CD49b	PE-conjugated mouse monocl	BD	20′ RT	-
CD49d	Alexa647-conjugated mouse monocl	eBioscience	20′ RT	-
CD73	PE-conjugated mouse monocl	BD	20′ RT	-
CD105	PE-conjugated mouse monocl	Serotec	20′ RT	-
KDR	PE-conjugated mouse monocl	Serotec	20′ RT	-
c-Kit	Unconjugated rabbit polyclonal	Dako	30′ 37°C	Alexa488, 1:600, 20′ 37°C

2.6 Immunofluorescence staining of cells

To analyze the expression of proteins typical of the states of proliferation and senescence, Vehicles- or drugs-conditioned-CSCs were immuno-stained with specific antibodies.

2.6.1 Staining for proliferation and senescence

For the quantification of senescence and proliferation markers in CSCs, cells were cultured in 96-well plates (with clear bottom specific for use in imaging) and at the third passage were fixed with 4% buffered paraformaldehyde (PFA) ((Sigma-Aldrich, Dorest, UK)). The culture medium was removed and discarded from the adherent cells and the cells were washed twice with PBS. The cells were incubated for 20 minutes at RT (in the dark) with freshly prepared PFA. After the incubation the PFA solution was discarded and the cells were washed three times with PBS. To permeabilize the fixed cells, a solution of 0.1% (v/v) Triton-X 100 (Sigma-Aldrich, Dorest, UK) diluted in PBS was incubated with the cells for 10 minutes at RT, followed by washings with PBS and finally a blocking step with 10% heat-inactivated donkey serum (Jackson ImmunoResearch) in PBS for 30 minutes at RT. Cells were incubated with a primary antibody in a humidified chamber, afterwhich the cells were washed with PBS three times, before incubation with the appropriate labeled secondary antibody, diluted in PBS, in a humidified chamber for 1 hour at 37°C, in the dark. The cells were again washed with PBS three times before staining of nuclei with 1μg/mL of DAPI (Sigma-Aldrich, Dorest, UK) diluted in PBS. DAPI stained cells were stored in a solution of 80% (v/v) Glycerol (Sigma-Aldrich, Dorest, UK) in PBS, at 4°C in the dark. The list of antibodies and the informations about their dilution, incubation time and temperature are reported in **Table 4**. For each staining, a negative

control without the primary antibody was included, in order to exclude the non-specific binding of the secondary antibody inside the cells. For multiple stainings, the order of incubation of primary antibodies is: 1. rabbit, 2. mouse.

Table 4. Cells immunofluorescence antibodies

Antigen	Antibody	Company	Time, Temp, dilution	secondary antibody (all from Invitrogen and produced in donkey)
$p16^{INK4A}$	mouse monoclonal	CIN-TEK	O/N, 4°C, prediluted	Alexa488, 1:600, 1h 37°C
γH2AX	mouse monoclonal	Millipore	2h, 37°C, 1:500	Alexa555, 1:800, 1h 37°C
Ki67	rabbit policlonal	Leica-Novocastra	O/N, 4°C, 1:1000	Alexa488, 1:600, 1h 37°C

2.6.2 Staining for apoptosis

Quantification of apoptosis in CSCs was performed using the *ApopTag® Plus Fluorescein In Situ Apoptosis Detection Kit* (Millipore,Watford, UK). The protocol was performed as per the manufacturer's instruction, but method used is described below.

CSCs were cultured in clear bottomed 96-well plates and at the third passage the plates were fixed with 1% buffered PFA for 10 minutes at RT. The cells were washed twice with PBS and permeabilized with pre-cooled Ethanol: Acetic Acid (Sigma-Aldrich, Dorest, UK) 2:1 for 5 minutes at -20°C. The cells were incubated with 50 μL Equilibration Buffer (provided in the ApopTag® Plus kit). The supernatant was then aspirated and the cells were incubated with the TdT Working Solution and the digoxigenin-labeled nucleotides (70% Reaction Buffer : 30% TdT Enzyme), in a humidified chamber for 1 hour at 37°C. The 50 μL of Stop/Wash buffer (1mL of concentrated Stop Buffer: 34mL of distilled water) was incubated on the cells for 10 minutes at RT, after which the cells were incubated with 50 μL anti-digoxigenin fluorescein antibody diluted as per manufacturer's instructions. This incubation was performed for 30 mins at RT avoiding light exposure. To stain the cell nuclei, the cells were incubated for 5 minutes at RT, in the dark, with a solution of 1μg/mL DAPI diluted in PBS. The cells were stored in a solution of 80% (v/v) Glycerol in PBS, at 4°C in the dark. For each staining, cells for a negative (without TdT incubation) and a positive (pretreated with Dnasi I, 3U/mL for 10 min at RT) control were included.

2.6.3 Quantification

Image analyses were performed employing a Leica DMI6000B setup (Leica microsystems, Germany) equipped with a 40X oil-immersion objective (numerical aperture: 1.25) or a 63X oil-

immersion objective (numerical aperture: 1.40). Experiments were performed in duplicates. For each marker, at least 400-500 cells were analyzed. Positive cells for each marker were expressed as percentage of the total cells.

2.7 Cell migration: scratch assay

In vitro cell migration of vehicles or drugs treated E-CSC was evaluated by a scratch assay on E-CSC seeded in 96well-plates. 8000 cells were seeded in each well; at 80% of confluence, cells were pharmacologically or vehicle treated for 3 days. At the end of the 48 hrs of release-period in drug-free medium - when cells should have reached an high confluence - scratches were created in the center of the well utilizing 10μl tips. Cells were washed with PBS and new fresh medium is added to the plate. Phase contrast images of the scratches were acquired immediately and after 2, 8 and 24h, until their complete closure. Images were then compared and quantified by the software ImageJ. The rate of cell migration, expressed as μm/h, was calculated in the interval of time between 2 and 8 hours from the creation of the scratch, measured in 3 different points of the scratch. Then the average migration speed was calculated. Each condition was performed at least in quadruplicated.
Images were acquired using the microscope Leica DMI6000B equipped with a 10X objective (numerical aperture: 0.25).

2.8 Analysis of CSC secretome

2.8.1 Flow cytometry assay

Inflammatory cytokines (IL-6, IL-8 and IL-1β) were analyzed by human Th1/Th2 11plex FlowCytomix Multiplex (eBioscience, San Diego, CA, USA) following manufacturer's instructions. This kit allows the measurement of 11 different cytokines, both Th1 cytokines (referred to also as Type-1 cytokines) and Th2 cytokines (referred to also as Type-2 cytokines) secreted by cells, using a principle similar to the ELISA assay.
Cell analysis was carried out with a FACSCanto analyzer (Becton Dickinson, Franklin Lakes, NJ, USA). The sample values are read off the standard curve. The values of cytokines have been normalized for the volume of the collected supernatant, the number of cells and the time of incubation.

2.8.2 ELISA assay

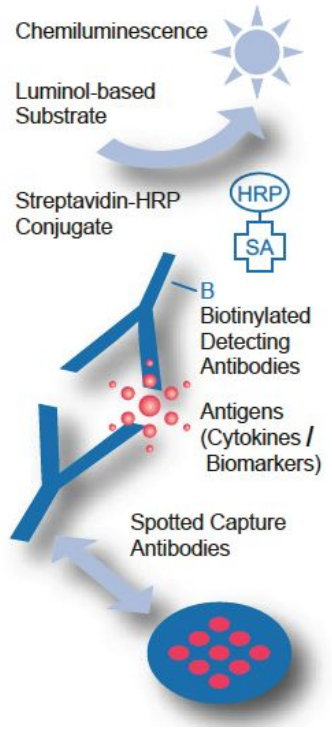

VEGF, bFGF, and HGF in CSCs supernatants were analyzed by *Searchlight angiogenesis array* (Aushon, Billerica, MA, USA) following manufacturer's instructions. This assay allows the simultaneous measurement of the cytokines combination.

The principle of the function of this assay is showed in the figure on the left, taken from the user guide. Capture antibodies specific for the cytokines are pre-coated onto the 96-well plate, in each well. Standards, control and samples were pipetted into the wells and incubated for 2 hours at RT, during which any specific protein present in the samples is bound by the immobilized antibody. After washing away any unbound substances (washing buffer 0.05% v/v Tween-20 (Sigma-Aldrich, Dorest, UK) diluted in PBS), a specific biotin-linked detecting antibody was added to the wells and incubated for 30 minutes at RT. Following a wash to remove any unbound antibody, a complex of Streptavidin (SA - which recognizes and binds the biotin) and the enzyme Horseradish Peroxidase (HRP) was added to the wells and incubated for 30 minutes at RT. Last, following a wash to remove any unbound SA-HRP complex, a Luminol-based substrate solution was added to the wells and incubated for 5 minutes. The resulting luminescence is proportional to the amount of protein bound in the initial step. The sample values were read off the standard curve. Measurements were performed in triplicates. The values of cytokines have been normalized for the volume of the collected supernatant, the number of cells and the time of incubation.

2.9 Determination of Nitric Oxide (NO)

2.9.1 Determination of intracellular NO

Determination of intracellular NO was performed using DAF-FM (4-amino-5-methylamino-2', 7'-difluorofluorescein diacetate), a reagent that allows the detection and quantification of low concentrations of nitric oxide. To analyze intracellular NO levels in cultured cells after detachment, CSCs were washed with HBSS and incubated with 1μM DAF-FM for 20 minutes at 37°C, in the dark. After an additional washing, cells were analyzed by flow-cytometry after 30 minutes to allow complete de-esterification of the intracellular diacetate.

Cell analysis was carried out with a FACSCanto analyzer (Becton Dickinson, Franklin Lakes, NJ, USA). Positive cells were expressed as percentage of total cells.

2.9.2 Determination of nitrites released in CSC supernatant

For the evaluation of the production and release of NO in CSC culture supernatants, endogenous nitrites have been dosed employing the *Total Nitric Oxide and Nitrate/Nitrite Parameter Assay Kit* (R&D Systems, Minneapolis, MN USA), following manufacturer's instructions. The reaction is followed by colorimetric detection of total nitrite as a chromophoric azo-derivative, product of the Griess Reaction, which absorbs light at 540-570 nm.

Working standards (provided inside the kit) and samples are pipetted into the wells of a 96-well plate. NADH and Nitrate Reductase were added to all wells. After an incubation of 30 minutes at 37 °C, Griess Reagent I and II were added to all wells and reagents are mixed well by gently tapping the side of the plate. After a further incubation for 10 minutes at RT, the optical density of each well was determined using a microplate reader set at 540 nm. Measurements was performed in duplicate. A standard curve was generated and the sample values were read off the standard curve. The values of nitrites were normalized for the volume of the collected supernatant, the number of cells and the time of incubation.

Before analysis, proteins that could interfere with the assay were removed from the culture supernatant through ultrafiltration using 10,000 molecular weight (MW) cut-off filters (Amicon, Millipore, Billerica, MA, USA).

2.10 Simulated Ischemia/ReOxygenation (SI/RO) on cardiomyocytes

Cardiomyocytes were isolated from 3 adult male Wistar rats. Experiments were performed in accordance with the Guide for the Care and Use of Laboratory Animals (Institute of Laboratory Animal Resources, 1996) and with approval of the British Home Office and the University of Bristol. Animals were killed by stunning and cervical dislocation prior to dissection of the heart.

2.10.1 Isolation and culture of adult rat cardiomyocytes

Ventricular cardiomyocytes were isolated by the Langendorff method as in (King et al, 2010)[233]. All solutions (see par. 6) are gassed with 100% O_2 and heated to 37 °C before perfusing through the heart. The solutions were perfused through the heart at a rate of 10 mL/min.

The heart was excised from the rat and placed in 4 °C solution B to stop contraction. The isolated heart was cannulated via the aorta onto a modified Langendorff apparatus (ADInstruments, UK) (illustrated in the figure below, taken from (Louch et al, 2011)[234]) and perfused retrogradely. Initially, solution B was perfused through the heart to restart contractile activity and wash out the blood (5 minutes).

The perfusing solution was then switched to solution C for a further 5 minutes. Hearts were then perfused with solution D, containing the enzymes Collagenase type-2 and Protease type XIV, to

break down extracellular matrix connections and assist the digestion of the heart. Solution D was perfused through the heart until it is soft to touch, generally between 20-25 minutes.

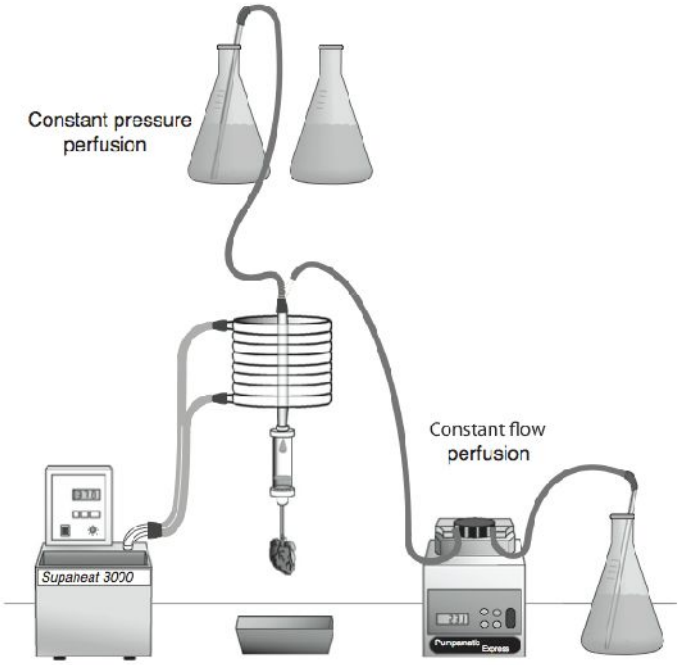

The enzyme solution was then washed out with solution E for 5 minutes; solution E has a low $CaCl_2$ concentration (150 μM). At this point, the ventricles were removed from the heart and chopped into several small pieces. The tissue undergoes mechanical disaggregation in a shaking water bath (100 rpm) (Stuart Scientific, UK) at 37°C for 5 minutes. The solution was then strained through muslin to remove the undigested tissue, topped up to 25 mL with solution E and allowed to settle for 10 minutes.

After 10 minutes the $CaCl_2$ concentration was increased from 150 μM to 500 μM using a 1M $CaCl_2$ stock solution. The cells were allowed to equilibrate in the new $CaCl_2$ concentration for a further 10 minutes. Finally, $CaCl_2$ is added to the cell solution to bring the final concentration to 1 mM. The cell suspension contains a mixture of healthy and dead cardiomyocytes.

At the end of the isolation procedure, Calcium was reintroduced gradually in cell suspension to further reach a concentration of 1.8 mM (the same of the culture medium) by two incremental additions of 0.4 mM $CaCl_2$ at a 4-minute interval. Cardiomyocytes were then centrifuged at 200xg for 3 minutes, resuspended in warm cardiomyocyte culture medium (see par. 6) and plated at a density of 10,000 cells/cm^2 on murine laminin (Sigma-Aldrich - 10μg/cm^2) coated 96-well plates.

Myocytes were subsequently incubated for 1hr at 37°C, 5% CO2 to allow attachment to culture dish. Afterwards, culture medium was replaced with fresh one and cells incubated for 4 more hours. After this time any cells which have not attached can be removed by gently changing the medium. Rounded and hyper-contracted myocytes would not attach to the culture surface, therefore the majority of myocytes remaining are rod-shaped and viable.

2.10.2 Ischemia-ReOxygenation injury

Cardiomyocytes were subjected to Simulated Ischemia (SI) for 40 minutes by replacing the medium with an "ischemia buffer" at pH6.2 (see par. 6) and incubating cells at 37°C, 1% O_2

and 5% CO_2. After the simulated ischemia cardiomyocytes were exposed to ReOxygenation (RO) incubating the cells for 17 hr at 37°C, 5%CO_2, in cardiomyocyte culture medium conditioned or not for 2 days by D- and E-CSC (see 2.2.1) and diluted 1:1 with fresh new myocyte medium. In particular, a pool of conditioned media was used for each condition: at this aim, the conditioned medium from the different CSC lines was mixed in the same proportions.

Specifically, in the first set of experiments, the effect of the pro-inflammatory IL1β - secreted by E-CSC - on cardiomyocytes has been analyzed. In order to do this, cardiomyocytes were incubated with the medium conditioned by CSCs supplemented or not of an IL1β-blocking antibody (Abcam, dilution 1:100). The medium was incubated with the antibody at 37°C for 1 hour before the addition to myocytes.

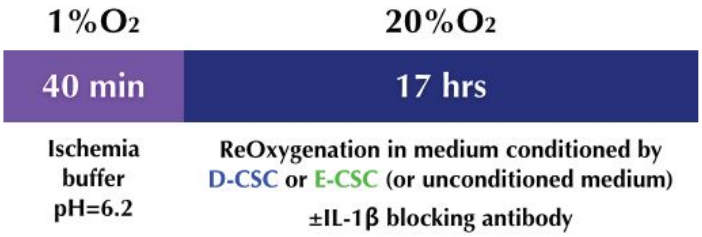

In the second set of experiments, the protective role of the secretome released by E-CSC treated or not for three days by drugs (10nM Rapamycin + 0.5μM Resveratrol) on cardiomyocytes was evaluated. Cells were incubated with the medium conditioned by CSCs for two days after the removal of either the drugs or the vehicles (see 2.2.1).

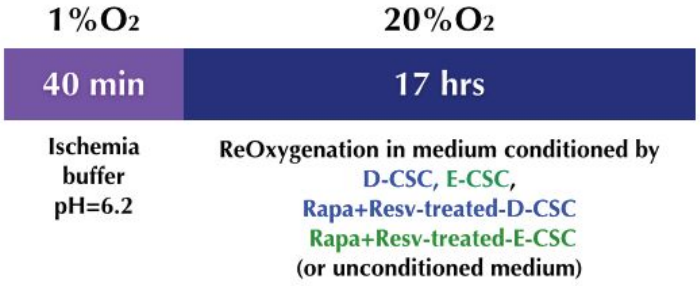

For each group, the experiments were performed at least in quadruplicate, for both the experiments.

2.10.3 Evaluation of cardiomyocytes apoptosis

For evaluation of cardiomyocytes apoptosis, a *Caspase Glo 3/7 assay* (Promega, UK) has been employed, following the manufacturer's instructions.

The *Caspase-Glo 3/7 Assay* was a homogeneous, luminescent assay that measures caspase-3 and -7 activities. The assay provided a luminogenic caspase-3/7 substrate. The Caspase-Glo 3/7

Reagent induces cell lysis, followed by caspase cleavage of the substrate and the release of a substrate for luciferase (aminoluciferin). Luminescence was proportional to the amount of caspase activity.

At the end of the 17 hours of ReOxygenation, the medium was removed and 30μL of fresh cardiomyocyte medium was added to all wells. A blank reaction (well without cells) was included for each group to measure the background luminescence associated with the cell culture system and the Kit reagents. 30μL of Caspase-Glo 3/7 Reagent were added to each well and the plate was incubated onto a plate shaker for 30 minutes at RT, in the dark. Luminescence was measured using a luminometer.

For the analysis, the values for the blank reaction were subtracted from experimental values. The levels of caspase activity in each experimental group were indicated as fold change respect to the control group (cardiomyocytes that received only their medium without any treatment).

2.10.4 Evaluation of cardiomyocytes senescence

To evaluate myocyte senescence, at the end of the ReOxygenation period cells were washed with PBS and fixed with 4% PFA for 20 minutes at RT. The cells were then washed and permeabilized for 10 minutes at RT with a 0.1% (v/v) Triton-X100 solution in PBS. Cells were incubated with a blocking solution (10% normal goat Serum in PBS) for 30 minutes at RT and incubated for 16h at 4°C with a mouse anti-p16^{INK4A} antibody (1:50 dilution, Clone F12, Santa Cruz Biotechnologies, USA). After washings with PBS to remove the unbound primary antibody, cells were incubated for 1hr at RT, in the dark, with an Alexa 488 goat anti-mouse secondary antibody (Invitrogen, 1:200 dilution). Myocyte cytoplasm was than stained with an antibody anti-alpha sarcomeric actin (Sigma, IgM, 1:100 dilution, 1hr 37°C), in the dark. After this incubation, the cells were incubated for 1hr at RT, in the dark, with a TRITC goat anti-mouse IgM secondary antibody (1:200 dilution). At the end, nuclei were stained by incubation for 5 minutes at RT with a solution of 1μg/mL DAPI diluted in PBS and cells are stored in a solution of 80% (v/v) Glycerol in PBS, at 4°C in the dark. All the incubations are performed in a humidified chamber.

For quantification, at least 500 cells were counted for each replicate. The analysis was performed using the microscope Leica DMI6000B, with a 40X objective (numerical aperture 1.25).

2.11 Matrigel assay

The capacity of CSCs to induce the formation of an endothelial cell network of human umbilical vein endothelial cells (HUVECs, Cambrex/Lonza) was evaluated using an ECM (extracellular matrix) gel assay (BD Bioscience, Oxford, UK).

70 μL of matrigel was added into each well of an ice-cold 96-well plate and incubated for 30 minutes at 37°C. This was performed on ice. 8000 HUVECs were resuspended in 100 μL of conditioned medium from CSCs previously diluted 1:1 with new fresh EGM-2 medium (Lonza) supplemented with 5% FBS. The cells were added on the top of the gelified matrigel (100 μL / well) and incubated for 20 hours at 37°C, 5% CO_2. Media conditioned by D- and E-CSC treated either with Rapamycin + Resveratrol or Vehicles were used for this assay. In particular, a pool of conditioned media was used for each condition. The conditioned medium from the different CSC lines was mixed in the same proportions. In addition, a control with medium not conditioned by CSCs was included.

The assay was performed in quintuplicate. Network formation was analyzed in an Axiovert microscope (Zeiss); an image for each well was acquired at a magnification of 50X. For quantification, the length of the networks was measured using the software ImageJ (http://rsb.info.nih.gov/ij/) and the cumulative tube length (in mm) per field was calculated.

3. *IN VITRO* EXPERIMENTS: MOLECULAR BIOLOGY

3.1 Analysis of micro-RNA-132 and micro-RNA-146a

3.1.1 RNA extraction and quantification

microRNAs were extracted from a CSC confluent 100mm diameter culture dish employing the miRVana kit, following the manufacturer's instructions (Life Technologies). Briefly, samples were disrupted in a denaturing lysis buffer and stored at -80°C if not immediately used. Samples are first subjected to Acid-Phenol:Chloroform (Sigma) extraction followed by the addition of 100% ethanol (Sigma-Aldrich, Dorest, UK) to isolate small RNAs. The ethanol was added so the final volume in the samples was 25% ethanol. When this lysate/ethanol mixture was passed through a glass-fiber filter, large RNAs are immobilized and the small RNA species are collected in the filtrate. The ethanol concentration of the filtrate was then increased to 55%, and the solution was passed through a second glass-fiber filter where the small RNAs become immobilized. This RNA was washed a few times with ethanol, eluted in RNAse-free water and stored at -80°C until required.

The concentration of RNA is determined by measuring the absorbance at 260 nm (A260) using a Nanodrop spectrophotometer (Nanodrop 1000, Thermo Scientific) according to the manufacturer's instructions. The ratio between the absorbance values at 260 and 280 nm gave an estimate of RNA purity. Pure RNA has an A260/A280 ratio of 1.9–2.1.

3.1.2 RNA reverse transcription

To reverse transcribe the RNA, the *miRNA Reverse Transcription Kit* (Applied Biosystems division of Life Technologies, Warrington, UK) was used, as per manufacturer's instructions. Briefly, the reaction of reverse transcription included dNTPS, multiscribe, RT buffer, RNA inhibitor, water, miR specific RT primer and total RNA. The reaction was run on a thermal cycler at 16°C for 30 min, 42°C for 30 min, 85°C for 5 min and held at 12°C before being stored at -20°C.

3.1.3 miR amplification by semiquantitative Real-Time PCR

The expression of hsa-miR-132 and hsa-miR-146a was evaluated by quantitative PCR-based amplification using TaqMan probes (Life Technologies, Paisley, UK) and a Roche LightCycler 480 Real-Time PCR System.

The reaction mixture of a 10 μL reaction comprises 5 μL of 2x Taqman Mastermix, 0.5 μL of probe, 3 μL of water and 1.5 μL of cDNA. Expression of hsa-miR-132 and -146a were normalized to hsa-miR-16 as reference. Relative Quantification was calculated using the $2^{-\Delta\Delta Ct}$ method previously described in (Livak et al, 2001)[235]. Results are expressed in fold-change respect to the control group.

3.2 Evaluation of IL-1β effects on IKKβ phosphorylation

E-CSC at the fourth passage in culture were incubated for 24 hours at 37°C, in growth medium added or not with 20 μg/ml IL1β-blocking antibody (Abcam, Cambridge, United Kingdom).

After incubation, treated and untreated E-CSC lysates were collected following the protocol employed for western blot analysis (see below) and analyzed for IKKβ and phospho-IKK^{Ser177}.

3.3 Western Blot analysis

3.3.1 Protein collection and extraction

For the preparation of total cell lysates, CSCs were harvested by trypsination, washed with ice-cold PBS, counted, pelleted (supernatant was discarded) and frozen.

Cell pellet was resuspended in lysis buffer (see par. 6), at a cell density of 10^7 cells/mL and rotated for 30 minutes at 4°C. After centrifugation at 12000xg for 10 minutes at 4°C, the supernatant was collected as total cell lysate and stored at -80°C until required.

3.3.2 Measurement of protein concentration

Concentration of protein extracts was measured using the Bradford assay (Bio-Rad protein assay reagent, Bio-Rad, Hercules, CA). The measurement of protein concentration was completed

following the Manufacture's instructions. The Bradford reagent was initially diluted to 1X with distilled water. BSA standards were prepared, ranging from 0 μg/ml to 20 μg/ml and diluted in 1x Bradford reagent (final volume 1ml). 2 μl protein lysate was then diluted in 998 μl Bradford reagent, before the lysates and standards absorbance was measured with a spectrophotometer set at 595 nm. The protein concentration of the lysates was calculated using a standard curve generated from the known concentration of the protein standards.

3.3.3 Electrophoresis and immunoblotting

For solutions, see par. 6. 30μg of total cell lysate was prepared for electrophoresis in sample loading buffer. Samples were boiled at 95°C for 5 minutes and then spun down. Samples were separated by a 12% SDS-PAGE gel.

The resolving gel is prepared at the right density for the protein of interest and polymerized between two glass plates in a gel caster. The gel was leveled using saturated butanol. After the resolving gel was polymerized, the stacking gel was poured on the first gel, with a comb inserted at the top to create the sample wells. Once polymerized the combs were removed. The gel was put into the Bio-Rad Tetra running tank with 500 mL of 1x running buffer, then the samples and 10 μL of protein ladder were loaded into the wells. The voltage was set a 120V for 1 hr.

Separated proteins were then transferred to nitrocellulose membranes (Schleicher & Schuell, Keene, NH). The "sandwich" was prepared with a sponge, 3X filter paper (Bio-Rad,Hercules, CA), gel, membrane, 3X filter paper and sponge and placed in the cassette. Paper and sponges were soaked in transfer buffer and the tank was filled with running buffer. The voltage was set at 30 volts for 12hrs at 4C. The resulting transferred proteins and membrane were then ready to be used in the antibody hybridization method.

3.3.4 Antibody hybridization

Membranes were saturated by incubation at RT for 1 hour with 5% (w/v) nonfat dry milk (Sigma-Aldrich, Dorest, UK) in TBS-T and incubated overnight at 4°C with the antibodies listed in **Table 5**. After three washes with TBS-T, membranes were incubated with an anti-rabbit antibody coupled to the enzyme peroxidase (HRP) (Sigma-Aldrich, Dorest, UK). After 2 hours of incubation at RT, membranes were washed 3 times with TBS-T and last with distilled water, to remove the Tween-20 detergent. The blots were developed using the ECL enhanced chemiluminescence procedure (GE Life Science, Buckinghamshire, Uk), which consists in the incubation of the membrane with a chemiluminescence solution, resulting in a production of a chemiluminescent signal that is captured onto a film.

Equal loading was confirmed by the use of a polyclonal anti-actin antibody (Sigma-Aldrich, Dorest, UK). Blots were quantified using a Gel Doc 2000 video densitometer (Bio-Rad,Hercules, CA).

Table 5. WESTERN BLOTTING antibodies

Antigen	Antibody	Company	Time, Temp, Dilution
mTOR	rabbit monoclonal	Cell Signaling	1:1000, O/N, 4°C
p-mTOR$^{(Ser248)}$	rabbit monoclonal	Cell Signaling	1:1000, O/N, 4°C
p70 S6K	rabbit monoclonal	Cell Signaling	1:1000, O/N, 4°C
p-p70 S6K$^{(Thr389)}$	rabbit monoclonal	Cell Signaling	1:1000, O/N, 4°C
Atg3	rabbit polyclonal	Cell Signaling	1:1000, O/N, 4°C
Atg7	rabbit polyclonal	Cell Signaling	1:1000, O/N, 4°C
Akt	rabbit monoclonal	Cell Signaling	1:1000, O/N, 4°C
p-Akt$^{(Ser473)}$	rabbit monoclonal	Cell Signaling	1:1000, O/N, 4°C
P62 SQSTM1	rabbit polyclonal	LifeSpan BioSciences	1:1000, O/N, 4°C
Sirt1	rabbit monoclonal	Cell Signaling	1:1000, O/N, 4°C
p-CREB$^{(ser133)}$	rabbit polyclonal	Cell Signaling	1:1000, O/N, 4°C
p-CREB	rabbit polyclonal	Cell Signaling	1:1000, O/N, 4°C
Beclin 1	rabbit monoclonal	Cell Signaling	1:1000, O/N, 4°C
LC3 B	rabbit monoclonal	Cell Signaling	1:1000, O/N, 4°C
Cleaved Caspase 1	rabbit polyclonal	BioVision	1:1000, O/N, 4°C
IKKβ	rabbit polyclonal	Cell Signaling	1:1000, O/N, 4°C
p-IKKβ$^{(ser177)}$ p-IKKα$^{(ser176)}$	rabbit polyclonal	Cell Signaling	1:1000, O/N, 4°C
AMPKα	rabbit monoclonal	Cell Signaling	1:1000, O/N, 4°C
p-AMPKα $^{(Thr172)}$	rabbit monoclonal	Cell Signaling	1:1000, O/N, 4°C

4. *IN VIVO* STUDIES

4.1 Experimental plan and Ethics

Animal experiments were performed in accordance with the Guide for the Care and Use of Laboratory Animals (Institute of Laboratory Animal Resources, 1996) and with approval of the British Home Office and the University of Bristol.

Female 8-week-old immunodeficient SCID/beige mice (Charles River) were anesthetized with 2,2,2 tribromo-ethanol (Avertin) at a dose of 250mg/kg, by intra-peritoneal injection.

Under anesthesia and artificial ventilation, the chest cavity was opened and, after careful dissection of the pericardium, the left anterior descending (LAD) coronary artery was permanently ligated using a 7-0 silk suture. This operation was performed by a highly trained person with an animal license.

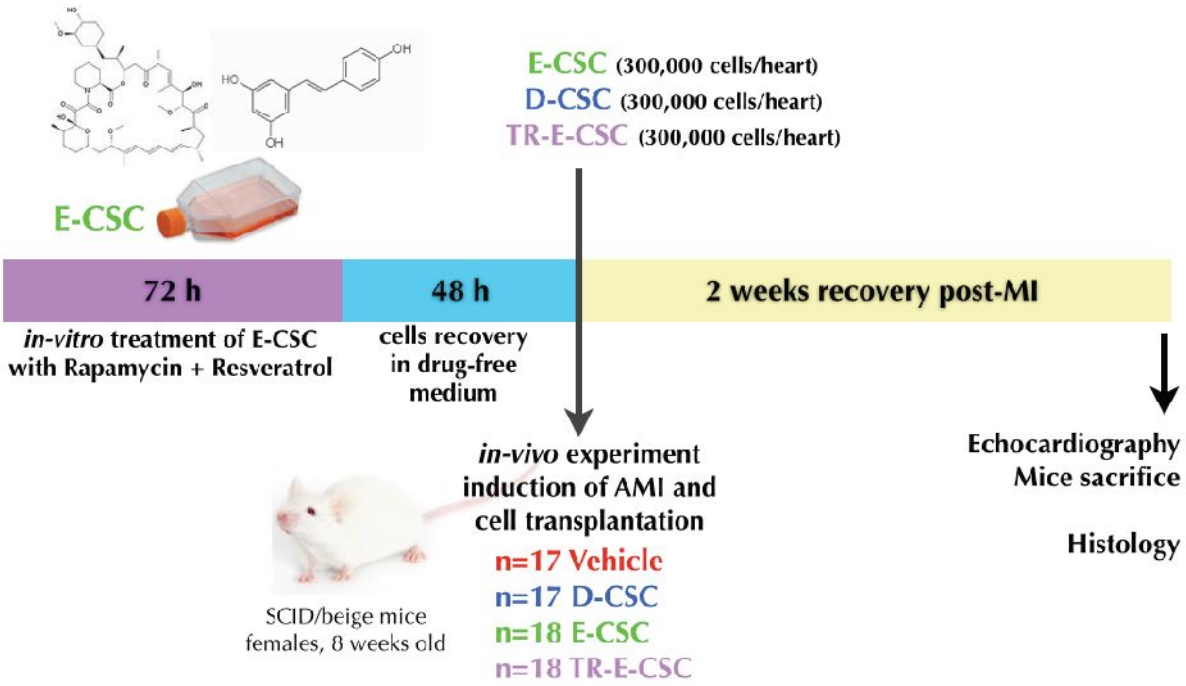

In the first set of experiments aimed at comparing the *in vivo* reparative ability of D-CSC vs E-CSC, myocardial infarction procedure was followed by injection of one of the following:

1. vehicle (PBS, n=5 mice),
2. CSCs obtained from 4 donor hearts (D-CSC, n=9 mice),
3. CSCs obtained from 3 explanted hearts (E-CSC, n=6 mice).

D-CSC and E-CSC were cultured until passage 3 and then injected.

In the second set of experiments aimed at comparing the *in vivo* reparative ability of drug-treated vs untreated-E-CSC, myocardial infarction procedure was followed by injection of one of the following (see figure above):

1. vehicle (PBS, n=17 mice),
2. CSCs obtained from 8 donor hearts (D-CSC, n=18 mice),
3. CSCs obtained from 7 explanted hearts pre-conditioned by vehicles (E-CSC, n=17 mice),
4. CSCs obtained from 5 explanted hearts and preconditioned *in-vitro* by Rapamycin and Resveratrol (TR-E-CSC, n=18 mice).

In both sets of experiments, $3 \cdot 10^5$ cells per animal were injected at 3 different sites (100,000 cells per site of injection) along the infarct border zone. Animals were allowed to recover with aseptic precautions and received analgesic medication (Buprenorphine, 0.1mg/kg s.c.) to reduce post-operative pain.

4.1.1 Hemodynamic measurements

Dimensional and functional parameters were measured with a mouse-dedicated high-frequency, high-resolution echocardiography system (Vevo 770, VisualSonics, Toronto, Canada) as described in (Katare et al, 2011)[223] on day 14 after MI. Intraventricular pressure measurement was done using a high-fidelity 1.4F transducer tipped catheter (Millar Instruments, Houston, TX, USA) inserted into the left ventricle through right carotid artery.

Hearts were imaged in the 2-dimensional parasternal short-axis view, and an M-mode measurement was recorded at the mid-ventricle, at the level of the papillary muscles. Heart rate, thickness of left ventricular wells, end-diastolic and end-systolic diameters and volumes were measured from the M-mode image, illustrated in (**fig. 4.1**). Stroke volume was defined as end-diastolic minus end-systolic volumes. Fractional shortening and ejection fraction were used as indexes of cardiac contractile function. Cardiac output was calculated multiplying stroke volume by heart rate.

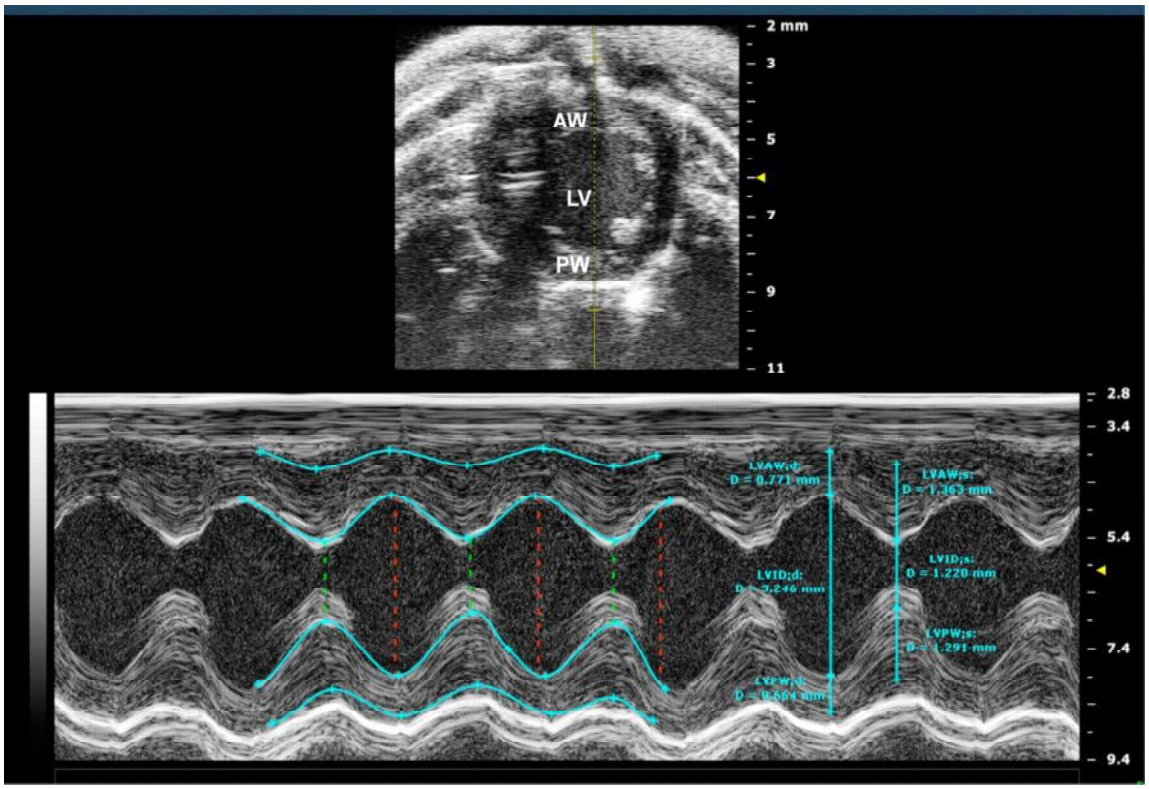

Figure 4.1 M-mode imaging. *M-mode image of the LV displays dimensions of the ventricular walls, LV cavity, and cardiac function measurements. y-axis represents the distance (in mm) from the transducer; time (in ms) is on the x-axis. The M-mode images show the LVAW, LV chamber, and LVPW throughout diastole (d) and systole (s). Echogenic peaks visible along the PW during systole represent the papillary muscle entering the field of view. LVIDs, left ventricular internal diameter (systole); LVID d, left ventricular internal diameter (diastole). Taken from*[236].

4.1.2 Collection and processing of heart samples for histology

Hearts were arrested in diastole by intra-cardiac injection of Cadmium Chloride 14 days after surgery and fixed by retrograde perfusion with formalin (a solution of 37% formaldehyde, (Sigma-Aldrich, Dorest, UK)) throughout the abdominal aorta. Hearts were then harvested for histological analysis and further fixed for 24h in formalin at 4°C, followed by washings with PBS and dissection at apical, mid-ventricular and basal level. Last, the tissues were processed for paraffin-embedding. Briefly, tissues underwent dehydration through an ascending scale of alcohols, a cycle of clearene (Sigma-Aldrich, Dorest, UK) to remove alcohol and a liquid paraffin wax bath to allow the complete penetration of paraffin within the samples.

After embedding in paraffin blocks, samples were cooled down to -20°C on a cold surface and cut using a microtome in 5μm thick tissue sections, mounted on positive-charged slides and dried first overnight at RT and then 3 hours at 56°C to melt the paraffin and ensure the sections adherence to the slides.

4.2 Histology on heart tissue sections

In advance to perform all the stainings described below, tissue sections were exposed to deparaffinization in xylene and rehydratation through passages in decreasing concentrations of alcohol (100%, 85%, 70%). Last sections were hydrated in distilled water.

4.2.1 Hematoxylin & Eosin staining

Hematoxylin & Eosin staining was performed to evaluate the tissue characteristics in terms of infarcted zone and inflammatory infiltration.

Briefly, the protocol consisted of sequential incubations of sections in the following solutions: Calcium formol, 20 sec.; running water, 10 sec.; Harris Hematoxylin, 60 sec.; running water, 60 sec.; distilled water, 10 sec.; 3% Eosin G in distilled water, 30 sec.; running water, 60 sec.; distilled water, 10 sec.; 95% and 100% Ethanol, 10 sec. each; xylene, 10 sec.; mounting with Eukitt.

4.2.2 Determination of Scar Size

To calculate the scar size, 3 sections were cut at different levels along the infarcted ventricle and stained with the Azan Mallory staining. See par. 6 for solutions.

Tissue sections were incubated for 1h in 0,1% Azocarmine G at 56°-60°C and allowed to cool down for 10 minutes. After rinsing in distilled water, the sections were incubated for 2h in 5% Phosphotungstic Acid. After a quick rinse in distilled water, sections were incubated for 1h in Mallory solution, followed by a rinse in distilled water. Sections were then dehydrated with two passages in EtOH 95% and 100% for 5 minutes each, cleared in clearene for 5 minutes and mounted in Eukitt.

The procedure allowed the cell structures to be visualized, with the staining of nuclei in red, collagen fibers (characteristic of the fibrotic scar) in blue and cell cytoplasm in orange. Images were acquired using the microscope Leica DMD108 and a 5X objective.

4.2.3 Immuno-histochemical staining for human mitochondria

At the aim to verify if human injected cells were engrafted and survived in the murine hearts 14 days after-MI and transplantation, sections were stained for a human cells specific marker.

To allow the exposition of the antigens (masked by cross-links between proteins created during the fixation process) and their recognition by antibodies, first a heat-induced antigen retrieval was performed by incubating the tissue slides for 30 minutes at 98°C in a 0.01M citrate buffer, pH 8.0. Slides were then cooled down at RT and washed in distilled water. Endogenous peroxidase was inactivated by incubation with a solution at 3.5% H_2O_2 (Sigma-Aldrich, Dorest, UK) in distilled water, for 10 mins at RT. After 2 rinses with PBS, sections were first incubated for 1hr at RT with a solution of 1% w/v BSA (Sigma-Aldrich, Dorest, UK) in PBS, then for 1hr at

RT with a primary antibody against human mitochondria (Ab-2 anti-human mitochondria, NeoMarkers) diluted 1:100 in PBS. After which sections were washed in PBS and incubated for 30 mins at RT with the Envision solution (DAKO Real Envision Detection Kit), a polymer which binds both secondary antibodies anti-mouse and rabbit, in addition to Peroxidase enzyme molecules. After further rinses with distilled water, sections were incubated for 2-5 mins at RT with the DAB (3,3'-Diaminobenzidine) chromogen substrate (DAKO Real Envision Detection Kit) prepared as per manufacturer's instructions. As soon as the reaction was visible (a precipitate colored brown could be observed), sections were washed with distilled water. Nuclei were counterstained with Harris' Hematoxylin, after which sections were washed for 2 mins in running water. Sections were dehydrated with two passages in EtOH 70%, 95% and 100% for 3 minutes each, cleared in clearene for 5 minutes and mounted in Eukitt.

For each staining, a section from human heart was included as positive control; furthermore, a section not incubated with the primary antibody was included as control to exclude the non-specific binding of the Envision polymer to the sections.

At least 6, possibly not sequential, sections were analyzed for each heart. Stained samples were analyzed at a microscope Leica DMD108 with a 40X objective.

4.2.4 Immunofluorescence stainings

For determination of cardiomyocyte proliferation, senescence and expression of markers of autophagy in the tissue sections as well to determine the density of primitive progenitor cells, sections were stained with specific antibodies (listed in **Table 6**).

To allow the exposition of the antigens (masked by cross-links between proteins created during the fixation process) and their recognition by antibodies, first a heat-induced antigen retrieval was performed by incubating the tissue slides for 40 minutes at 98°C in a 0.01M citrate buffer, pH 6.0. Slides were then cooled down at RT and washed in distilled water and PBS. After an incubation for 30 minutes at RT with a solution of 10% donkey serum (Jackson ImmunoResearch) in PBS, aimed at blocking the non-specific secondary antibody binding-sites, sections were incubated sequentially with the primary antibodies followed by their specific fluorochrome-labeled secondary antibodies (all produced in donkey). All the antibodies were diluted in PBS and incubations were performed in humidified chambers in the dark. The order for the incubation of the antibodies was determined by the host in which the antibodies have been produced. It was performed in following manner: 1. mouse IgG, 2. goat IgG, 3. rabbit IgG, 4. mouse IgM. Between the different incubations, sections were washed in PBS to remove the unbound antibodies. For each staining, a section incubated only with the secondary antibodies was prepared to check for any non-specific binding to the tissue.

At the end, to decrease the autofluorescence of the tissue, sections were last incubated for 30 minutes with a solution of 0.1% Sudan Black B (SBB) in 70% Ethanol (Sigma-Aldrich, Dorest,

UK), as explained in (Baschong et al., 2001)[237]. After washing in PBS to completely remove the SBB, sections were mounted with a solution of 80% (v/v) Glycerol (Sigma-Aldrich, Dorest, UK) in PBS added of 1μg/mL of DAPI (Sigma) and stored at 4°C in the dark.

Table 6. Tissues immunofluorescence antibodies

Antigen	Antibody	Company	Time, Temp, dilution	secondary antibody (all from Invitrogen)
α-Sarcomeric Actin	mouse monoclonal	Sigma Aldrich	1h, 37°C, 1:100	TRITC or DyLight649, 1:400, 1h 37°C
ki67	mouse monoclonal	Leica-Novocastra	O/N, 4°C, 1:1000	Alexa555, 1:800, 1h 37°C
γH2AX	mouse monoclonal	Millipore	2h, 37°C, 1:500	Alexa488, 1:600, 1h 37°C
c-Kit	goat polyclonal	R&D	2h, 37°C, 1:100	Alexa555, 1:800, 1h 37°C
GATA4	rabbit polyclonal	Santa Cruz	2h, 37°C, 1:80	Alexa488, 1:600, 1h 37°C
Tryptase	mouse monoclonal	Abcam	2h, 37°C, 1:600	Alexa488, 1:600, 1h 37°C
LC3A/B	rabbit polyclonal	Cell Signaling	O/N, 4°C, 1:100	Alexa555, 1:800, 1h 37°C
α-Smooth Muscle Actin	Cy3 conjugated rabbit policlonal	Sigma Aldrich	1h, RT, 1:400	N/A
IsolectinB-4	biotinilated mouse monoclonal	Invitrogen	O/N, 4°C, 1:100	Streptavidin Alexa488, 1:100, 1h RT

Apoptotic cells were identified by TdT-mediated dUTP-X nick end labeling (TUNEL) assay (Apoptag, EMD Millipore Corporation, USA), following manufacturer's instructions. Antigens were unmasked incubating sections with a solution of 10μg/mL Protease K (Sigma-Aldrich, Dorest, UK) in PBS, for 15 minutes at RT. After washings with PBS, the protocol was followed as already described for cells in 2.6.2, including also in this case a positive control (tissue treated with DNase) and a negative control (without TdT incubation to exclude non-specific binding of nucleotides).

Epifluorescence images were obtained using a Leica DMI 6000B microscope connected to a Leica DFC350FX camera (Leica microsystems, Germany) and equipped with a 63X oil immersion objective (numerical aperture: 1.40) or a 40X oil immersion objective (numerical aperture: 1.25). z-stacking and deconvolution were performed using AF6000 software. Confocal images were obtained using Leica TCS SP2 equipped with a 63X oil immersion objective (numerical aperture: 1.40) or a 40X oil immersion objective (numerical aperture: 1.25). Adobe Photoshop (Adobe) software was utilized to compose, overlay the images and to adjust contrast.

4.2.5 Markers quantification

Only the left infarcted ventricle was analyzed. At least 3 sections, possibly not sequential, were analyzed for each marker.

Scar size was expressed as the percentage of fibrotic area of the left ventricle. The calculation of areas were performed using the free imaging software ImageJ (http://rsb.info.nih.gov/ij/); the blue area was considered the fibrotic scar.

For quantification of cardiomyocytes and cardiac primitive cells in the tissue sections, the area of each section analyzed was subdivided in 3 portions: the infarct zone (IZ), the tissue bordering the infarct or border zone (BZ) and the non-infarcted myocardium or remote zone (RZ), depicted in the figure on the right. The imageJ software allows the calculation of the infarct zone (depicted in blue in the Azan Mallory staining), after splitting the channels of the RGB image and the selection of the proper channel. The non-infarcted area or spared myocardium (=BZ+RZ) was calculated by subtraction of the infarct area to the total area of the left ventricle. Last, the area corresponding to the border zones was calculated as the 20% of the area of the spared myocardium (10% on each side of the fibrotic scar), as in Olivetti et. al[238].

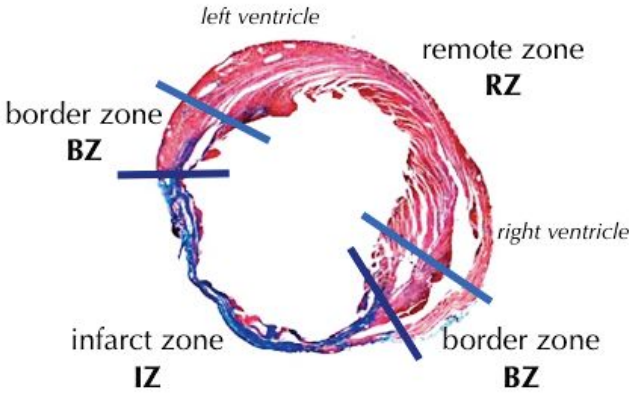

Proliferation, senescence and apoptosis (nuclear markers) of cardiomyocytes were expressed as the number of positive cardiomyocyte nuclei for 10^5 myocyte nuclei.

Autophagy (cytoplasmic marker) in cardiomyocytes was expressed as the number of positive cardiomyocytes for 10^6 cardiomyocytes. For the calculation of the number of cardiomyocytes in the sections, 10 images were randomly acquired at a magnification of 630X and the number of myocytes was calculated using the ImageJ software. In particular the plug-in "Grid Cycloic Arc" was installed and used for the morphometric analysis (instructions can be found on http://rsbweb.nih.gov/ij/plugins/grid-cycloid-arc.html). For the countings of the number of myocytes was preferable to stain the sections with an antibody anti-Laminin, to simplify the recognition of cells.

Cardiac primitive cells were expressed as cell density (cells/cm^2).

Angiogenesis was expressed as the density of capillaries and small and large arterioles (profiles/mm^2).

5. STATISTIC ANALYSIS

Characteristics of the study population are described using means±SEM. The data were analyzed for normal distribution using the Kolmogorov-Smirnov test.

T-test, or Mann-Whitney test, was used to compare continuous variables between two groups.

Drug-treatment assays were analyzed by repeated measurements one-way Anova followed by Bonferroni post-test or by Kruskal-Wallis followed by Dunn's post-test, as appropriate.

In order to distinguish the effects of age and pathology on CSC senescence parameters (dependent variables), a univariate general linear model was employed in which pathology was considered as fixed factor and age as covariate.

Probability values (p) less than 0.05 were considered significant. Analyses were conducted with Prism, version 4.0c and SPSS20 for Macintosh software.

6. SOLUTIONS AND CULTURE MEDIA

All chemical reagents have been purchased from Sigma-Aldrich, Dorest, UK otherwise differently specified.

Basic Dissociation Buffer (BDB)

Minimum Essential Medium Joklik (J-MEM, Gibco, Life Technologies, Paisley) reconstituted in 1 L ultrapure H_2O, 3 mM HEPES, 2 mM Glutamine, 20 U Insulin, 100 μg/L Streptomycin, 100 U Penicillin; pH to 7.3 with NaOH.

HBSS (Calcium free, Magnesium free Hank's Balanced Salt Solution)

Add the content of 1 package in 1 L ultrapure H_2O, adjust the pH to 7.3.

Expansion Medium for CSCs (starting from the second passage in culture)

60% low glucose DMEM (GIBCO, Life Technologies, Paisley), 40% MCDB-201, 1 mg/mL linoleic acid-BSA, 10^{-8} M dexamethasone, 10^{-4} M ascorbic acid-2 phosphate, 5 g/mL insulin, 5 g/mL transferrin, 30 nM sodium selenite, 2% fetal bovine serum (STEMCELL Technologies, Manchester,UK), 1X Penicillin/Streptomycin (from 100X concentrated stock, GIBCO, Life Technologies, Paisley), 10ng/mL human PDGF-BB (Peprotech, NJ, USA), 10ng/mL human EGF (Peprotech, NJ, USA); adjust the pH to 7.4.

PBS (Phosphate Buffered Saline) with Calcium and Magnesium

137 mM NaCl, 27 mM KCl, 4.3 mM Na_2HPO_4, 1.4 mM KH_2PO_4, 0.1mM $MgCl_2$, 0.1mM $CaCl_2 2H_20$; adjust the pH to 7.4

PFA solution (4%w/v)

4% PFA in PBS gently heated at 55°C and agitated with a magnetic flea, until the powder dissolved. Solution prepared in a chemical hood and pH to 7.4.

Citrate buffer for antigen retrieval

SOLUTION A: Citric Acid 0.1M (21.01g Citric Acid dissolved in 1L dH_2O)

SOLUTION B: Sodium Citrate 0.1M (29.41g sodium citrate dissolved in 1L dH_2O)

CITRATE BUFFER pH=6 (0.01M): 18mL sol. A + 82mL sol. B, in 1L dH_2O. Adjust pH to 6.

Solutions for cardiomyocytes isolation

- Solution A (Tyrode buffer, $CaCl_2$-free)

137 mM NaCl, 5 mM KCl, 1.2 mM $MgSO_4 \cdot 7H_2O$, 1.2 mM $NaH_2PO_4 \cdot 2H_2O$, 20 mM HEPES, 16 mM D-glucose anhydrous, 5 mM pyruvate, 1.8 mM $MgCl_2$; adjust the pH to 7.25 with NaOH.

- Solution B

Solution A + 750 μM $CaCl_2$

- Solution C

Solution A + 90 μM EGTA

- Solution D

Solution A, 1 g/L Collagenase type-1, 0.02 g/L Protease type XIV

- Solution E

Solution A + 150 μM $CaCl_2$

Cardiomyocyte ischemia buffer

118 mM NaCl, 24 mM $NaHCO_3$, 1.0 mM NaH_2PO_4, 2.5 mM $CaCl_2$-$2H_2O$, 1.2 mM $MgCl_2$, 20 mM sodium DL-lactate, 16 mM KCl, 10 mM 2-deoxy-D-glucose; adjust the pH to 6.2.

Cardiomyocyte culture medium

medium 199 (GIBCO, Life Technologies, Paisley), 2g/L BSA, 2% FBS, 2mM Carnitine, 5mM Creatine, 5mM Taurine, 1mM Butanedione, 1X Penicillin/Streptomycin (from 100X concentrated stock, GIBCO, Life Technologies, Paisley); adjust the pH to 7.35.

Lysis buffer for protein extraction

50 mM Tris HCl (pH 7.4), 150 mM NaCl, 1 mM EDTA, 1% v/v Triton X-100, 1X protease inhibitor cocktail, 0.5 mM phenylmethylsulfonyl fluoride (PMSF), 1 mM NaF, 1 mM Na_3VO_4.

Western Blot solutions

- Resolving gel 12% Acrilamide

distilled water 3.3 mL, 30% Acrilamide mix 4 mL, TrisHCl pH 8.8 2.5 mL, 10% SDS 100 μL, 10% APS 100 μL, TEMED 4 μL.

- Stacking gel

distilled water 3.4 mL, 30% Acrilamide mix 830 μL, TrisHCl pH 8.8 630 μL, 10% SDS 50 μL, 10% APS 50 μL, TEMED 5 μL.

- TBS 10X pH=7.5

Tris 100 mM, NaCl 150 mM in distilled water. Adjust pH to 7.5. Store at RT.

- TBS-T

TBS (1X) + 0.1% (v/v) Tween-20

- Transfer buffers

dissolve 3 g Tris base and 11.3 g Glycine in a final volume of 800mL in distilled water. Add 200 mL Methanol. Store at 4°C.

- Running Buffer 10X

For a final volume of 2L in distilled water: Tris 60.6g, Glycine 288g, SDS 20g

- SDS samples loading buffer 5X

250 mM TrisHCl pH6.8, 10% SDS, 30% Glycerol, 5% β-mercaptoethanol, 0.02% bromophenol blue.

Solutions for Azan Mallory staining

- Azocarmine G

Dissolve 0.1g Azocarmine G in 100mL dH_2O and let it boil for 3-4 minutes; cool down and filter; before the use, add 1mL of Acetic acid.

- Phosphotungstic Acid

Prepare 100mL of a 5% w/v solution

- Mallory solution

Dissolve 0.5g of Methyl blue together with 2g Orange G in 100mL dH_2O; just boil the solution, add 8mL Acetic acid, cool it down and filter.

List of references

1. Roger, V. L. (2013). Epidemiology of heart failure. *Circ Res* **113**, 646-59.
2. Yancy, C. W., Jessup, M., et al. (2013). 2013 ACCF/AHA Guideline for the Management of Heart Failure: A Report of the American College of Cardiology Foundation/American Heart Association Task Force on Practice Guidelines. *Circulation*.
3. Jessup, M. & Brozena, S. (2003). Heart failure. *The New England journal of medicine* **348**, 2007-18.
4. Long, D. L. (2012). Harrison. Principi di medicina interna - diciottesima edizione.
5. Roger, V. L. (2013). Epidemiology of heart failure. *Circulation research* **113**, 646-59.
6. Mann, D. L. (1999). Mechanisms and models in heart failure: A combinatorial approach. *Circulation* **100**, 999-1008.
7. Leonard, B. L., Smaill, B. H., et al. (2012). Structural remodeling and mechanical function in heart failure. *Microscopy and microanalysis : the official journal of Microscopy Society of America, Microbeam Analysis Society, Microscopical Society of Canada* **18**, 50-67.
8. Beltrami, C. A., Finato, N., et al. (1994). Structural basis of end-stage failure in ischemic cardiomyopathy in humans. *Circulation* **89**, 151-63.
9. Chen, F. M., Zhao, Y. M., et al. (2012). Prospects for translational regenerative medicine. *Biotechnology advances* **30**, 658-72.
10. Sanganalmath, S. K. & Bolli, R. (2013). Cell therapy for heart failure: a comprehensive overview of experimental and clinical studies, current challenges, and future directions. *Circulation research* **113**, 810-34.
11. Austin, S. (2006). A glossary for stem-cell biology. *Nature*.
12. Kolios, G. & Moodley, Y. (2013). Introduction to stem cells and regenerative medicine. *Respiration; international review of thoracic diseases* **85**, 3-10.
13. Verfaillie, C. M., Pera, M. F., et al. (2002). Stem cells: hype and reality. *Hematology / the Education Program of the American Society of Hematology. American Society of Hematology. Education Program*, 369-91.
14. Takahashi, K., Tanabe, K., et al. (2007). Induction of pluripotent stem cells from adult human fibroblasts by defined factors. *Cell* **131**, 861-72.
15. Raff, M. (2003). Adult stem cell plasticity: fact or artifact? *Annual review of cell and developmental biology* **19**, 1-22.
16. Wagers, A. J. & Weissman, I. L. (2004). Plasticity of adult stem cells. *Cell* **116**, 639-48.
17. Hoggatt, J. & Scadden, D. T. (2012). The stem cell niche: tissue physiology at a single cell level. *The Journal of clinical investigation* **122**, 3029-34.
18. Beltrami, A. P., Cesselli, D., et al. (2011). At the stem of youth and health. *Pharmacology & therapeutics* **129**, 3-20.
19. Iglesias-Bartolome, R. & Gutkind, J. S. (2011). Signaling circuitries controlling stem cell fate: to be or not to be. *Current opinion in cell biology* **23**, 716-23.
20. Zoncu, R., Efeyan, A., et al. (2011). mTOR: from growth signal integration to cancer, diabetes and ageing. *Nature reviews. Molecular cell biology* **12**, 21-35.
21. Bhattacharyya, S., Kumar, A., et al. (2012). The voyage of stem cell toward terminal differentiation: a brief overview. *Acta biochimica et biophysica Sinica* **44**, 463-75.
22. Nelson, T. J., Behfar, A., et al. (2008). Strategies for therapeutic repair: The "R(3)" regenerative medicine paradigm. *Clinical and translational science* **1**, 168-171.
23. Anversa, P. & Kajstura, J. (1998). Ventricular myocytes are not terminally differentiated in the adult mammalian heart. *Circ Res* **83**, 1-14.

24. Anversa, P., Kajstura, J., et al. (2006). Life and Death of Cardiac Stem Cells - A paradigm Shift in Cardiac Biology. *Circulation* **113**, 1451-1463.
25. Soonpaa, M. H. & Field, L. J. (1998). Survey of studies examining mammalian cardiomyocyte DNA synthesis. *Circ Res* **83**, 15-26.
26. Beltrami, A. P., Urbanek, K., et al. (2001). Evidence that human cardiac myocytes divide after myocardial infarction. *N Engl J Med* **344**, 1750-1757.
27. Urbanek, K., Quaini, F., et al. (2003). Intense myocyte formation from cardiac stem cells in human cardiac hypertrophy. *Proc Natl Acad Sci U S A* **100**, 10440-10445.
28. Bergmann, O., Bhardwaj, R. D., et al. (2009). Evidence for cardiomyocyte renewal in humans. *Science* **324**, 98-102.
29. Kajstura, J., Rota, M., et al. (2012). Cardiomyogenesis in the aging and failing human heart. *Circulation* **126**, 1869-81.
30. Beltrami, A., Cesselli, D., et al. (2011). Multiple Sources for Cardiac Stem Cells and Their Cardiogenic Potential. In *Regenerating the Heart* (Cohen, I. S. & Gaudette, G. R., eds.), pp. 149-171-171. Humana Press.
31. Quaini, F., Urbanek, K., et al. (2002). Chimerism of the transplanted heart. *N Engl J Med* **346**, 5-15.
32. Muller, P., Pfeiffer, P., et al. (2002). Cardiomyocytes of noncardiac origin in myocardial biopsies of human transplanted hearts. *Circulation* **106**, 31-5.
33. Leri, A., Kajstura, J., et al. (2005). Cardiac stem cells and mechanisms of myocardial regeneration. *Physiol Rev* **85**, 1373-416.
34. Beltrami, A. P., Barlucchi, L., et al. (2003). Adult cardiac stem cells are multipotent and support myocardial regeneration. *Cell* **114**, 763-776.
35. Urbanek, K., Cesselli, D., et al. (2006). Stem cell niches in the adult mouse heart. *Proc Natl Acad Sci U S A* **103**, 9226-31.
36. Bearzi, C., Rota, M., et al. (2007). Human cardiac stem cells. *Proc Natl Acad Sci U S A* **104**, 14068-73.
37. Hsieh, P. C., Segers, V. F., et al. (2007). Evidence from a genetic fate-mapping study that stem cells refresh adult mammalian cardiomyocytes after injury. *Nat Med* **13**, 970-4.
38. Senyo, S. E., Steinhauser, M. L., et al. (2013). Mammalian heart renewal by pre-existing cardiomyocytes. *Nature* **493**, 433-6.
39. Malliaras, K., Zhang, Y., et al. (2013). Cardiomyocyte proliferation and progenitor cell recruitment underlie therapeutic regeneration after myocardial infarction in the adult mouse heart. *EMBO molecular medicine* **5**, 191-209.
40. Duran, J. M., Makarewich, C. A., et al. (2013). Bone-derived stem cells repair the heart after myocardial infarction through transdifferentiation and paracrine signaling mechanisms. *Circulation research* **113**, 539-52.
41. Da Silva, J. S. & Hare, J. M. (2013). Cell-Based Therapies for Myocardial Repair: Emerging Role for Bone Marrow-Derived Mesenchymal Stem Cells (MSCs) in the Treatment of the Chronically Injured Heart. *Methods in molecular biology* **1037**, 145-63.
42. Orlic, D., Kajstura, J., et al. (2001). Mobilized bone marrow cells repair the infarcted heart, improving function and survival. *Proc Natl Acad Sci U S A* **98**, 10344-10349.
43. Cesselli, D., Beltrami, A. P., et al. (2011). Effects of Age and Heart Failure on Human Cardiac Stem Cell Function. *Am J Pathol* **179**, 349-366.
44. Itzhaki-Alfia, A., Leor, J., et al. (2009). Patient characteristics and cell source determine the number of isolated human cardiac progenitor cells. *Circulation* **120**, 2559-66.
45. Chimenti, C., Kajstura, J., et al. (2003). Senescence and death of primitive cells and myocytes lead to premature cardiac aging and heart failure. *Circ Res* **93**, 604-13.
46. Fransioli, J., Bailey, B., et al. (2008). Evolution of the c-kit-positive cell response to pathological challenge in the myocardium. *Stem Cells* **26**, 1315-24.
47. Martin-Puig, S., Wang, Z., et al. (2008). Lives of a heart cell: tracing the origins of cardiac progenitors. *Cell Stem Cell* **2**, 320-31.

48. Dey, D., Han, L., et al. (2013). Dissecting the molecular relationship among various cardiogenic progenitor cells. *Circulation research* **112**, 1253-62.
49. Edling, C. E. & Hallberg, B. (2007). c-Kit--a hematopoietic cell essential receptor tyrosine kinase. *The international journal of biochemistry & cell biology* **39**, 1995-8.
50. Dawn, B., Stein, A. B., et al. (2005). Cardiac stem cells delivered intravascularly traverse the vessel barrier, regenerate infarcted myocardium, and improve cardiac function. *Proc Natl Acad Sci U S A* **102**, 3766-3771.
51. Ellison, G. M., Vicinanza, C., et al. (2013). Adult c-kit(pos) cardiac stem cells are necessary and sufficient for functional cardiac regeneration and repair. *Cell* **154**, 827-42.
52. Ellison, G. M., Torella, D., et al. (2007). Acute beta-adrenergic overload produces myocyte damage through calcium leakage from the ryanodine receptor 2 but spares cardiac stem cells. *J Biol Chem* **282**, 11397-409.
53. Wu, S. M., Fujiwara, Y., et al. (2006). Developmental origin of a bipotential myocardial and smooth muscle cell precursor in the mammalian heart. *Cell* **127**, 1137-50.
54. Koudstaal, S., Jansen Of Lorkeers, S. J., et al. (2013). Concise review: heart regeneration and the role of cardiac stem cells. *Stem cells translational medicine* **2**, 434-43.
55. Bolli, R., Chugh, A. R., et al. (2011). Cardiac stem cells in patients with ischaemic cardiomyopathy (SCIPIO): initial results of a randomised phase 1 trial. *Lancet* **378**, 1847-57.
56. Chugh, A. R., Beache, G. M., et al. (2012). Administration of cardiac stem cells in patients with ischemic cardiomyopathy: the SCIPIO trial: surgical aspects and interim analysis of myocardial function and viability by magnetic resonance. *Circulation* **126**, S54-64.
57. Makkar, R. R., Smith, R. R., et al. (2012). Intracoronary cardiosphere-derived cells for heart regeneration after myocardial infarction (CADUCEUS): a prospective, randomised phase 1 trial. *Lancet* **379**, 895-904.
58. Messina, E., De Angelis, L., et al. (2004). Isolation and expansion of adult cardiac stem cells from human and murine heart. *Circ Res* **95**, 911-21.
59. Smith, R. R., Barile, L., et al. (2007). Regenerative potential of cardiosphere-derived cells expanded from percutaneous endomyocardial biopsy specimens. *Circulation* **115**, 896-908.
60. Lee, J. & Terracciano, C. M. (2010). Cell therapy for cardiac repair. *British medical bulletin* **94**, 65-80.
61. Tang, X. L., Rokosh, G., et al. (2010). Intracoronary administration of cardiac progenitor cells alleviates left ventricular dysfunction in rats with a 30-day-old infarction. *Circulation* **121**, 293-305.
62. Lee, S. T., White, A. J., et al. (2011). Intramyocardial injection of autologous cardiospheres or cardiosphere-derived cells preserves function and minimizes adverse ventricular remodeling in pigs with heart failure post-myocardial infarction. *Journal of the American College of Cardiology* **57**, 455-65.
63. Malliaras, K., Li, T. S., et al. (2012). Safety and efficacy of allogeneic cell therapy in infarcted rats transplanted with mismatched cardiosphere-derived cells. *Circulation* **125**, 100-12.
64. Murry, C. E., Soonpaa, M. H., et al. (2004). Haematopoietic stem cells do not transdifferentiate into cardiac myocytes in myocardial infarcts. *Nature*.
65. Balsam, L. B., Wagers, A. J., et al. (2004). Haematopoietic stem cells adopt mature haematopoietic fates in ischaemic myocardium. *Nature* **428**, 668-73.
66. Kajstura, J., Rota, M., et al. (2005). Bone marrow cells differentiate in cardiac cell lineages after infarction indipendently of cell fusion. *Circ Res* **96**, 127-137.
67. Gnecchi, M., Zhang, Z., et al. (2008). Paracrine mechanisms in adult stem cell signaling and therapy. *Circ Res* **103**, 1204-19.

68. Rota, M., Padin-Iruegas, M. E., et al. (2008). Local activation or implantation of cardiac progenitor cells rescues scarred infarcted myocardium improving cardiac function. *Circ Res* **103**, 107-16.
69. Sharpless, N. E. & DePinho, R. A. (2007). How stem cells age and why this makes us grow old. *Nat Rev Mol Cell Biol* **8**, 703-713.
70. Hayflick, L. (1965). The Limited in Vitro Lifetime of Human Diploid Cell Strains. *Experimental cell research* **37**, 614-36.
71. Campisi, J. & d'Adda di Fagagna, F. (2007). Cellular senescence: when bad things happen to good cells. *Nat Rev Mol Cell Biol* **8**, 729-40.
72. Naylor, R. M., Baker, D. J., et al. (2013). Senescent cells: a novel therapeutic target for aging and age-related diseases. *Clin Pharmacol Ther* **93**, 105-16.
73. Rodier, F. & Campisi, J. (2011). Four faces of cellular senescence. *J Cell Biol* **192**, 547-56.
74. Campisi, J. (2005). Senescent cells, tumor suppression, and organismal aging: good citizens, bad neighbors. *Cell* **120**, 513-22.
75. Kosar, M., Bartkova, J., et al. (2011). Senescence-associated heterochromatin foci are dispensable for cellular senescence, occur in a cell type- and insult-dependent manner and follow expression of p16(ink4a). *Cell Cycle* **10**, 457-68.
76. Narita, M., Nunez, S., et al. (2003). Rb-mediated heterochromatin formation and silencing of E2F target genes during cellular senescence. *Cell* **113**, 703-16.
77. Acosta, J. C., Banito, A., et al. (2013). A complex secretory program orchestrated by the inflammasome controls paracrine senescence. *Nature cell biology* **15**, 978-90.
78. d'Adda di Fagagna, F., Reaper, P. M., et al. (2003). A DNA damage checkpoint response in telomere-initiated senescence. *Nature* **426**, 194-8.
79. Nakamura, A. J., Chiang, Y. J., et al. (2008). Both telomeric and non-telomeric DNA damage are determinants of mammalian cellular senescence. *Epigenetics & chromatin* **1**, 6.
80. Ramirez, R. D., Morales, C. P., et al. (2001). Putative telomere-independent mechanisms of replicative aging reflect inadequate growth conditions. *Genes & development* **15**, 398-403.
81. Beltrami, A. P., Cesselli, D., et al. (2011). At the stem of youth and health. *Pharmacol Ther* **129**, 3-20.
82. Cesselli, D., Caragnano, A., et al. (2012). Pharmacologic Inhibition of Cardiac Stem Cell Senescence. In *Senescence* (Nagata, T., ed.). InTech, Rijeka, Croatia.
83. Baker, D. J. & Sedivy, J. M. (2013). Probing the depths of cellular senescence. *J Cell Biol* **202**, 11-3.
84. Dimri, G. P., Lee, X., et al. (1995). A biomarker that identifies senescent human cells in culture and in aging skin in vivo. *Proc Natl Acad Sci U S A* **92**, 9363-7.
85. Krishnamurthy, J., Torrice, C., et al. (2004). Ink4a/Arf expression is a biomarker of aging. *J Clin Invest* **114**, 1299-307.
86. Collado, M. & Serrano, M. (2006). The power and the promise of oncogene-induced senescence markers. *Nature reviews. Cancer* **6**, 472-6.
87. Takai, H., Smogorzewska, A., et al. (2003). DNA damage foci at dysfunctional telomeres. *Curr Biol* **13**, 1549-56.
88. Kinner, A., Wu, W., et al. (2008). Gamma-H2AX in recognition and signaling of DNA double-strand breaks in the context of chromatin. *Nucleic acids research* **36**, 5678-94.
89. Lawless, C., Wang, C., et al. (2010). Quantitative assessment of markers for cell senescence. *Exp Gerontol* **45**, 772-8.
90. Vasile, E., Tomita, Y., et al. (2001). Differential expression of thymosin beta-10 by early passage and senescent vascular endothelium is modulated by VPF/VEGF: evidence for senescent endothelial cells in vivo at sites of atherosclerosis. *FASEB journal : official publication of the Federation of American Societies for Experimental Biology* **15**, 458-66.
91. Hayflick, L. & Moorhead, P. S. (1961). The serial cultivation of human diploid cell strains. *Exp Cell Res* **25**, 585-621.

92. Xue, W., Zender, L., et al. (2007). Senescence and tumour clearance is triggered by p53 restoration in murine liver carcinomas. *Nature* **445**, 656-60.
93. Baker, D. J., Wijshake, T., et al. (2011). Clearance of p16Ink4a-positive senescent cells delays ageing-associated disorders. *Nature*.
94. Drummond-Barbosa, D. (2008). Stem cells, their niches and the systemic environment: an aging network. *Genetics* **180**, 1787-97.
95. Parrinello, S., Samper, E., et al. (2003). Oxygen sensitivity severely limits the replicative lifespan of murine fibroblasts. *Nat Cell Biol* **5**, 741-7.
96. Freund, A., Orjalo, A. V., et al. Inflammatory networks during cellular senescence: causes and consequences. *Trends Mol Med* **16**, 238-46.
97. Coppe, J. P., Desprez, P. Y., et al. (2010). The senescence-associated secretory phenotype: the dark side of tumor suppression. *Annu Rev Pathol* **5**, 99-118.
98. Nelson, G., Wordsworth, J., et al. (2012). A senescent cell bystander effect: senescence-induced senescence. *Aging cell* **11**, 345-9.
99. Tasdemir, N. & Lowe, S. W. (2013). Senescent cells spread the word: non-cell autonomous propagation of cellular senescence. *The EMBO journal* **32**, 1975-6.
100. Campisi, J. (2013). Aging, cellular senescence, and cancer. *Annu Rev Physiol* **75**, 685-705.
101. Hoare, M. & Narita, M. (2013). Transmitting senescence to the cell neighbourhood. *Nature cell biology* **15**, 887-9.
102. Tchkonia, T., Zhu, Y., et al. (2013). Cellular senescence and the senescent secretory phenotype: therapeutic opportunities. *The Journal of clinical investigation* **123**, 966-72.
103. Hubackova, S., Krejcikova, K., et al. (2012). IL1- and TGFbeta-Nox4 signaling, oxidative stress and DNA damage response are shared features of replicative, oncogene-induced, and drug-induced paracrine 'bystander senescence'. *Aging* **4**, 932-51.
104. Strowig, T., Henao-Mejia, J., et al. (2012). Inflammasomes in health and disease. *Nature* **481**, 278-86.
105. Wajapeyee, N., Serra, R. W., et al. (2008). Oncogenic BRAF induces senescence and apoptosis through pathways mediated by the secreted protein IGFBP7. *Cell* **132**, 363-74.
106. Kuilman, T., Michaloglou, C., et al. (2008). Oncogene-induced senescence relayed by an interleukin-dependent inflammatory network. *Cell* **133**, 1019-31.
107. Lujambio, A., Akkari, L., et al. (2013). Non-cell-autonomous tumor suppression by p53. *Cell* **153**, 449-60.
108. Bhaumik, D., Scott, G. K., et al. (2009). MicroRNAs miR-146a/b negatively modulate the senescence-associated inflammatory mediators IL-6 and IL-8. *Aging (Albany NY)* **1**, 402-11.
109. McMillan, D. H., Woeller, C. F., et al. (2013). Attenuation of inflammatory mediator production by the NF-kappaB member RelB is mediated by microRNA-146a in lung fibroblasts. *American journal of physiology. Lung cellular and molecular physiology* **304**, L774-81.
110. Taganov, K. D., Boldin, M. P., et al. (2006). NF-kappaB-dependent induction of microRNA miR-146, an inhibitor targeted to signaling proteins of innate immune responses. *Proc Natl Acad Sci U S A* **103**, 12481-6.
111. Zoncu, R., Efeyan, A., et al. (2011). mTOR: from growth signal integration to cancer, diabetes and ageing. *Nat Rev Mol Cell Biol* **12**, 21-35.
112. Hay, N. & Sonenberg, N. (2004). Upstream and downstream of mTOR. *Genes & development* **18**, 1926-45.
113. Bhaskar, P. T. & Hay, N. (2007). The two TORCs and Akt. *Dev Cell* **12**, 487-502.
114. Magnuson, B., Ekim, B., et al. (2012). Regulation and function of ribosomal protein S6 kinase (S6K) within mTOR signalling networks. *Biochem J* **441**, 1-21.
115. Huang, J. & Manning, B. D. (2009). A complex interplay between Akt, TSC2 and the two mTOR complexes. *Biochem Soc Trans* **37**, 217-22.

116. Zhang, W., Haines, B. B., et al. (2012). Evidence of mTOR Activation by an AKT-Independent Mechanism Provides Support for the Combined Treatment of PTEN-Deficient Prostate Tumors with mTOR and AKT Inhibitors. *Translational oncology* **5**, 422-9.
117. Hands, S. L., Proud, C. G., et al. (2009). mTOR's role in ageing: protein synthesis or autophagy? *Aging* **1**, 586-97.
118. Harrison, D. E., Strong, R., et al. (2009). Rapamycin fed late in life extends lifespan in genetically heterogeneous mice. *Nature* **460**, 392-5.
119. Korotchkina, L. G., Leontieva, O. V., et al. (2010). The choice between p53-induced senescence and quiescence is determined in part by the mTOR pathway. *Aging (Albany NY)* **2**, 344-52.
120. Iglesias-Bartolome, R., Patel, V., et al. (2012). mTOR inhibition prevents epithelial stem cell senescence and protects from radiation-induced mucositis. *Cell stem cell* **11**, 401-14.
121. Gan, B. & DePinho, R. A. (2009). mTORC1 signaling governs hematopoietic stem cell quiescence. *Cell Cycle* **8**, 1003-6.
122. Castilho, R. M., Squarize, C. H., et al. (2009). mTOR mediates Wnt-induced epidermal stem cell exhaustion and aging. *Cell Stem Cell* **5**, 279-89.
123. Chen, C., Liu, Y., et al. (2009). mTOR regulation and therapeutic rejuvenation of aging hematopoietic stem cells. *Sci Signal* **2**, ra75.
124. Yilmaz, O. H., Valdez, R., et al. (2006). Pten dependence distinguishes haematopoietic stem cells from leukaemia-initiating cells. *Nature* **441**, 475-82.
125. Harrington, L. S., Findlay, G. M., et al. (2005). Restraining PI3K: mTOR signalling goes back to the membrane. *Trends in biochemical sciences* **30**, 35-42.
126. Johnson, S. C., Rabinovitch, P. S., et al. (2013). mTOR is a key modulator of ageing and age-related disease. *Nature* **493**, 338-45.
127. Glick, D., Barth, S., et al. (2010). Autophagy: cellular and molecular mechanisms. *The Journal of pathology* **221**, 3-12.
128. Mizushima, N. & Komatsu, M. (2011). Autophagy: renovation of cells and tissues. *Cell* **147**, 728-41.
129. Klionsky, D. J. (2004). Cell biology: regulated self-cannibalism. *Nature* **431**, 31-2.
130. Klionsky, D. J., Meijer, A. J., et al. (2005). Autophagy and p70S6 kinase. *Autophagy* **1**, 59-60; discussion 60-1.
131. Shah, O. J., Wang, Z., et al. (2004). Inappropriate activation of the TSC/Rheb/mTOR/S6K cassette induces IRS1/2 depletion, insulin resistance, and cell survival deficiencies. *Curr Biol* **14**, 1650-6.
132. Um, S. H., Frigerio, F., et al. (2004). Absence of S6K1 protects against age- and diet-induced obesity while enhancing insulin sensitivity. *Nature* **431**, 200-5.
133. Scott, R. C., Schuldiner, O., et al. (2004). Role and regulation of starvation-induced autophagy in the Drosophila fat body. *Dev Cell* **7**, 167-78.
134. Klionsky, D. J., Cregg, J. M., et al. (2003). A unified nomenclature for yeast autophagy-related genes. *Developmental cell* **5**, 539-45.
135. Salminen, A., Kaarniranta, K., et al. (2013). Beclin 1 interactome controls the crosstalk between apoptosis, autophagy and inflammasome activation: impact on the aging process. *Ageing research reviews* **12**, 520-34.
136. Johansen, T. & Lamark, T. (2011). Selective autophagy mediated by autophagic adapter proteins. *Autophagy* **7**, 279-96.
137. Komatsu, M., Waguri, S., et al. (2007). Homeostatic levels of p62 control cytoplasmic inclusion body formation in autophagy-deficient mice. *Cell* **131**, 1149-63.
138. Alvers, A. L., Wood, M. S., et al. (2009). Autophagy is required for extension of yeast chronological life span by rapamycin. *Autophagy* **5**, 847-9.
139. Narita, M., Young, A. R., et al. (2011). Spatial coupling of mTOR and autophagy augments secretory phenotypes. *Science* **332**, 966-70.

140. Young, A. R. & Narita, M. (2010). Connecting autophagy to senescence in pathophysiology. *Curr Opin Cell Biol* **22**, 234-40.
141. Young, A. R., Narita, M., et al. (2009). Autophagy mediates the mitotic senescence transition. *Genes Dev* **23**, 798-803.
142. Salminen, A., Kaarniranta, K., et al. (2012). Inflammaging: disturbed interplay between autophagy and inflammasomes. *Aging* **4**, 166-75.
143. Xie, M., Morales, C. R., et al. (2011). Tuning flux: autophagy as a target of heart disease therapy. *Current opinion in cardiology* **26**, 216-22.
144. Cao, D. J., Gillette, T. G., et al. (2009). Cardiomyocyte autophagy: remodeling, repairing, and reconstructing the heart. *Current hypertension reports* **11**, 406-11.
145. Kassiotis, C., Ballal, K., et al. (2009). Markers of autophagy are downregulated in failing human heart after mechanical unloading. *Circulation* **120**, S191-7.
146. Salminen, A. & Kaarniranta, K. (2012). AMP-activated protein kinase (AMPK) controls the aging process via an integrated signaling network. *Ageing research reviews* **11**, 230-41.
147. Mihaylova, M. M. & Shaw, R. J. (2011). The AMPK signalling pathway coordinates cell growth, autophagy and metabolism. *Nature cell biology* **13**, 1016-23.
148. Muller, F. L., Lustgarten, M. S., et al. (2007). Trends in oxidative aging theories. *Free radical biology & medicine* **43**, 477-503.
149. Salminen, A. & Kaarniranta, K. (2010). ER stress and hormetic regulation of the aging process. *Ageing research reviews* **9**, 211-7.
150. Salminen, A. & Kaarniranta, K. (2009). Regulation of the aging process by autophagy. *Trends in molecular medicine* **15**, 217-24.
151. Franceschi, C., Capri, M., et al. (2007). Inflammaging and anti-inflammaging: a systemic perspective on aging and longevity emerged from studies in humans. *Mechanisms of ageing and development* **128**, 92-105.
152. Kim, J., Kundu, M., et al. (2011). AMPK and mTOR regulate autophagy through direct phosphorylation of Ulk1. *Nat Cell Biol* **13**, 132-41.
153. Denu, J. M. (2003). Linking chromatin function with metabolic networks: Sir2 family of NAD(+)-dependent deacetylases. *Trends Biochem Sci* **28**, 41-8.
154. Boily, G., Seifert, E. L., et al. (2008). SirT1 regulates energy metabolism and response to caloric restriction in mice. *PLoS ONE* **3**, e1759.
155. Finkel, T., Deng, C. X., et al. (2009). Recent progress in the biology and physiology of sirtuins. *Nature* **460**, 587-91.
156. Langley, E., Pearson, M., et al. (2002). Human SIR2 deacetylates p53 and antagonizes PML/p53-induced cellular senescence. *EMBO J* **21**, 2383-96.
157. Kawahara, T. L., Michishita, E., et al. (2009). SIRT6 links histone H3 lysine 9 deacetylation to NF-kappaB-dependent gene expression and organismal life span. *Cell* **136**, 62-74.
158. Canto, C., Gerhart-Hines, Z., et al. (2009). AMPK regulates energy expenditure by modulating NAD+ metabolism and SIRT1 activity. *Nature* **458**, 1056-60.
159. Lin, J. N., Lin, V. C., et al. (2010). Resveratrol modulates tumor cell proliferation and protein translation via SIRT1-dependent AMPK activation. *J Agric Food Chem* **58**, 1584-92.
160. Lee, I. H., Cao, L., et al. (2008). A role for the NAD-dependent deacetylase Sirt1 in the regulation of autophagy. *Proc Natl Acad Sci U S A* **105**, 3374-9.
161. Mattagajasingh, I., Kim, C. S., et al. (2007). SIRT1 promotes endothelium-dependent vascular relaxation by activating endothelial nitric oxide synthase. *Proc Natl Acad Sci U S A* **104**, 14855-60.
162. Altarejos, J. Y. & Montminy, M. (2011). CREB and the CRTC co-activators: sensors for hormonal and metabolic signals. *Nature reviews. Molecular cell biology* **12**, 141-51.
163. Hansen, R. T., 3rd & Zhang, H. T. (2013). Senescent-induced dysregulation of cAMP/CREB signaling and correlations with cognitive decline. *Brain Res* **1516**, 93-109.

164. Thomson, D. M., Herway, S. T., et al. (2008). AMP-activated protein kinase phosphorylates transcription factors of the CREB family. *Journal of applied physiology* **104**, 429-38.
165. Fusco, S., Ripoli, C., et al. (2012). A role for neuronal cAMP responsive-element binding (CREB)-1 in brain responses to calorie restriction. *Proc Natl Acad Sci U S A* **109**, 621-6.
166. Chin, J. H., Okazaki, M., et al. (1996). Impaired cAMP-mediated gene expression and decreased cAMP response element binding protein in senescent cells. *Am J Physiol* **271**, C362-71.
167. Du, K. & Montminy, M. (1998). CREB is a regulatory target for the protein kinase Akt/PKB. *J Biol Chem* **273**, 32377-9.
168. Noriega, L. G., Feige, J. N., et al. (2011). CREB and ChREBP oppositely regulate SIRT1 expression in response to energy availability. *EMBO Rep* **12**, 1069-76.
169. Alvarez-Saavedra, M., Antoun, G., et al. (2011). miRNA-132 orchestrates chromatin remodeling and translational control of the circadian clock. *Hum Mol Genet* **20**, 731-51.
170. Salminen, A., Hyttinen, J. M., et al. (2012). Context-Dependent Regulation of Autophagy by IKK-NF-kappaB Signaling: Impact on the Aging Process. *International journal of cell biology* **2012**, 849541.
171. Vaughan, S. & Jat, P. S. (2011). Deciphering the role of nuclear factor-kappaB in cellular senescence. *Aging* **3**, 913-9.
172. Hayden, M. S. & Ghosh, S. (2008). Shared principles in NF-kappaB signaling. *Cell* **132**, 344-62.
173. Oeckinghaus, A., Hayden, M. S., et al. (2011). Crosstalk in NF-kappaB signaling pathways. *Nature immunology* **12**, 695-708.
174. Kriete, A., Mayo, K. L., et al. (2008). Cell autonomous expression of inflammatory genes in biologically aged fibroblasts associated with elevated NF-kappaB activity. *Immunity & ageing : I & A* **5**, 5.
175. Lane, N. (2003). A unifying view of ageing and disease: the double-agent theory. *Journal of theoretical biology* **225**, 531-40.
176. Adler, A. S., Sinha, S., et al. (2007). Motif module map reveals enforcement of aging by continual NF-kappaB activity. *Genes & development* **21**, 3244-57.
177. Franceschi, C., Valensin, S., et al. (2000). The network and the remodeling theories of aging: historical background and new perspectives. *Experimental gerontology* **35**, 879-96.
178. de Magalhaes, J. P., Curado, J., et al. (2009). Meta-analysis of age-related gene expression profiles identifies common signatures of aging. *Bioinformatics* **25**, 875-81.
179. Singh, T. & Newman, A. B. (2011). Inflammatory markers in population studies of aging. *Ageing research reviews* **10**, 319-29.
180. Helenius, M., Kyrylenko, S., et al. (2001). Characterization of aging-associated up-regulation of constitutive nuclear factor-kappa B binding activity. *Antioxidants & redox signaling* **3**, 147-56.
181. Rubinsztein, D. C., Marino, G., et al. (2011). Autophagy and aging. *Cell* **146**, 682-95.
182. Zhang, Y. & Herman, B. (2002). Ageing and apoptosis. *Mechanisms of ageing and development* **123**, 245-60.
183. Salminen, A., Ojala, J., et al. (2011). Apoptosis and aging: increased resistance to apoptosis enhances the aging process. *Cellular and molecular life sciences : CMLS* **68**, 1021-31.
184. Freund, A., Patil, C. K., et al. (2011). p38MAPK is a novel DNA damage response-independent regulator of the senescence-associated secretory phenotype. *EMBO J* **30**, 1536-48.
185. Salminen, A., Kauppinen, A., et al. (2012). Emerging role of NF-kappaB signaling in the induction of senescence-associated secretory phenotype (SASP). *Cellular signalling* **24**, 835-45.

186. Djavaheri-Mergny, M., Amelotti, M., et al. (2006). NF-kappaB activation represses tumor necrosis factor-alpha-induced autophagy. *The Journal of biological chemistry* **281**, 30373-82.
187. Lee, D. F., Kuo, H. P., et al. (2007). IKK beta suppression of TSC1 links inflammation and tumor angiogenesis via the mTOR pathway. *Cell* **130**, 440-55.
188. Kim, S., Domon-Dell, C., et al. (2004). Down-regulation of the tumor suppressor PTEN by the tumor necrosis factor-alpha/nuclear factor-kappaB (NF-kappaB)-inducing kinase/NF-kappaB pathway is linked to a default IkappaB-alpha autoregulatory loop. *The Journal of biological chemistry* **279**, 4285-91.
189. Vasudevan, K. M., Gurumurthy, S., et al. (2004). Suppression of PTEN expression by NF-kappa B prevents apoptosis. *Molecular and cellular biology* **24**, 1007-21.
190. Salminen, A. & Kaarniranta, K. (2010). Insulin/IGF-1 paradox of aging: regulation via AKT/IKK/NF-kappaB signaling. *Cellular signalling* **22**, 573-7.
191. Sarkar, S., Korolchuk, V. I., et al. (2011). Complex inhibitory effects of nitric oxide on autophagy. *Mol Cell* **43**, 19-32.
192. Beltrami, A. P., Cesselli, D., et al. (2012). Stem Cell Senescence and Regenerative Paradigms. *Clinical Pharmacology & Therapeutics* **91**, 21-29.
193. Capasso, J. M., Fitzpatrick, D., et al. (1992). Cellular mechanisms of ventricular failure: myocyte kinetics and geometry with age. *The American journal of physiology* **262**, H1770-81.
194. Torella, D., Rota, M., et al. (2004). Cardiac stem cells and myocyte aging, heart failure, and insulin-like growth factor-1 overexpression. *Circ Res* **95**, 514-524.
195. Sussman, M. & Anversa, P. (2004). Myocardial aging and senescence: where have the stem cells gone? *Annu Rev Physiol.* **66**, 29-48.
196. Urbanek, K., Torella, D., et al. (2005). Myocardial regeneration by activation of multipotent cardiac stem cells in ischemic heart failure. *Proc Natl Acad Sci U S A* **102**, 8692-7.
197. Burgess, M. L., McCrea, J. C., et al. (2001). Age-associated changes in cardiac matrix and integrins. *Mechanisms of ageing and development* **122**, 1739-56.
198. Dimmeler, S. & Leri, A. (2008). Aging and disease as modifiers of efficacy of cell therapy. *Circ Res* **102**, 1319-30.
199. D'Amario, D., Cabral-Da-Silva, M. C., et al. (2011). Insulin-like growth factor-1 receptor identifies a pool of human cardiac stem cells with superior therapeutic potential for myocardial regeneration. *Circ Res* **108**, 1467-81.
200. Mohsin, S., Khan, M., et al. (2013). Rejuvenation of Human Cardiac Progenitor Cells with Pim-1 Kinase. *Circulation research*.
201. Petrovski, G., Gurusamy, N., et al. (2011). Resveratrol in cardiovascular health and disease. *Ann N Y Acad Sci* **1215**, 22-33.
202. Gorbunov, N., Petrovski, G., et al. (2012). Regeneration of infarcted myocardium with resveratrol-modified cardiac stem cells. *Journal of cellular and molecular medicine* **16**, 174-84.
203. Blagosklonny, M. V. (2009). Inhibition of S6K by resveratrol: in search of the purpose. *Aging* **1**, 511-4.
204. Rajapakse, A. G., Yepuri, G., et al. (2011). Hyperactive S6K1 mediates oxidative stress and endothelial dysfunction in aging: inhibition by resveratrol. *PLoS One* **6**, e19237.
205. Park, S. J., Ahmad, F., et al. (2012). Resveratrol ameliorates aging-related metabolic phenotypes by inhibiting cAMP phosphodiesterases. *Cell* **148**, 421-33.
206. Pitozzi, V., Mocali, A., et al. (2013). Chronic resveratrol treatment ameliorates cell adhesion and mitigates the inflammatory phenotype in senescent human fibroblasts. *The journals of gerontology. Series A, Biological sciences and medical sciences* **68**, 371-81.
207. Morselli, E., Galluzzi, L., et al. (2009). Autophagy mediates pharmacological lifespan extension by spermidine and resveratrol. *Aging (Albany NY)* **1**, 961-70.

208. Blagosklonny, M. V. (2010). Calorie restriction: decelerating mTOR-driven aging from cells to organisms (including humans). *Cell Cycle* **9**, 683-8.
209. Hudes, G., Carducci, M., et al. (2007). Temsirolimus, interferon alfa, or both for advanced renal-cell carcinoma. *The New England journal of medicine* **356**, 2271-81.
210. Adelman, S. J. (2010). Sirolimus and its analogs and its effects on vascular diseases. *Current pharmaceutical design* **16**, 4002-11.
211. Chan, A. Y., Dolinsky, V. W., et al. (2008). Resveratrol inhibits cardiac hypertrophy via AMP-activated protein kinase and Akt. *The Journal of biological chemistry* **283**, 24194-201.
212. Smoliga, J. M., Baur, J. A., et al. (2011). Resveratrol and health--a comprehensive review of human clinical trials. *Molecular nutrition & food research* **55**, 1129-41.
213. Pearson, K. J., Baur, J. A., et al. (2008). Resveratrol delays age-related deterioration and mimics transcriptional aspects of dietary restriction without extending life span. *Cell Metab* **8**, 157-68.
214. Ming, X. F., Montani, J. P., et al. (2012). Perspectives of Targeting mTORC1-S6K1 in Cardiovascular Aging. *Frontiers in physiology* **3**, 5.
215. Beltrami, A. P., Cesselli, D., et al. (2007). Multipotent cells can be generated in vitro from several adult human organs (heart, liver and bone marrow). *Blood* **110**, 3438-3446.
216. D'Amario, D., Fiorini, C., et al. (2011). Functionally competent cardiac stem cells can be isolated from endomyocardial biopsies of patients with advanced cardiomyopathies. *Circ Res* **108**, 857-61.
217. Das, A., Salloum, F. N., et al. (2012). Rapamycin protects against myocardial ischemia-reperfusion injury through JAK2-STAT3 signaling pathway. *Journal of molecular and cellular cardiology* **53**, 858-69.
218. Portal, L., Martin, V., et al. (2013). A Model of Hypoxia-Reoxygenation on Isolated Adult Mouse Cardiomyocytes: Characterization, Comparison With Ischemia-Reperfusion, and Application to the Cardioprotective Effect of Regular Treadmill Exercise. *J Cardiovasc Pharmacol Ther*.
219. Factor, S. M., Sonnenblick, E. H., et al. (1978). The histologic border zone of acute myocardial infarction--islands or peninsulas? *Am J Pathol* **92**, 111-24.
220. Houser, S. R., Margulies, K. B., et al. (2012). Animal models of heart failure: a scientific statement from the American Heart Association. *Circulation research* **111**, 131-50.
221. Beltrami, C. A., Finato, N., et al. (1994). Structural basis of end-stage failure in ischemic cardiomyopathy in humans. *Circulation* **89**, 151-163.
222. Armour, S. M., Baur, J. A., et al. (2009). Inhibition of mammalian S6 kinase by resveratrol suppresses autophagy. *Aging (Albany NY)* **1**, 515-28.
223. Katare, R., Riu, F., et al. (2011). Transplantation of Human Pericyte Progenitor Cells Improves the Repair of Infarcted Heart Through Activation of an Angiogenic Program Involving Micro-RNA-132. *Circ Res* **109**, 894-906.
224. Riccio, A., Alvania, R. S., et al. (2006). A nitric oxide signaling pathway controls CREB-mediated gene expression in neurons. *Mol Cell* **21**, 283-94.
225. Habib, S. L. (2011). Mechanism of activation of AMPK and upregulation of OGG1 by rapamycin in cancer cells. *Oncotarget* **2**, 958-9.
226. Li, H., Xia, N., et al. (2012). Cardiovascular effects and molecular targets of resveratrol. *Nitric Oxide* **26**, 102-10.
227. Vaz, A. R., Silva, S. L., et al. (2011). Pro-inflammatory cytokines intensify the activation of NO/NOS, JNK1/2 and caspase cascades in immature neurons exposed to elevated levels of unconjugated bilirubin. *Exp Neurol* **229**, 381-90.
228. Mirotsou, M., Jayawardena, T. M., et al. (2011). Paracrine mechanisms of stem cell reparative and regenerative actions in the heart. *J Mol Cell Cardiol* **50**, 280-9.
229. Beauloye, C., Bertrand, L., et al. (2011). AMPK activation, a preventive therapeutic target in the transition from cardiac injury to heart failure. *Cardiovasc Res* **90**, 224-33.

230. Rahman, S. & Islam, R. (2011). Mammalian Sirt1: insights on its biological functions. *Cell Commun Signal* **9**, 11.
231. Lin, J. F., Wu, S., et al. (2011). Resveratrol protects left ventricle by increasing adenylate kinase and isocitrate dehydrogenase activities in rats with myocardial infarction. *Chin J Physiol* **54**, 406-12.
232. Cesselli, D., D'Aurizio, F., et al. (2013). Cardiac stem cell senescence. *Methods Mol Biol* **976**, 81-97.
233. King, N., Lin, H., et al. (2010). Cysteine protects freshly isolated cardiomyocytes against oxidative stress by stimulating glutathione peroxidase. *Molecular and cellular biochemistry* **343**, 125-32.
234. Louch, W. E., Sheehan, K. A., et al. (2011). Methods in cardiomyocyte isolation, culture, and gene transfer. *Journal of molecular and cellular cardiology* **51**, 288-98.
235. Livak, K. J. & Schmittgen, T. D. (2001). Analysis of relative gene expression data using real-time quantitative PCR and the 2(-Delta Delta C(T)) Method. *Methods* **25**, 402-8.
236. Ram, R., Mickelsen, D. M., et al. (2011). New approaches in small animal echocardiography: imaging the sounds of silence. *American journal of physiology. Heart and circulatory physiology* **301**, H1765-80.
237. Baschong, W., Suetterlin, R., et al. (2001). Control of autofluorescence of archival formaldehyde-fixed, paraffin-embedded tissue in confocal laser scanning microscopy (CLSM). *The journal of histochemistry and cytochemistry : official journal of the Histochemistry Society* **49**, 1565-72.
238. Olivetti, G., Ricci, R., et al. (1986). Response of the border zone to myocardial infarction in rats. *Am J Pathol* **125**, 476-483.

List of references for Table 3.1

Baba, S., T. Heike, et al. (2007). "Flk1(+) cardiac stem/progenitor cells derived from embryonic stem cells improve cardiac function in a dilated cardiomyopathy mouse model." Cardiovascular research **76**(1): 119-131.

Bearzi, C., A. Leri, et al. (2009). "Identification of a coronary vascular progenitor cell in the human heart." Proc Natl Acad Sci U S A **106**(37): 15885-15890.

Bearzi, C., M. Rota, et al. (2007). "Human cardiac stem cells." Proc Natl Acad Sci U S A **104**(35): 14068-14073.

Beltrami, A. P., L. Barlucchi, et al. (2003). "Adult cardiac stem cells are multipotent and support myocardial regeneration." Cell **114**(6): 763-776.

Cai, C. L., X. Liang, et al. (2003). "Isl1 identifies a cardiac progenitor population that proliferates prior to differentiation and contributes a majority of cells to the heart." Dev Cell **5**(6): 877-889.

Cai, C. L., J. C. Martin, et al. (2008). "A myocardial lineage derives from Tbx18 epicardial cells." Nature **454**(7200): 104-108.

Chimenti, I., R. R. Smith, et al. (2010). "Relative roles of direct regeneration versus paracrine effects of human cardiosphere-derived cells transplanted into infarcted mice." Circulation research **106**(5): 971-980.

Dawn, B., A. B. Stein, et al. (2005). "Cardiac stem cells delivered intravascularly traverse the vessel barrier, regenerate infarcted myocardium, and improve cardiac function." Proc Natl Acad Sci U S A **102**: 3766-3771.

Ellison, G. M., C. Vicinanza, et al. (2013). "Adult c-kit(pos) cardiac stem cells are necessary and sufficient for functional cardiac regeneration and repair." Cell **154**(4): 827-842.

Goumans, M. J., T. P. de Boer, et al. (2007). "TGF-beta1 induces efficient differentiation of human cardiomyocyte progenitor cells into functional cardiomyocytes in vitro." Stem cell research **1**(2): 138-149.

Hierlihy, A. M., P. Seale, et al. (2002). "The post-natal heart contains a myocardial stem cell population." FEBS Lett **530**(1-3): 239-243.

Johnston, P. V., T. Sasano, et al. (2009). "Engraftment, differentiation, and functional benefits of autologous cardiosphere-derived cells in porcine ischemic cardiomyopathy." Circulation **120**(12): 1075-1083, 1077 p following 1083.

Kattman, S. J., T. L. Huber, et al. (2006). "Multipotent flk-1+ cardiovascular progenitor cells give rise to the cardiomyocyte, endothelial, and vascular smooth muscle lineages." Dev Cell **11**(5): 723-732.

Laugwitz, K. L., A. Moretti, et al. (2005). "Postnatal isl1+ cardioblasts enter fully differentiated cardiomyocyte lineages." Nature **433**(7026): 647-653.

Liang, S. X., L. M. Khachigian, et al. (2011). "In vitro and in vivo proliferation, differentiation and migration of cardiac endothelial progenitor cells (SCA1+/CD31+ side-population cells)." Journal of thrombosis and haemostasis : JTH **9**(8): 1628-1637.

Limana, F., A. Zacheo, et al. (2007). "Identification of myocardial and vascular precursor cells in human and mouse epicardium." Circ Res **101**(12): 1255-1265.

Makkar, R. R., R. R. Smith, et al. (2012). "Intracoronary cardiosphere-derived cells for heart regeneration after myocardial infarction (CADUCEUS): a prospective, randomised phase 1 trial." Lancet **379**(9819): 895-904.

Martin, C. M., A. P. Meeson, et al. (2004). "Persistent expression of the ATP-binding cassette transporter, Abcg2, identifies cardiac SP cells in the developing and adult heart." Dev Biol **265**(1): 262-275.

Martin-Puig, S., Z. Wang, et al. (2008). "Lives of a heart cell: tracing the origins of cardiac progenitors." Cell Stem Cell **2**(4): 320-331.

Messina, E., L. De Angelis, et al. (2004). "Isolation and expansion of adult cardiac stem cells from human and murine heart." Circ Res **95**(9): 911-921.

Moretti, A., L. Caron, et al. (2006). "Multipotent embryonic isl1+ progenitor cells lead to cardiac, smooth muscle, and endothelial cell diversification." Cell **127**(6): 1151-1165.

Mouquet, F., O. Pfister, et al. (2005). "Restoration of cardiac progenitor cells after myocardial infarction by self-proliferation and selective homing of bone marrow-derived stem cells." Circ Res **97**: 1090-1092.

Oh, B. H., S. B. Bradfute, et al. (2003). "Cardiac progenitor cells from adult myocardium: homing, differentiation, and fusion after infarction." Proc Natl Acad Sci U S A **100**: 12313-12318.

Ott, H. C., T. S. Matthiesen, et al. (2007). "The adult human heart as a source for stem cells: repair strategies with embryonic-like progenitor cells." Nature clinical practice. Cardiovascular medicine **4 Suppl 1**: S27-39.

Oyama, T., T. Nagai, et al. (2007). "Cardiac side population cells have a potential to migrate and differentiate into cardiomyocytes in vitro and in vivo." J Cell Biol **176**(3): 329-341.

Serradifalco, C., P. Catanese, et al. (2011). "Embryonic and foetal Islet-1 positive cells in human hearts are also positive to c-Kit." European journal of histochemistry : EJH **55**(4): e41.

Simpson, D. L., R. Mishra, et al. (2012). "A strong regenerative ability of cardiac stem cells derived from neonatal hearts." Circulation **126**(11 Suppl 1): S46-53.

Smith, R. R., L. Barile, et al. (2007). "Regenerative potential of cardiosphere-derived cells expanded from percutaneous endomyocardial biopsy specimens." Circulation **115**(7): 896-908.

Smits, A. M., P. van Vliet, et al. (2009). "Human cardiomyocyte progenitor cells differentiate into functional mature cardiomyocytes: an in vitro model for studying human cardiac physiology and pathophysiology." Nature protocols **4**(2): 232-243.

Wang, X., Q. Hu, et al. (2006). "The role of the sca-1+/CD31- cardiac progenitor cell population in postinfarction left ventricular remodeling." Stem cells **24**(7): 1779-1788.

Yamashita, J. K., M. Takano, et al. (2005). "Prospective identification of cardiac progenitors by a novel single cell-based cardiomyocyte induction." FASEB journal : official publication of the Federation of American Societies for Experimental Biology **19**(11): 1534-1536.

Zhou, B., Q. Ma, et al. (2008). "Epicardial progenitors contribute to the cardiomyocyte lineage in the developing heart." Nature **454**(7200): 109-113.

CONFERENCE PROCEEDINGS

1. Trieste (IT), 30.05 – 2.06.2012: *Frontiers in Cardiac and Vascular Regeneration***.**
Poster presentation: "**Pharmacological attenuation of Cardiac Stem Cell senescence *in vitro* increases their reparative ability *in vivo***". Elisa Avolio, Angela Caragnano, Carlo Vascotto, Giuseppe Gianfranceschi, Ugolino Livi, Rajesh Katare, Paolo Madeddu, Daniela Cesselli, Carlo Alberto Beltrami and Antonio Paolo Beltrami

2. Venezia (IT), 7.06.2012: *11th european Congress on Telepathology and 5th International Congress on Virtual Microscopy*.
Poster presentation: "**An in vitro, image-based platform to evaluate human stem cell senescence**". Elisa Avolio, Angela Caragnano, Giuseppe Gianfranceschi, Daniela Cesselli, Antonio Paolo Beltrami, Ugolino Livi and Carlo Alberto Beltrami

3. Ferrara (IT), 20-22.06.2012: *Stem Cell Research Italy - International Society For Cellular Therapy - Europe AICC JOINT MEETING*.
Poster presentation: "**Rapamycin and Resveratrol attenuate human Cardiac Stem Cell senescence *in vitro* and ameliorate their regenerative potential *in vivo***". A. Caragnano, E. Avolio, G. Gianfranceschi, V. Zanon, R. Katare, N. Bergamin, M. Sorrentino, N. Finato, U. Livi, P. Madeddu, D. Cesselli, A.P. Beltrami, C.A. Beltrami.

4. Cambridge (UK), 20-23.07.2013: "Cell senescence in Cancer and Ageing".
Poster presentation: "**Fighting senescence in the Heart: a novel intervention protocol is able to revert human Cardiac Stem Cells senescence *in vitro* enhancing their regenerative potential *in vivo***". Elisa Avolio, Giuseppe Gianfranceschi, Angela Caragnano, Emmanouil Athanasakis, Rajesh Katare, Marco Meloni, Anita Palma, Arianna Barchiesi, Carlo Vascotto, Barbara Toffoletto, Elisa Mazzega, Nicoletta Finato, Giuseppe Aresu, Ugolino Livi, Costanza Emanueli, Carlo Alberto Beltrami, Paolo Madeddu, Daniela Cesselli and Antonio Paolo Beltrami

PUBLISHED ABSTRACT

E. Avolio, G. Aresu, A. Caragnano, R. Katare, C. Vascotto, P. Madeddu, U. Livi, C. Beltrami, D. Cesselli, A. Beltrami. "***Pharmacologic Attenuation of Cardiac Stem Cell Senescence".***
1st Joint Meeting of Pathology and Laboratory Diagnostics, 2012 September 12–15, Udine, Italy. Am J Pathol 2012, 181(Suppl):S30 Abstract SC7